Rhodium-Catalyzed Asymmetric Hydroformylation of Alkenes Using Diazaphospholane Ligands and Application With Wittig Olefination

by

Gene W. Wong

A dissertation submitted in partial fulfillment

of the requirements for the degree of

Doctor of Philosophy

(Chemistry)

at the

UNIVERSITY OF WISCONSIN-MADISON

2012

Date of final oral examination: 11/9/12

The dissertation is approved by the following members of the Final Oral Committee:

Clark R. Landis, Professor, Chemistry
Shannon S. Stahl, Professor, Chemistry
Tehshik P. Yoon, Associate Professor, Chemistry
Steve D. Burke, Professor, Chemistry
Mahesh K. Mahanthappa, Associate Professor, Chemistry

Rhodium-Catalyzed Asymmetric Hydroformylation of Alkenes Using Diazaphospholane Ligands and Application With Wittig Olefination

Gene W. Wong

Under the supervision of Professor Clark R. Landis

At the University of Wisconsin-Madison

Hydroformylation is a large-scale commodity process in the synthesis of aldehydes from alkene, carbon monoxide and hydrogen gas starting materials; in contrast, *asymmetric* hydroformylation (AHF) is underutilized in the synthesis of chiral aldehydes. Because rhodium-catalyzed hydroformylation exhibits perfect atom-economy, high turnover numbers, and fast rates, this is a desirable reaction in synthesis of branched chiral aldehydes. Challenges in AHF include control of selectivity (chemo-, regio-, and enantio-), slow rates of reaction, and a limited substrate scope. Currently, only a handful of chiral phosphorus-containing ligands exhibit state-of-the-art rates of reaction and high levels of enantioselectivity in rhodium-catalyzed hydroformylation for a broad range of substrates; even less of these have found applications in complex molecule and natural product synthesis. This work describes the synthesis of a bis-3,4-diazaphospholane ligand library, hydroformylation of O-functionalized alkenes, and application with Wittig olefination in the synthesis of complex organic molecules. A library of bis-3,4-diazaphospholanes ligands was generated by varying the steric bulk in the secondary coordination sphere and applied to the hydroformylation of three terminal alkenes. Styrene exhibited modest variations in regio- and enantioselectivity, whereas, vinyl acetate and allyloxy-*t*-butyldimethylsilane exhibited fairly minor changes. Enantioselective hydroformylation of allyl

ethers with bisdiazaphospholane ligands yield synthetically useful building blocks for organic synthesis; one prominent example, chiral “Roche aldehyde” can be accessed from inexpensive allyl alcohol. AHF of 5-grams of an allyl silyl ether and a protected acrolein demonstrate scalable syntheses of chiral building blocks relevant for natural product synthesis. One-pot asymmetric hydroformylation-Wittig olefinations (AHF-WO) is performed with various alkenes using Rh-bisdiazaphospholane catalysts resulting in γ-chiral α,β-unsaturated carbonyl products. In these experiments multiple AHF-WO iterations demonstrate the utility of the synthesis of complex molecules with various functionalities, multiple carbon-carbon double bonds, and stereocenters. Overall this body of work promotes the use of bisdiazaphospholane ligands for enantioselective hydroformylation and organic synthesis.

Acknowledgements

The work described in this Thesis was only possible by the unyielding support from various people during my time in graduate school. Tremendous thanks goes to Professor Clark Landis for his tireless devotion in providing guidance, suggestions, and wisdom in the past five and a half years. I acknowledge Professor Charles Casey, Professor Shannon Stahl, Professor Tehshik Yoon, Professor Mahesh Mahanthappa, and Professor Steve Burke for serving on various committees during my graduate school education, and or for helpful comments and suggestions in supergroup meetings. A lot of the characterization work reported herein could not be done without the assistance and expertise of Dr. Charlie Fry, Dr. Monika Ivancic, Dr. Martha Vestling, and Dr. Ilia Guzei.

I am grateful to my coworkers in the Landis group, especially Poon Chotchatchawankul, Allice Dang, Anna Dunn, Leigh Abrams, Tyler Adint, Nick Beach, Ian Tonks, Julia Wildt, Andrew Yan, Helen Dauer, Nuru Stracey, and Emily Tan, for friendship and excellent chemistry/scientific discussions. I would not be where I am today without the friendship and support from fellow classmates: Eugenia Turov, Kasia Kornecki, Michael Nippe, Aaron Smith, Ryan Pakula, Travis Sunderland, Katie Freeman, and Juana Du. To my teammates on The Mighty Hucks, many thanks for friendship and fun during Ultimate frisbee. Thanks go to colleagues and co-workers in the Stahl, Berry, Yoon, and Burke research groups for various chemicals and chemistry discussions. Thanks to Professor Brian Frost (University of Nevada, Reno) and Jeff Weinert for early mentorship and guidance in my chemical education.

Many thanks to my friends for the many fun road trips to unexplored places. Thanks go to Kim Wong, for being the best sister in listening to my numerous rants and uncompromising

support of the family. Finally, my thesis would not be possible without the upbringing of Mei and Harvey Wong; you two have taught me to value education and to always keep pushing.

Table of Contents

Chapter 1

Catalysis

1.1 Introduction

Every person in the modern world has directly benefited from products generated from catalysis. Many have come to unknowingly depend on catalysis in our current way-of-life: impacts can be found from food to transportation to health care and more. The production of key ingredients in fertilizers or agrochemicals allow for in maximized crop cultivation or farming of food come from catalytic processes. The components found in fuels for various modes of transportation are accessed from various catalytic processes. Key constituents and materials found in products we use everyday has improved our standard of living (e.g., plastics, synthetic materials, detergents, fragrances, etc.) were accessed from catalysis. Catalysis enables improved manufacturing of medicine with less generated waste. These real-life examples demonstrate the silent role of catalytic technology that plays in our modern way of life. Undoubtedly catalysis will increase in importance in sustaining and advancing our modern society.

What is catalysis? To understand catalysis we must ask, "What is a catalytic reaction?" A generic catalytic reaction is a transformation between starting materials (A and B) to a more valuable product (C), enabled by the addition of a small amount of a catalyst. A catalyst is another chemical component added to a reaction that is not created or consumed in the reaction. At the molecular level, a catalyst begins a catalytic reaction by interacting with one of the starting materials, A, followed by the subsequent addition, B (Scheme 1.1). Through another step, components A and B attached to the catalyst react to form C and regenerating the catalyst; one rotation around this "cycle" represents one catalytic transformation and formation of the product C. Because the catalyst is not consumed in the reaction, this allows for many more revolutions about the cycle and increased product formation. Two desirable attributes catalysts exhibit are high selectivity and activity for a desirable product that may be difficult to attain

through any other means. In many situations the choice of a catalyst allows precise control of a particularly product, thus minimizing undesired byproducts. Most importantly, catalytic reactions often occur faster than an uncatalyzed reaction and with less energy.

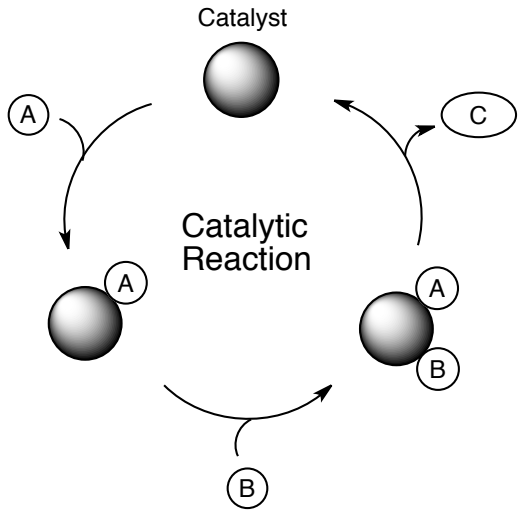

Scheme 1.1 A reaction "cycle" between A, B, and a catalyst.

In an uncatalyzed reaction, there is large energy barrier between the starting materials (A and B) and the product (C) (Figure 1.1). A way to visualize barrier is by analogy to elevation in geography: the difference between "valley" of starting materials and the top of the "mountain" is the barrier to the transformation of A and B into C. In contrast, the reaction between A, B, and a catalyst happens to exhibit lower overall energy barriers for the catalytic reaction (Figure 1.2). The "valleys" of the catalytic intermediates are close in energy relative to one another, and more importantly, the largest of the "hills" is relatively modest. Comparing these plots, a lower energy is required for the catalyzed reaction in comparison to the uncatalyzed reaction, thus requiring less energy and time to complete the transformation (Figure 1.3).

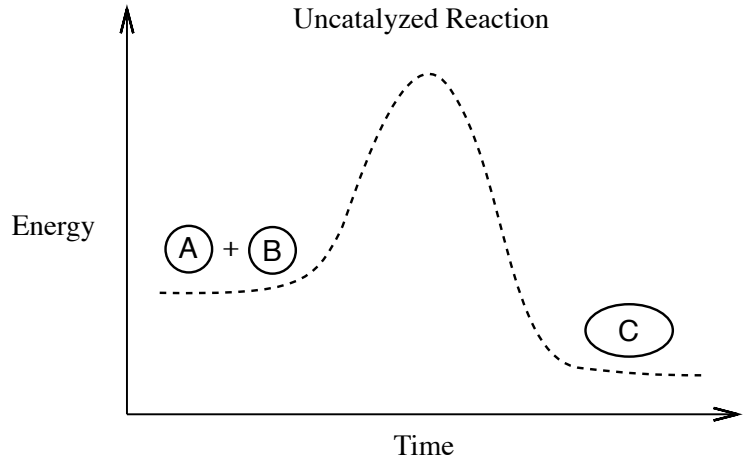

Figure 1.1 Reaction progress vs. energy of an uncatalyzed reaction.

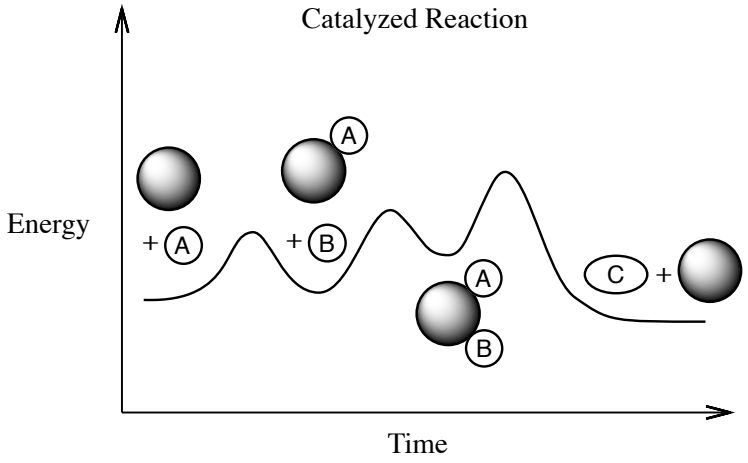

Figure 1.2 Time vs. energy of a catalyzed reaction.

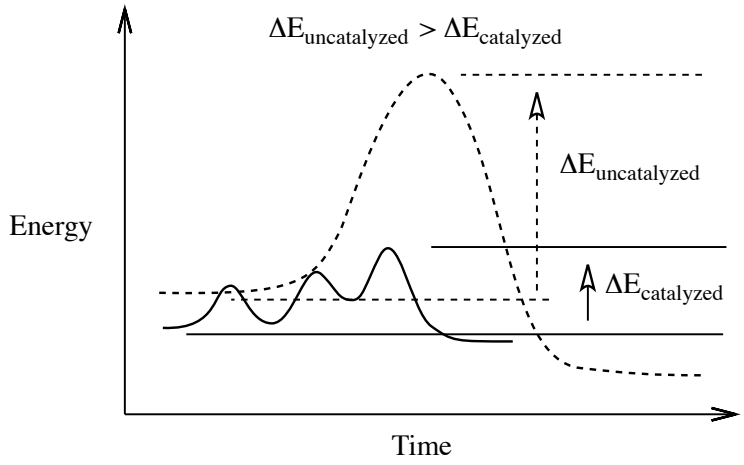

Figure 1.3 Comparison of reaction profiles between uncatalyzed and catalyzed reactions.

The generic catalytic reaction described here applies to all types of catalysis. The attributes of catalysis, lower energy consumption, synthesis of desirable products, and high levels of productivity make catalytic processes highly attractive in sustaining and advancing technologies that contribute to a modern way-of-life.

1.2 Prominent Examples of Catalysis

Two main efforts that use catalysis today are in commodities production and in fine chemical synthesis. Commodity-scale production is only feasible using catalysis—the practical synthesis of large amounts of a material or product can only be done efficiently using a catalyst (otherwise, enormous amounts of waste result). Fine chemicals and medicines are increasingly made using catalysis to minimize the amount of waste generated. Described briefly herein is a broad overview of select types of catalysis and some implications in our way-of-life.

The advent of the Haber-Bosch process contributed in the world's exponential increase in population because it enabled catalytic production of ammonia from nitrogen and hydrogen gases using iron and ruthenium catalysts (Scheme 1.2). Ammonia is used in the production of

nitrates used as fertilizers in agriculture. The availability of cheap and abundant fertilizers enabled more efficient farming and better crop yields that lead to readily available and cheaper food. Enzymes found in nature, nitrogenases, have been discovered to reduce dinitrogen to ammonia; efforts to study and mimic these natural catalysts for less energy intensive production of ammonia is an on-going area of chemical research.

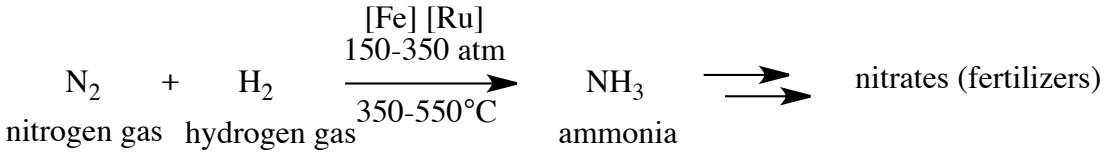

Scheme 1.2 Haber-Bosch process.

New materials were required to help store and contain available foods for longer amounts of time. One solution came from Drs. Karl Ziegler and Giulio Natta, in the development large-scale polyolefin polymerization (e.g., polyethylene, Scheme 1.3). Polymers are large molecules made up of from smaller components, called monomers. Because polymers are typically lightweight and available through a wide range of physical properties, they are utilized today for numerous applications and situations: one example, food packaging. Other synthetic polymers include polyesters, Styrofoam, rubber, PVC (polyvinyl chloride), nylon, Teflon, polycarbonates, etc. Different catalysts exhibit a range of selectivity in polymer synthesis enable the development of different polymers with varying physical properties. Many commodity-scale plastics and synthetic materials are cheap and readily available due to highly efficient and cheap catalysts.

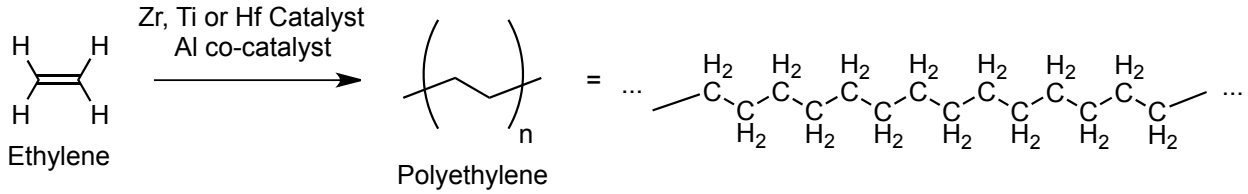

Scheme 1.3 Ethylene polymerization.

Hydrogenation is a significant catalytic transformation between an unsaturated molecule and hydrogen gas, resulting in a saturated analogue. Some examples include hydrogenation of vegetable and plant oils in the production of margarine and shortenings, or aldehydes (made from hydroformylation) into alcohols for detergents and surfactants. In Scheme 1.4 depicts hydrogenation of a triglyceride molecule into it's saturated analogue by addition of an equivalent of hydrogen gas across each of the carbon-carbon double bonds; commonly, these molecules are commonly called unsaturated and saturated fats, respectively. Typically hydrogenation of liquid oils to solid fats yield increased stability and longer self-life. The Haber-Bosch process previously mentioned, is an example of an inorganic hydrogenation of atmospheric nitrogen to ammonia.

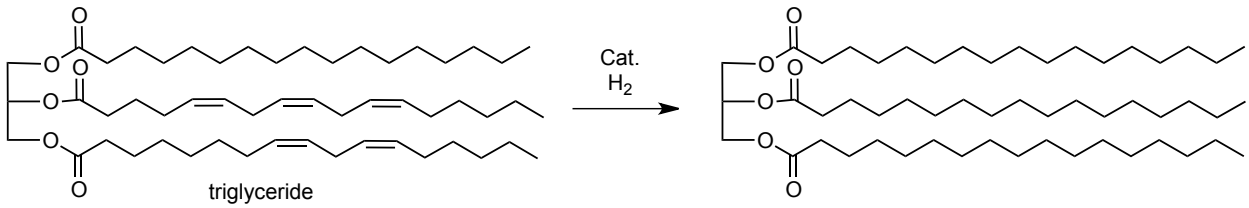

Scheme 1.4 Hydrogenation of a triglyceride (an example of a polyunsaturated fat found in vegetable oils).

In 2001, the Nobel Prize was awarded to Drs. William S. Knowles, Ryori Noyori, and K. Barry Sharpless, for their work in asymmetric hydrogenation and oxidation catalysis. Asymmetric hydrogenation and oxidation catalysis allow chemists to carefully control the synthesis of chiral molecules using metal catalysts in a specialized structural configurations and functionalities. For example, chiral amino acids have been made from asymmetric hydrogenation (e.g., synthesis of alanine, Scheme 1.5). These reactions are often used in organic synthesis and medicine where the correct configuration of a molecule is paramount in biological function.

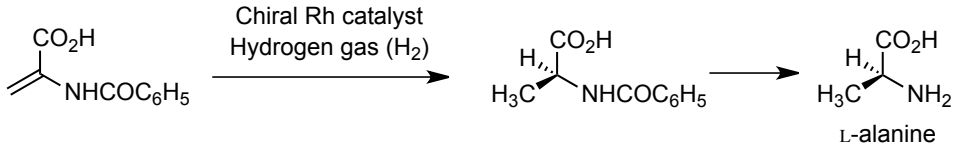

Scheme 1.5 Asymmetric hydrogenation in the synthesis of L-alanine.

1.3 Chirality

Chirality is found ubiquitously throughout nature and because organisms react differently to certain stereoisomers of a drug molecule, there is a demand in synthetic chemistry to make one selectively over another. The importance of chirality was unfortunately learned from one of the greatest tragedies in modern medicine involving a chiral drug, thalidomide, prescribed as a morning sickness drug for pregnant women. One of the drug's stereoisomers, an enantiomer, caused thousands of cases of birth defects in children worldwide. This discovery enforced the importance of thorough testing of chiral drugs in their enantiomerically pure forms. Thus, drug synthesis required the development of highly selective reactions to attain sufficient purity chiral building blocks and biologically active molecules.

A chiral molecule is asymmetric in their 3-dimensional (3-D) structures and its mirror image is not superimposable. One real-world example of a chiral object is a human hand. A left hand is not superimposable with the right although both contain the same composition (fingers), but in different spatial arrangements—by analogy, chiral molecules such as sugars and amino acids can be explained a same manner (an individual configuration is called a stereoisomer). Illustrated in Figure 1.4 is an amino acid, alanine, in its left- and right-handed forms. These two molecules have the same elemental formula ($C_3H_7NO_2$) but their components are arranged differently—they're mirror images with respect to one another. If you were to overlay these molecules you would find they do not have the same spatial arrangement. These molecules are designated as *S* or *R*-stereochemistry (L- or D-alanine, respectively) based on the priority of the groups bound to the central carbon for scientific nomenclature. It is this difference in configuration between chiral molecules plays a significant role in therapeutic properties of chiral drugs as found with thalidomide.

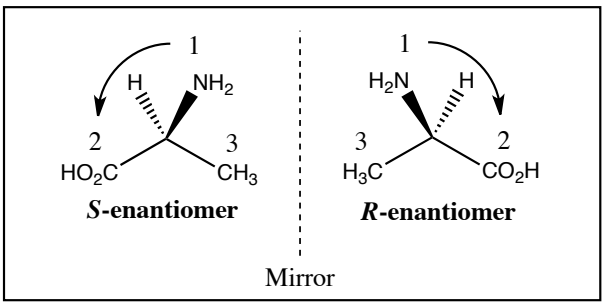

Figure 1.4 Two enantiomers of alanine.

A major advance in the production of chiral molecules came from asymmetric *hydrogenation* (as the example of the synthesis of alanine in Scheme 1.5) and oxidation. My work reported herein is in the development of an underutilized reaction, asymmetric

hydroformylation (AHF), with focus in producing chiral building blocks in the synthesis of biologically active molecules.

1.4 This Work

In the past five years, my work has been based on the development of asymmetric hydroformylation (AHF), for practical use in organic synthesis. Hydroformylation is a reaction between an alkene, carbon monoxide, hydrogen gas, and in the presence of a rhodium or cobalt catalyst, to yield branched and linear aldehydes (Scheme 1.6). Typically hydroformylation is a large-scale commodity process in the production of linear aldehydes for a variety of purposes: detergents, plasticizers, agrochemicals, and fine chemical production. Our interest in the Landis research group is based on studying catalysts to improve selectivity and activity; one on-going project in the group is development of ligands for hydroformylation and related catalytic reactions. Hydroformylation exhibits "green" chemical ideals: perfect atom economy, high turnover numbers, and fast rates of reaction. These attributes make AHF a practical and attractive method in the synthesis of chiral aldehydes. My work in the past five years consisted of developing ligands for AHF and promote its application in organic synthesis.

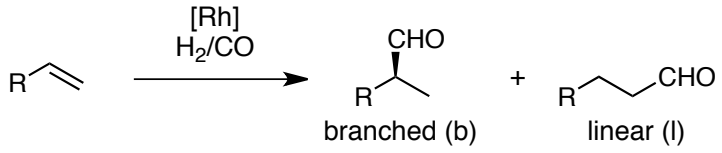

Scheme 1.6 Hydroformylation reaction.

Chapter 2 contains a review the current state-of-the-art in rhodium-catalyzed AHF (>90% ee) with a focus on the chiral ligands and hydroformylation selectivity on various substrates. The purpose of this review is to highlight reported AHF work and its use in the synthesis of chiral

aldehydes in organic synthesis. Only a handful of these ligands lead to highly selective and active catalysts, bisdiazaphospholanes ligands among them (developed by our group) have opportunity to impact organic synthesis in hydroformylation catalysis.

One major facet in the Landis group is the development of diazaphospholane ligands for transition-metal catalysis; Chapter 3 presents synthesis of a bisdiazaphospholane ligand library for optimizing hydroformylation selectivity. This work was conducted with a fellow group member, Tyler Adint, in synthesis and testing these ligands in catalysis. The results of this project gave us insight between the molecular structure of the catalyst and the affect on hydroformylation selectivity. Efforts in this study attempt to improve and maximize desirable selectivity for alkenes of interest.

Another interest of our group is to identify problems in organic synthesis that could be solved using AHF; one example is the synthesis of chiral "Roche aldehyde." The current method in the synthesis of chiral Roche *aldehyde* is inefficient requiring tedious functional group manipulation from expensive Roche *ester* (Scheme 1.7). Enantioselective hydroformylation of allyl ethers and acrylates described in Chapter 4 presents an efficient alternative in the synthesis of Roche aldehyde and related analogues. Hydroformylations performed with five-grams of alkene using very low amounts of catalyst demonstrate synthesis of the chiral Roche aldehyde in practical amounts of Roche aldehyde.

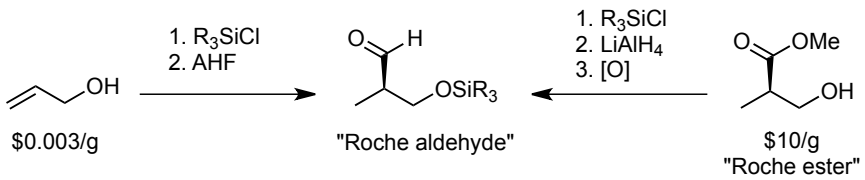

Scheme 1.7 AHF of allyl alcohol as an alternative in the synthesis of chiral "Roche aldehyde."

The Roche aldehyde is a common building block in total synthesis of biologically active molecules. In Chapter 5, I describe hydroformylation and Wittig olefination (WO) in a one-pot tandem reaction in the synthesis of useful organic molecules. These set of experiments demonstrate rhodium-diazaphospholane catalysts are competent in the presence of other reagents for multicomponent reactions in the synthesis of complex products. Overall, the collection of this work described herein looks at advancing enantioselective hydroformylation as a practical method for use in organic synthesis.

Chapter 2

Highly Enantioselective Rhodium-Catalyzed Hydroformylation of Alkenes Using Chiral Phosphorus Ligands and Applications in Organic Synthesis

2.1 Introduction

As increasing number of pharmacologically active drugs are delivered as their enantiomerically pure form, there is a need to synthesize these molecules selectively using scalable asymmetric transformations. We cannot help to look at asymmetric hydroformylation (AHF) as a possible method that provides chiral and functional products. Hydroformylation is a large-scale commodity process yielding billions of pounds of linear aldehydes per year; in contrast, rhodium-catalyzed asymmetric hydroformylation (Scheme 2.1) is an underutilized transformation due to the limited number of ligands preferentially giving the branched aldehyde in high enantioselectivity. Perfect atom economy, inexpensive reactants, neutral reaction conditions, simple purification, and high turnover numbers make rhodium-catalyzed enantioselective hydroformylation a very attractive process for the synthesis of α-chiral aldehydes. Although asymmetric hydroformylation is promising, there are three challenges that remain: a wide substrate scope, modular ligands for substrate optimization, and fast rates that yield desirable selectivity.

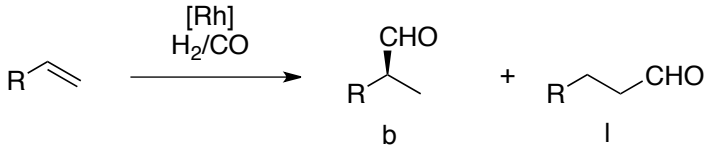

Scheme 2.1 Asymmetric hydroformylation (AHF).

Noyori has described asymmetric catalysis as four-dimensional chemistry; not only is perfect stereochemistry for a molecule (x, y, z) a requisite, but attaining optically active materials in a reasonable amount of time (t) is also paramount.[1] *Asymmetric hydrogenation catalysis* of C—C and C—X double bonds with dihydrogen have achieved these goals while establishing

itself as a powerful method in establishing stereocenters in organic synthesis. Asymmetric hydroformylation offers similar draws although comparatively with less precedence in fine chemical synthesis. Operationally, AHF is similar to asymmetric hydrogenation; both reactions use gaseous reagents under pressurized conditions. Hydroformylations are commonly performed using autoclaves (high pressures, 150—5000 psi) or glass bottles (low pressure, 15-150 psi). The demand for higher gas pressure in these reactions is due to two empirical factors: (1) generation of the active hydroformylation catalysts and (2) to attain high rates and/or selectivity of reaction. Both of these factors depend on the efficiency of gas-liquid mixing and effective gas concentration in solution. Due to these reasons, the use of balloons with H_2 and CO has found minimal practice in AHF. Throughout this review, an emphasis of focus will be the specific reaction conditions used in enantioselective hydroformylation.

There have been excellent reviews highlighting the recent advances in hydroformylation;[2-5,6] this manuscript offers an in-depth look at rhodium-catalyzed highly enantioselective hydroformylation (≥90% ee) of structurally diverse alkenes comparing the current state-of-the-art ligands (Figure 2.1). The focus of these criteria neglects other important factors pertaining to hydroformylation: chemoselectivity, regioselectivity, substrate scope, reaction conditions, catalyst activity, and scalability. The mechanism of enantioselective hydroformylation of styrene will be discussed with rhodium-bisdiazaphospholane catalysts. Herein, a sampling of exceptional results is summarized with various substrate classes with various ligands: aryl alkenes, vinyl acetate and amides, functionalized allylic alkenes, heterocycles, 1,3-dienes, and alkyl alkenes. Relevant reports of application of enantioselective hydroformylation in organic synthesis will be included throughout this Chapter.

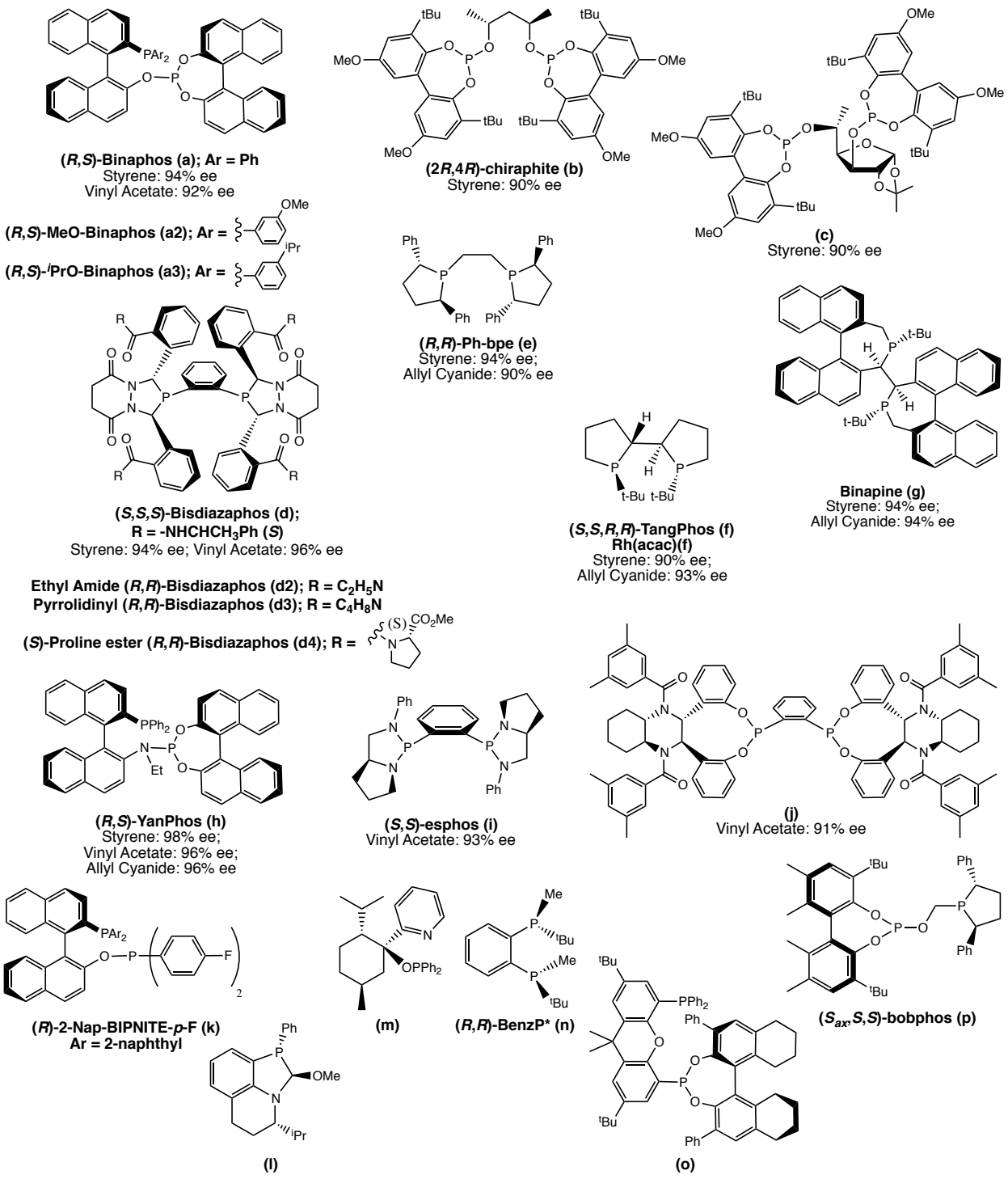

Figure 2.1 Chiral phosphorus-containing ligands that exhibit 90%+ ee in rhodium-catalyzed AHF of various alkenes.

2.2 Enantioselective Hydroformylation of Alkenes

In general, the relative rate of reactivity of rhodium-catalyzed hydroformylation corresponds with the number of substitutions bound to the alkene (Figure 2.2).[7-9] Terminal alkenes have been the most common substrates found in AHF due to the ease of hydroformylation under mild conditions (low pressures and temperatures). 1,2-Disubstituted alkenes have seen less attention in enantioselective hydroformylation because the requisite of higher temperatures to access reasonable rates. In some systems, higher temperature has been found to be detrimental to the regio- and enantioselectivity of hydroformylation. Enantioselective hydroformylation of 1,1-disubstituted alkenes leading to β-chiral aldehydes or quaternary aldehydes have been sparsely reported. Little to no precedence for AHF of trisubstituted and tetrasubstituted alkenes with significant enantio-enrichment has appeared.

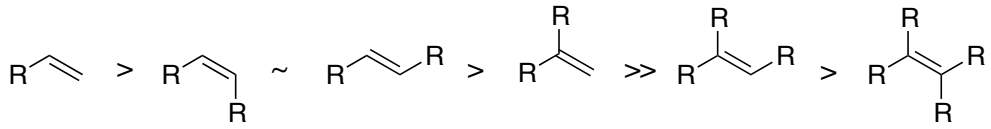

Figure 2.2 Relative rates of reactivity of various substituted alkenes in rhodium-catalyzed hydroformylation arranged by decreasing activity.

2.2.1 Styrenes and Aromatic Alkenes

Styrenes have been most common substrates to be explored in AHF due to the attractive aldehyde products that constitute intermediates in the synthesis of pharmacologically active, anti-inflammatory analgesics (such as ibuprofen, ketoprofen, and naproxen). The hydroformylation of aryl alkenes with rhodium and platinum phosphine complexes intrinsically give desirable regioselectivity with higher yields of the branched aldehyde compared to other terminal alkenes

(i.e. alkyl alkenes). Hydroformylation of styrene that exhibited interesting temperature, carbon monoxide and dihydrogen pressure effects with regio- and enantioselectivity prompted mechanistic studies from rhodium-bisdiazaphospholane[10] and platinum systems.[11]

(*S*,*R*)-Binaphos **a** (Figure 2.1) and related analogues developed by Nozaki and coworkers reported some of the earliest examples of rhodium-catalyzed enantioselective hydroformylation of styrene (Table 2.2, entry 1, 94% ee).[12] Zhang and coworkers developed a related phosphine-phosphoramidite ligand **h** exhibiting 98% ee in styrene hydroformylation (entry 8).[13] For brevity, ligand libraries derived from (*S*,*R*)-Binaphos **a**,[14-16] bisdiazaphospholanes **d**,[17] (*R*,*R*)-Ph-bpe **e**,[18] and (*R*,*S*)-YanPhos **h**[19] have generally demonstrated comparable or less regio- and enantioselective results to their parent ligand, and superior results for a particular substrate will be specified. Bisphosphites such as (*2R*,*4R*)-Chiraphite[20,21] **b** (entry 2) and a D-(+)-glucose derived bisphosphite[22] **c** (entry 3) enabled highly regio- (up to 99% branched aldehyde) and enantioselective hydroformylation (90% ee for both ligands) albeit low conversions due to lower reaction temperatures. Other examples include cyclic bisphosphines yielding less active hydroformylation catalysts such as Binapine **g** (entry 6, 12% conversion) and ((*S*,*S*,*R*,*R*)-TangPhos)Rh(acac) (entry 7, 12% conversion) exhibiting 94% and 90% ee, respectively.[23] In comparison, using bisphospholanes in rhodium hydroformylation formed more active catalysts for styrene hydroformylation; for example using (*R*,*R*)-Ph-bpe as a ligand, 57% conversion and 94% ee were observed (**e**, entry 4, 57% conversion, 94% ee).[18,24] Optimized conditions with (*S*,*S*,*S*)-bisdiazaphospholane was accomplished to obtain highly regioselective and enantioselective hydroformylation of styrene **d** (entry 5, 98% branched and 93% ee).[25]

Table 2.1 Styrene AHF using various chiral phosphorus-containing ligands.

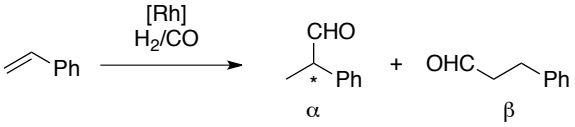

	Ligand/Catalyst	Sub/Cat Loading	H_2/CO Pressure	T (°C)	t (h)	Conv. (%)	α:β	ee (%)
1	**(*S*,*R*)-(a)**	2,000:1	1470 psi (1:1)	60	43	99	88:12	94 (*S*)
2	**b**	40,000:1	500 psi (1:1)	25	-	-	98:2	90
3	**c**	1,000:1	145 psi (2:1)	20	48	83	99:1	90 (*S*)
5	**d**	200:1	160 psia (1:3)	40	8	96	98:2	93 (*R*)
4	**e**	5,000:1[a]	150 psi (1:1)	80	3	57	98:2	94 (*R*)
7	Rh(acac)(**f**)	3,000:1[a]	150 psi (1:1)	80	3	12	94:6	90
6	**g**	3,000:1[a]	150 psi (1:1)	80	3	12	91:9	94 (*S*)
8	**h**	1,000:1	290 psi (1:1)	60	24	99	88:12	98 (*R*)

a. Total substrate/catalyst loading with styrene in a one-pot three-substrate screening.

Three ligands from this group have been demonstrated effective enantioselective hydroformylation of various substituted styrene's and 1,2−disubstituted aryl alkenes (Table 2.2). The highest reported enantioselectivities of various substituted styrenes have been predominantly with the two hybrid ligands: (*R*,*S*)-Binaphos **a** and (*S*,*R*)-YanPhos **h**. (*R*,*S*)-Binaphos **a** was utilized to obtain a range of 86—88% branched aldehyde for non-fluorinated (entries 1, 3, 7) and 89—96% for fluorinated styrene's (entries 9, 11, 13) while exhibiting high stereoselectivity (92—98% ee).[12,15] Zhang and coworkers reported 98%+ ee for various aryl-substituted styrene's and comparable regioselectivities to (*R*,*S*)-binaphos **a** using their (*R*,*S*)-YanPhos ligand **h**.[13,19] In comparison, AHF with (*S*,*S*,*S*)-diazaphospholane ligand **d** of substituted styrene's gave 95%+ regioselectivity and 70-89% ee for the α-aldehyde under unoptimized conditions (not listed in the table).[25] Hydroformylation of para-substituted styrenes found that the branched selectivity increased towards electron-withdrawing groups (up to 98.5% branched aldehyde). The Hammett plot, where the σ_{para} vs. log(α:β), is linear with a positive slope ($\sigma = +0.56$, $R^2 = 0.93$). These data suggest negative charge build-up in the regioselectivity-determining transition state.

Table 2.2 AHF of substituted styrenes.

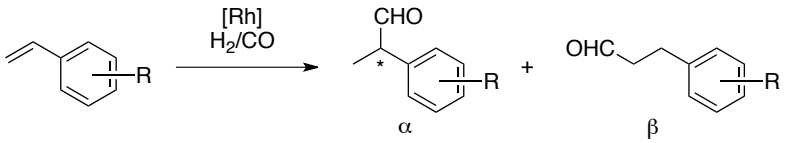

	Substrate	Ligand	Sub/Cat Loading	T (°C)	t (h)	Conv. (%)	α:β	ee (%)
1[a]	4-methylstyrene	**(*S*,*R*)-(a)**	1,000:1	60	20	97	86:14	95 (+)
2[b]		**h**	1,000:1	60	24	98	87:13	99 (*R*)
3[a]	4-isobutylstyrene	**(*S*,*R*)-(a)**	300:1	60	66	99	88:12	92 (*S*)
4[b]		**h**	1,000:1	60	24	98	89:11	98 (*R*)
5[c]	4-methoxystyrene	**c**	1,000:1	20	48	81	99:1	91 (−)
6[b]		**h**	1,000:1	60	24	97	86:14	98 (*R*)
7[a]	4-chlorostyrene	**(*S*,*R*)-(a)**	1,000:1	60	34	99	87:13	93 (+)
8[b]		**h**	1,000:1	60	24	99	87:13	98 (*R*)
9[a]	4-fluorostyrene	**a**	2,000:1	40	39	43	89:11	92 (−)
10[b]		**h**	1,000:1	60	24	99	88:12	98 (*R*)
11[a]	2-fluorostyrene	**a**	2,000:1	40	30	52	91:9	95 (−)
12[b]		**(*S*,*R*)-(h)**	1,000:1	60	24	99	91:9	98 (*R*)
13[a]	2,3,4,5,6-pentafluorostyrene	**a**	1,000:1	35	24	72	96:4	98 (*R*)
14[b]	2-vinylnaphthalene	**a3**	1,000:1	60	4	99	88:12	93 (*R*)
15[d]		**d**	500:1	40	8	99	98:2	94 (*R*)

16[d]	6-methoxy-2-vinylnaphthalene	**d**	500:1	40	8	99	98:2	96 (*R*)

a. 1470 psi H_2/CO (1:1). b. 290 psi H_2/CO (1:1). c. 145 psi H_2/CO (1:0.5). d. 40 psia H_2 and 120 psia CO.

Hydroformylation of *trans*-β-methylstyrene can be accomplished with (*R*,*S*)-Binaphos **a** (Table 2.3, Entry 1) to yield the 97% of the α-aldehyde in 92% ee.[26] AHF of *cis*-β-methylstyrene using (*S*,*S*,*S*)-diazaphospholane ligand **d** resulted in corresponding α- and β-aldehydes with high enantioselectivity: 92% ee and 94% ee, respectively.[25] *Cis*-stilbene, a symmetrical *Z*-alkene, undergoes enantioselective hydroformylation using ligand **d** resulting in one regioisomer in 93% ee.[25] Cyclic aryl *Z*-alkenes such as 1,2-Dihydronaphthalene can undergo hydroformylation yielding 96% of the α-aldehyde in 96% ee with Nozaki's (*R*,*S*)-binaphos **a** ligand.[26] Hydroformylation of indene (not shown), gave 88% ee using (*S*,*R*)-BIPHEMPHOS, a related Binaphos analogue.[16]

Table 2.3 AHF of 1,2-disubstituted styrenes.

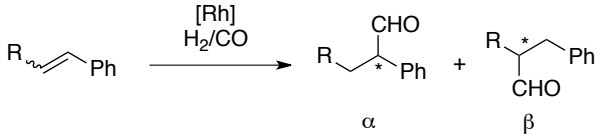

	Substrate	Ligand	Sub/Cat Loading	H_2/CO Pressure	T (°C)	t (h)	Conv. (%)	α:β	ee (%)
1	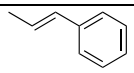	**a**	250:1	1470 psi (1:1)	60	50	10	97:3	92 (*R*)
2	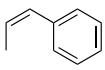	**d**	500:1	150 psia (1:1)	40	24	37	92:8	92 (*R*)/ 94[a]
3	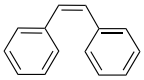	**d**	500:1	70 psia (1:1)	40	24	67	-	93 (*R*)
4	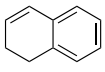	**a**	300:1	1470 psi (1:1)	60	20	79	96:4	96 (−)

a. α-aldehyde/β-aldehyde.

Nozaki and coworkers explored hydroformylation of vinyl-substituted heteroaromatic alkenes with (*R*,*S*)-MeO-Binaphos ligand **a2** (Table 2.4). Hydroformylation of 3-vinylfuran[27] and 3-vinylthiophene[28] resulted in 99% and 91% ee respectively, and in good regioselectivity (92% α-aldehyde for both substrates). 2-vinylthiophene and 4-methyl-2-vinylthiophene also exhibited high enantio- (93% and 99% ee) and regioselectivity (94% and 95% α-aldehyde) in hydroformylation.[28]

Table 2.4 AHF of vinyl heteroaromatic alkenes.

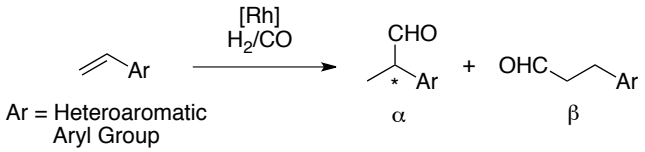

	Substrate	Isolated Yield (%)	α:β	ee (%)
1	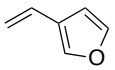	80	92:8	99 (*R*)
2[a]		73[b]	88:12	98 (*R*)
3	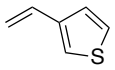	91	92:8	91 (*R*)
4	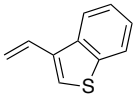	69[b]	-	92 (*R*)
5[c]	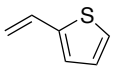	93	94:6	93 (*S*)
6[c]	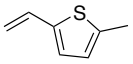	92	95:5	95 (*S*)

Standard reaction conditions: 200:1 substrate:catalyst loading using **a2** ligand at 60°C and 290 psi H_2/CO (1:1) for 6 h reaction time. a. Standard reaction conditions except with (*R*,*S*)-Binaphos **a** ligand. b. NMR yield. c. Standard reaction conditions except 3 h reaction time.

2.2.2 Vinyl Acetate and *N*-Vinyl Carboxamides

Vinyl acetate has been another commonly investigated substrate due to intrinsically high regioselectivity observed in hydroformylation. AHF of vinyl acetate and related protected enols yields α-hydroxyaldehydes that are useful in the organic synthesis. Only a handful of ligand classes have demonstrated highly enantioselective rhodium-catalyzed hydroformylation of vinyl acetate with greater than 90% ee (Table 2.5). Hydroformylation with (*R*,*S*)-binaphos **a** gave the α-aldehyde in 86% regioselectivity and in 92% ee (entry 1).[12] (*S*,*S*,*S*)-Diazaphospholane ligand **d**[17] with $Rh(acac)(CO)_2$ generates a highly active catalyst (TOF 19,400 h^{-1}) in vinyl acetate hydroformylation (entry 2) achieving high conversion (97%), regioselectivity (96%), and stereoselectivity (96% ee).[29] Phosphine-phosphoramidite (*R*,*S*)-YanPhos **h**[13] and related ligand analogues[19] demonstrates high enantioselectivity (entry 3, up to 96% ee) for vinyl acetate at low catalyst loadings (1,000:1 substrate:catalyst loading). Changing the steric bulk at the vinyl carboxylate R-group has a minimal affect on the selectivity of the hydroformylation: AHF of vinyl esters using (*R*,*S*)-YanPhos **h** ligand gave 93—98% ee and 94—96% branched regioselectivity (Table 2.6).[19] Wills and coworkers developed ESPHOS **i** (Table 2.5, entry 4),[30] a diazaphospholidine ligand exhibiting high regioselectivity (94% branched aldehyde) and optical purity for vinyl acetate (90% ee). Xia and Ding has developed C_2-symmetric bisphosphonite ligands and with ligand **j** to exhibit high regio- (98% α-aldehyde) and enantioselectivity (91% ee) in vinyl acetate hydroformylation (entry 5).[31]

Table 2.5 AHF of vinyl acetate.

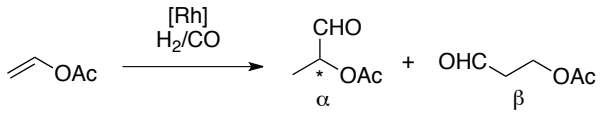

	Ligand	Sub/Cat Loading	H_2/CO Pressure	T (°C)	t (h)	Conv. (%)	α:β	ee (%)
1	**a**	400:1	1470 psi (1:1)	60	36	99	86:14	92 (*S*)
2	**d**	100,000:1	300 psi (1:1)	80	5	97	96:4	96 (*S*)
3	**h**	1,000:1	290 psi (1:1)	60	24	75	93:7	96 (*S*)
4	**i**	200:1	116 psi (1:1)	60	2	80	94:6	90 (*S*)
5	**j**	500:1[a]	726 psi (4:1)	60	2	99	98:2	91 (*S*)

a. Total substrate/catalyst loading with vinyl acetate in a one-pot three-substrate screening.

Table 2.6 AHF of vinyl esters.

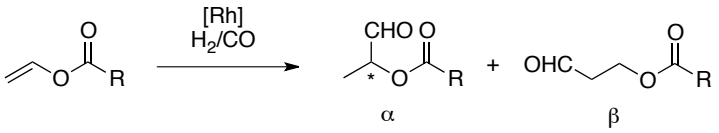

	R	Ligand	t (h)	Conv. (%)	α:β	ee (%)
1	ethyl	**a**	78	99	85:15	90 (*S*)
2		**h**	24	67	96:4	93 (*S*)
3	*n*-propyl	**h**	24	53	94:6	94 (*S*)
5	*t*-butyl	**a**	74	99	88:12	93 (*S*)
6		**h**	24	40	94:6	98 (*S*)
7	*n*-heptyl	**h**	24	56	94:6	94 (*S*)
8	*n*-nonyl	**h**	24	69	94:6	96 (*S*)
9	phenyl	**h**	24	69	96:4	93 (*S*)

a. Reaction conditions: 500:1 substrate:catalyst loading at 60°C and 1450 psi H_2/CO (1:1). b. Reaction conditions: 1,000:1 substrate:catalyst loading at 60°C and 290 psi H_2/CO (1:1).

Thomas, Klosin, and coworkers reported 150—180 gram-scale hydroformylations of vinyl acetate using rhodium-diazaphospholane catalysts, achieving remarkable TONs up to 100,000 and TOFs approaching 20,000 h^{-1}.[29] Both enantiomers of the α-aldehyde aldehyde were distilled in excellent purity [(*S*)-**1**/(*R*)-**1**: 99.3%/99.0% regioselectivity and 96%/94% ee] and used in the synthesis of chiral small molecules (Scheme 2.2). Aminoalcohol, **2** was synthesized from condensation of (*R*)-**1** with hydroxylamine hydrochloride, followed by LAH reduction with no degradation in optical purity (94% ee). Chlorination of aldoxime leads to hydroximoyl

chloride followed by substitution with allylbenzylamine, activation/protection with pentafluorobenzoyl chloride, and a Heck reaction yields a chiral imidazole **3**. Chiral isoxazolines, **4a-c** can be accessed through aldoxime, followed oxidation to the nitrile oxide and by addition of various styrenes (64—65% yield). These sequences demonstrate optically enriched intermediates obtained from hydroformylation can be used for the synthesis of chiral heterocycles without racemization of the stereocenter.

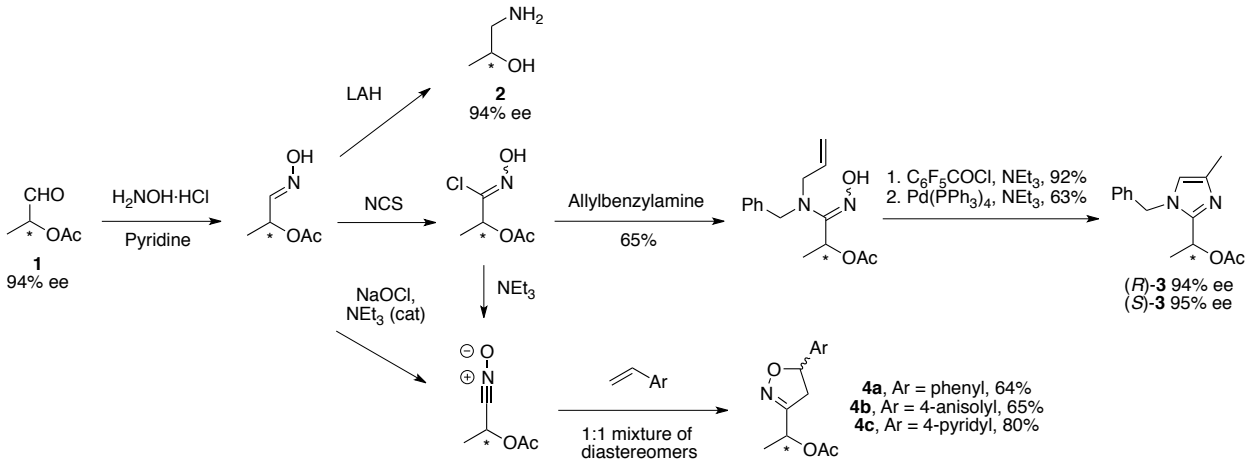

Scheme 2.2 Synthesis of enantioenriched a 1,2-aminoalcohol **2**, an imidazole **3**, and isoxazolines **4a-c** from lactaldehyde **1**.

Recently, Burke and Risi has demonstrated AHF of a 1,2-disubstituted (*Z*)-vinyl ester for the use in the synthesis of (+)-Patulolide C (Scheme 2.3).[32] In a sequential tandem AHF-olefination of a 1,2-disubstituted (*Z*)-vinyl ester **5** (made from a rhodium-catalyzed hydroacetoxylation of (*2R*)-8-nonyn-2-ol) using bisdiazaphospholane **d** yielded an enantiomerically enriched α-hydroxyaldehyde followed by addition of the Bestmann ylide to result in the acetyl-protected (+)-Patulolide C. After acetyl hydrolysis, a total of three short steps were required to complete the synthesis in 49% overall yield from (*2R*)-8-nonyn-2-ol.

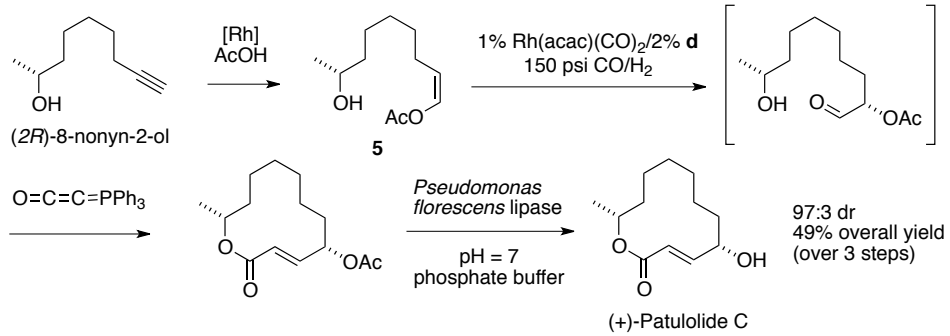

Scheme 2.3 Three-step synthesis of (+)-Patulolide C from AHF of a 1,2-disubstituted (*Z*)-vinyl ester **5**.

Enantioselective hydroformylation of protected *N*-vinyl amides using (*S*,*S*,*S*)-bisdiazaphospholane **d** and $Rh(acac)(CO)_2$ catalyzes the formation of 1,2-aminoaldehydes in quantitative conversion and in high enantioselectivity (90—99% ee; Table 2.7, entries 1-4).[33] Similar to vinyl acetate hydroformylation using (*R*,*S*)-YanPhos **h**,[19] the steric bulk of the protection group on the carboxamide has a minimal effect on the hydroformylation regio- and enantioselectivity with bisdiazaphospholane **d**. Hydroformylation of *cis*-1-acetoamido-1-propene (entry 5), a (*Z*)-1,2-disubstituted alkene (commonly a difficult substrate class in AHF), yields the corresponding 1,2-aminoaldehyde in 90% ee under mild conditions. In comparison with *trans*-1,2-disubstituted alkene, poor regio- (α:β ratio 82:18) and enantioselectivity (32% ee) was observed (not shown). *Z*-alkene stereochemistry is required for high enantioselectivity using a bisdiazaphospholane-ligated catalyst.

Table 2.7 AHF of vinyl amides.

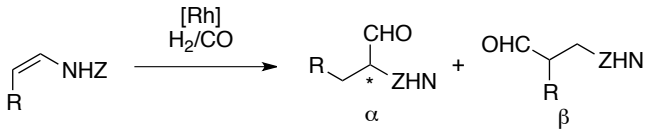

	Z	R	T (°C)	t (h)	Conv. (%)	α:β	ee (%)
1[a]	Phth	H	40	8	99	98:2	95
2[a]	Cbz	H	40	12	99	98:2	94
3[a]	BOC	H	40	12	99	97:3	99
4[a]	TFA	H	40	6	99	98:2	99
5[a]	Ac	Me	70	20	99	97:3	90

a. Reaction was performed using a 200:1 substrate:catalyst loading with (*S*,*S*,*S*)-bisdiazaphospholane **d** at 140 psia of H_2/CO (1:1).

2.2.3 Functionalized Allylic Substrates

Enantioselective hydroformylation of functionalized allylic substrates yields optically active aldehyde intermediates that constitute useful building blocks for organic synthesis. Generally, regioselective control of this substrate class in hydroformylation is a challenge for all ligands due to the lack of a strongly σ-electron-deficient group as with styrene, vinyl acetate, and *N*-vinyl enamides. A particular aim has been hydroformylation of allyl cyanide to yield the corresponding α-aldehyde **6**, a precursor intermediate for drug syntheses (Figure 2.3). For example, 2-methyl-4-aminobutanol **7** (accessed from reduction of formyl and nitrile functionalities in the α-aldehyde from allyl cyanide hydroformylation) has been identified as a key building block[34,35] in the synthesis of two particular pharmacologically-active targets: a

gonadotropin releasing hormone (GnRH) antagonist[36] and a tachykinin NK_1 receptor antagonist.[37,38]

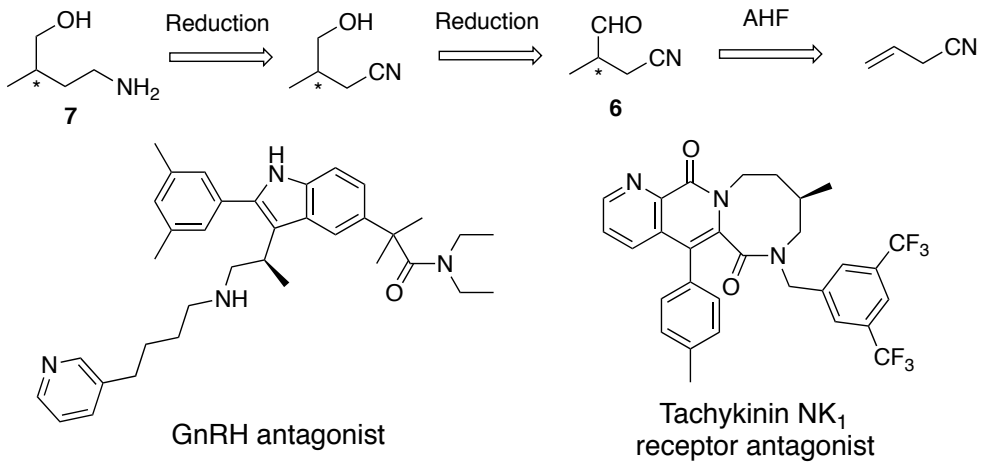

Figure 2.3 Synthetic strategy of 2-methyl-4-aminobutanol **7** from allyl cyanide for the synthesis of pharmacologically active targets.

Several ligands recently demonstrated effective hydroformylation of allyl cyanide in greater than 90% ee. Hydroformylation using (*R*,*R*)-Ph-bpe **e** (Table 2.8, entry 2) at a 5,000:1 total substrate to catalyst loading exhibited 96% conversion and 90% ee. Hydroformylation using Rh(acac)(**f**) (entry 2) provided comparable results: 61% conversion, 88:12 α:β ratio, and 93% ee. Binapine **g**, a bisphosphine containing two 7-member phosphacycle rings (g, entry 3), enables hydroformylation of allyl cyanide in 87% regioselectivity and 94% ee for the α-aldehyde. Using Zhang's phosphine-phosphoramidite ligand, the α-aldehyde can be obtained at 96% ee and complete conversion at 60°C (entry 4).

Table 2.8 AHF of allyl cyanide.

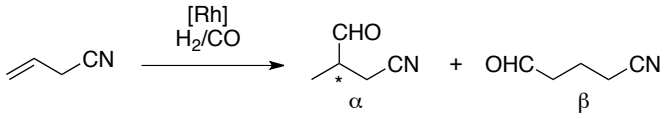

	Ligand/catalyst	Sub/Cat Loading[a]	H_2/CO Pressure	T (°C)	t (h)	Conv. (%)	α:β	ee (%)
1[a]	**e**	5,000:1	150 psi (1:1)	80	3	96	88:12	90 (*R*)
2[a]	Rh(acac)(**f**)	3,000:1	150 psi (1:1)	80	3	61	88:12	93 (*S*)
3[a]	**g**	3,000:1	150 psi (1:1)	80	3	49	87:13	94 (*S*)
4	**h**	1,000:1	290 psi (1:1)	60	18	99	80:20	96 (*R*)

a. Total substrate/catalyst loading with allyl cyanide in a one-pot three-substrate screening.

Zhang and co-workers have investigated the AHF of allyl carbamates, allyl-*N*-benzylamine, allyl sulfonamides, and N-allylphthalimide yielding modest-to-good regioselectivity (Table 2.9, 66—84% for the α-aldehyde) and high enantioselectivity (92—99% ee) in result in chiral β-aminoaldehydes. For comparison, hydroformylation of Cbz-protected allyl amine using (*S*,*S*,*S*)-bisdiazaphospholane (not shown) resulted in 86% ee for the α-aldehyde (82% regioselectivity). Nozaki has demonstrated AHF of a chiral vinyl lactam **8** in high diastereomeric ratios using (*R*)-2-Nap-BINITE-*p*-F ligand **k** (Scheme 2.4).[39] Products **9** and **9-ent** can be viewed as potential intemediates in the synthesis of 1β-methylcarbapenem antibiotics.[40-44]

Table 2.9 AHF of protected allylamines.

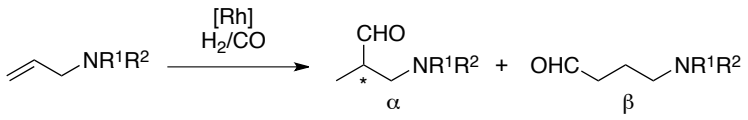

	R^1	R^2	Conv. (%)	α:β	ee (%)
1	Boc	H	99 (97)[b]	66:34 (66:34)[b]	94 (94)[b]
2	Bz	H	99	78:22	95
3	Ts	H	99	67:33	94
4	*p*-NO_2-$C_6H_4SO_2$	H	99	72:28	92
5	*p*-MeO-$C_6H_4SO_2$	H	99	71:29	96
6	Ts	Me	99	67:33	94
7	Boc	Boc	99	72:28	99
8	Phthaloyl		99	84:16	96

a. Reaction performed using a 1,000:1 substrate:catalyst loading using (*R*,*S*)-YanPhos **h** at 60°C and 290 psi H_2/CO (1:1) for 20 h. b. Reaction was conducted with a 10,000:1 substrate:catalyst ratio on a 1.57g (10.0 mmol) scale for 24 h.

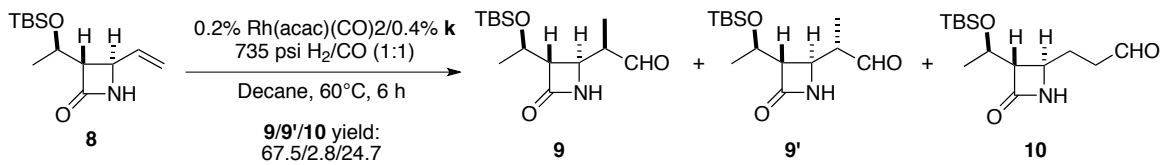

Scheme 2.4 AHF of chiral lactam **8** using (*R*)-2-Nap-BIPNITE-*p*-F ligand **l**.

Specialized approaches such as directing groups and catalytic amounts of scaffolding ligands have been developed to control the regioselectivity of hydroformylation in application to organic synthesis. Breit and co-workers have demonstrated the use of a stoichiometric amount of a covalently bound planar-chiral phosphine that acts as a directing group for use in diastereoselective hydroformylation of 1,1-disubstituted and trisubstituted olefins.[45-49] Similarly with 1,2-disubstituted allylic amines, Tan and co-workers have developed a labile chiral scaffolding ligand[50,51] that is functionalized with a hemiaminal.[52] In the presence of catalytic amounts of *p*-toluenesulfonic acid, PMP-protected allyl amine and ligand **l** equilibrate in benzene to the products favoring the phosphine-tethered alkene (Scheme 2.5, K_{eq} = 3.8 ± 0.5). Hydroformylation of (*Z*)-1,2-disubstituted allylamines using scaffolding-ligand **l** in 15 hours yields the corresponding chiral primary alcohols (after a sodium borohydride reduction of the β-aminoaldehyde) with moderate-to-high enantioselectivities (Table 2.10, 73—93% ee).[52,53] Reduction to alcohols or oxidation to carboxylic acids, are commonly used in the isolation of hydroformylation products. In optimizing the reaction conditions using ligand **l**, 56—72% α-regioselectivity was commonly observed for the substrate in entry 1. High enantioselectivity was predominantly observed with 1,2-disubstituted *Z*-alkenes and less enantioenrichment with analogous *E*-alkenes. Analogous to reports by Breit, Tan's ligand **l** also enables regioselective hydroformylation of 1,1-disubstituted[54] and trisubstituted allyl alcohols[55] using catalytic amounts of an analogous racemic scaffolding ligand.

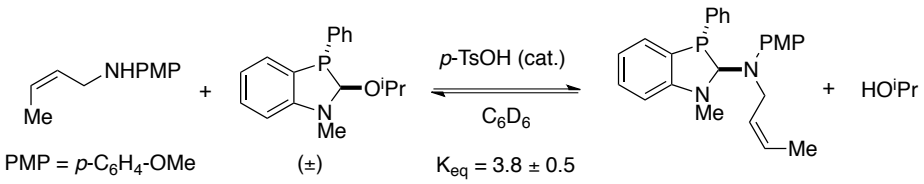

Scheme 2.5 *p*-Toluenesulfonic acid catalyzed equilibration of an allylamine and a scaffolding ligand.

Table 2.10 AHF of 1,2-disubstituted allylamines using Tan's scaffolding ligand **l**.

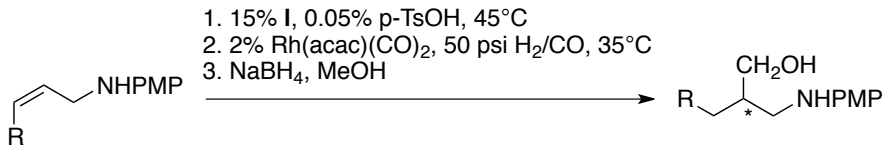

	Substrate	Product	Yield (%)	ee (%)
1[a]	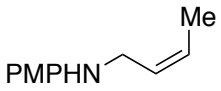	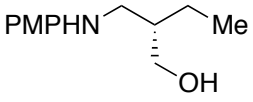	69	92
2[b,c]			61	92
3[d]	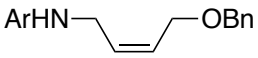	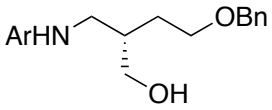	77	91
	Ar = Ph			
4[b]	Ar = *p*-C_6H_4-OMe (PMP)		70	92
5[d]	Ar = *p*-C_6H_4-Me		79	92
6[e]	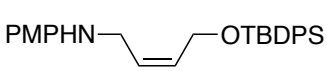	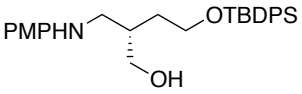	66	90
7[d]	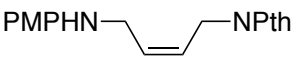	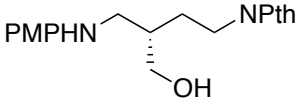	55	93
8[e]	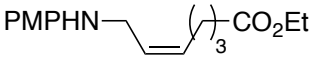	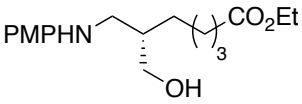	68	90

a. Standard conditions: 1) 15% **l**, 0.05% p-TsOH, 45°C, benzene; 2) 2% Rh(acac)$(CO)_2$, 35°C, 50 psi H_2/CO 15 h; 3) $NaBH_4$, MeOH. b. Standard conditions except 1.75% Rh(acac)$(CO)_2$ and 0.03% p-TsOH. c. Hydroformylation performed with 0.5 g of alkene. d. Standard conditions except 1.75% Rh(acac)$(CO)_2$. e. Standard conditions except 1.5% Rh(acac)$(CO)_2$.

Enantioselective hydroformylation of O-functionalized allylic substrates (Table 2.11) have been demonstrated with (*S*,*S*,*S*)-bisdiazaphospholane **d**[33] and (*R*,*S*)-YanPhos **h**,[56] following Nozaki's unprecedented work using (*R*,*S*)-Binaphos **a** (not shown).[57] Allyl alcohol hydroformylation using (*S*,*S*,*S*)-bisdiazaphospholane **d** yields predominately the achiral linear aldehyde (23% α-aldehyde), although the branched aldehyde was observed in high enantioselectivity (95% ee). In comparison, allyl and silyl/phenyl ethers undergo effective hydroformylation yielding the α-aldehyde in excellent enantioselectivity (92—96% ee) and increased regioselectivity (64—72 α:β). Zhang reported hydroformylation of allyl phenyl ether and allyl acetate using (*R*,*S*)-YanPhos **h** both demonstrating 94% ee. 1,3-alkoxyaldehydes and 1,3-silyloxyaldehydes have been found use in polyketide total synthesis and enantioselective hydroformylation offers an alternative, scalable method in accessing the "Roche aldehyde" from allyl alcohol (Scheme 2.6).[33,58] The existing method in Roche aldehyde synthesis typically involves functional group manipulation of the Roche ester through protection, reduction to the primary alcohol, and oxidation to the aldehyde. Hydroformylation of 1,2-Disubstituted allyl alcohol substrates, TMS-protected Z-crotyl alcohol (74:26 1:2 ratio; 94% ee) and cinnamyl alcohol (<2:98 1:2 ratio; 90% ee) proceeds in reasonable 15 and 16-hour reaction times with (*S*,*S*,*S*)-Bisdiazaphospholane ligand **d**.[33]

Table 2.11 AHF of allyl alcohols and ethers.

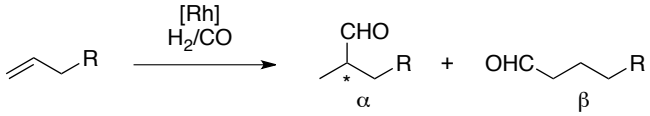

	Substrate	Ligand	Conv. (%)	α:β or 1-formyl:2-formyl	ee (%)
1[a]	R = OH	**d**	99	23:77	95
2[a]	R = OTMS	**d**	99	67:33	97
3[a]	R = OTBS	**d**	99	67:33	96
4[b]		**d**	99	64:36	92
5[c]	R = OAc	**h**	-	30:70	94
6[b]	R = OPh	**d**	99	72:28	96
7[c]		**h**	-	71:29	94
8[d]	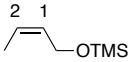	**d**	99	74:26	94
9[e]	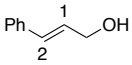	**d**	99	<2:98	90

a. Standard reaction conditions: 200:1 substrate:catalyst loading at 40°C and 140 psig H_2/CO (1:1) for 4 h in toluene. b. Using a 10,000:1 substrate:catalyst ratio, hydroformylation was performed on a 5.17 g (30.0 mmol) scale for 5 h reaction time. c. Reaction conditions and conversion data were not reported. d. Standard conditions except 15 h reaction time. e. Standard conditions except 80°C for 16 h reaction time.

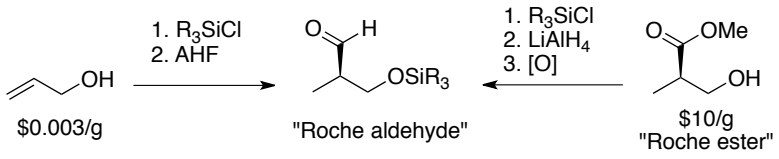

Scheme 2.6 AHF of allyl alcohol as an alternative route to "Roche aldehyde."

Enantioselective hydroformylation of α,β-unsaturated carbonyl substrates is not common because the branched dicarbonyl product can undergo a rapid racemization due to a very acidic enolizable proton. Faraone and co-workers has reported hydroformylation of methyl acrylate using a (-)-menthol derived phosphonite-pyridinyl bidentate ligand, **l**, in 95% conversion and 92% ee to the branched aldehyde (Table 2.12, entry 1).[59] Clarke and co-workers have utilized (*S*,*S*,*S*)-bisdiazaphospholane **d** in the AHF of dialkylacrylamides and observed moderate enantioselectivity (up to 82% ee; not shown).[60] Buchwald and Wang have demonstrated effective AHF of 1,1-disubstituted alkenes (α-alkylacrylates) to yield β-substituted aldehydes in 54-91% isolated yield and in good to excellent enantioselectivity (entries 2-4, 81-94% ee).[61] The α-regioisomer was not observed in appreciable amounts following Keulemans' rule with 1,1-disubstituted alkenes.[62,63] Hydroformylation of α-alkylacrylates provides a synthetic route to 1,4-dicarbonyl structures that are present in pharmacologically active ingredients and biologically relevant molecules (Figure 2.4). Because the hydroformylation products of α,β-unsaturated carbonyls can be sensitive, protected analogues provide increased stability for the corresponding hydroformylation products. AHF of protected acrolein derivatives as a 1,3-dixolane (entry 5) and diacetoxy acetal (entry 7) with bisdiazaphospholane **d** yield modest regio- (81% and 88% α:β ratio) and high enantioselectivity (92% and 93% ee, respectively).[33] Analogously, with 2-methyl-2-vinyl-1,3-dioxolane of methyl vinyl ketone, 70% α-aldehyde and 96% ee was observed (entry 6). Burke and Risi has reported hydroformylation of a vinyl ortho ester (entry 8) with improved

regioselectivity (92% a:b ratio) while maintaining high enantioselectivity (93% ee) using (*R*,*R*,*S*)-**(d)**.[64]

Table 2.12 AHF of acrylates and related analogues.

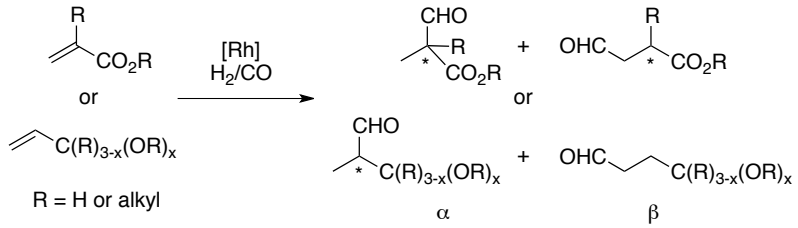

	Substrate	Ligand	Conv. (%)	α:β ratio	ee (%)
1[a]		**m**	95	97:3	92
2[b]	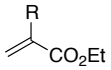 R = ^{i}Pr	**n**	91[c]	only β	92
3[b]	R = C_6H_{11}	**n**	84[c]	only β	94
4[b]	R = C_5H_9	**n**	85[c]	only β	93
5[d]	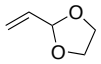	**d**	99	81:19	92
6[d]	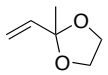	**d**	99	70:30	96
7[e]	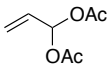	**d**	99	88:12	93
8[f]	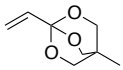	(*R*,*R*,*S*)-**(d)**	100	92:8	93

a. [Rh(CO)(PPh_3)(**m**)]ClO_4 at a 500:1 substrate:catalyst loading, at 60°C and 882 psi H_2/CO (1:1) for 16 h reaction time. b. 1% Rh(acac)$(CO)_2$, 1.2% (*R*,*R*)-BenzP* **n**, 145 psi CO/H_2 (1:5 ratio), for 4—8 h in dodecane. c. Isolated yield. d. 200:1 substrate:catalyst loading at 40°C and 140 psig H_2/CO (1:1) for 4 h in toluene. e. 2,500:1 substrate:catalyst loading at 40°C and 140 psig H_2/CO (1:1) for 18 h on a 1 g (6.3 mmols) scale. Product contained ~25% 1,3-diacetoxy-2-methylprop-1-ene. f. 200:1 substrate:catalyst loading at 40°C, 120 psi CO, and 40 psi H_2.

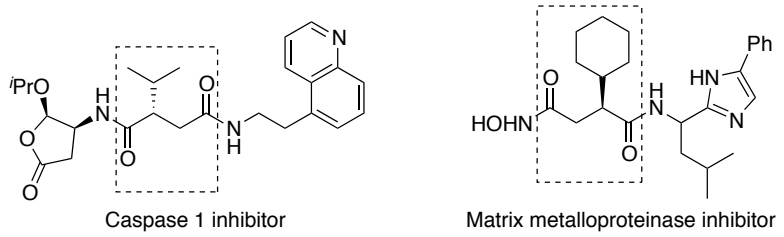

Figure 2.4 Examples of biologically relevant molecules with 1,4-dicarbonyl structures.

Burke and Risi have highlighted the use hydroformylation of a vinyl orthoester in the synthesis of the Prelog-Djerassi Lactone (Scheme 2.7).[64] Using a sequential tandem protocol, AHF of a vinyl orthoester **11** yielded the corresponding branched aldehyde followed by a crotylation to yield a homoallylic alcohol in good yield (83% isolated yield) and favorable diastereoselectivity (>95:5) using bisdiazaphospholane (*R*,*R*,*S*)-**(d)**. This tandem sequence established three stereocenters out of four in route towards their synthetic goal. The homoallylic alcohol was further elaborated through ozonolysis, Wittig olefination, and an asymmetric hydrogenation towards the target Prelog-Djerassi lactone. After deprotection and esterification, the synthesis of Prelog-Djerassi lactone was achieved in a 57% overall yield.

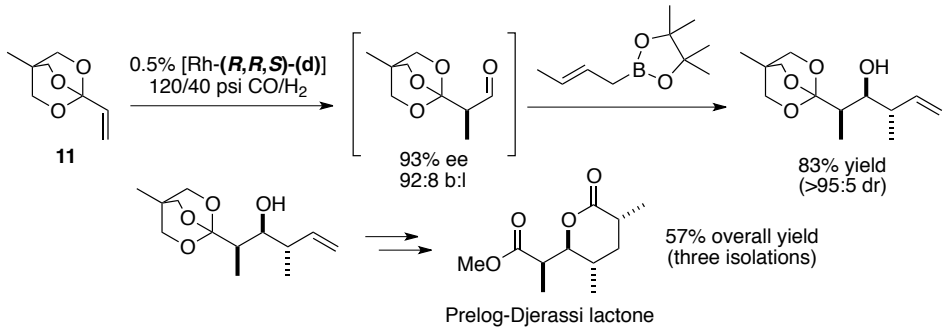

Scheme 2.7 AHF of a vinyl orthoester **11** and use in the synthesis of Prelog-Djerassi lactone.

2.2.4 Heterocycles

Chiral heterocycles such as pyrrolidines and tetrahydropyrans are common structural motifs in natural products. Hydroformylation of 2,3-dihydropyrrole can be performed to obtain the α-formyl product, a intermediate to proline, in 97% ee for both (*R*,*S*)-binaphos **a**[65] and (*S*,*S*,*S*)-Bisdiazaphos **d**[33] ligands (Table 2.13, entries 1 and 2). Conversely, the β-formyl isomer (intermediate to the β-aminoacid) can be accessible from hydroformylation of 2,5-dihydropyrrole using ligand **d** yielding 94% regioselectivity and 91% ee (entry 3).[33] Reek and co-workers analogously accomplished hydroformylation on 2,5-dihydrofuran using a phosphine-phosphite ligand **o**, to only give the corresponding β-formyl regioisomer in 90% ee (entry 5).[66,67] Interestingly, rhodium-catalyzed isomerization-hydroformylation can be accomplished with ligand **o**, on 2,3-dihydrofuran to give the β-formyl aldehyde in high enantioselectivity (91% ee) in low conversion. Hydroformylation of 2,3-dihydrofuran using bisdiazaphospholane ligands **d3** and **d4**, yields the α-formyl product (78-79% regioselectivity and 90% ee) while the 2,5-dihydrofuran preferentially gives the β-formyl product (97% regioselectivity and 95% ee for both ligands).[68] Burke and Clemens have reported the hydroformylation of an oxazolidine to produce the synthetically useful Garner's aldehyde in high regio- (95%) and enantioselectivity (97%) using bisdiazaphospholane **d**.[69]

Table 2.13 AHF of heterocycles.

	Substrate	Ligand	H_2/CO Pressure	T (°C)	t (h)	Conv. (%)	α-formyl: β-formyl	ee (%) major isomer
1[a]	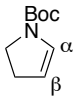	**a**	1470 psi (1:1)	60	72	99	67:33	97
2[a]		**d**	140 psig (1:1)	60	15	99	91:9	97
3[a]	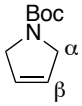	**d**	140 psig (1:1)	60	18	99	6:94	91
4[a]		**o**	363 psi (1:1)	25	40	5	20:80	91
5[b]		**d3**	150 psig (1:1)	30	18	45	79:21	90
6[b]		**d4**	150 psig (1:1)	40	4	27	78:22	90
7[a]		**o**	290 psi (1:1)	45	48	97	0:100	90
8[b]		**d3**	150 psig (1:1)	40	4	94	<3:97	95
9[b]		**d4**	150 psig (1:1)	40	4	92	<3:97	95
10[c]		**d**	140 psi (1:1)	55	72	70[d]	95:5	97

a. Standard reaction conditions: 200:1 substrate:catalyst loading. b. Reaction performed using a 670:1 substrate:catalyst loading. c. Reaction conducted using 2.0% $Rh(acac)(CO)_2$ and 2.5% ligand **d**. d. Isolated yield.

2.2.5 1,3-dienes

Hydroformylation of 1,3-dienes provides access to β,γ-unsaturated chiral aldehydes—intermediates that have been found to be useful in polyketide synthesis. For example, Jacobsen and Lui demonstrated the use of hydroformylation of 1,3-diene **12** with ligand (*S*,*R*)-Binaphos **a** to set a stereocenter at C15 in the total synthesis of (+)-Ambruticin (Figure 2.5).[70] Similarly, Smith and coworkers have demonstrated the use of both enantiomers of Binaphos **a** in the AHF of a model diene **13** (Table 2.14; 93:7 er or better) and **14** leading to a C1-C12 fragment of Tedanolide C (Scheme 2.8) in excellent diastereoselectivity (>95:5).[71]

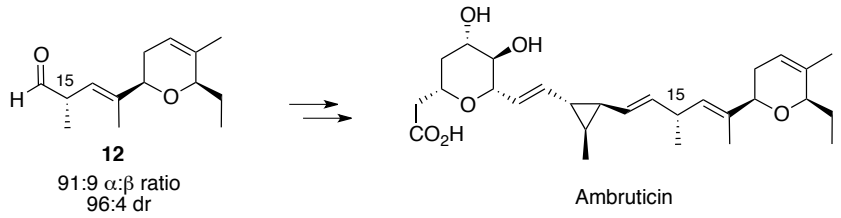

Figure 2.5 Synthesis of Ambruticin from hydroformylation of 1,3-diene **12**.

Table 2.14 AHF of a model 1,3-diene **13**.

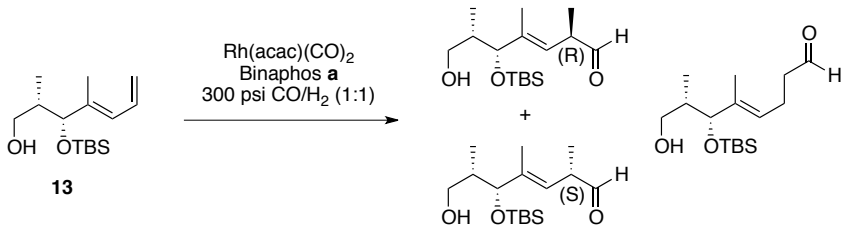

	Ligand	T (°C)	t (h)	conv.	b:l ratio	er
1	(*R*,*S*)-**a**	35	113	100	96:4	93:7
2	(*S*,*R*)-**a**	35	113	100	92:8	6:94

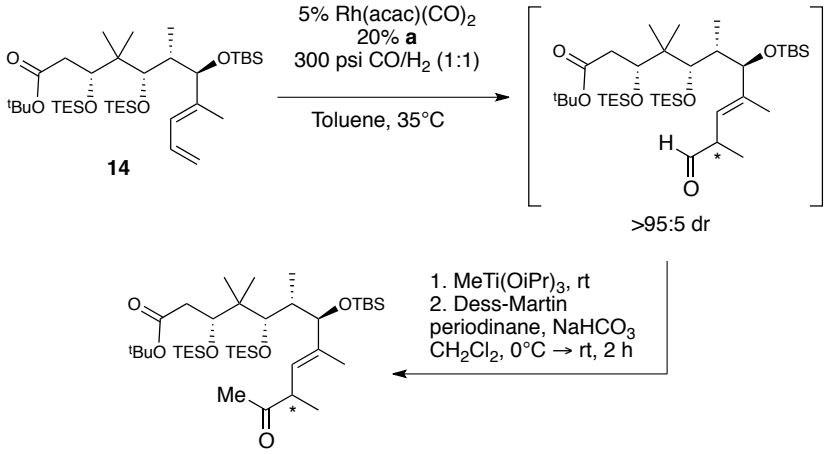

Scheme 2.8 AHF of 1,3-diene **14** leading to a C1-C12 fragment of Tedanolide C.

Hydroformylation of 1,3-butadienes potentially results in various regioisomers: 1-formyl, 2-formyl, and 4-formyl products (see equation in Table 2.15 for product numbering scheme), and products from alkene isomerization. With Nozaki's (*R*,*S*)-Binaphos **a**[72] and (*S*,*S*,*S*)-Bisdiazaphospholane **d**[73] ligand, hydroformylation of (*E*)-1-phenyl-1,3-butadiene yields the 2-formyl product in high regio- (entries 1 and 2; 92% and 99%, respectively) and enantioselectivity (90% and 91% ee). Similarly, AHF of (*E*)-1-(2-furyl)-1,3-butadiene using (*S*,*S*,*S*)-Bisdiazaphospholane **d** enables selective formation of the 2-formyl product in 99% regioselectivity and 97% ee (entry 3). (*E*)-1-methoxy-1,3-butadiene (entry 4), (*E*)-1-acetyloxy-1,3-butadiene (entry 5), and (*E*)-1-triisopropylsilyloxy-1,3-butadiene (entry 6) undergoes effective hydroformylation with high enantioselectivity (94%, 91%, and 90%, respectively for the (*E*)-β,γ-unsaturated aldehyde). Interestingly, hydroformylation of the other geomeric isomer ((*Z*)-1-triisopropylsilyloxy-1,3-butadiene, Scheme 2.9), results in the opposite absolute stereoisomer configurations (in 70% ee) using the same enantiomer of the ligand. For this reason, geometrically pure samples of (3*E*)-1,3-diene are required to achieve highly enantioenriched samples.

Table 2.15 AHF of 1,3-dienes.

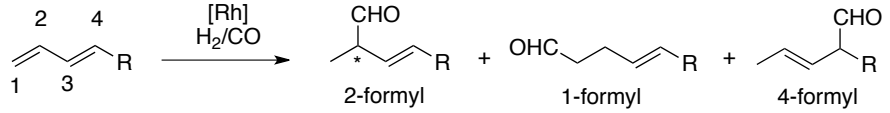

	2-formyl	%	other	%	L	t (h)	Conv. (%)	*E*:*Z*	ee (%)
1[a]	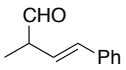	92	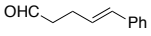	5	**a**	24	88	-	90(*E*)
2		99			**d**	4	99	>99:1	91(*E*)
3	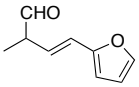	99			**d**	4	99	>99:1	97(*E*)
4	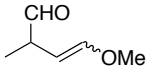	99			**d**	4	99	50:50	94(*E*) 67(*Z*)
5	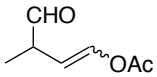	60	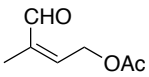	40	**d**	1.5	99	50:50	91(*E*) 88(*Z*)
6	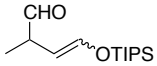	99			**d**	4	99	71:29	90(*E*)
7	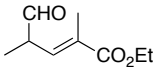	95	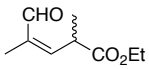	5	**d**	1.5	99	>99:1	91(*E*)
8[b]	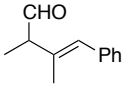	88	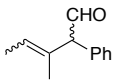	12	(*R*,*R*,*S*)-**(d)**	4	99	>99:1	93(*E*)
9[b]	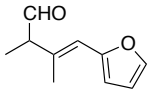	98	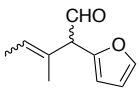	2	(*R*,*R*,*S*)-**(d)**	4	99	>99:1	93(*E*)
10[c]		86		14	**a**	18	85	-	96(*E*)
11[b]		88	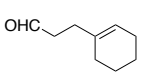	12	(*R*,*R*,*S*)-**(d)**	4	99	>99:1	92(*E*)
12	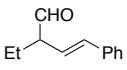	99			(*R*,*R*)-**(d2)**	12	99	>99:1	91(*E*)

Standard reaction conditions: 200:1 substrate:catalyst loading using 150 psi H_2/CO (1:1) at 40°C. a. Standard reaction conditions except using 588 psi H_2/CO (1:1) at 30°C. b. Standard reaction conditions except using 40 psi H_2 and 120 psi CO. c. Standard reaction conditions except using 1470 psi H_2/CO (1:1) at 60°C.

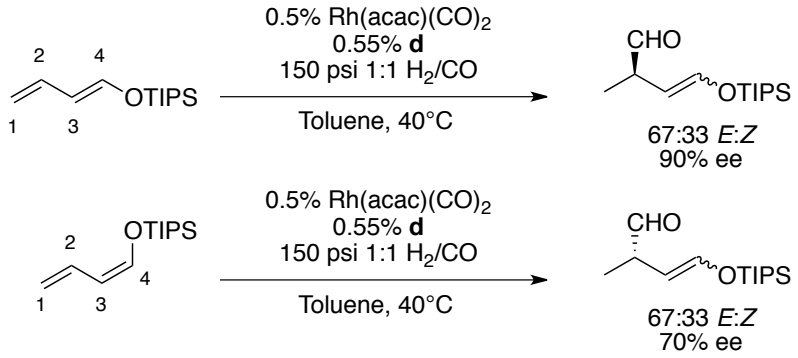

Scheme 2.9 Stereochemical outcomes in the AHF of (*E*)- and (Z)-isomers of 1-trisisopropylsilyoxy-1,3-diene.

Enantioselective hydroformylation of (*E*)-1-carboethoxy-1,3-butadiene (Table 2.15, entry 7, 91% ee) with (*S*,*S*,*S*)-bisdiazaphospholane **d**,[73] offers a shorter synthetic route to the same aldehyde intermediate used in total synthesis of Iejimalide B[74] (Figure 2.6). Fürstner and co-workers employed six steps to synthesize β,γ-unsaturated aldehyde from the Roche ester while in comparison, the same intermediate can be accessed from an achiral 1,3-diene in one step. Hydroformylation of 1,3-dienes with a methyl-substitution at position C2 (entry 8 and 9) with a higher CO pressure and the (*R*,*R*,*S*)-**(d)** ligand diastereomer, results in 88% and 98% regioselectivity respectively, for the desired β,γ-unsaturated aldehyde in 93% ee (for both substrates). 1-Vinyl-cyclohex-1-ene hydroformylation with ligands **a** or **d** affords ratios of 86% and 88% for the 2-formyl product, in 96% ee and 92% ee (entries 10 and 11), respectively.

Selective hydroformylation can be accomplished on two geometrically differentiated double bonds in a 1,3-diene with rhodium-bisdiazaphospholane catalysts. With a sample of (1*E*,3*Z*)-1-phenyl-1,3-pentadiene (entry 12), hydroformylation occurs at the *Z*-alkene instead of an adjacent *E*-alkene, to produce the desired 2-formyl product in 99% regioselectivity and 91% ee, with an ethyl branching substituent.

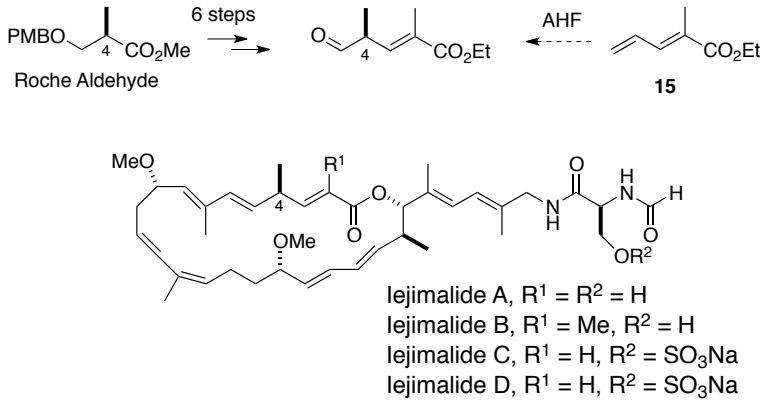

Figure 2.6 AHF of a 1,3-diene **15** as an alternative route to an intermediate in the synthesis of lejimalides.

AHF of (*E*)-1-trisisopropylsilyloxy-1,3-diene using ligand bisdiazaphospholane **d** results in a 67:33 *E*:*Z* mixture of 2-formyl isomers, with the (3*E*)-2-formyl product in 90% ee. In contrast, (*Z*)-1-trisisopropylsilyloxy-1,3-diene hydroformylates in 70% ee with the predominant product in the opposite sense of chirality. At partial conversion there is no change in the *E*:*Z* ratios and suggest that the isomerization occurs "on" cycle during catalysis. The proposed mechanism of (*E*)-1,3-diene hydroformylation involves insertion of the terminal alkene into a [Rh]-H to yield both π-[Rh]-allyls and σ-[Rh]-alkyls (Scheme 2.10; left portion) during the catalysis, and through a C-C bond rotation, leads to form the other 2-formyl geometric isomer.

Analogously in hydroformylation of (*Z*)-1,3-diene, produces the opposite 2-formyl enantiomer for both geometric isomers operative through the similar intermediates.

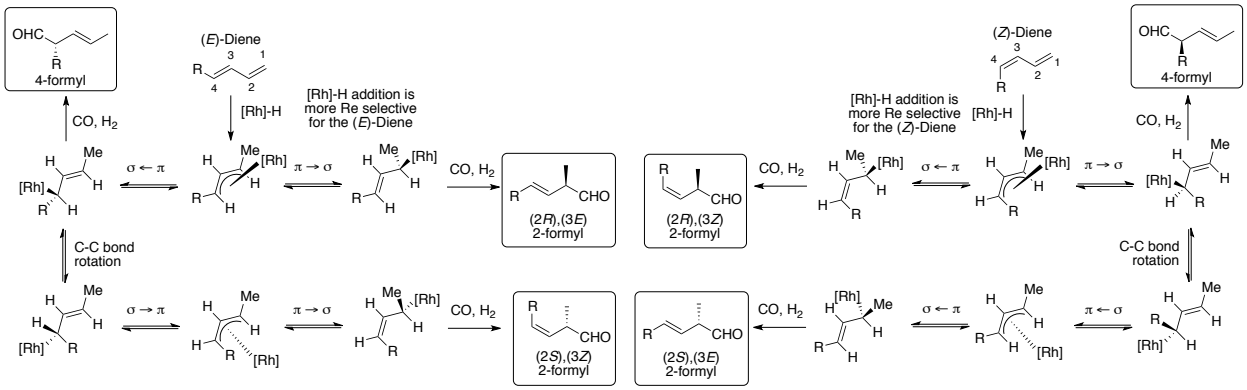

Scheme 2.10 Proposed mechanism for Rh-catalyzed AHF of 1,3-dienes using ligand **d**.

2.2.6 Alkyl Alkenes

Hydroformylation of alkyl alkenes, such as 1-hexene or 1-octene, has been mainly aimed at optimizing linear aldehyde formation; whereas, enantioselective hydroformylation of these substrates has been sparsely demonstrated due to low observed selectivities for the branched aldehyde. Nozaki has accomplished AHF of various aliphatic alkenes with (*R*,*S*)-Binaphos **a** and related ligands with varying levels of enantioselectivity (75—90% ee).[75] Hydroformylation of 1-hexene with (*R*,*S*)-MeO-Binaphos **a2** exhibits 90% ee for the α-aldehyde in 30% regioselectivity (Table 2.16, entry 1).[16] Comparatively Clarke and Cobley has used (S_{ax},*S*,*S*)-Bobphos **n** in the hydroformylation of 1-hexene with improved selectivity: 75% branched regioselectivity and 93% ee (entry 2).[76] AHF of 4,4-dimethyl-pentene using (*R*,*S*)-Binaphos **a** results in 94% conversion, 43% regioselectivity and 92% ee for the branched aldehyde (entry 3).[75] Changing to a trityl substituent result in higher regio- (entry 4, 60%) and in superior enantioselectivity (99% ee). The Zhang group has used (*R*,*S*)-YanPhos **h** in the hydroformylation of allyltrimethylsilane and

allylbenzene (entries 5 and 6, respectively) to give 72% and 42% regioselectivity respectively for the α-aldehyde, and in 94% ee (both substrates).[56] Clarke and Cobley reported use of (S_{ax},*S*,*S*)-Bobphos **p** in AHF of allyl benzene (entry 7) and related analogues (entries 8 and 9) in higher branch selectivity (75-86%) and at 90-92% enantioselectivity at 16°C.[76]

Table 2.16 AHF of allyl alkenes.

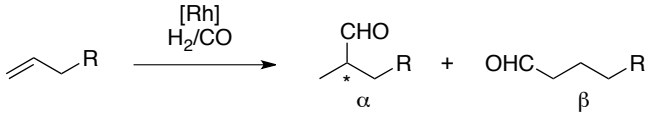

	Substrate	Ligand	H_2/CO Pressure	T (°C)	t (h)	Conv. (%)	α:β	ee (%)
1[a]	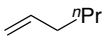	**a2**	1470 psi (1:1)	30	40	66	30:70	90 (*R*)
2[b]		**p**	72 psi (1:1)	16	46	78	75:25	93
3[c]	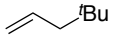	**a**	1470 psi (1:1)	50	87	94	43:57	92 (−)
4[b]	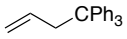	**a**	1470 psi (1:1)	50	20	99	60:40	99 (+)
5[d]	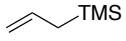	**h**	-	-	-	-	72:28	94
6[d]	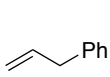	**h**	-	-	-	-	42:58	94
7[b]		**p**	72 psi (1:1)	16	72	64	80:20	90
8[b]	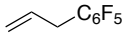	**p**	72 psi (1:1)	16	21	81	86:14	91
9[b]	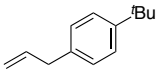	**p**	72 psi (1:1)	16	66	99	75:25	92
10[b]	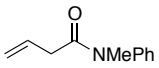	**p**	72 psi (1:1)	16	29	72	82:18	92

a. Reaction was conducted at a 2000:1 substrate:catalyst loading. b. Reaction was conducted with a 250:1 substrate:catalyst loading. c. Reaction was performed with a 500:1 substrate:catalyst loading. d. Reaction conditions and conversion data were not reported.

Nozaki has demonstrated hydroformylation of 3,3,3-trifluoropropene, with (*R*,*S*)-Binaphos ligand **a**, giving the α-aldehyde in 95% regioselectivity and 93% ee (Scheme 2.11).[15] Olefins containing a strongly σ-electron deficient substituent, a trifluoromethyl (-*C*F_3) in this example, to exhibit a large preference for the desired α-aldehyde in hydroformylation—consistent with observed regioselectivity seen with vinyl acetate and *N*-vinyl amides.

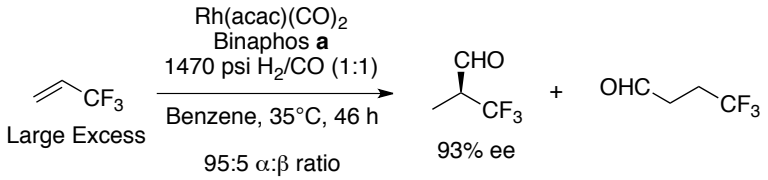

Scheme 2.11 AHF of 3,3,3-trifluoropropene.

Huang, Bunel, and coworkers have accomplished enantioselective rhodium-catalyzed hydroformylation of norbornenes using (*R*,*R*,*S*,*S*)-TangPhos **f**. Effective hydroformylation norbornene at a substrate-to-catalyst loading of 200:1, can be accomplished to yield quantitative conversion for the *exo*-product at 92% ee (Table 2.17, entry 1). This particular reaction can be scaled to 750-grams with the same results. (*R*)-*exo*-norbornylamine **16** can be synthesized in 71% overall yield over five steps from norbornene without degradation of optical purity (Scheme 2.12). Other [2.2.1]-bicyclic olefins, such as aryl substituted and functionalized as an anhydride, undergo hydroformylation to yield high enantioselectivity for the desymmetrized product (entries 2 and 3, 92% and 93% ee, respectively). Interestingly, the *exo*-substituted anhydride gives a mixture of *exo*- and *endo*-aldehydes in high enantioselectivity (*endo*-substituted anhydride resulted in solely the *exo*-aldehyde product). Hydroformylation of structurally analogous *meso*-

Bicyclic hydrazines (not shown) using tangphos **f** yielded low-to-modest enantioselectivities (13-78% ee at high conversion).

Table 2.17 AHF of bicyclic alkenes.

	Substrate	Product	Conv. (%)	ee (%)
1[a]		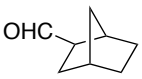	99	92
2[b]			99	92
3[a]	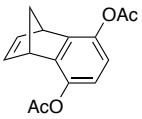	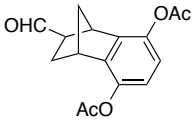	99	92
4[a]	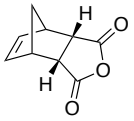	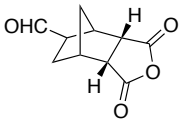	99	93
5[c]	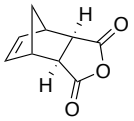	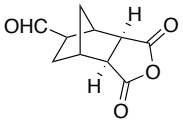	99 (25/75)[d]	92/91

Standard reaction conditions: 200:1 substrate:catalyst loading using $Rh(acac)(CO)_2$ and (*R*,*R*,*S*,*S*)-TangPhos **f**. a. 120 psi H_2/CO (1:1) at room temperature. b. Reaction conducted on 750 g of norbornene using 60 psi H_2/CO (1:1). c. 500 psi H_2/CO (1:1) at 60°C. d. Exo and endo assignments were arbitrary assigned by the authors from GC analysis.

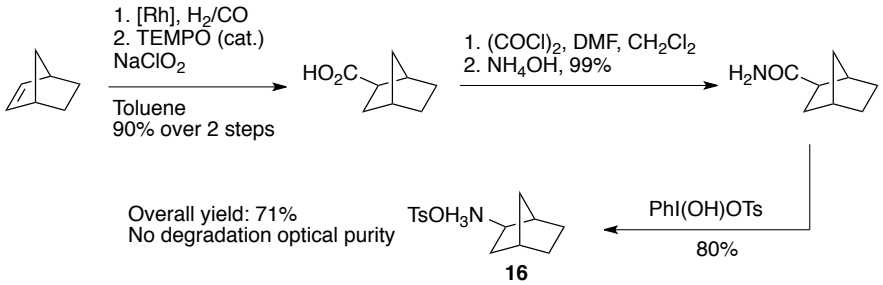

Scheme 2.12 Synthesis of (*R*)-*exo*-norbornylamine **16**.

2.3 Hydroformylation of Styrene Mechanism with Diazaphospholane Ligands

In the generally accepted mechanism of rhodium-catalyzed hydroformylation (Scheme 2.13) established by Heck and Breslow, the product regio- and stereoselectivity may be set in one of four stages: (1) irreversible alkene coordination to rhodium, (2) reversible alkene coordination followed by irreversible rhodium hydride addition, (3) reversible rhodium hydride addition followed by irreversible alkyl migratory insertion to the rhodium acyl intermediate, or (4) reversible acyl formation followed by irreversible rhodium acyl hydrogenolysis. Recently, Landis and Watkins have developed a kinetic model that extends this mechanism that accounts for the diastereomeric pathways leading to the two branched aldehyde enantiomers and linear aldehyde in AHF of styrene using diazaphospholane ligands.

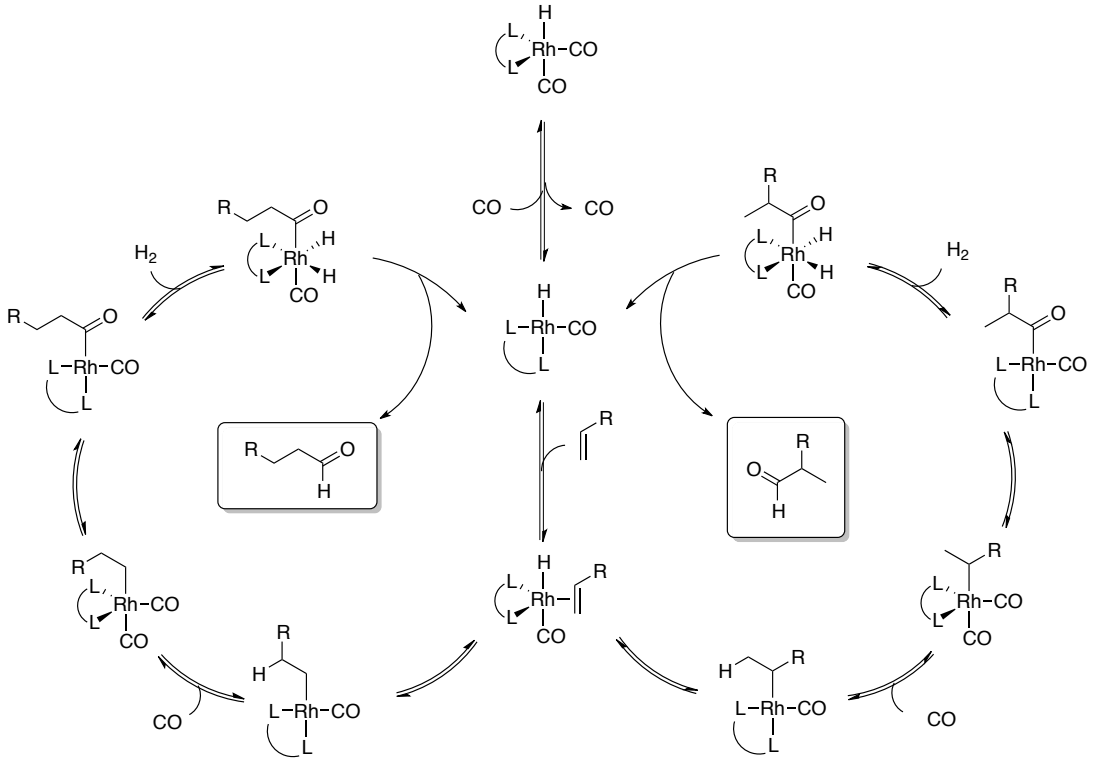

Scheme 2.13 Mechanism of rhodium-catalyzed hydroformylation of alkenes.

To account diastereomeric pathways in AHF, three fundamental investigations was used in the development of an extended mechanism: (1) deuterioformylation to explore the extent of the reversibility of alkene insertion into the rhodium-deuteride, (2) the affect of CO and H_2 pressures on the relative rates of formation for the three aldehyde products (both branched aldehyde enantiomers and the linear aldehyde), and (3) investigation into the origin of the linear aldehyde selectivity from *re* or *si* faces of styrene.

Enantioselective hydroformylation of styrene using rhodium-bisdiazaphospholane catalysts exhibits interesting carbon monoxide pressure dependence: at higher CO pressure, higher branched-to-linear aldehyde ratios and higher enantioselectivity was observed.[17] These observations prompted further attention to investigate the origin of regio- and enantioselectivity in AHF starting by determining the extent of reversibility of the styrene insertion into the

rhodium-hydride bond. Deuteroformylation experiments were performed on styrene hydroformylation to determine the extent of the labeling that gets incorporated into products. If the rhodium-alkyl formation was irreversible, the aldehyde products should contain deuterium in the formyl group and β to the carbonyl group (Scheme 2.14). If olefin insertion into Rh-D was reversible, the incorporation of deuterium would be observed in vinyl-resonances of styrene (through β-hydride elimination from the rhodium-alkyl) and the aldehyde products would contain less than two equivalence deuterium by NMR integrations.

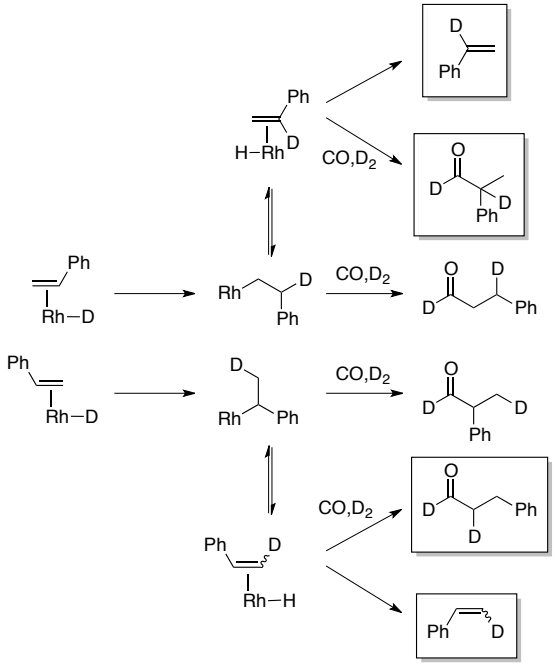

Scheme 2.14 Products expected from deutrioformylation of styrene.

Deuteroformylation of styrene at 80°C at low conversion (88.6% unconverted styrene), yield products with varying levels of deuterium incorporation observed by ^{1}H and ^{2}H NMR spectroscopy (Figure 2.7). Aldehyde products I—IV contain 100% deuterium incorporation in the formyl group and about 20% deuterium was found in the β position (II and III versus VII and VIII). Of the styrene observed, 5.9% was found to contain deuterium incorporation in the β-

position due to reversible olefin insertion into the rhodium-deuteride and β-Hydride elimination to yield β-labeled styrene (VI) (Scheme 2.15). This process was found to be approximately 7 times faster than the competitive reaction of alkyl migratory insertion to rhodium acyls, leading to the corresponding branched aldehyde (51.2% VI versus 7.2% III). Conversely, only trace amounts (<1%) of α-labeled styrene (V) were observed that would result from β-hydride elimination from the linear Rh-alkyl. In comparison to branched Rh-alkyls, the linear Rh-alkyls appears to be much more likely to undergo a migratory insert to form linear rhodium acyls. Most of the aldehydes formed in deuterioformylation contain only one deuterium found in the formyl group. In contrast, the β-position of these aldehyde products was found to be mostly protio (80% (VII + VIII)), and this observation implies a higher steady state concentration of Rh-H species over the Rh-D (approximately 4-fold). Hydrogenolysis with D_2 produces rhodium-deuterides but undergoes a rapid exchange with all protio-styrene to generate rhodium-hydrides along with the observed β-deuteriostyrene.

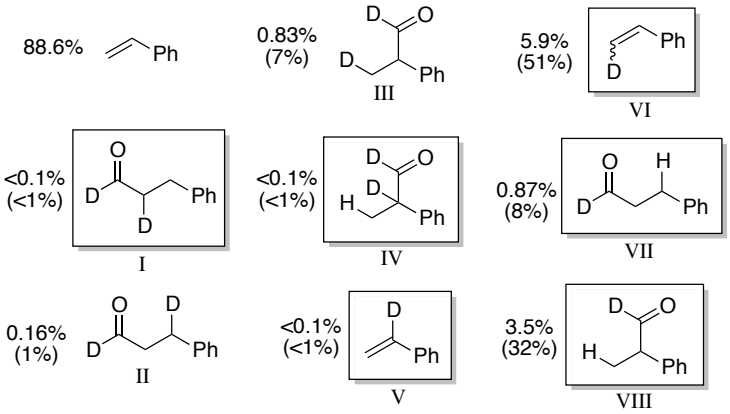

Figure 2.7 Product distribution observed in the deuterioformylation of styrene.

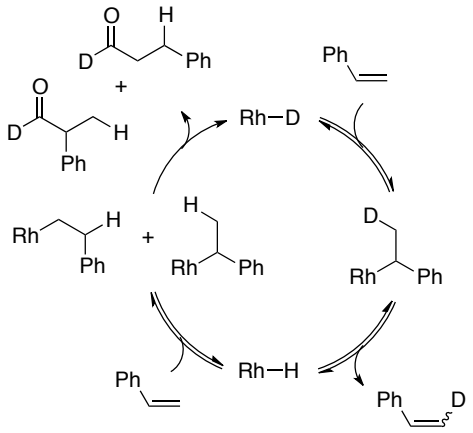

Scheme 2.15 Mechanistic pathways in which β-d_1-styrene and d_1-aldehydes are produced.

Pressure studies by varying the CO and H_2 partial pressure have demonstrated an interesting effect on the regio- and enantioselectivity in styrene hydroformylation using rhodium catalysts bearing (*S*,*S*,*S*)-bisdiazaphospholane **d** ligand. Performing hydroformylations at 80°C and increasing CO pressures (15—200 psi), while holding dihydrogen pressure constant (40 psi), resulted in increasing levels of b:l (branched:linear) and enantiomeric ratios (Figure 2.8). Interestingly only conjugated alkenes (styrenes and 1,3-dienes) have been demonstrated to exhibit these pressure effects in optimizing desirable regio- and enantioselectivity. In comparison, hold the carbon monoxide pressure constant at 40 psi and varying dihydrogen pressures (15—160 psi), neither regioselectivity and enantioselectivity varied substantially. From these data, the regio- and enantioselectivity of styrene hydroformylation are likely set before the rhodium acyl hydrogenolysis step.

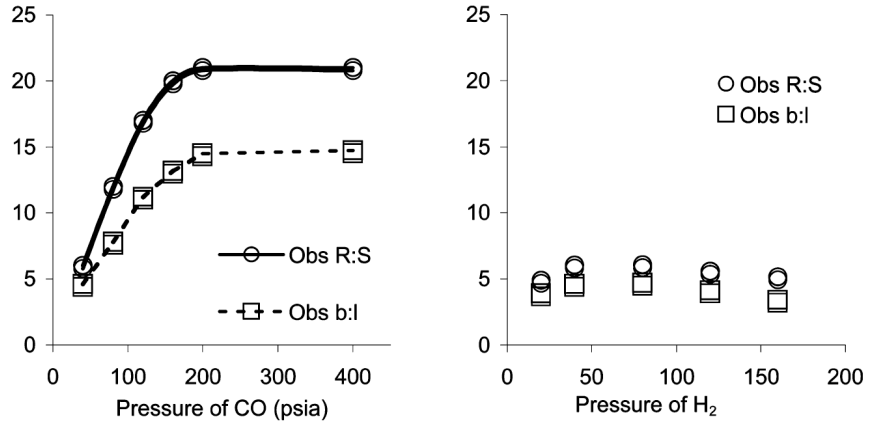

Figure 2.8 Plots depicting the influence of carbon monoxide and dihydrogen pressure on regioselectivity (branched:linear) and stereoselectivity [(*R*)-enantiomer:(*S*)-enantiomer] ratios in Rh-catalyzed hydroformylation of styrene using bisdiazaphos **d** (from reference 10).

Hydroformylation of α-deuteriostyrene demonstrates the preference of *re* and *si* faces of the alkene towards aldehyde products depending on the facial selectivity of the (*S*,*S*,*S*)-**d**-rhodium catalysts (Scheme 2.16). Under the conditions evaluated, the addition of the rhodium hydride to the *re* face of coordinated styrene predominantly leads to the formation of the major aldehyde product (*R*)-**17** in 67% stereoselectivity. The minor aldehyde enantiomer, (*S*)-**17**, can be obtained from binding of the *si* face styrene to rhodium catalysts. The formation of the linear aldehyde, 3-phenylpropanal (**18**) is largely the result from binding of the *si* face of styrene (16%) to rhodium. The linear aldehyde is accessible from the *re* face but to a lesser extent (3%).

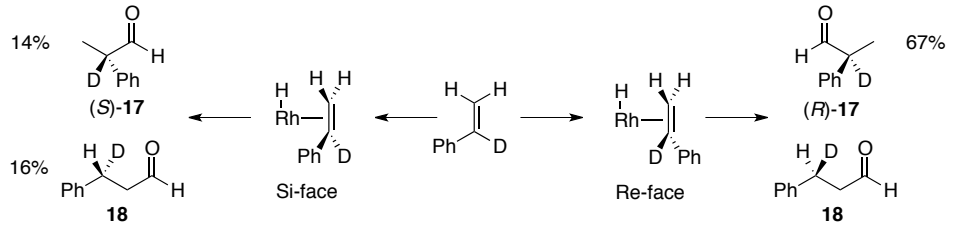

Scheme 2.16 Stereochemical outcome of AHF of α-d_1-styrene.

A proposed mechanistic model (Scheme 2.17) was developed from these investigations to account for the diastereomeric pathways not originally presented in Heck and Breslow's mechanism in the enantioselective hydroformylation of styrene by rhodium-bisdiazaphospholane catalysts. Starting from the 18 e^- complex **A**, loss of CO leads to the proposed active catalyst **B**. Styrene coordination to **B** leads to two diastereomeric styrene intermediates **C**(*R*) and **C**(*S*). From **C**(*S*) where styrene is coordinated at the *si* face, generates the linear rhodium alkyl (Dl) or the branched rhodium alkyl (**Db**(*S*)). These two pathways are irreversible in the rhodium-hydride addition eventually leading to the linear aldehyde and the minor branched aldehyde enantiomer. The other diastereomer, **C**(*R*), where the styrene is coordinated at the *re* face, can proceed irreversibly to the linear aldehyde through intermediate **Dl** or reversibly to the other branched rhodium alkyl (**Db**(*R*)). The reversibility of **C**(*R*) to (**Db**(*R*)) depends on the CO pressure, where the branched rhodium-alkyl intermediate can undergo β-hydride elimination proceeding to the styrene coordinated complex. At the higher-pressure limit of CO, intermediate (**Db**(*R*)) can be trapped so that migratory insertion to rhodium acyl is faster than β-hydride elimination. At low pressures of CO, β-hydride elimination is faster than migratory insertion to the corresponding rhodium acyl intermediate. The mechanism of styrene hydroformylation and these pressure dependent variables can be best visualized from depictions of hypothetical free energy reaction coordinate diagrams.

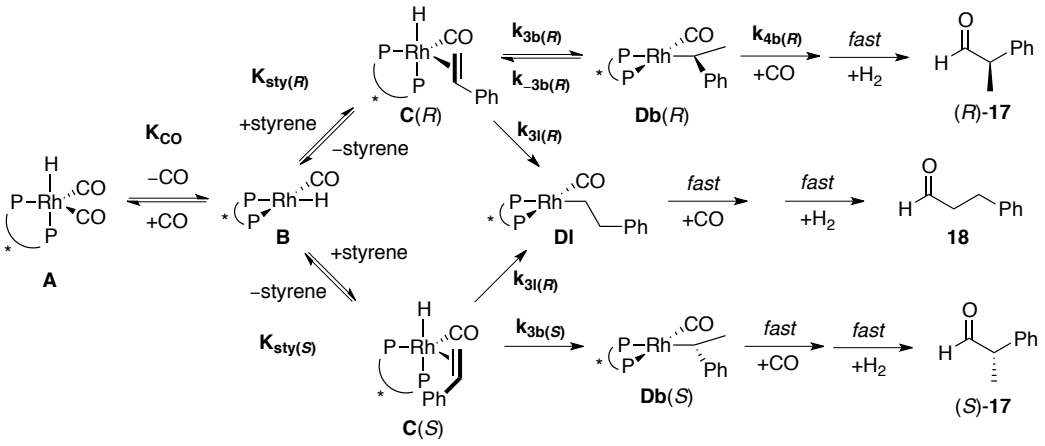

Scheme 2.17 Proposed kinetic model for the AHF of styrene using bisdiazaphos **d**.

Simple free energy surface models that qualitatively accounts for the kinetic data are depicted to account for the two differing CO pressure regimes in the formation of each of the branched aldehyde enantiomers (Figure 2.9). The pathways leading to the two aldehyde enantiomers presented in these graphs are as follows: major enantiomer (*R*)-**17** is presented in dashed blue and the minor enantiomer (*S*)-**17** is in solid red. The pathway leading to 3-phenylpropanal (linear aldehyde from styrene) is not shown but tracks similarly with the formation of the minor aldehyde enantiomer. At low CO pressure, the barrier between the branched rhodium alkyl **Db**(*R*) and the olefin adduct, **C**(*R*) is lower than the forward reaction to produce the branched rhodium acyl. In contrast, for the other diastereomeric pathway leading to the minor aldehyde enantiomer, a higher barrier between **C**(*S*) to the branched rhodium **Db**(*S*) intermediate leads to olefin insertion into the rhodium-hydride bond to be the irreversible step. At high CO pressure, the pathway leading to the minor enantiomer is similar and remains irreversible from **C**(*S*) to **Db**(*S*); the pathway towards the major enantiomer between **C**(*R*) and **Db**(*R*) rises slightly higher in energy and becomes irreversible. The rational behind this kinetic

behavior is at higher CO pressure, the free energy of states changes due to the two free CO's in intermediates **B**, **C**(*R*) and **Db**(*R*). Considering the diastereomeric pathways in formation of the linear aldehyde (under both CO conditions) tracks similarly with the production of the minor enantiomer correlates with the CO pressure effect observed with enantioselectivity and regioselectivity. Depending on the conditions in this regard, the use of terms to characterize selectivity or activity based on a single step in the mechanism (such as enantiodetermining, regiodetermining, or turnover-limiting) remains to be to simplistic to describe the kinetic behavior of this complex catalytic system.

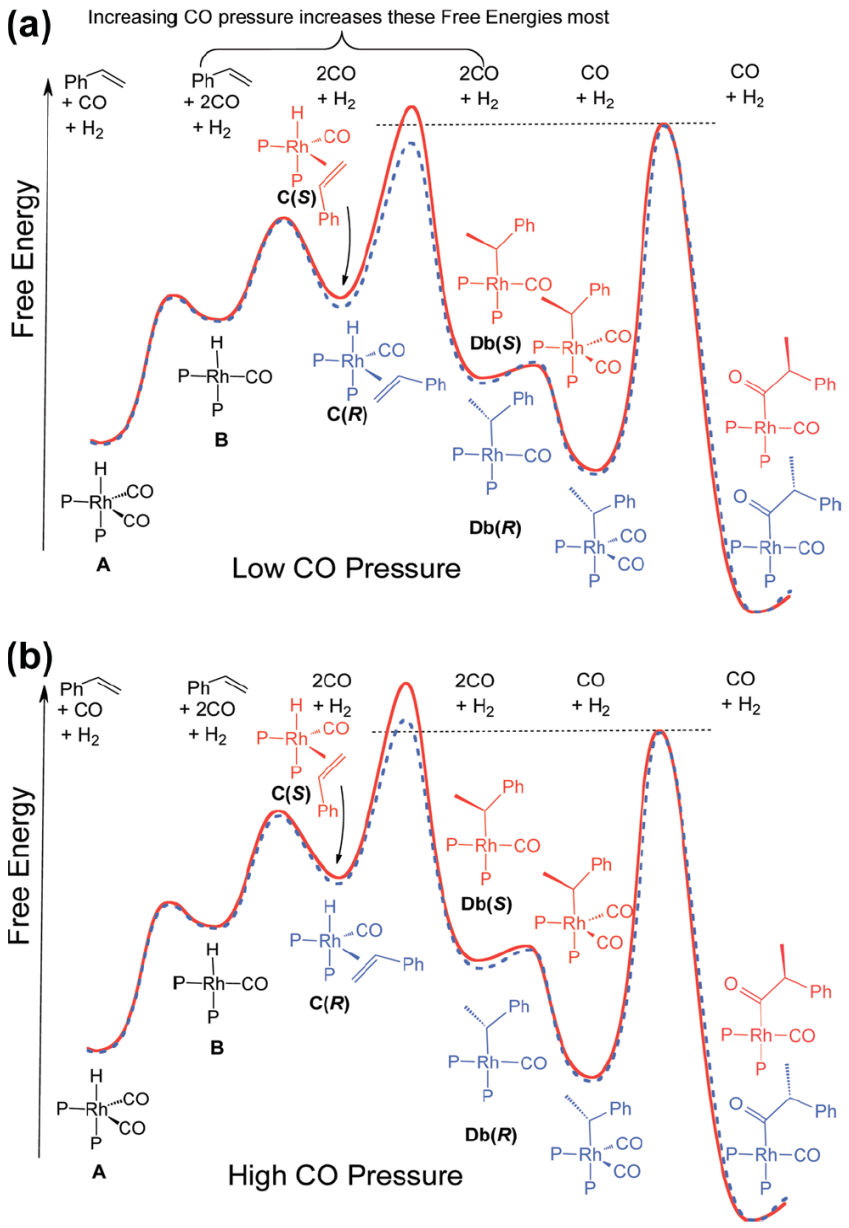

Figure 2.9 Graphical depiction of hypothetical free energy surfaces that rationalize kinetic behavior of rhodium-bisdiazaphospholane catalysts in styrene hydroformylation under the following conditions: low CO pressure and high CO pressure (from reference 10). Plots for the major branched (red, solid) and minor branched mechanistic pathways (blue, dashed) are as indicated. These plots aid in describing the current working hypothesis and no additional information (such as computed energies) is represented.

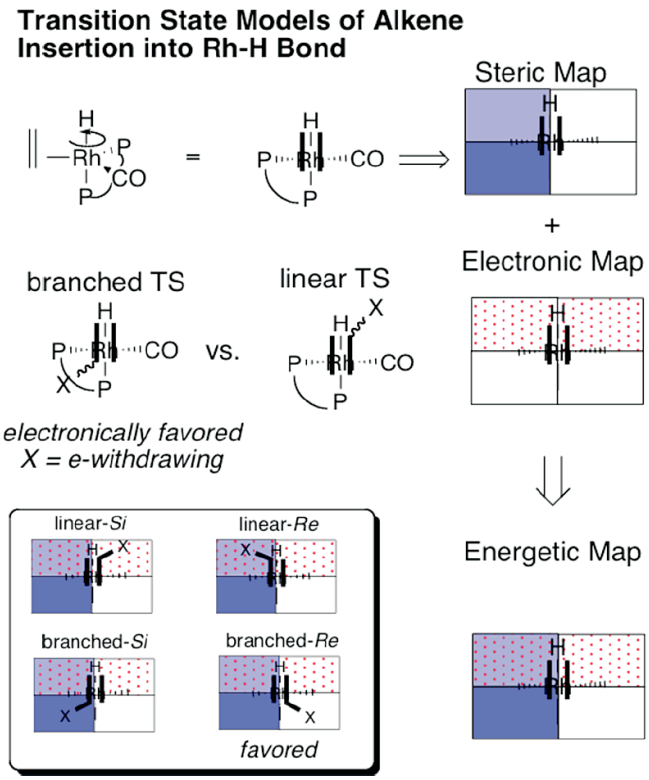

Figure 2.10 Energetic map (combination of steric and electronic maps) that rationalizes observed regioselectivity in the Rh-catalyzed AHF of terminal alkenes using bisdiazaphospholane ligands (from reference 10).

Landis and Watkins have developed an energetic quadrant map that combines steric and electronic contributions from rhodium-bisdiazaphospholane catalysts to qualitatively describe empirical observations in the hydroformylation of terminal olefins (Figure 2.10). We presume equatorial-axial coordination of bisdiazaphospholane ligands in trigonal bipyramidal coordination geometry of the rhodium-alkene complexes. Terminal alkenes coordinate from the top of the page onto the rhodium metal center that contain a hydride and one of the phosphorus atoms ligands in plane of the paper. Pointed away from the rhodium metal center are the other phosphorus atom and carbonyl ligands. In the steric map, the white quadrants indicate little-to-no

steric congestion (right side) from the carbonyl ligand whereas the light blue (upper left) and dark blue (lower left) show increasing amounts of steric bulk from the bisdiazaphospholane ligand. The electronic map depicts red dots in the upper half to indicate the orientation of the terminal alkene with respect to the substituent X, that would not be favorable in leading to linear aldehyde. The map indicates branched-*Re* coordination of a terminal alkene to the rhodium metal in the transition state is more favorable compared to the linear-*Re*. The inductive strength of the substituent X dictates the overall degree of regiocontrol in hydroformylation. Combination of these two maps as an energetic map provides a hypothetical model to rationalize observed trends in regioselectivity found with AHF of terminal alkenes.

2.4 Summary and Outlook

Enantioselective *hydroformylation* of alkenes offers a practical method in the synthesis of functionalized chiral building blocks that approach similar efficiency found with asymmetric *hydrogenation* catalysis; however, AHF remains underdeveloped due to the availability of chiral ligands that exhibit desirable chemo-, regio-, and enantioselectivity at reasonable reaction rates. Ligands that have demonstrated high regio- and enantioselectivity selectivity in hydroformylation for a variety of structurally diverse alkenes include (*R*,*S*)-Binaphos **a**, bis-3,4-diazaphospholane **d**, and YanPhos **h**. AHF of styrenes yields precursors to pharmacologically active, anti-inflammatory analgesics such as ibuprofen and naproxen. α-hydroxyaldehydes from vinyl ester hydroformylation have been demonstrated in the synthesis of chiral oxazolines and imidazoles, and the synthesis of (+)-Patulolide C. Hydoformylation of vinyl amides provide access to protected α-aminoaldehydes. Allyl ethers, acrylates and related analogues undergo AHF to synthetically useful precursors (e.g., “Roche aldehyde”) for polyketide total syntheses

(e.g., Prelog-Djerassi lactone was enabled by hydroformylation of a vinyl orthoester). Enantioselective hydroformylation of heterocycles yields useful carboaldehydes such as Garner's aldehyde or precursors to proline or β-proline. Most ligands exhibited desirable results for a particular substrate or substrate class: for example, Tan's scaffolding ligand, **k**, in hydroformylation of allylic alcohols or amines, or hydroformylation of 1,1-disubstituted alkene hydroformylation with ligand (*R*,*R*)-BenzP* **m**. AHF of 1,3-dienes yield chiral β,γ-unsaturated aldehydes and constitute useful and complex intermediates for natural product synthesis (e.g., (+)-Ambruticin and Tedanolide C). Simple alkyl alkenes remain a challenge in hydroformylation due to low levels of regioselectivity control but several hybrid ligands have demonstrate high levels of enantioselectivity.

New chiral ligands leading to highly active catalysts, which can access large libraries and or ligand-substrate interactions, will continue to challenge unsolved problems in hydroformylation such with traditionally difficult substrates. Hydroformylation of 1,2- and 1,1-disubstituted, and trisubstituted alkenes will receive increased attention because they lead to products with more diverse branching substitutents. Tandem reactions (hydrogenation, oxidation, olefination, hydroaminomethylation, etc.) coupled with hydroformylation utilize inherent the draws with hydroformylation: gaseous reagents, essentially neutral conditions, high selectivity, and large turnover numbers. Examples in organic synthesis will continue to emerge due to the availability of ligands that exhibit predicable and desirable selectivity in enantioselective hydroformylation. The use of synthesis gas and rhodium is ubiquitous in hydroformylation; alternative sources of H_2/CO equivalent (such as formalin or paraformaldehyde) and base metals will supplement work towards "greener" catalytic syntheses.

2.5 References

(1) Noyori, R.; Kitamura, M.; Ohkuma, T. *Proc. Natl. Acad. Sci. U.S.A.* **2004**, *101*, 5356-5362.

(2) Breit, B.; Seiche, W. *Synthesis* **2001**, *2001*, 0001-0036.

(3) Dieguez, M.; Pamies, O.; Claver, C. *Tetrahedron: Asymmetry* **2004**, *15*, 2113-2122.

(4) Breit, B. In *Metal Catalyzed Reductive C–C Bond Formation*; Krische, M., Ed.; Springer Berlin / Heidelberg: 2007; Vol. 279, p 139-172.

(5) Gual, A.; Godard, C.; Castillón, S.; Claver, C. *Tetrahedron: Asymmetry* **2010**, *21*, 1135-1146.

(6) Franke, R.; Selent, D.; Borner, A. Applied Hydroformylation. Chem. Rev. [Online early access]. DOI: 10.1021/cr3001803. Published Online: Aug 31, 2012. http://pubs.acs.org/doi/abs/10.1021/cr3001803 (accessed Aug 31, 2012).

(7) Brown, C. K.; Wilkinson, G. *Tetrahedron Lett.* **1969**, *10*, 1725-1726.

(8) Brown, C. K.; Wilkinson, G. *J. Chem. Soc. A* **1970**, 2753-2764.

(9) van Leeuwen, P. W. N. M.; Roobeek, C. F. *J. Organomet. Chem.* **1983**, *258*, 343-350.

(10) Watkins, A. L.; Landis, C. R. *J. Am. Chem. Soc.* **2010**, *132*, 10306-10317.

(11) Casey, C. P.; Martins, S. C.; Fagan, M. A. *J. Am. Chem. Soc.* **2004**, *126*, 5585-5592.

(12) Sakai, N.; Mano, S.; Nozaki, K.; Takaya, H. *J. Am. Chem. Soc.* **1993**, *115*, 7033-7034.

(13) Yan, Y.; Zhang, X. *J. Am. Chem. Soc.* **2006**, *128*, 7198-7202.

(14) Higashizima, T.; Sakai, N.; Nozaki, K.; Takaya, H. *Tetrahedron Lett.* **1994**, *35*, 2023-2026.

(15) Nozaki, K.; Sakai, N.; Nanno, T.; Higashijima, T.; Mano, S.; Horiuchi, T.; Takaya, H. *J. Am. Chem. Soc.* **1997**, *119*, 4413-4423.

(16) Nozaki, K.; Matsuo, T.; Shibahara, F.; Hiyama, T. *Adv. Synth. Catal.* **2001**, *343*, 61-63.

(17) Clark, T. P.; Landis, C. R.; Freed, S. L.; Klosin, J.; Abboud, K. A. *J. Am. Chem. Soc.* **2005**, *127*, 5040-5042.

(18) Axtell, A. T.; Klosin, J.; Whiteker, G. T.; Cobley, C. J.; Fox, M. E.; Jackson, M.; Abboud, K. A. *Organometallics* **2009**, *28*, 2993-2999.

(19) Zhang, X. W.; Cao, B. N.; Yan, Y. J.; Yu, S. C.; Ji, B. M.; Zhang, X. M. *Chem.—Eur. J.* **2010**, *16*, 871-877.

(20) Babin, J. E.; Whiteker, G. T. WO 93/03839, 1993.

(21) Babin, J. E.; Whiteker, G. T. U.S. Patent 5,360,938, 1994.

(22) Dieguez, M.; Pamies, O.; Ruiz, A.; Castillon, S.; Claver, C. *Chem.—Eur. J.* **2001**, *7*, 3086-3094.

(23) Axtell, A. T.; Klosin, J.; Abboud, K. A. *Organometallics* **2006**, *25*, 5003-5009.

(24) Axtell, A. T.; Cobley, C. J.; Klosin, J.; Whiteker, G. T.; Zanotti-Gerosa, A.; Abboud, K. A. *Angew. Chem. Int. Ed.* **2005**, *44*, 5834-5838.

(25) Watkins, A. L.; Hashiguchi, B. G.; Landis, C. R. *Org. Lett.* **2008**, *10*, 4553-4556.

(26) Sakai, N.; Nozaki, K.; Takaya, H. *J. Chem. Soc., Chem. Commun.* **1994**, 395-396.

(27) Nakano, K.; Tanaka, R.; Nozaki, K. *Helv. Chim. Acta* **2006**, *89*, 1681-1686.

(28) Tanaka, R.; Nakano, K.; Nozaki, K. *J. Org. Chem.* **2007**, *72*, 8671-8676.

(29) Thomas, P. J.; Axtell, A. T.; Klosin, J.; Peng, W.; Rand, C. L.; Clark, T. P.; Landis, C. R.; Abboud, K. A. *Org. Lett.* **2007**, *9*, 2665-2668.

(30) Breeden, S.; Cole-Hamilton, D. J.; Foster, D. F.; Schwarz, G. J.; Wills, M. *Angew. Chem. Int. Ed.* **2000**, *39*, 4106-4108.

(31) Zhao, B.; Peng, X.; Wang, Z.; Xia, C.; Ding, K. *Chemistry – A European Journal* **2008**, *14*, 7847-7857.

(32) Risi, R. M.; Burke, S. D. *Org. Lett.* **2012**, *14*, 1180-1182.

(33) McDonald, R. I.; Wong, G. W.; Neupane, R. P.; Stahl, S. S.; Landis, C. R. *J. Am. Chem. Soc.* **2010**, *132*, 14027-14029.

(34) Lambers-Verstappen, M. M. H.; de Vries, J. G. *Adv. Synth. Catal.* **2003**, *345*, 478-482.

(35) Cobley, C. J.; Gardner, K.; Klosin, J.; Praquin, C.; Hill, C.; Whiteker, G. T.; Zanotti-Gerosa, A.; Petersen, J. L.; Abboud, K. A. *J. Org. Chem.* **2004**, *69*, 4031-4040.

(36) Simeone, J. P.; Bugianesi, R. L.; Ponpipom, M. M.; Goulet, M. T.; Levorse, M. S.; Desai, R. C. *Tetrahedron Lett.* **2001**, *42*, 6459-6461.

(37) Ikeura, Y.; Doi, T.; Fujishima, A.; Natsugari, H. *Chem. Commun.* **1998**, 2141-2142.

(38) Natsugari, H.; Ikeura, Y.; Kamo, I.; Ishimaru, T.; Ishichi, Y.; Fujishima, A.; Tanaka, T.; Kasahara, F.; Kawada, M.; Doi, T. *J. Med. Chem.* **1999**, *42*, 3982-3993.

(39) Nozaki, K.; Li, W.-g.; Horiuchi, T.; Takaya, H.; Saito, T.; Yoshida, A.; Matsumura, K.; Kato, Y.; Imai, T.; Miura, T.; Kumobayashi, H. *J. Org. Chem.* **1996**, *61*, 7658-7659.

(40) Shih, D. H.; Baker, F.; Cama, L.; Chrisrtensen, B. G. *Heterocycles* **1984**, *21*, 29-40.

(41) Shih, D. H.; Cama, L.; Christensen, B. G. *Tetrahedron Lett.* **1985**, *26*, 587-590.

(42) Shirai, F.; Nakai, T. *J. Org. Chem.* **1987**, *52*, 5491-5492.

(43) Nagao, Y.; Nagase, Y.; Kumagai, T.; Matsunaga, H.; Abe, T.; Shimada, O.; Hayashi, T.; Inoue, Y. *J. Org. Chem.* **1992**, *57*, 4243-4249.

(44) Tsukada, N.; Shimada, T.; Gyoung, Y. S.; Asao, N.; Yamamoto, Y. *J. Org. Chem.* **1995**, *60*, 143-148.

(45) Breit, B. *Eur. J. Org. Chem.* **1998**, 1123-1134.

(46) Breit, B.; Heckmann, G.; Zahn, S. K. *Chem.—Eur. J.* **2003**, *9*, 425-434.

(47) Breit, B.; Breuninger, D. *J. Am. Chem. Soc.* **2004**, *126*, 10244-10245.

(48) Breit, B.; Breuninger, D. *Eur. J. Org. Chem.* **2005**, *2005*, 3930-3941.

(49) Rousseau, G.; Breit, B. *Angew. Chem. Int. Ed.* **2011**, *50*, 2450-2494.

(50) Tan, K. L. *ACS Catal.* **2011**, *1*, 877-886.

(51) Yeung, C. S.; Dong, V. M. *Angew. Chem. Int. Ed.* **2011**, *50*, 809-812.

(52) Worthy, A. D.; Joe, C. L.; Lightburn, T. E.; Tan, K. L. *J. Am. Chem. Soc.* **2010**, *132*, 14757-14759.

(53) Joe, C. L.; Tan, K. L. *J. Org. Chem.* **2011**, *76*, 7590-7596.

(54) Sun, X.; Frimpong, K.; Tan, K. L. *J. Am. Chem. Soc.* **2010**, *132*, 11841-11843.

(55) Lightburn, T. E.; De Paolis, O. A.; Cheng, K. H.; Tan, K. L. *Org. Lett.* **2011**, *13*, 2686-2689.

(56) Zhang, X.; Cao, B.; Yu, S.; Zhang, X. *Angew. Chem. Int. Ed.* **2010**, *49*, 4047-4050.

(57) Nozaki, K.; Li, W. G.; Horiuchi, T.; Takaya, H. *Tetrahedron Lett.* **1997**, *38*, 4611-4614.

(58) Wong, G. W.; Adint, T. A.; Landis, C. R. *Org. Synth.* **2012**, *89*, 243-254.

(59) Arena, C. G.; Nicolo, F.; Drommi, D.; Bruno, G.; Faraone, F. *J. Chem. Soc., Chem. Commun.* **1994**, 2251-2252.

(60) Noonan, G. M.; Newton, D.; Cobley, C. J.; Suarez, A.; Pizzano, A.; Clarke, M. L. *Adv. Synth. Catal.* **2010**, *352*, 1047-1054.

(61) Wang, X.; Buchwald, S. L. *J. Am. Chem. Soc.* **2011**, *133*, 19080-19083.

(62) Keulemans, A. I. M.; Kwantes, A.; van Bavel, T. *Recl. Trav. Chim. Pays-Bas* **1948**, *67*, 298-308.

(63) Uhlemann, M.; Borner, A. *Chemcatchem* **2012**, *4*, 753-754.

(64) Risi, R. M.; Burke, S. D. *Org. Lett.* **2012**, *14*, 2572-2575.

(65) Horiuchi, T.; Ohta, T.; Shirakawa, E.; Nozaki, K.; Takaya, H. *J. Org. Chem.* **1997**, *62*, 4285-4292.

(66) Chikkali, S. H.; Bellini, R.; Berthon-Gelloz, G.; van der Vlugt, J. I.; Bruin, B.; Reek, J. N. H. *Chem. Commun.* **2010**, *46*, 1244-1246.

(67) Chikkali, S. H.; Bellini, R.; de Bruin, B.; van der Vlugt, J. I.; Reek, J. N. H. *J. Am. Chem. Soc.* **2012**, *134*, 6607-6616.

(68) Adint, T. A.; Wong, G. W.; Landis, C. R. University of Wisconsin-Madison, Madison, WI. Unpublished work, 2012.

(69) Clemens, A. J. L.; Burke, S. D. *J. Org. Chem.* **2012**, *77*, 2983-2985.

(70) Liu, P.; Jacobsen, E. N. *J. Am. Chem. Soc.* **2001**, *123*, 10772-10773.

(71) Smith, T. E.; Fink, S. J.; Levine, Z. G.; McClelland, K. A.; Zackheim, A. A.; Daub, M. E. *Org. Lett.* **2012**, *14*, 1452-1455.

(72) Horiuchi, T.; Ohta, T.; Shirakawa, E.; Nozaki, K.; Takaya, H. *Tetrahedron* **1997**, *53*, 7795-7804.

(73) Watkins, A. L.; Landis, C. R. *Org. Lett.* **2011**, *13*, 164-167.

(74) Fürstner, A.; Nevado, C.; Waser, M.; Tremblay, M.; Chevrier, C.; Teplý, F.; Aïssa, C.; Moulin, E.; Müller, O. *J. Am. Chem. Soc.* **2007**, *129*, 9150-9161.

(75) Nozaki, K.; Nanno, T.; Takaya, H. *J. Organomet. Chem.* **1997**, *527*, 103-108.

(76) Noonan, G. M.; Fuentes, J. A.; Cobley, C. J.; Clarke, M. L. *Angew. Chem. Int. Ed.* **2012**, *51*, 2477-2480.

Chapter 3

Synthesis of a Library of Bis-3,4-diazaphospholane Ligands and Their Application in Rhodium-Catalyzed Asymmetric Hydroformylation

Acknowledgement: Mr. Tyler A. Adint performed the hydroformylation work reported in Table 3.1, entries 1, 4, and 5.

3.1 Introduction

Rhodium-catalyzed hydroformylation is a large-scale commodity process that exhibits perfect atom economy, high turnover numbers, and simple product separation used to generate 18 billion pounds of linear aldehyde per year.[1] In comparison, asymmetric hydroformylation (AHF) has been underutilized in the synthesis of α-chiral aldehydes.[2] Our group[3-7] and others[8-15] have previously demonstrated effective enantioselective hydroformylation of various alkenes at mild conditions and with low catalyst loadings. Many phosphorus-containing ligands have been reported for rhodium-catalyzed AHF; nevertheless, a highly modular class of ligands that exhibits desirable regio- and enantioselectivity in hydroformylation provides enhanced opportunity for selectivity optimization. One core ligand structure that has found success in rhodium-catalyzed AHF is bisphospholane ligand systems.[16]

A phospholane is a 5-member ring containing a tertiary phosphorus atom (three P−C bonds).[17] Bisphospholanes, such as MeDuPHOS or (*R*,*R*)-Ph-bpe, enables high levels of enantioselectivity in rhodium-catalyzed asymmetric *hydrogenation* of various multisubstituted alkenes.[18,19] Landis and Clark hypothesized that bisphospholanes could impart high selectivity in asymmetric *hydroformylation* catalysis.[17] Indeed, C_2-symmetric bisphospholanes such as (*R*,*R*)-Ph-bpe, enables good enantioselectivities in the hydroformylation of vinyl acetate (82%), styrene (94%), and allyl cyanide (90%). Bisphospholane (*R*,*R*)-Ph-bpe differs from typical chiral ligands reported for rhodium-catalyzed AHF because it exhibits desirable enantioselectivity with these three substrates at reasonable rates (often a ligand is found to only work well with a particular substrate class). A drawback with bisphospholanes is their lack of functionality for chemical variation that could enable the synthesis of a large library for combinatorial approach to

catalysis. Modular bisphospholanes would provide enhanced opportunity for selectivity optimization in hydroformylation and yield improvement for other areas of asymmetric catalysis.

3.2 Synthesis of Bis-3,4-Diazaphospholanes

Landis and co-workers developed a Mannich-type reaction leading to 3,4-diazaphospholanes made from readily available starting materials: aldehydes, acid chlorides, and primary phosphines.[20] The cyclization of a primary phosphine with an azine (condensation product of hydrazine and two equivalents of an aldehyde) in the presence of a Bronsted acid or an acid chloride forms a 3,4-diazaphospholane (Scheme 3.1). The ease of synthesis and high functional group compatibility enable numerous variations and tuning of the ligand in application to transition metal catalysis.

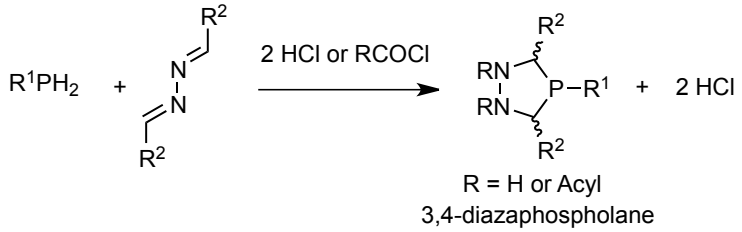

Scheme 3.1 Mannich-type cyclization of a primary phosphine and an azine, in the presence of HCl or an acid chloride produces a 3,4-diazaphospholane.

Bis-3,4-diazaphospholanes modified at the 2,5-positions on the phospholane ring with 2-benzamides provide state-of-the-art activity and good selectivity in rhodium-catalyzed asymmetric hydroformylation of styrene, vinyl acetate, and allyl cyanide.[3] These ligands were accessed from a common precursor, tetraacid bisdiazaphos **1**, synthesized from 2-formylbenzoic acid azine, 1,2-bisphosphinobenzene, and succinyl chloride. Crystal structures were obtained of

tetraacid bisdiazaphos **1** (Figure 3.1) and of a related bisdiazaphospholane analogue, tetraester bisdiazaphos **2** (Figure 3.2).

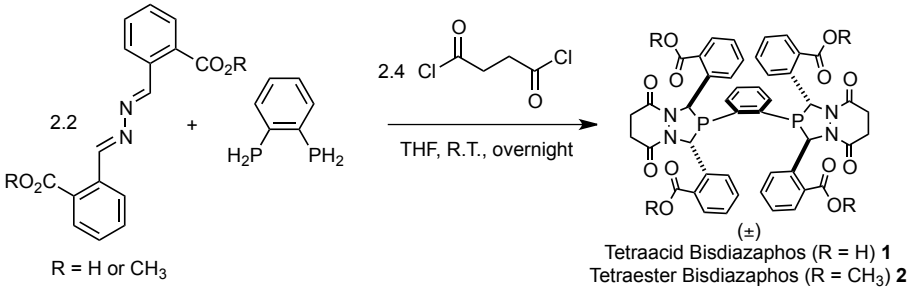

Scheme 3.2 Synthesis of bisdiazaphospholanes **1** and **2**.

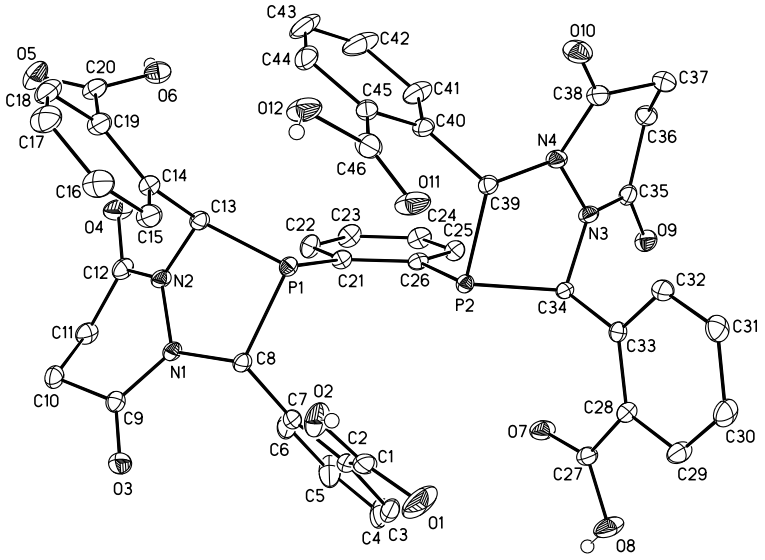

Figure 3.1 ORTEP drawing of tetraacid bisdiazaphos **1**. Thermal ellipsoids are drawn at the 30% probability level. All hydrogens, except for the four carboxylic acids moieties, are omitted for clarity. Only the (*S*,*S*) stereoisomer is shown; however, both exist in the structure.

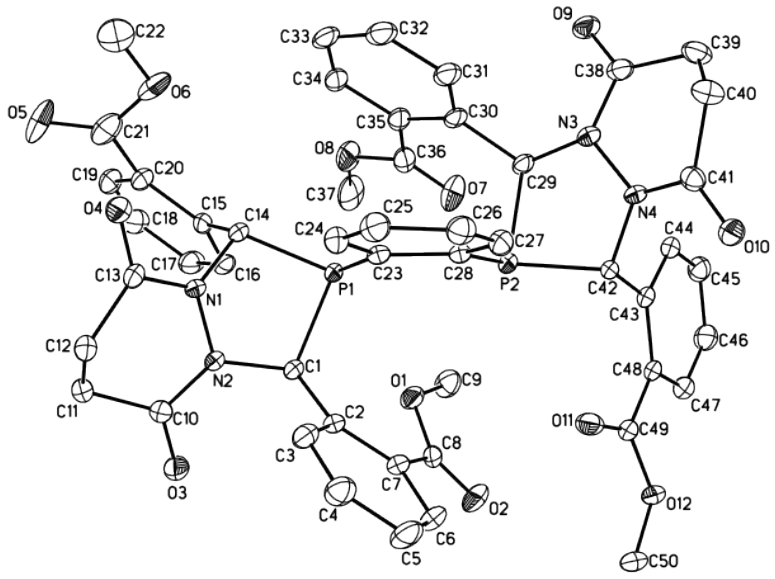

Figure 3.2 ORTEP drawing of tetraester bisdiazaphos **2**. Thermal ellipsoids are drawn at the 40% probability level. All hydrogens and THF solvent molecules are omitted for clarity. Only the (*S*,*S*) stereoisomer is shown; however, both exist in the structure.

Previously Landis and Clark have demonstrated resolution of a monodentate diazaphospholane by diastereomeric salt formation as α-methylbenzylammonium carboxylates.[21] Diastereomeric salt formation of tetraacid bisdiazaphos **1** with chiral amines was not achieved after a survey of crystallization attempts in preliminary experiments. In collaboration with Merck & Co. Inc. (Dr. Neil Strotman), preparative-scale resolution of tetraacid bisdiazaphos can be conducted using chiral supercritical fluid chromatography (SFC). Resolved tetraacid bisdiazaphos **1** enables the synthesis of a library of ligands in coupling with a variety of amines. Three new ligand subsets were synthesized to compare bisdiazaphospholane secondary coordination sphere steric bulk and hydroformylation selectivity: type **I**, secondary carboxamides

with slight steric modifications from previously reported (*S*,*S*)-**3** ligand; type **II**, secondary carboxamides with achiral R-groups with varying steric bulk; and structurally different type **III**, tertiary carboxamides (synthesized by Tyler A. Adint and is not reported here).

3.3 Synthesis of a Library of Tetraamide Bis-3,4-Diazaphospholanes

A previously reported bisdiazaphospholane ligand, (*S*,*S*)-**3**, has demonstrated fast reaction rates and high selectivity in Rh-catalyzed AHF of styrene, vinyl acetate, and allyl cyanide. Tetraamide bis-3,4-diazaphospholane ligands can be accessed from coupling of the tetraacid bisdiazaphospholane **1** with various amines with an appropriate coupling reagent. Most primary amines underwent coupling using PyBOP/DIEA to form secondary carboxamide bisdiazaphospholane ligands (Scheme 3.3; Type I and II ligands). Tritylamine does not undergo coupling using PyBOP/DIEA (presumably due to steric bulk of the amine) and a bisdiazaphospholane containing benzotriazole ester (OBt) was isolated instead (Scheme 3.4).

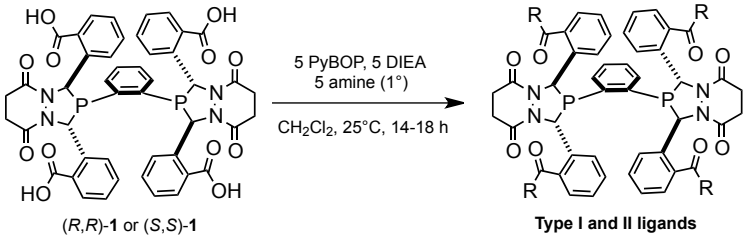

Type I	R =	Type II	R =
(*S*,*S*)-**3**		(*R*,*R*)-**6**	
(*R*,*R*)-**3**		(*R*,*R*)-**7**	
(*S*,*S*)-**4**		(*R*,*R*)-**8**	
(*S*,*S*)-**5**		(*R*,*R*)-**9**	

Scheme 3.3 Synthesis of tetraamide bisdiazaphos analogues with varying steric bulk.

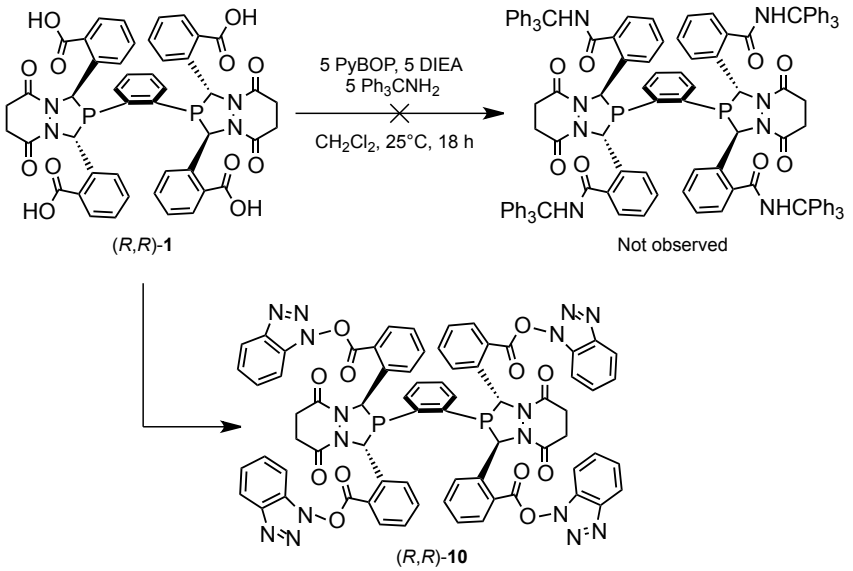

Scheme 3.4 Unsuccessful PyBOP coupling of (*R*,*R*)-tetraacid bisdiazaphos **1** with tritylamine.

Bisdiazaphospholane (*R*,*R*)-**10** is a competent intermediate in the formation of carboxamides substituted bisdiazaphospholanes. For example, the addition of excess (*R*)-(+)-α-methylbenzylamine to a sample of **10** yield quantitative conversion to (*R*,*R*,*R*)-**3** (enantiomer of (*S*,*S*)-**3**) by $^{31}P\{^{1}H\}$ and ^{1}H NMR.

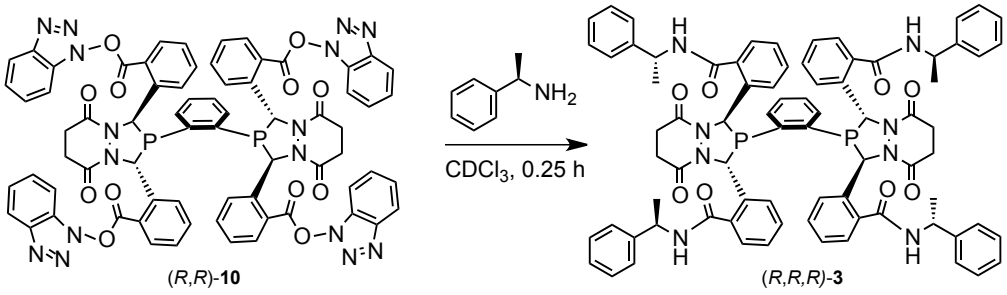

Scheme 3.5 Addition of (*R*)-(+)-α-methylbenzylamine to bisdiazaphospholane (*R*,*R*)-**10**.

3.4 Application of a Library of Tetraamide Bis-3,4-Diazaphospholanes in Rh-Catalyzed Asymmetric Hydroformylation

Similar to previously reported studies,[3,22] an one-pot AHF of three substrates was used as a screening protocol to systematically test changes of the bis-3,4-diazaphospholane secondary coordination sphere sterics on AHF regio- and enantioselectivity. Styrene, vinyl acetate, and allyloxy-*tert*-butyldimethylsilane underwent effective hydroformylation in glass pressure bottles at 150 psig H_2/CO (1:1) at 60˚C, screening the three types of bis-3,4-diazaphospholane ligands (Table 3.1). The precursor tetraacid ligand (*R*,*R*)-**1** forms complexes competent for catalysis (entry 1) exhibiting modest enantioselectivity. Type **I** ligands include our previously reported (*S*,*S*)-**3** and less selective diastereomer (*R*,*R*)-**3** (entries 2 and 3, respectively) along with ligands that contain slight steric changes to the carboxamide R group. Slight steric modifications in (*S*,*S*)-**3** and (*S*,*S*)-**4** (exchanging phenyl for cyclohexyl in the R group; entries 2 and 4) resulted in decreases in regio- (18.3:1 vs. 7.5:1) and enantioselectivity (87% ee vs. 63% ee) in hydroformylation of styrene, but exhibited minor effects on vinyl acetate and allyl silyl ether hydroformylation. This comparison contrasts the differences between (*S*,*S*)-**2** and (*S*,*S*)-**4** (entries 2 and 5), where these ligands contain phenyl and t-butyl substituted carboxamides, which resulted in decreased regioselectivity but retained high enantioselectivity. Type **II** ligands contain secondary carboxamides with increasing R-group steric bulk (ethyl, benzyl, diphenylmethyl, and 1-adamantyl) decrease styrene regio- and enantioselectivity in AHF while leaving selectivities with vinyl acetate and allyl silyl ether relatively unaffected (entries 6—9). Hydroformylations performed by tetraamide bisdiazaphospholanes **3**-**9** were at least 50% conversation or better (in many cases, 95%+) and only draw comparisons for selectivity.

Table 3.1 One-pot AHF of vinyl acetate, styrene, and allyloxy-*tert*-butyldimethylsilane using ligands **1**, and **3**-**9**.

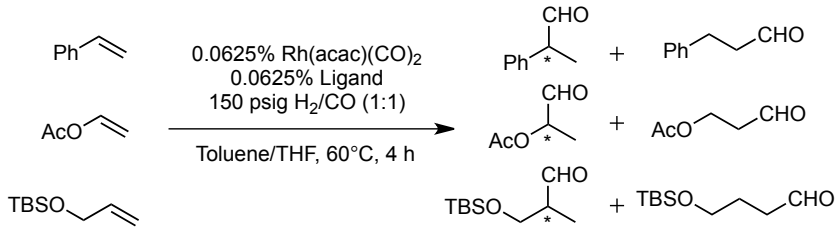

Entry	Type	Ligand	Styrene		Vinyl acetate		Allyloxy-*t*-butyldimethylsilane	
			b:l ratio[a]	% ee[b]	b:l ratio[a]	% ee[b]	b:l ratio[a]	% ee[b]
1[c]		(*R*,*R*)-**1**	10.9:1	53	15:1	83	1.6:1	75
2		(*S*,*S*)-**3**	18.3:1	87	53:1	98	2:1	96
3		(*R*,*R*)-**3**	9.2:1	75	29:1	84	1.7:1	80
4	**I**	(*S*,*S*)-**4**	7.5:1	63	53:1	97	1.9:1	91
5		(*S*,*S*)-**5**	6.2:1	88	55:1	95	1.5:1	90
6		(*R*,*R*)-**6**	9:1	87	34:1	95	1.8:1	94
7		(*R*,*R*)-**7**	8:1	89	33:1	97	1.8:1	97
8	**II**	(*R*,*R*)-**8**	6.7:1	82	36:1	90	1.6:1	97
9		(*R*,*R*)-**9**	3.2:1	68	40:1	94	1.9:1	95

Conditions: 4 h, 60°C, 150 psig H_2/CO (1:1), 1200:1 total substrate:Rh, [each alkene] = 1.4 M, [Rh] = 3.5 mM, [L] = 4.2 mM. a. Determined by ^{1}H NMR spectroscopy. b. Determined by chiral GC analysis. c. 1mL MeOH as solvent with 1eq. Et_3N to (*R*,*R*)-**1** to solubilize ligand.

3.5 Conclusions

A library of bis-3,4-diazaphospholane ligands was synthesized for use in rhodium-catalyzed AHF of three substrates: styrene, vinyl acetate, and alloxy-*tert*-butyldimethylsilane. These ligands examined secondary carboxamides with varying levels of steric bulk and tested their impact on hydroformylation selectivity. Hydroformylation of styrene demonstrated the most variation while vinyl acetate and alloxy-*tert*-butyldimethylsilane gave modest changes with respect to bisdiazaphospholane carboxamide steric bulk. Allyl alcohols remain a challenge in hydroformylation and new ligand-based approaches to optimize the regioselectivity such as invoking secondary interactions are underway in the Landis research group.

3.6 Experimental

General considerations. Routine NMR experiments (^{1}H, ^{13}C, ^{31}P) were carried out on a Bruker AC-300 or a Varian Mercury-300. Proton (^{1}H) and carbon (^{13}C) NMR spectra were referenced to residual solvent relative to tetramethylsilane. Phosphorus (^{31}P) chemical shifts were referenced to an external 85% phosphoric acid (H_3PO_4) sample. Mass spectra were collected on a Waters (Micromass) LCT® for electrospray ionization experiments with a sample cone voltage of 20. Gas chromatographic analysis was performed on a Varian Chrompack system using a β-DEX 225 capillary column from Supelco, 30 m x 0.25 mm ID x 0.25 μm film thickness. Resolution conditions for the hydroformylation products of styrene, vinyl acetate, and allyloxy-*t*-butyldimethylsilane have been reported.[3,5,7]

General Synthesis of Enantiopure Tetraamide Bisdiazaphospholanes

In an oven dried 50 mL Schlenk flask added 0.200 to 0.300 g (0.22 – 0.33 mmols; 1 eq.) of tetraacid bisdiazaphos **1**, 0.58 - 0.87 g (1.1 - 1.65 mmols; 5 eq.) PyBOP and approximately 20-30 mL of dichloromethane. Upon addition of 5 eq. of Hünig's base (DIEA, 0.20 – 0.30 mL 1.1-1.65 mmols) resulted in a homogeneous yellow solution. After the tetraacid bisdiazaphos dissolved, 5 eq. of primary amine (1.1 – 1.65 mmols) was added and stirred overnight. The reaction mixture was washed with $NaHCO_3$ (sat.), 1 M HCl, $NaHCO_3$ (sat.), and brine (sat.) solutions, dried over $MgSO_4$, and the solvent was removed by rotatory evaporation. The yellow solid was purified by flash column chromatography or recrystallized.

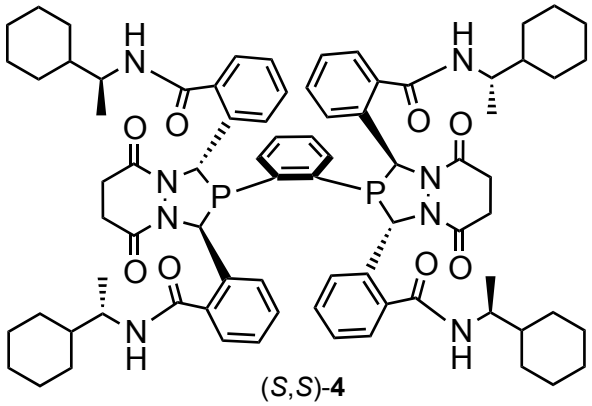

(*S*,*S*)-**4**

(*S*,*S*)-**4** was isolated from silica gel chromatography using 2:1 ethyl acetate and dichloromethane (R_f = 0.43) solvent mixture in 69% isolated yield. ^{1}H NMR (300 MHz, $CDCl_3$) δ: 0.72 ppm (d, J = 6.6 Hz, NHCH(Cy)CH_3), 0.81 – 0.93 (m, Cy), 1.03 – 1.22 (m, Cy and NHCH(Cy)CH_3), 1.46 – 1.82 (m, Cy), 2.41 – 2.71 (m, C(O)CH_2CH_2C(O)), 3.53 – 3.60 (m, NHC*H*(Cy)CH_3), 3.99 – 4.09 (m, NHC*H*(Cy)CH_3), 6.14 – 6.16 (m), 6.64 – 6.69 (m), 6.90 – 6.94 (m), 7.03 – 7.11 (m), 7.23 – 7.26 (m, overlap with $CHCl_3$ residual solvent peak), 7.33 – 7.40 (m), 7.45 – 7.50 (m), 7.54 – 7.56

(m), 7.62 – 7.68 (m), 7.75 – 7.78 (m), 8.06 – 8.08 (m). ^{13}C NMR (75 MHz, $CDCl_3$) δ: 17.3 (s, NHCH(Cy)*C*H_3), 17.8 (s, NHCH(Cy)*C*H_3), 25-35 ppm have not been assigned, 42.6 (s, NHCH(CH_3)*C*H(CH_2)$_5$), 42.9 (s, NHCH(CH_3)*C*H(CH_2)$_5$), 50.5 (s, NHC*H*(CH_3)CH(CH_2)$_5$), 51.3 (s, NHC*H*(CH_3)CH(CH_2)$_5$), 55.6 (br s, P*C*HN), 57.6 (br s, P*C*HN), peaks 125-150 have not been assigned, 165.7 (s, *C*(O)NH), 167.3 (s, *C*(O)NH), 168.3 (s, *C*(O)NN), 168.6 (s, *C*(O)NN). ^{31}P{^{1}H} NMR (120 MHz, $CDCl_3$) δ: 5.6 (broad s). HRMS-ESI (m/z): $[M + Na]^+$ calcd for $C_{78}H_{96}N_8NaO_8P_2$, 1357.6719; found, 1357.6763 (Δ = 3.2 ppm).

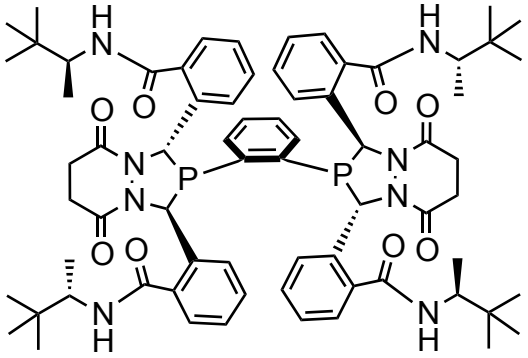

(*S*,*S*)-**5**

(*S*,*S*)-**5** was isolated from silica gel chromatography using 4:1 ethyl acetate and dichloromethane solvent mixture in 51% isolated yield. ^{1}H NMR (300 MHz, $CDCl_3$) δ: 0.81 ppm (d, J = 6.6 Hz, NHCH(^{t}Bu)C*H*$_3$), 0.90 (s, CH(C(C*H*$_3$)$_3$)CH$_3$), 1.00 (s, CH(C(C*H*$_3$)$_3$)CH$_3$), 1.20 (d, J = 6.9, NHCH(^{t}Bu)C*H*$_3$), 2.38 – 2.69 (m, C(O)C*H*$_2$C*H*$_2$C(O)), 3.49 – 3.54 (m, NHC*H*(^{t}Bu)CH$_3$), 4.12 – 4.17 (m, NHC*H*(^{t}Bu)CH$_3$), 6.20 (d, J = 8.1 Hz), 6.35 (br s), 6.66 – 6.80 (m), 6.98 (br d, J = 9.0 Hz), 7.16 (br s), 7.30 – 7.40 (m), 7.45 – 7.52 (m), 7.66 – 7.69 (m), 7.76 – 7.79 (m), 7.90 (br d, J = 9.3 Hz). ^{13}C NMR (75 MHz, $CDCl_3$) δ: 15.8 (s, NHCH(^{t}Bu)*C*H$_3$), 16.1 (s, NHCH(^{t}Bu)*C*H$_3$), 26.7 (s, CH(C(*C*H$_3$)$_3$)CH$_3$), 26.9 (s, CH(C(*C*H$_3$)$_3$)CH$_3$), 29.2 (s, C(O)*C*H$_2$CH$_2$C(O)), 29.4 (s, C(O)*C*H$_2$CH$_2$C(O)), 34.3 (s, CH(*C*(CH$_3$)$_3$)CH$_3$), 34.6 (s, CH(*C*(CH$_3$)$_3$)CH$_3$), 54.1 (s, NH*C*H(^{t}Bu)CH$_3$), 54.7 (s, NH*C*H(^{t}Bu)CH$_3$), 55.3 (br s, P*C*HN), 57.2 (m, P*C*HN), peaks 110-150

have not been assigned, 165.7 (s, *C*(O)NH), 166.7 (s, *C*(O)NH), 168.7 (s, *C*(O)NN), 169.4 (s, *C*(O)NN). $^{31}P\{^{1}H\}$ NMR (120 MHz, $CDCl_3$) δ: 10.4 (broad s). HRMS-ESI (m/z): $[M + Na]^+$ calcd for $C_{70}H_{88}N_8NaO_8P_2$, 1253.6093; found, 1253.6074 (Δ = 1.5 ppm).

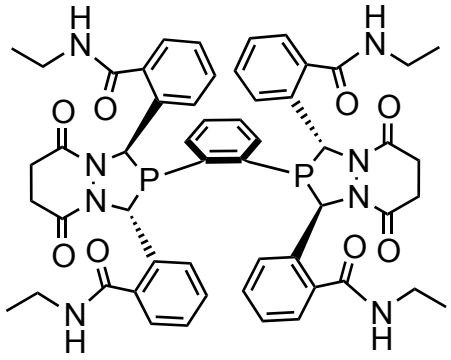

(*R*,*R*)-**6**

(*R*,*R*)-**6** can be recrystallized from 8:1 hexane:ethyl acetate solution obtaining a white solid (30% isolated yield). ^{1}H NMR (300 MHz, $CDCl_3$) δ: 1.04 (t, J = 7.3 Hz, $NHCH_2CH_3$, 6H), 1.24 (t, J = 7.3 Hz, $NHCH_2CH_3$ 6H), 2.40 – 2.85 (m, $C(O)CH_2CH_2C(O)$, 8 H), 3.12 – 3.30 (m, $NHCH_2CH_3$, 3H), 3.45 – 3.75 (m, $NHCH_2CH_3$, 5H), 6.17 (d, J = 7.5 Hz, 2H), 6.33 (s, 2H), 6.67 (m, 2H), 6.85 – 7.00 (m, 4 H) 7.05 – 7.30 (m, overlap with $CHCl_3$ residual solvent peak), 7.40 – 7.68 (m, 9H), 8.61 (broad t, J = 5.2 Hz, 2H). ^{13}C NMR (75 MHz, $CDCl_3$) δ: 14.8 (s, $NHCH_2CH_3$), 15.0 (s, $NHCH_2CH_3$), 29.1 (s, $C(O)CH_2CH_2C(O)$), 29.4 (s, $C(O)CH_2CH_2C(O)$), 34.6 (s, $NHCH_2CH_3$), 35.0 (s, $NHCH_2CH_3$), 55.1 (s, PCHN), 57.5 (s, PCHN), peaks 125-150 have not been assigned, 165.7 (s, *C*(O)N), 167.3 (s, *C*(O)N), 168.1 (s, *C*(O)N), 169.0 (s, *C*(O)N). $^{31}P\{^{1}H\}$ NMR (120 MHz, $CDCl_3$) δ: 9.2 (s). HRMS-ESI (m/z): $[M + NH_4]^+$ calcd for $C_{54}H_{60}N_9O_8P_2$, 1024.4035; found, 1024.4059 (Δ = 2.3 ppm).

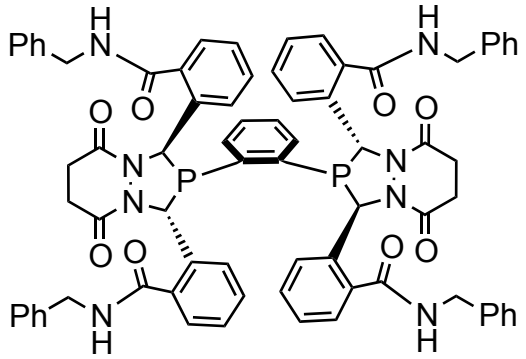

(*R*,*R*)-**7**

(*R*,*R*)-**7** was purified by flash column chromatography using ethyl acetate as elutant (Rf = 0.05) in a 32% yield. ^{1}H NMR (300 MHz, $CDCl_3$) δ: 2.30 – 2.63 (m, C(O)CH_2CH_2C(O), 8 H), 3.64 (dd, J = 15.6, 5.1 Hz, NHCH_2Ph, 2H), 4.26 (dd, J = 15.1, 6.4 Hz, NHCH_2Ph, 2H), 4.29 – 4.71 (m, NHCH_2Ph, 4H), 6.16 (d, J = 7.8 Hz, 2H), 6.22 (s, 2H), 6.61 – 6.67 (m, 2H), 6.78 – 6.86 (m, 4H), 7.03 – 7.12 (m, 9 H), 7.18 – 7.40 (m, overlap with $CHCl_3$ residual solvent peak), 7.49 – 7.52 (m, 2H), 7.60 – 7.80 (m, 2H), 8.68 (broad s, 1H). ^{13}C NMR (75 MHz, $CDCl_3$) δ: 29.0 (s, C(O)*C*H_2CH_2C(O)), 29.4 (s, C(O)*C*H_2CH_2C(O)), 43.3 (s, NH*C*H_2Ph), 44.4 (s, NH*C*H_2Ph), 55.7 (broad s, P*C*HN), 57.7 (t, J = 17.5 Hz, P*C*HN), peaks 125-150 have not been assigned, 165.5 (s, *C*(O)N), 167.3 (s, *C*(O)N), 168.6 (s, *C*(O)N), 169.6 (s, *C*(O)N). ^{31}P{^{1}H} NMR (120 MHz, $CDCl_3$) δ: 7.3 (s). HRMS-ESI (m/z): $[M + NH_4]^+$ calcd for $C_{74}H_{68}N_9O_8P_2$, 1272.4661; found, 1272.4634 (Δ = 2.1 ppm).

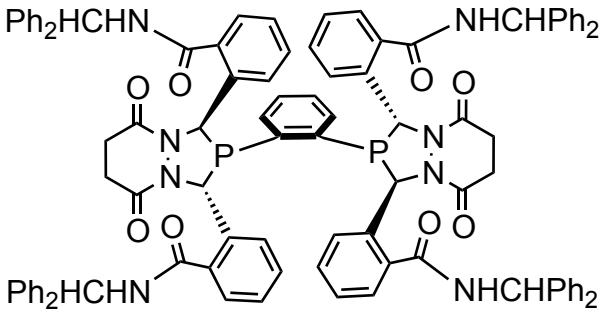

(*S*,*S*)-**8**

Ligand (*S*,*S*)-**8** was isolated by way of flash column chromatography using 2:1 ethyl acetate and dichloromethane (R_f = 0.30) solvent mixture in 64% isolated yield. ^{1}H NMR (300 MHz, $CDCl_3$) δ: 2.30 – 2.63 (m, C(O)CH_2CH_2C(O), 8 H), 4.29 – 4.71 (m, NHCH_2Ph, 4H), 6.16 (d, J = 7.8 Hz, 2H), 6.22 (s, 2H), 6.61 – 6.67 (m, 2H), 6.78 – 6.86 (m, 4H), 7.03 – 7.12 (m, 9 H), 7.18 – 7.40 (m, overlap with $CHCl_3$ residual solvent peak), 7.49 – 7.52 (m, 2H), 7.60 – 7.80 (m, 2H), 8.68 (broad s, 1H). ^{13}C NMR (75 MHz, $CDCl_3$) δ: 28.9 (s, C(O)*C*H_2CH_2C(O)), 29.1 (s, C(O)*C*H_2CH_2C(O)), 57.7 (m, P*C*HN), 57.9 (s, HN*C*HPh_2), peaks 125-150 have not been assigned, 166.1 (s, *C*(O)N), 167.0 (s, *C*(O)N), 168.4 (s, *C*(O)N), 168.6 (s, *C*(O)N). ^{31}P{^{1}H} NMR (120 MHz, $CDCl_3$) δ: 9.8 (broad s). HRMS-ESI (m/z): $[M + Na]^+$ calcd for $C_{98}H_{80}N_8NaO_8P_2$, 1581.5467; found, 1581.5500 (Δ = 2.1 ppm).

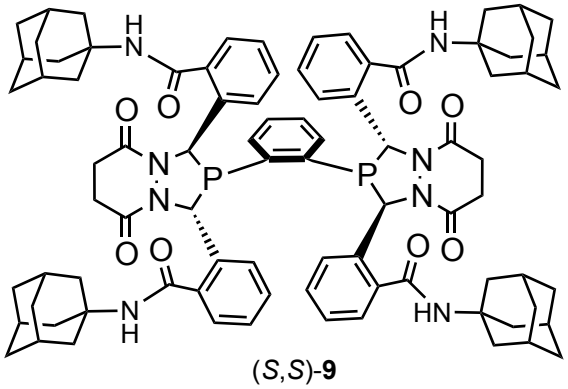

(*S*,*S*)-**9**

1-adamantylamine was dissolved in dichloromethane solution and cannula transferred to the tetraacid bisdiazaphos **1**, PyBOP, and Hünig's base mixture. After 4 hours stirring, a white solid precipitated out of solution; this material was separated from the supernatant. The solvent from the filtrate was removed and (*S*,*S*)-**9** was purified by way of silica gel chromatography utilizing ethyl acetate (R_f = 0.05) as an elutant, resulting in a white solid in 41% isolated yield. ^{1}H NMR (500 MHz, CD_2Cl_2) δ: 1.54 (apparent Abs, $\Delta\upsilon_{AB}$ = 61.6 Hz, J = 11.8 Hz, aliphatic H, 14 H), 1.74 (m, aliphatic H, 13H), 1.89 (m, aliphatic H, 16H), 2.14 (m, aliphatic H, 17H) 2.25 – 2.55 (m, C(O)CH_2CH_2C(O), 8H), 6.23 (broad s, 2H), 6.45 – 6.70 (m), 6.78 (broad s), 6.92 (m), 7.18 – 7.40 (m), 7.40 – 7.50 (m), 7.60 – 7.85 (m). ^{31}P{^{1}H} NMR (120 MHz, $CDCl_3$) δ: 10.9 (broad s). HRMS-ESI (m/z): $[M + Na]^+$ calcd for $C_{86}H_{96}N_8NaO_8P_2$, 1453.6719; found, 1453.6727 (Δ < 1 ppm).

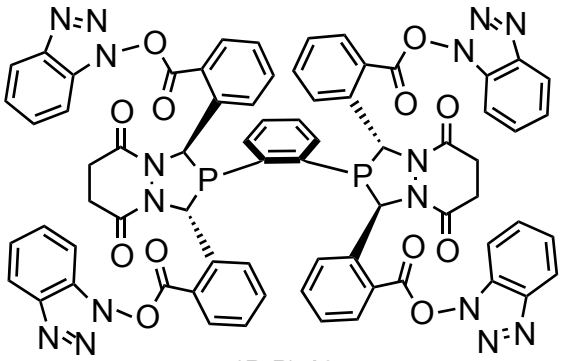

(*R*,*R*)-**10**

(*R*,*R*)-**10** was isolated in 62% yield from silica gel chromatography using 2:1 ethyl acetate:dichloromethane column conditions. ^{1}H NMR (300 MHz, $CDCl_3$) δ: 2.26 – 3.04 (m, C(O)CH_2CH_2C(O), 8 H), 6.08 – 6.39 (m), 6.45 (d, J = 7.8 Hz), 6.71 – 6.78 (m), 6.86 – 6.91 (m), 7.05 – 7.18 (m), 7.22 – 7.48 (m), 7.44 – 7.52 (m), 7.57 – 7.66 (m), 7.71 – 7.78 (m), 7.89 – 7.97 (m), 8.11 – 8.15 (m), 8.22 – 8.25 (m). ^{13}C NMR (75 MHz, $CDCl_3$) δ: 29.3 (s, C(O)*C*H_2CH_2C(O)), 29.7 (s, C(O)*C*H_2CH_2C(O)), 54.1 (t, J = 4.7 Hz, P*C*HN), 58.4 (t, J = 19.8

Hz, P*C*HN), peaks 105-145 have not been assigned, 162.3 (s, *C*(O)O), 162.7 (s, *C*(O)O), 164.9 (s, *C*(O)NN), 167.9 (s, *C*(O)NN). $^{31}P\{^{1}H\}$ NMR (120 MHz, $CDCl_3$) δ: 0.4 (s). HRMS-ESI (m/z): $[M + Na]^+$ calcd for $C_{70}H_{48}N_{16}NaO_{12}P_2$, 1389.3006; found, 1389.2952 (Δ = 3.9 ppm).

General protocol for asymmetric hydroformylation for one-pot AHF of vinyl acetate, styrene, and allyloxy-tert-butyldimethylsilane

An oven dried 15 mL Ace Glass pressure bottle and magnetic stir bar was charged with solutions of $Rh(acac)(CO)_2$ (2.4 μmols; toluene), bisdiazaphospholane ligand (2.9 μmols; THF), and substrates (0.94 mmols of styrene, vinyl acetate, and allyloxy-*t*-butyldimethylsilane) using a 1000μL Dependent® pipette in a dinitrogen filled glove box. The assembled reactor was removed from the glovebox, placed in the fume hood, connected to the synthesis gas source, and taken through 5 cycles of pressurization (150 psig of 1:1 H_2:CO)/depressurization(0 psig) to replace the dinitrogen atmosphere with synthesis gas. A carbon monoxide detector is installed near the gas cylinder. The pressure tube portion of the reactor was then submerged in a heated silicon oil bath at 60°C for four hours. The reactor was depressurized and a sample of reaction solution was dissolved in d^8-toluene for proton (^{1}H) NMR, and a ~100μL aliquot was diluted with 2 mL of toluene for chiral GC analysis.

3.7 References

(1) Thayer, A. *Chem. Eng. News* **2005**, *83*, 7.

(2) Klosin, J.; Landis, C. R. *Acc. Chem. Res.* **2007**, *40*, 1251-1259.

(3) Clark, T. P.; Landis, C. R.; Freed, S. L.; Klosin, J.; Abboud, K. A. *J. Am. Chem. Soc.* **2005**, *127*, 5040-5042.

(4) Watkins, A. L.; Hashiguchi, B. G.; Landis, C. R. *Org. Lett.* **2008**, *10*, 4553-4556.

(5) McDonald, R. I.; Wong, G. W.; Neupane, R. P.; Stahl, S. S.; Landis, C. R. *J. Am. Chem. Soc.* **2010**, *132*, 14027-14029.

(6) Watkins, A. L.; Landis, C. R. *Org. Lett.* **2011**, *13*, 164-167.

(7) Wong, G. W.; Adint, T. A.; Landis, C. R. *Org. Synth.* **2012**, *89*, 243-254.

(8) Thomas, P. J.; Axtell, A. T.; Klosin, J.; Peng, W.; Rand, C. L.; Clark, T. P.; Landis, C. R.; Abboud, K. A. *Org. Lett.* **2007**, *9*, 2665-2668.

(9) Worthy, A. D.; Joe, C. L.; Lightburn, T. E.; Tan, K. L. *J. Am. Chem. Soc.* **2010**, *132*, 14757-14759.

(10) Zhang, X.; Cao, B.; Yu, S.; Zhang, X. *Angew. Chem. Int. Ed.* **2010**, *49*, 4047-4050.

(11) Joe, C. L.; Tan, K. L. *J. Org. Chem.* **2011**, *76*, 7590-7596.

(12) Clemens, A. J. L.; Burke, S. D. *J. Org. Chem.* **2012**, *77*, 2983-2985.

(13) Noonan, G. M.; Fuentes, J. A.; Cobley, C. J.; Clarke, M. L. *Angew. Chem. Int. Ed.* **2012**, *51*, 2477-2480.

(14) Risi, R. M.; Burke, S. D. *Org. Lett.* **2012**, *14*, 2572-2575.

(15) Risi, R. M.; Burke, S. D. *Org. Lett.* **2012**, *14*, 1180-1182.

(16) Axtell, A. T.; Cobley, C. J.; Klosin, J.; Whiteker, G. T.; Zanotti-Gerosa, A.; Abboud, K. A. *Angew. Chem. Int. Ed.* **2005**, *44*, 5834-5838.

(17) Clark, T.; Landis, C. *Tetrahedron: Asymmetry* **2004**, *15*, 2123-2137.

(18) Burk, M. J. *J. Am. Chem. Soc.* **1991**, *113*, 8518-8519.

(19) Burk, M. J. *Acc. Chem. Res.* **2000**, *33*, 363-372.

(20) Landis, C. R.; Jin, W.; Owen, J. S.; Clark, T. P. *Angew. Chem. Int. Ed.* **2001**, *40*, 3432-3434.

(21) Clark, T. P.; Landis, C. R. *J. Am. Chem. Soc.* **2003**, *125*, 11792-11793.

(22) Cobley, C. J.; Klosin, J.; Qin, C.; Whiteker, G. T. *Org. Lett.* **2004**, *6*, 3277-3280.

Chapter 4

Rhodium-Catalyzed Enantioselective Hydroformylation of O-Functionalized Alkenes

Portions of this chapter is published in:

McDonald, R. I.; Wong, G. W.; Neupane, R. P.; Stahl, S. S.; Landis, C. R. *J. Am. Chem. Soc.* **2010**, *132*, 14027-14029.

Wong, G. W.; Adint, T. A.; Landis, C. R. *Org. Synth.* **2012**, *89*, 243-254.

Acknowledgement: Dr. Richard I. McDonald and Mr. Ram P. Neupane performed hydroformylation of *N*-Boc-2-pyrroline (Scheme 4.2) and preliminary hydroformylation experiments (in Table 4.1) respectively, described in this chapter.

4.1 Introduction

Perfect atom economy, fast rates, and high turnover numbers under mild conditions as well as the synthetic utility of the aldehyde products enable rhodium-catalyzed alkene hydroformylation to be one of the largest homogeneous metal-catalyzed processes, producing billions of pounds of achiral aldehydes per year.[1] In contrast, *enantioselective* hydroformylation is underdeveloped. Relatively few chiral rhodium catalysts effect high selectivity and useable rates for a broad range of substrates.[2-7] Chiral aldehydes are versatile synthetic intermediates, and new catalysts capable of selective asymmetric hydroformylation (AHF) could dramatically impact the synthesis of chiral molecules on research and production scales. We recently demonstrated that bis-3,4-diazaphospholanes, produced in two steps from 1,2-bisphosphinobenzene and azine, and $Rh(acac)(CO)_2$ catalyze highly selective hydroformylation of vinyl acetate, allyl cyanide, and styrene derivatives with turnover frequencies approaching 20 000 h^{-1} under mild reaction conditions.[8-10] Takaya and Nozaki first reported AHF of allyl alcohols using (*R*,*S*)-Binaphos, a hybrid phosphine-phosphite ligand, to yield synthetically useful 1,3-alkoxyaldehydes in low regio- and enantioselectivity in the desired branched product (Scheme 4.1).[11] Examples of 1,3-alkoxyaldehydes include "Roche Aldehydes" find prominent use in the total syntheses.

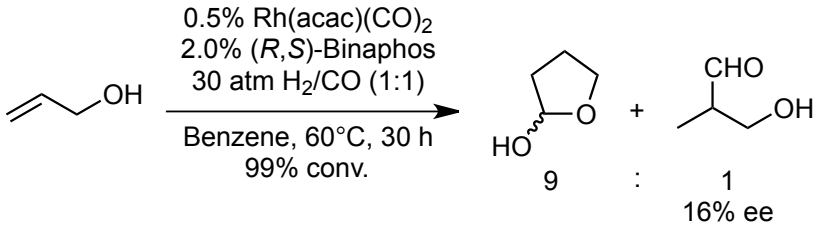

Scheme 4.1. Rh-catalyzed AHF of allyl alcohol using (*R*,*S*)-Binaphos ligand.

4.2 Rh-Catalyzed Highly Enantioselective Hydroformylation of Allyl Ethers

Diazaphospholane ligands are effective for the AHF of O- and N-functionalized allyl substrates. Regioselective control for these alkenes is challenging; prior work has demonstrated a high preference for the achiral linear aldehyde.[11] For example, the AHF of allyl alcohol using the phosphine-phosphite ligand BINAPHOS yields a 1:9 ratio of branched to linear aldehyde and affords the α-aldehyde in 16% ee.[11] With diazaphospholane ligand **1** (Figure 4.1), AHF of allyl alcohol proceeds in 95% enantioselectivity, although the regioselectivity still favors the linear aldehyde in a 1:3.4 branched-to-linear ratio (Table 4.1, entry 1). Analogous allyl *ethers*, however, react with much higher levels of selectivity. Silyl ethers and the phenyl ether react in 99% conversion to afford the chiral 1,3-alkoxyaldehydes with excellent enantioselectivity (96-97%, entries 2-4) and increased levels of regioselectivity (up to 2.6:1). Substituted allyl alcohols undergo facile and effective AHF: trimethyl silyl protected cis-crotyl alcohol reacts with complete conversion in 15 hours at 40°C (entry 5). The products of these reactions are 1,3-alkoxy- and 1,3-silyloxyaldehydes, which are common starting materials for the synthesis of biologically active compounds.[12-15] AHF of allyl silyl ethers with **1** as the ligand proceed with turnover frequencies > 2000 h-1 and turnover numbers exceeding 10 000 at 80 °C.[16] Because of the low cost of allyl alcohol, a commodity chemical, and low catalyst loadings, AHF provides an attractive route to the Roche aldehyde. High pressure is not a prerequisite for effective AHF. For example, AHF of the TBS allyl ether (Table 2, entry 3) at standard loadings and reaction times, but gas pressures of 15 psig and 60 psig *yields complete conversion to aldehydes with selectivities identical to those of reactions performed at 140 psig*.

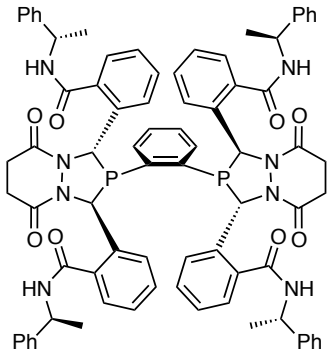

(*S*,*S*,*S*)-Bisdiazaphos **1**

Figure 4.1 Bisdiazaphopholane **1** used in Rh-catalyzed AHF.

Many other synthetically valuable aldehydes are accessible via AHF. For example, 1,3-aminoaldehydes are synthesized from Cbz-protected allyl amine in 86% enantioselectivity with increased levels of regioselectivity relative to the allyloxy substrates (entry 6). Hydroformylation of α,β-unsaturated carbonyl substrates commonly results in high levels of olefin hydrogenation. This limitation may be overcome, however, by protecting the carbonyl group of acrolein and methyl vinyl ketone as a dioxolane. Hydroformylation of the acrolein derivative with ligand **1** gives the desired aldehyde in 92% ee (entry 7) and 4.2:1 regioselectivity; even higher regioselectivity (7:1) is obtained with acrolein protected as the diacetoxy acetal (entry 9). Similarly useful results were obtained for the vinyl ketone derivative (entry 8). Hydroformylation uniquely provides rapid access to synthetically useful malondialdehyde and related dicarbonyls that are chiral and stable by virtue of having one masked carbonyl and one aldehyde functionality.

Table 4.1 AHF of allyl alcohol, carbamate, ethers, acrylates and related analogues.

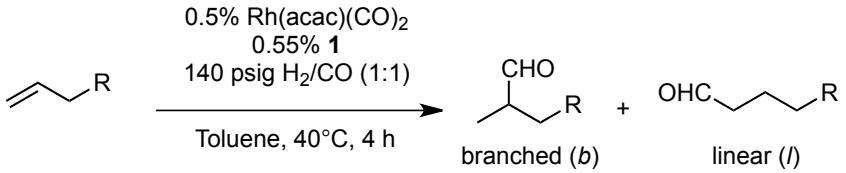

	Alkene	% conv[b]	b:l	% ee[c]
1	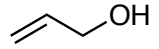	99	1:3.4	95
2	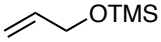	99	2.0:1	97
3	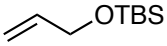	99	2.0:1	96
4	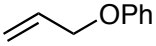	99	2.6:1	96
5	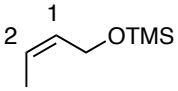	99[d]	2.8:1[e]	94[f]
6	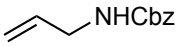	99	4.4:1	86
7	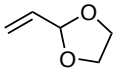	99	4.2:1	92
8	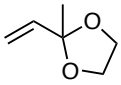	99	2.3:1	96
9	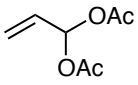	99[g]	7.1:1	93

a. CO/H_2 = 1:1, [alkene] = 0.75 M in toluene. b. Determined via ^1H NMR spectroscopy. c. See supporting information for determination of enantiomeric excess. d. 15 hour reaction time. e. 1-formyl:2-formyl ratio. f. 1-formyl product. g. 18 hours, 0.04% $Rh(acac)(CO)_2$, [diacetoxypropene] = 1M. Product contained ~25% 1,3-diacetoxy-2-methylprop-1-ene.

Enantioselective hydroformylation of heterocycles lead to useful chiral carbaldehydes. For example, AHF of Boc-protected five-membered nitrogen heterocycles, 2- and 3-pyrroline exhibited desirable of regio- (Scheme 4.2, 10.4:1 vs. 1:15 1-formyl:2-formyl ratio, respectively) and enantioselectivity (97% and 91% ee). These aldehydes constitute precursors to proline and β-proline amino acids.

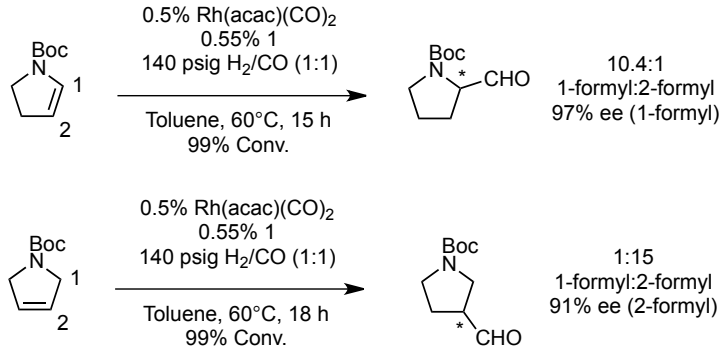

Scheme 4.2 AHF of Boc-protected 2- and 3-pyrroline using bisdiazaphospholane **1**.

4.3 Five-Gram Hydroformylations of Allyloxy-*tert*-butyldimethylsilane and 2-Vinyl-1,3-Dioxolane

Protected "Roche Aldehydes" (e.g., (2*R*)-3-[[(1,1-dimethylethyl)dimethylsilyl]oxy]-2-methylpropanal) are common starting materials for the synthesis of polyketides and related molecules.[17-21] Compared with the common reduction-to-alcohol-followed-by-selective-oxidation-to-aldehyde route to (2*R*)-3-[[(1,1-dimethylethyl)dimethylsilyl]oxy]-2-methylpropanal from "Roche Ester", hydroformylation of the protected commodity monomer, allyl alcohol, provides Roche Aldehyde derivatives rapidly, at low cost, and in an easily scalable process (Scheme 4.3). For comparison purposes we have collected the following approximate costs of substrates, normalized to 25 g units, from a common supplier: Roche ester ($350/25g), allyl alcohol ($1.00/25g). The only byproducts of the enantioselective hydroformylation of allyl ethers

is the corresponding linear aldehyde; although achiral the linear aldehyde is isolated cleanly and constitutes a useful synthetic material also. On larger scales, it should be possible to separate the linear and branched aldehydes by careful vacuum distillation; we have not yet optimized the distillation conditions. An advantage of hydroformylation routes to chiral aldehydes is the absence of acids or bases in the reaction solution that catalyze racemization and condensation reactions. We note that although the Roche *Ester* has been synthesized by asymmetric hydrogenation of the methyl 2-(hydroxymethyl)-prop-2-enoate,[22-27] there is no report of a catalytic hydrogenation route to enantiopure Roche *Aldehyde*.

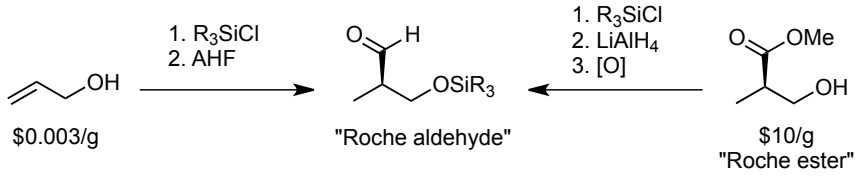

Scheme 4.3 AHF as an alternative route to Roche aldehyde.

Hydroformylation of five grams of allyloxy-*t*-butyldimethylsilane using 0.020 mol% of $Rh(acac)(CO)_2$ and 0.024 mol% of bisdiazaphospholane **1** in a pressure bottle, produces TBS-protected Roche aldehyde [**3**, (2*R*)-3-[[(1,1-dimethylethyl)dimethylsilyl]oxy]-2-methylpropanal, Scheme 4.4] in 45% yield after silica gel chromatography. High levels of enantioselectivity were observed (90-94% ee) in synthesis of the Roche aldehyde from enantioselective hydroformylation of allyl silyl ether. Checkers of this procedure with *Organic Syntheses* reported 55-58% isolated yield and 94-96% ee of the Roche aldehyde using a Symyx Heated Orbital Shaker System.

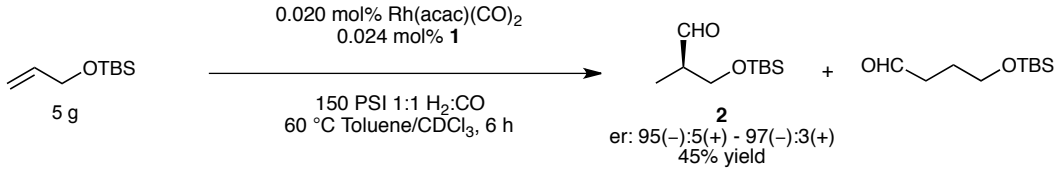

Scheme 4.4 Five-gram hydroformylation of allyloxy-*t*-butyldimethylsilane.

Rhodium-catalyzed AHF of 2-vinyl-1,3-dioxolane yield (2*S*)-2-(1,3-dioxolan-2-yl)-propanal (**3**, Scheme 4.5) in moderate yields (71-74% isolated yield) and in high enantioselectivity (92-95% ee). The synthesis of (2*S*)-2-(1,3-dioxolan-2-yl)-propanal and use as a chiral building block enables potential for fewer functional group manipulations in total syntheses. The chiral desymmetrized methylmalonaldehyde is set-up to undergo facile deprotection for further modification and elaboration in polyketide and related natural product synthesis.

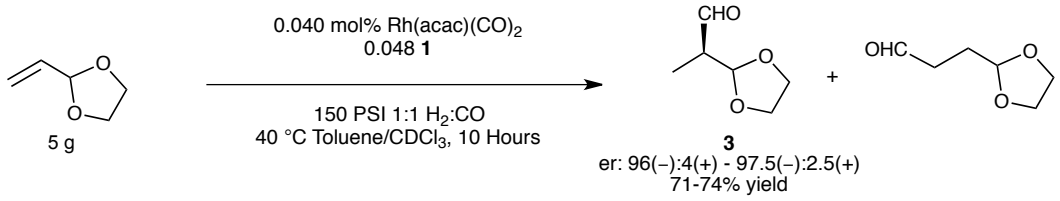

Scheme 4.5 AHF of 2-vinyl-1,3-dioxolane on a five-gram scale.

4.4 General Considerations for Gram-Scale AHF

High Purity Reagents. Optimizing hydroformylations to very low catalyst loadings (e.g., 0.05 mol% of catalyst or lower) require the solvents and alkene to be at their highest possible purity: distill and degas samples. Because small amounts of poison could kill the catalyst in scale-up experiments, success depend on purity of starting materials and solvent used.

Catalyst Activation. For more reliable catalysis, reaction of $Rh(acac)(CO)_2$, bisdiazaphospholane, syngas, and in the absence of alkene at 50-60°C for half an hour produces more robust catalysts. After activation, injection of the alkene sample to proceed normally with hydroformylation. In many situations this is the preferred procedure because the catalyst precursors are sensitive to poisons while active catalysts are comparatively more robust.

Less Solvent. Generally, the use of higher concentrations of alkene is preferred because the rate of hydroformylation is first order in alkene with Rh-bisdiazaphospholane catalysts. In most situations, hydroformylation selectivity is unaffected by alkene concentration. Hydroformylations can be performed neat in alkene but solubility is often a concern using rhodium-diazaphospholane catalysts. Typically small amounts of an aprotic polar organic solvent (e.g., THF, chloroform, and dichloromethane) are commonly used in solubilizing the ligand.

Gas-Liquid Mixing. Vigorous mixing of the reaction solution is required in hydroformylation to obtain sufficient gas-liquid mixing for effective concentrations of dihydrogen and carbon monoxide. Since mass-transport of the gas dissolution into the liquid phase is a realistic possibility, vigorous mixing is recommended in gram-scale reactions (to maximize reactor surface area-liquid contact).

Troubleshooting: Aldehyde Racemization. There are a few possibilities that could lead to racemization of the aldehyde: hydroformylation temperature and pH of the reaction solution. Although higher temperature leads to better AHF activity, diminished regioselectivity and or

enantioselectivity could result in some situations. Lower temperatures (40−60°C) are typically preferred for substrates without strong σ-electron withdrawing groups (e.g. some allylic substrates). Some substrates use Brønsted acids or bases in their synthesis; small amounts of these impurities could racemize α-chiral aldehydes (note: the sensitivity of the aldehydes vary considerably).

4.5 Determination of Absolute Stereochemistry of (2*S*)-2-(1,3-dioxolan-2-yl)-Propanal 3

The absolute stereochemical determination of 2-(1,3-dioxolan-2-yl)-propanal **3**, was determined by way of chemical transformation to an molecule with known stereochemistry. TBS-protected Roche Aldehyde (*R*)-**2** was subjected to ethylene glycol with 20% PPTS in refluxing toluene resulting in an ethylene diacetal-protected Roche Aldehyde (*R*)-**5**. To obtain the same derivative from 2-(1,3-dioxolan-2-yl)-propanal **3**, a sample was reduced with sodium borohydride, followed by alcohol protection with *tert*-butyldimethylsilyl chloride, resulting in **5** in unknown configuration. Optical rotation was obtained for both samples of **5**, resulted in the assignment of (*S*)-absolute stereochemistry for the derivative made from 2-(1,3-dioxolan-2-yl)-propanal **3** (Scheme 4.6). To confirm this assignment, (2*S*)-2-(1,3-dioxolan-2-yl)-propanal was condensed with 2,4-dinitrophenylhydrazine forming (2*S*)-2-(1,3-dioxolan-2-yl)-propanal 2,4-dinitrophenylhydrazone **6** in ethanol resulting in X-ray diffraction-quality crystals. The structure of (2*S*)-2-(1,3-dioxolan-2-yl)-propanal 2,4-dinitrophenylhydrazone **6** (Figure 4.2) confirmed the assignment from optical rotation measurements.

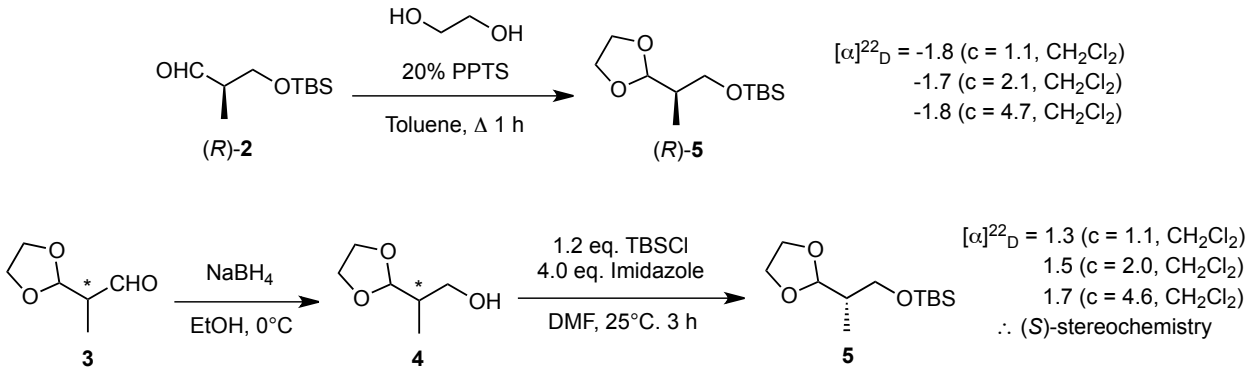

Scheme 4.6 Chemical transformation of 2-(1,3-dioxolan-2-yl)-propanal **3** to a common stereochemical intermediate **5** (ethylene diacetal protected "Roche Aldehyde").

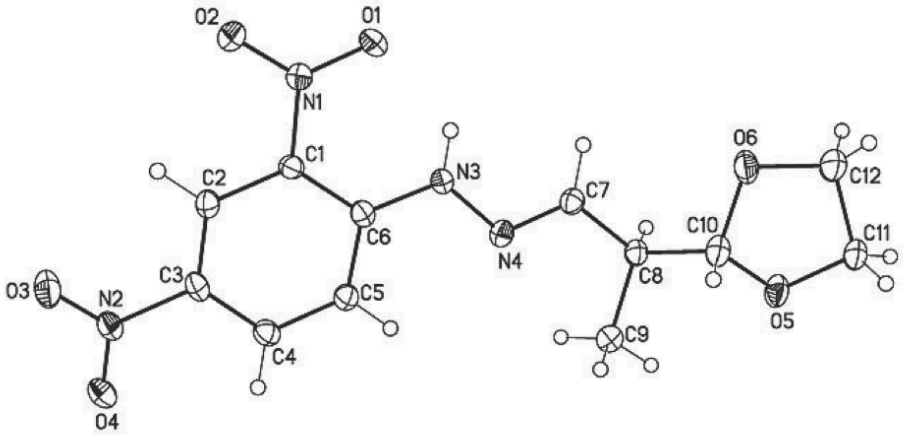

Figure 4.2 ORTEP drawing of (2*S*)-2-(1,3-dioxolan-2-yl)-propanal 2,4-dinitrophenylhydrazone **6**. Thermal ellipsoids are drawn at the 50% probability level.

This assignment reinforces the facial preference of the active hydroformylation catalyst: diastereoselective hydride addition into the coordinated olefin occurs on the same face for vinyl acetate, styrene, allyl cyanide, allyloxy-t-butyl-dimethylsilane and 2-vinyl-1,3-dioxolane using (*S*,*S*,*S*)-bisdiazaphospholane **1**.

4.6 Conclusions

Enantioselective hydroformylation with diazaphospholane ligands enables scalable atom-efficient synthesis of chiral amino- and alkoxyaldehydes from simple substrates under mild conditions. Allyl ethers and silyl ethers hydroformylate using rhodium-diazaphospholane catalysts accesses useful 1,3-alkoxyaldehydes in 92-97% ee; a prominent example includes "Roche aldehyde." Hydroformylation of related analogues, protected acrolein and acrylates, yield the desired branched aldehyde in higher regioselectivity compared to allyl ethers (up to 7.1:1 vs. 2.0:1). Hydroformylation of *N*-Boc pyrrolines yield chiral carbaldehydes analogous to proline and β-proline. Hydroformylations of allyloxy-*t*-butyldimethylsilane and 2-vinyl-1,3-dioxolane on five-gram scale, demonstrate the synthesis of practical amounts of "Roche aldehyde" and related analogues as a feasible alternative to existing procedures. These results extend the range of chiral aldehydes that can be practically and effectively produced by asymmetric hydroformylation and used in the synthesis of more complex organic molecules.

4.7 Experimental

General Considerations.

All commercially available compounds were used as received. Solvents were distilled over Na/benzophenone prior to use. For hydroformylation reactions, dried solvents were further deoxygenated by three freeze-thaw cycles, then taken into a nitrogen filled glove box. $Rh(acac)(CO)_2$ was recrystalized from toluene/hexanes (green needles) prior to use. ^{1}H and ^{13}C NMR spectra were recorded on Bruker or Varian 300 MHz spectrometers. The chemical shifts are given in parts per million relative to internal TMS (0.00 ppm for 1H) or $CDCl_3$ (77.23 ppm

for ^{13}C). Silica gel chromatography was performed using Siliaflash Å silica gel (Silicyle, particle size 40–63 μm, 230–400 mesh). Optical rotations were measured using a 1 mL cell with a 0.5 dm path length on a Randolph digital polarimeter. Chiral gas chromatography (GC) analysis was performed on a Varian Chrompack system using commercial Supelco columns. Chiral super critical fluid chromatography (SFC) analysis was performed on a Berger analytical supercritical fluid chromatograph with commercial Chiralpak columns. Carbon monooxide and synthesis gas (custom H_2/CO 1:1 mixture) cylinders were used without further manipulation from Airgas, Inc.

Proton (^1H) NMR spectra was collected on a Varian MercuryPlus 300 or a Bruker AC+ 300 spectrometer and referenced to tetramethylsilane (TMS). Carbon (^{13}C) NMR spectra was obtained on a Varian MercuryPlus 300 spectrometer and referenced to $CDCl_3$ (77.23 ppm). Splitting patterns from spectra were denoted as follows: single (s), doublet (d), triplet (t), quartet (q), pentet, and sextet. Non-first order splitting was denoted as (m) for a multiplet.

Caution! Carbon monoxide is a highly toxic gas and manipulations should be conducted in a well-ventilated fume hood in the vicinity of a carbon monoxide detector. Hydrogen gas is highly flammable and explosive gas. Precautions should be taken when using synthesis gas (H_2/CO mixtures).

General protocol for asymmetric hydroformylation of oxygen-containing substrates

An oven dried 15 mL Ace Glass reaction tube and magnetic stir bar was charged with solutions of $Rh(acac)(CO)_2$, followed by Bis[(*S*,*S*,*S*)-DiazaPhos-SPE], alkene substrate (typically 1.0 mmol), and toluene using a 1000μL Eppendoft® pipette in a dinitrogen filled glove box. The assembled reactor was removed from the glovebox, clamped down in a fume hood, connected to

the synthesis gas source, and taken through 5 cycles of pressurization (150 psig of 1:1 H_2:CO)/depressurization (0 psig) (Figure 4.4). The pressure tube portion of the reactor was then submerged in a heated silicon oil bath at the desired temperature. At the end of the reaction time, the reactor was removed from the oil bath, cooled, and depressurized. A sample of reaction solution was dissolved in d^8-toluene for proton (^{1}H) NMR for percent conversion and a ~100μL aliquote was diluted with toluene for chiral GC analysis.

Literature protocols were followed for the synthesis of allyloxy-*t*-butyldimethylsilane,[28] 2-methyl-2-vinyl-1,3-dioxolane,[29] *N*-(benzyloxycarbonyl) allylamine,[30] and *N*-Boc-3-pyrroline.[31] Characterization data for aldehydes (2*R*)-3-[[(1,1-dimethylethyl)dimethylsilyl]oxy]-2-methylpropanal (*R*)-**2** and (2*S*)-2-(1,3-dioxolan-2-yl)-propanal (*S*)-**3** can be found in the "General protocol for five gram asymmetric hydroformylation reactions."

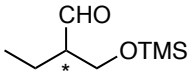

^{1}H NMR (300 MHz, $CDCl_3$): δ 0.11 (s, 9H), δ 0.95 (t, J = 7.8 Hz, 3H), δ 1.45-1.62 (m, 1H), δ 1.63-1.76 (m, 1H), δ 2.32-2.47 (m, 1H), δ 3.75-3.87 (m, 2H), δ 9.70 (d, J = 2.4 Hz, 1H). ^{13}C NMR (75 MHz, $CDCl_3$): δ –0.45, δ 11.6, δ 18.9, δ 55.9, δ 61.2, δ 205.0. HRMS: m/z (ESI) calculated $[M+Na]^+$ = 197.0969, measured 197.0972 (Δ < 1.5 ppm). Enantiomeric excess was determined to be 94% by chiral GC analysis (β-DEX 225, 70 °C, isothermal); $t_{R(major)}$ = 20.5 min., $t_{R(minor)}$ = 21.2 min.

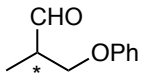

^{1}H NMR (300 MHz, $CDCl_3$): δ 1.26 (d, J = 7.5 Hz, 3H), δ 2.8 – 2.9 (m, 1H), δ 4.14 (dd, J = 5.3,

9.5 Hz, 1H), δ 4.20 (dd, J = 6.4, 9.5 Hz, 1H), δ 6.9 – 7.0 (m, 3H), δ 7.2 – 7.3 (m, 2H), δ 9.81 (d, J = 1.8 Hz, 1H). ^{13}C NMR (75 MHz, $CDCl_3$): δ 11.0, δ 46.5, δ 67.9, δ 114.8, δ 121.4, δ 129.7, δ 158.8, δ 203.2. HRMS: m/z (ESI) calculated $[M+Na]^+$ = 187.0730, measured, 187.0733 (Δ = 1.6 ppm). Gas chromatographic analysis was performed on a Varian Chrompack system using a β-DEX 225 capillary column from Supelco, 30 m x 0.25 mm ID x 0.25 mm film thickness. The analytical method used to resolve the enantiomers as follow: 120˚C hold for 40 minutes, $t_{R(major)}$ = 27.6 min., $t_{R(minor)}$ = 28.2 min. on chiral GC.

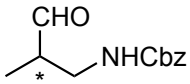

^{1}H NMR (300 MHz, $CDCl_3$): δ 1.15 (d, J = 7.2 Hz, 3H), δ 2.60-2.69 (m, 1H), δ 3.31-3.47 (m, 2H), δ 5.04 (broad s, 1H), δ 7.29-7.39 (m, 5H), δ 9.67 (broad s, 1H). ^{13}C NMR (75 MHz, $CDCl_3$): δ 11.5, δ 41.2, δ 47.2, δ 67.0, δ 128.3, δ 128.4, δ 128.7, δ 136.6, δ 156.7, δ 204.0. HRMS: m/z (ESI) calculated $[M+Na]^+$ = 244.0945, measured, 244.0948 (Δ = 1.2 ppm). $NaBH_4$ reduction to form the alcohol was required to determine the enantiomeric excess, which was 86% by chiral SFC analysis (Chiralpak OD-H, 3% MeOH for 5 min, then 20% MeOH at a rate of 0.5 %/min, 3.0 mL/min, = 254 nm); $t_{R(major)}$ = 19.4 min., $t_{R(minor)}$ = 20.1 min.

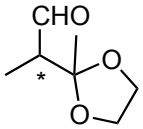

^{1}H NMR (300 MHz, $CDCl_3$): δ 1.13 (d, J = 6.9 Hz, 3H), δ 1.31 (s, 3H), δ 2.65 (qd, J = 7.2, 1.8 Hz, 1H), δ 3.9-4.1 (m, 4H), δ 9.77 (d, J = 1.8 Hz, 1H). ^{13}C NMR (75 MHz, $CDCl_3$): δ 9.4, δ 22.5, δ 54.6, δ 64.9, δ 65.1, δ 101.4, δ 203.5. HRMS: m/z (ESI) calculated $[M+Na]^+$ = 167.0679,

measured, 167.0671 (Δ = 4.8 ppm). Gas chromatographic analysis was performed on a Varian Chrompack system using a β-DEX 225 capillary column from Supelco, 30 m x 0.25 mm ID x 0.25 mm film thickness. The analytical method used to resolve the enantiomers as follow: 100˚C hold for 60 minutes, $t_{R(minor)}$ = 10.3 min., $t_{R(major)}$ = 11.2 min. on chiral GC.

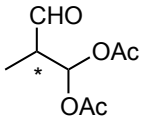

^{1}H NMR (300 MHz, $CDCl_3$): δ 1.18 (d, J = 7.2 Hz, 3H), δ 2.10 (s, 3H), δ 2.11 (s, 3H), δ 2.84 (qdd, J = 7.2, 4.2, 1.5 Hz, 1H), δ 7.06 (d, J = 4.2 Hz, 1H), δ 9.79 (d, J = 1.5, 1H). ^{13}C NMR (75 MHz, $CDCl_3$): δ 8.6, δ 20.8, δ 20.9, δ 49.6, δ 89.5, δ 168.8, δ 168.9, δ 200.0. HRMS: m/z (ESI) calculated $[M+NH_4]^+$ = 206.1023, measured, 206.1024 (Δ < 1 ppm). $[\alpha]^{22}_D$ = -31.0 (c = 1.0, CH_2Cl_2). Gas chromatographic analysis was performed on a Varian Chrompack system using a β-DEX 225 capillary column from Supelco, 30 m x 0.25 mm ID x 0.25 mm film thickness. The analytical method used to resolve the enantiomers as follow: 100˚C hold for 60 minutes, $t_{R(major)}$ = 25.3 min., $t_{R(minor\ enantiomer)}$ = 25.9 min. on chiral GC.

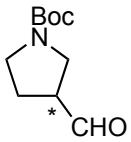

^{1}H NMR (300 MHz, $CDCl_3$): δ 1.46 (s, 9H), δ 2.0 – 2.3 (m, 2H), δ 2.90 – 3.10 (m, 1H), δ 3.2 – 3.8 (m, 4H), δ 9.70 (d, J = 1.5, 1H); ^{13}C NMR (75 MHz, $CDCl_3$): δ 25.6, δ 26.0, δ 28.7, δ 45.0, δ 45.3, δ 49.9, δ 50.8, δ 79.9, δ 154.5, δ 200.8; $[\alpha]^{22}_D$ = −24.7 (c = 1.02, CH_2Cl_2). HRMS: m/z (ESI) calculated $[M+H]^+$ = 199.1203, measured, 199.1193 (Δ = 5 ppm). Gas chromatographic

analysis was performed on a Varian Chrompack system using a β-DEX 225 capillary column from Supelco, 30 m x 0.25 mm ID x 0.25 mm film thickness. The analytical method used to resolve the enantiomers as follow: 125˚C hold for 70 minutes, $t_{R(major)}$ = 60.9 min., $t_{R(minor\ enantiomer)}$ = 62.9 min on chiral GC.

General protocol for five-gram asymmetric hydroformylation reactions

In a dinitrogen filled glovebox, a 185 mL Ace Glass reaction tube and magnetic stir bar (Note 1) was charged with solutions of $Rh(acac)(CO)_2$ (Note 2) followed by Bis[(S,S,S)-DiazaPhos-SPE] (Note 3) using a 1000μL Eppendoft® pipette. Five grams of substrate (Note 4) were weighed in a vial and added to the light yellow catalyst solution (Note 5). The vial was rinsed with 200 μL of toluene and the reaction tube was attached to the reactor head (Note 6). The assembled reactor was removed from the glovebox, placed in the fume hood, connected to the synthesis gas source (Note 7), and taken through 5 cycles of pressurization (150 psig of 1:1 H_2:CO)/depressurization (0 psig) to replace the dinitrogen atmosphere with synthesis gas (Note 8, Figure 2). The reactor was then submerged in a heated silicon oil bath (Note 9) at the desired temperature. As synthesis gas was consumed, the reactor was repressurized to 150 psi to maintain approximately constant pressure (Note 10). At the end of the reaction time, the reactor was depressurized. A sample of reaction solution was checked by proton (^{1}H) NMR to assure >99% conversion of alkene, and reaction product was subjected to flash column chromatography without further manipulation. Details can be found for each substrate below:

Synthesis of (2*R*)-3-[[(1,1-dimethylethyl)dimethylsilyl]oxy]-2-methylpropanal (*R*)-2

A substrate to catalyst ratio of 5,000:1 enables quantitative hydroformylation of allyloxy-*tert*-butyldimethylsilane, at 60˚C in a convenient 6 hour reaction time. The following amount of reagents were used: 290 μL of a 20 mM toluene solution of $Rh(acac)(CO)_2$ (0.0058 mmols), 232 μL of a 30 mM d^1-chloroform solution of ligand **1** (0.0070 mmols), and 5g of allyloxy-*tert*-butyldimethylsilane (29.0 mmols). Notably, the addition of the alkene to the catalyst solution resulted in a yellow-white suspension due to partial precipitation of ligand and/or catalyst-ligand complex. After 2-3 hours (~30-40 psi of synthesis gas consumed) the suspension transformed to a homogeneous yellow solution. In six hours, ~90 psi of synthesis was consumed. Proton (^1H) NMR of the crude product mixture revealed 64% to 67% yield of branched aldehyde and >99% conversion of alkene (b:l, 1.8:1 to 2.0:1). The hydroformylation reaction mixture was purified immediately (Note 11) by flash column chromatography (Note 12). Colorless oils of (*R*)-**2** (2.64 g, 45% isolated yield, Note 13) and the linear aldehyde (1.69 g, 29% isolated yield) resulted. Typically, the percent enantiomeric excess of **2** was 95-97% after chromatography (Note 14). The aldehyde can be stored at -5˚C in air with less than 10% oxidation.

Synthesis of (2*S*)-2-(1,3-dioxolan-2-yl)-Propanal (*S*)-3

Convenient conditions for the hydroformylation of 2-vinyl-1,3-dioxolane (Note 15) comprise a 2500:1 substrate to catalyst ratio, a reaction temperature of 40˚C and a 10 hour reaction time. The following reagent quantities were used: 1000 μL of a 20 mM solution of $Rh(acac)(CO)_2$ (0.020 mmols), 31 mg of ligand **1** in 500 μL d^1-chloroform (0.024 mmols), and 5g of 2-vinyl-1,3-dioxolane (50.0 mmols). The reaction solution was yellow and homogeneous after addition of alkene to catalyst solution. After reaction at 40˚C for 10 hours, during which ~180 psi of synthesis gas was consumed, the reactor was depressurized, disassembled, and the reaction

solution was checked by proton (^{1}H) NMR. Proton (^{1}H) NMR of the crude product mixture revealed 75% to 81% yield of branched aldehyde and complete conversion of alkene to aldehydes (b:l, 3.0:1 to 4.3:1). The crude product was purified by flash column chromatography (Note 16). Two colorless oils resulted: **3** (4.63-4.81g, 71-74 % isolated yield, Note 17) and the linear aldehyde (1.25-1.77 g, 19-27 % isolated yield). The percent enantiomeric excess was typically 92-95% after chromatography (Note 18). The aldehyde can be stored at -5˚C in air without appreciable oxidation (purity remains >95% by ^{1}H NMR two weeks later).

Experimental Notes

1. A Heavy-wall pressure tube/bottle and a 0.5 in. x 0.125 in. magnetic stir bar was dried in a 125˚C oven overnight. Specifically, a #15 Ace-Tread®, 30 cm (length) x 38.1 mm (O.D.) 185 mL capacity (approx.) pressure tube was used (Ace Glass® product #: 8648-33).

2. Dicarbonylacetylacetonato rhodium(I) was recrystallized from toluene and hexanes as fine green crystals. Toluene (≥99.9%) was obtained from Sigma-Aldrich, distilled over sodium benzophenone ketyl under nitrogen, and degassed via 3 freeze-pump-thaw cycles.

3. Bis[(S,S,S)-DiazaPhos-SPE], 2,2′,2″,2‴-(1,2-Phenylenebis[(1S,3S)-tetrahydro-5,8-dioxo-1H-[1,2,4]diazaphospholo[1,2-a]pyridazine-2,1,3(3H)-triyl])tetrakis(N-[(1S)-1-phenylethyl])benzamide, was synthesized as reported.[8] Deuterated chloroform (99.8% atom % D, w/ 0.03 TMS, v/v) was obtained from Aldrich and sparged with dinitrogen prior to use.

4. Allyloxy-*tert*-butyldimethylsilane (97%) was obtained from Aldrich and sparged with dinitrogen prior to use. 2-vinyl-1,3-dioxolane (≥99.0%) was obtained from Fluka, purified by bulb-to-bulb distillation on a vacuum line, and degassed with 3 freeze-pump-thaw cycles prior to use.

5. The addition of allyloxy-*tert*-butyldimethylsilane to the catalyst solution at a 5000:1 substrate to catalyst loading resulted in some precipitation. The addition of 2-vinyl-1,3-dioxolane at a 2500:1 substrate to catalyst loading resulted in a homogeneous yellow solution.

6. A custom-made reactor head used for hydroformylations is shown in Figure 1. The following parts were used to assemble the reactor head: **a**, Alltech® septum (High-temp, 3/8 in., AT79231) for aliquot-abstractions using a gas-tight syringe, **b**, Swagelok® Brass 1-Piece 40 Series Ball Valve (1.6 Cv, 1/4 in. MNPT x 1/4 in. Swagelok Tube Fitting; product #: B-43M4-S4), **c**, Swagelok® Brass Pipe Fitting, Cross (1/4 in. Female NPT; product #: B-4-CS), **d**, Brass Pipe Fitting, Hex Nipple (1/4 in. Male NPT), **e**, Swagelok® Brass Pipe Fitting, Elbow (1/4 in. Female NPT; product #: B-4-E), **f**, Ashcroft® 0-160 psig pressure gauge (1/4 in. NPT, 3.5 in. Dial; McMaster-Carr 3846K311 0-160 psig range), **g**, Brass Pipe Fitting, Close Nipple (1/4 in. Male NPT), **h**, #15 Ace-Thred® (15mm thread, 1/4 in. NPT PTFE Swagelok adapter; Prod. #: 5844-74), **i**, Kalrez® 6375 O-ring (9.30 mm x 2.40 mm Part #: K31016K6375), **j**, #15 Ace Glass® pressure tube (30.5 cm L, 38.1 mm OD, Prod. #: 8648-33), **k**, Swagelok® Brass 1-Piece 40 Series 3-Way Ball Valve (0.75 Cv, 1/4 in. FNPT; product #: B-43XF4), **l**, Brass Pipe Fitting (1/4 in. male NPT to 1/4 in. male Swagelok Tube Fitting), **m**, SS tubing (1/4 in OD, 2 1/2 in. length), and **n**, Swagelok® SS Instrumentation Quick-Connect Stem w/ Valve, (0.2 Cv, 1/4 in. Swagelok Tube Fitting, Part #: SS-QC4-D-400). Threads **b**, **d**, **f**, **g**, and **l** were wrapped with PTFE tape prior to assembly. A thorough pressure check of reactor should be taken before conducting an experiment. The most common source of a leak is between the brass pipe fitting **g** and the plastic #15 Ace-Thred adapter **h**. Once assembled with the 185 mL pressure tube, the reactor is rather cumbersome to transport—the use of an 11.5” (W) x 13.5” (L) x 5.25” (D) Rubbermaid®

dishpan with a 3”(D) x 1” (W) rectangle cut in the tub on the width side was used to partially hold the reactor.

The use of a blast shield is suggested whenever the reactor is pressurized and safety procedures described for pressure tubes in the Ace-Glass® catalog should be observed.

7. A reverse-threaded regulator was connected to a synthesis gas cylinder and used of Swagelok® Quick-Connects to attach to the reactor manifold. The synthesis gas cylinder was obtained from AirGas Inc. as a custom mixture (48.3±2% carbon monoxide balanced with hydrogen gas).

8. The reactor has two possible points of entry: Swagelok® Ball valve **b** fitted with a GC septum, for gas-tight syringe aliquots, and the Swagelok® 3-way Ball Valve **k**, for pressurizing and depressurizing the reactor. In Figure 2, **k** is opened carefully to the synthesis gas cylinder, charging the apparatus to 150 psig (it is advisable to set the regulator on the cylinder to ca. 150 psig and to have a safety shield in place). The valve on **k** is then opened to vent, releasing synthesis gas from the apparatus. After the pressure is reduced to <40 psi, the valve is turned back to the original closed position constituting one cycle. This procedure is repeated for five cycles and the reactor pressure is set at 150 psi. The glass tube of the reactor is lowered into the oil bath for hydroformylation as seen in the far-right picture.

9. Silicone oil was obtained from Sigma-Aldrich and used to fill (approximately halfway) a VWR Pyrex 125 mm x 65 mm crystallization dish. This oil bath was equipped with a heating coil and the temperature was controlled by a Variac.

10. Synthesis gas is added manually to maintain at least 100 psig reactor pressure. It is not advisable to maintain reactor pressure by keeping the reactor open to the regulator on the synthesis gas cylinder because, in the event of a leak on the reactor or supply lines, large amounts of H_2 and CO could be released. A carbon monoxide detector is installed near the gas cylinder. Commonly we detach the synthesis gas line from the reactor at the Swagelok® Quick-Connect during reaction and reconnect when adding more gas. However, if the synthesis gas line is not needed for other reactions, the Swagelok® Quick-Connect system can remain assembled throughout the reaction.

11. Aldehyde (*R*)-**2** is air-sensitive and flash chromatography should be performed immediately after depressurizing the reactor and the purified product stored in a freezer.

12. A 8.0" (L) x 2.0" (I.D.) column was prepared using 200 g 230-400 mesh (40-63μm) of silica gel and eluted with 5% v:v ethyl acetate in hexane [$R_{f,(R)\text{-}\mathbf{2}} = 0.45$, $R_{f,linear} = 0.35$, visualized with potassium permanganate stain]. The eluent was collected in 20 x 150 mm disposable culture tubes as ~30 mL for a total of 48 fractions: 18-29 for (*R*)-**2** and 31-41 for the linear aldehyde. Specifically, Silicycle SiliaFlash® P60 silica gel, 230-400 mesh (40-63μm) was used. Ethyl acetate (≥99.8%) was obtained from Sigma-Aldrich and hexane (≥98.5%) from CCI Chemical. Potassium permanganate stain was prepared as follows: 3 g $KMnO_4$, 20 g potassium carbonate, 5 mL of a 5% (w/w) solution of aqueous sodium hydroxide, and 300 mL of deionized water. Potassium permanganate was obtained from Mallinckrodt Chemicals, potassium carbonate (≥ 99.0%) from Sigma-Aldrich, and sodium hydroxide (99.5%) from Fischer Scientific. This stain was stored at room temperature and away from light.

13. Typically (*R*)-**2** was isolated in ≥95% purity by proton (^{1}H) NMR. The product exhibits the following properties: $[\alpha]_D^{23}$ –34.6 (c 1.0, CH_2Cl_2); ^{1}H NMR (300 MHz, $CDCl_3$) δ: 0.06 (s, -

$Si(CH_3)_2C(CH_3)_3$, 6H), 0.88 (s, -$Si(CH_3)_2C(CH_3)_3$, 9H), 1.10 (d, J = 6.9 Hz, -CHCH_3, 3H), 2.47-2.60 (m, -C$H$$CH_3$, 1H), 3.82 (dd, J = 6.5, 10.2 Hz, -CH_2OSi, 1H), 3.86 (dd, J = 5.2 Hz, 10.2, -CH_2OSi, 1H), 9.74 (d, J = 1.8 Hz, CHO-CH); ^{13}C NMR (75 MHz, $CDCl_3$) δ: –5.33, –5.30, 10.5, 18.4, 26.0, 49.0, 63.7, 204.9; IR (neat): 2957, 2931, 2859, 1736 (C=O), 1473, 1258, 1101, 1033, 838, 778 cm^{-1}; GC-MS (EI, 70 eV) m/z: 202.9 (M^+), 130.0, 119.0, 109.0, 85.0, 83.0 (Major Fragment), 70.0, 47.0; Anal. Calcd. for $C_{10}H_{22}O_2Si$: C, 59.35, H, 10.96. Found: C, 58.78, H, 11.01.

14. Gas chromatographic analysis was performed on a Varian Chrompack system using a β-DEX 225 capillary column from Supelco, 30 m x 0.25 mm ID x 0.25 μm film thickness. The analytical method used to resolve the enantiomers as follow: 65˚C hold for 70 minutes, $t_{R,(R)\text{-}\mathbf{2}}$ = 60.8 min., $t_{R,(S)\text{-}\mathbf{2}}$ = 62.4 min.

15. Increasing the temperature (60˚C) and substrate to catalyst (5000:1) loading, resulted in a slight decrease in percent enantiomeric excess (91%) and branched to linear (2.6:1) ratio.

16. A 8.0” (L) x 2.0” (I.D.) column was prepared using 200 g of 230-400 mesh (40-63μm) silica gel and eluted with 40% v:v diethyl ether in pentane [$R_{f,(S)\text{-}\mathbf{3}}$ = 0.45, $R_{f,linear}$ = 0.35, visualized with potassium permanganate stain]. The eluent was collected in 20 x 150 mm disposable culture tubes as ~30 mL for a total of 48 fractions: 14-28 for (*S*)-**3** and 36-48 for the linear aldehyde. Diethyl ether (anhydrous, 99.9%) was obtained from Fisher Scientific and pentane (98%) from Sigma-Aldrich and used without further purification.

17. Typically (*S*)-**3** was isolated in ≥95% purity by proton (^{1}H) NMR. The product exhibits the following properties: $[\alpha]_D^{22}$ –72.9 (c 2.1, $CHCl_3$); ^{1}H NMR (300 MHz, $CDCl_3$) δ: 1.18 (d, J = 7.2 Hz, -CHCH_3, 3H), 2.74 (qdd, J = 7.2, 4.1, 1.4 Hz, C$H$$CH_3$ 1H), 3.88-4.05 (m, (OCH_2CH_2O)CH, 4H), 5.08 (d, J = 4.1 Hz, (OCH_2CH_2O)CH, 1H), 9.80 (d, J = 1.3 Hz, CHO-CH, 1H); ^{13}C NMR

(75 MHz, $CDCl_3$) δ: 8.9, 50.1, 65.4, 65.5, 104.3, 202.5; IR (NaCl, thin film): 2982, 2888, 2739, 1728 (C=O), 1458, 1402, 1068, 1031, 995, 940 cm^{-1}; GC-MS (EI, 70 eV) m/z: 129.1 (M^+), 115.1, 102.1, 85.1, 73.0 (Major Fragment, $C_3H_5O_2$), 57.1, 45.1; Anal. Calcd. for $C_6H_{10}O_3$: C, 55.37, H, 7.74 Found: C, 54.10, H, 7.82.

18. Gas chromatographic analysis was performed on a Varian Chrompack system using a β-DEX 225 capillary column from Supelco, 30 m x 0.25 mm ID x 0.25 μm film thickness. The analytical method used to resolve the enantiomers as follow: 100˚C hold for 25 minutes, $t_{R,(R)\text{-}\mathbf{2}}$ = 11.3 min., $t_{R,(S)\text{-}\mathbf{2}}$ = 11.5 min.

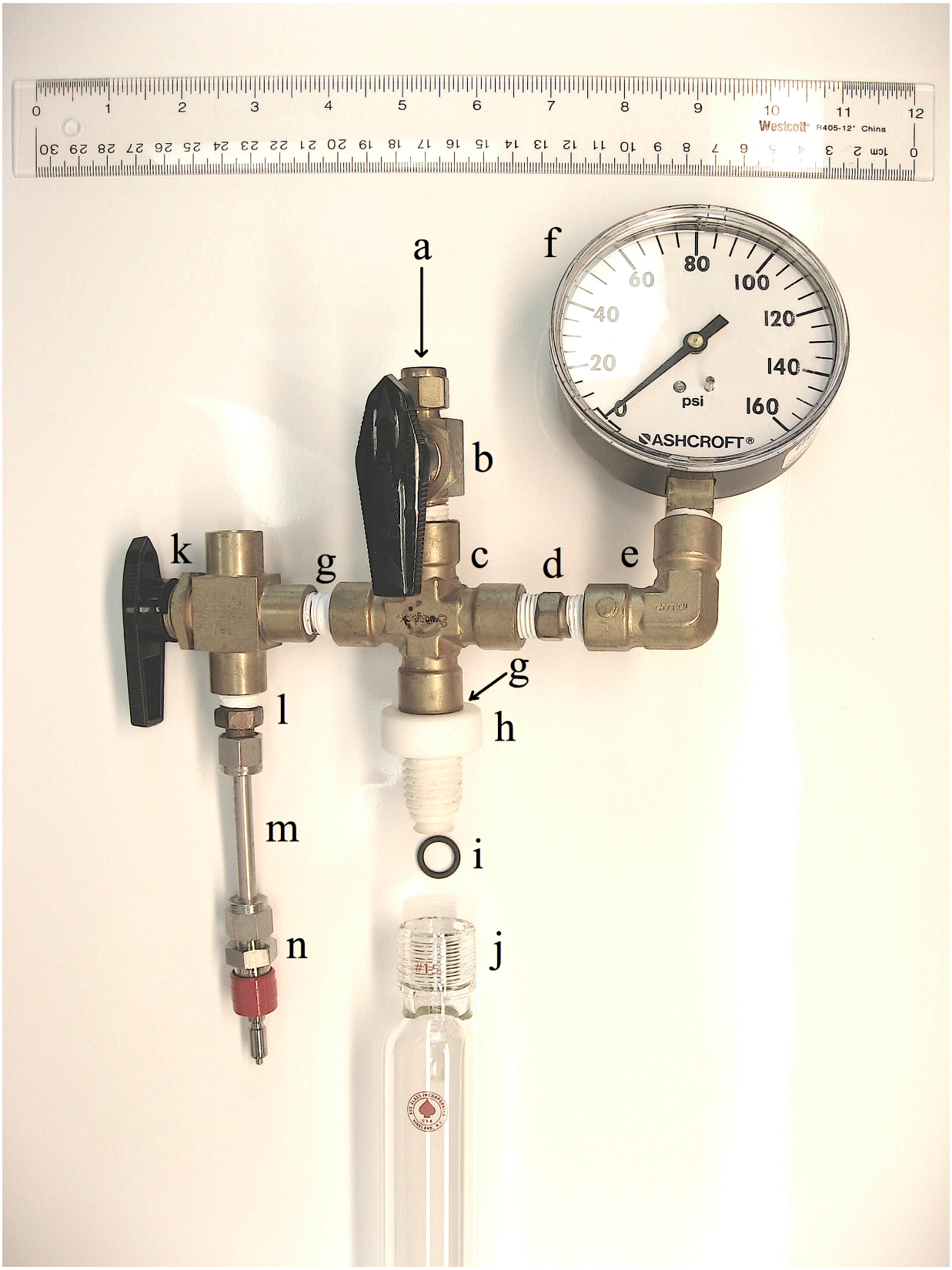

Figure 4.3 The assembled reactor with parts indicated.

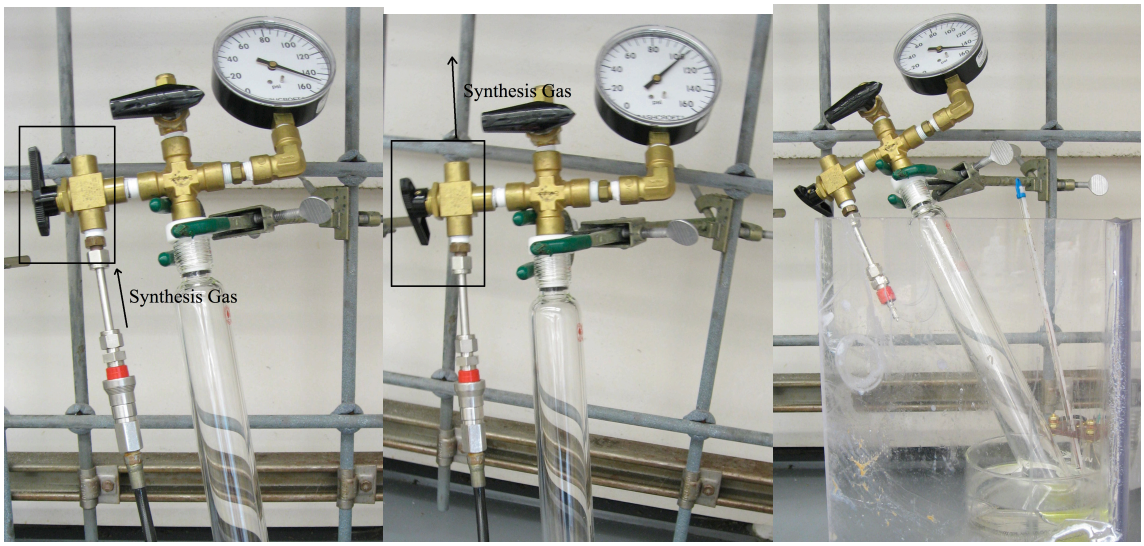

Figure 4.4 Reactor in-use.

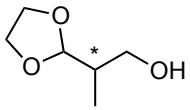

4

^{1}H NMR (300 MHz, $CDCl_3$) δ: 0.98 (d, J = 7.2 Hz, -CHC*H*$_3$, 3H), 1.93 − 2.05 (m, CHC*H*(CH_2OH)CH_3, 1H), 2.62 (br s, CHCH(CH_2O*H*)CH_3, 1H), 3.57 − 3.70 (m, CHCH(C*H*$_2$OH)CH_3, 2H), 3.83 − 4.04 (m, (OC*H*$_2$C*H*$_2$O)CH, 4H), 4.79 (d, J = 4.8 Hz, (OCH_2CH_2O)C*H*, 1H); ^{13}C NMR (75 MHz, $CDCl_3$) δ: 11.9, 39.0, 64.6, 65.0, 65.2, 107.7.

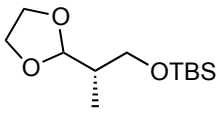

5

^{1}H NMR (300 MHz, $CDCl_3$) δ: 0.05 (s, Si(C*H*$_3$)$_2$(C(CH_3)$_3$), 6H), 0.90 (s, Si(CH_3)$_2$(C(C*H*$_3$)$_3$), 9H), 0.96 (d, J = 6.9 Hz, -CHC*H*$_3$, 3H), 1.86 − 1.99 (m, CHC*H*(CH_2OSi)CH_3, 1H), 3.67 (dd, J = 9.8, 6.0 Hz, 1H), 3.55 (dd, J = 9.8, 6.6, 1H), 3.83 − 3.97 (m, (OC*H*$_2$C*H*$_2$O)CH, 4H), 4.83 (d, J =

4.8 Hz, (OCH_2CH_2O)C*H*, 1H); ^{13}C NMR (75 MHz, $CDCl_3$) δ: -5.2, 11.1, 18.5, 26.1, 40.0, 64.7, 65.2, 105.3.

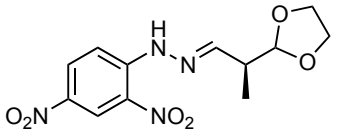

6

Synthesis of (2*S*)-2-(1,3-dioxolan-2-yl)-propanal 2,4-dinitrophenylhydrazone 6.

In a disposable culture tube, 165 mg of 2,4-dinitrophenylhydrazine (DNP) was dissolved in 10 mL of absolute ethanol. The orange solution was filtered through a pipette with a glass wool plug to remove any undissolved DNP. Added 95 mg of (2*S*)-2-(1,3-dioxolan-2-yl)-propanal in 3 mL of ethanol and removed approximately half of the ethanol with a gentle stream of nitrogen. The culture tube was left open to air for 11 days, at which point X-ray quality crystals formed at the bottom of the vessel. ^{1}H NMR (300 MHz, $CDCl_3$) δ: 1.29 (d, J = 7.2 Hz, -CHC*H*$_3$, 3H), 2.91 (m, C*H*CH_3 1H), 3.90-4.05 (m, (OC*H*$_2$C*H*$_2$O)CH, 4H), 4.93 (d, J = 3.9 Hz, (OCH_2CH_2O)C*H*, 1H), 7.55 (ap d, J = 5.1 Hz, C*H*N-NH, 1H), 7.96 (d, J = 9.6 Hz, Ar H) 8.31 (dd, J = 9.6, 2.4 Hz, Ar H), 9.13 (d, J = 2.4 Hz, Ar H, 1H), 11.1 (broad s, NH).

4.8 References

(1) Claver, C.; van Leeuwen, P. W. N. M. *Rhodium Catalyzed Hydroformylation*; Kluwer Academic Publishers: Dordrecht, The Netherlands, 2000.

(2) Babin, J. E.; Whiteker, G. T. WO 93/03839, 1993.

(3) Breeden, S.; Cole-Hamilton, D. J.; Foster, D. F.; Schwarz, G. J.; Wills, M. *Angew. Chem. Int. Ed.* **2000**, *39*, 4106-4108.

(4) Cobley, C. J.; Gardner, K.; Klosin, J.; Praquin, C.; Hill, C.; Whiteker, G. T.; Zanotti-Gerosa, A.; Petersen, J. L.; Abboud, K. A. *J. Org. Chem.* **2004**, *69*, 4031-4040.

(5) Klosin, J.; Landis, C. R. *Acc. Chem. Res.* **2007**, *40*, 1251-1259.

(6) Zhao, B.; Peng, X.; Wang, Z.; Xia, C.; Ding, K. *Chemistry – A European Journal* **2008**, *14*, 7847-7857.

(7) Zhang, X. W.; Cao, B. N.; Yan, Y. J.; Yu, S. C.; Ji, B. M.; Zhang, X. M. *Chem.—Eur. J.* **2010**, *16*, 871-877.

(8) Clark, T. P.; Landis, C. R.; Freed, S. L.; Klosin, J.; Abboud, K. A. *J. Am. Chem. Soc.* **2005**, *127*, 5040-5042.

(9) Thomas, P. J.; Axtell, A. T.; Klosin, J.; Peng, W.; Rand, C. L.; Clark, T. P.; Landis, C. R.; Abboud, K. A. *Org. Lett.* **2007**, *9*, 2665-2668.

(10) Watkins, A. L.; Hashiguchi, B. G.; Landis, C. R. *Org. Lett.* **2008**, *10*, 4553-4556.

(11) Nozaki, K.; Li, W. G.; Horiuchi, T.; Takaya, H. *Tetrahedron Lett.* **1997**, *38*, 4611-4614.

(12) Smith, A. B.; Beauchamp, T. J.; LaMarche, M. J.; Kaufman, M. D.; Qiu, Y.; Arimoto, H.; Jones, D. R.; Kobayashi, K. *J. Am. Chem. Soc.* **2000**, *122*, 8654-8664.

(13) Mickel, S. J.; Sedelmeier, G. H.; Niederer, D.; Schuerch, F.; Koch, G.; Kuesters, E.; Daeffler, R.; Osmani, A.; Seeger-Weibel, M.; Schmid, E.; Hirni, A.; Schaer, K.; Gamboni, R.; Bach, A.; Chen, S.; Chen, W.; Geng, P.; Jagoe, C. T.; Kinder, F. R.; Lee, G. T.; McKenna, J.; Ramsey, T. M.; Repič, O.; Rogers, L.; Shieh, W.-C.; Wang, R.-M.; Waykole, L. *Org. Process Res. Dev.* **2003**, *8*, 107-112.

(14) Smith, A. B.; Adams, C. M.; Barbosa, S. A. L.; Degnan, A. P. *Proc. Natl. Acad. Sci. U.S.A.* **2004**, *101*, 12042-12047.

(15) Lawhorn, B. G.; Boga, S. B.; Wolkenberg, S. E.; Colby, D. A.; Gauss, C.-M.; Swingle, M. R.; Amable, L.; Honkanen, R. E.; Boger, D. L. *J. Am. Chem. Soc.* **2006**, *128*, 16720-16732.

(16) Reaction conditions: allyloxy-tert-butyldimethylsilane (30 mmol, 4.5 M), $Rh(acac)(CO)_2$ (3 μmol), 1 (3 μmol), 80°C, 5 h. The reaction proceeded with 99% conversion to aldehydes, α:β 1.8:1, 92% ee. The linear aldehyde can be separated from the branched by flash chromatography to provide the pure chiral aldehyde with no degradation of enantioenrichment.

(17) Smith, A. B.; Brandt, B. M. *Org. Lett.* **2001**, *3*, 1685-1688.

(18) Ehrlich, G.; Kalesse, M. *Synlett* **2005**, *2005*, 655-657.

(19) Ferrié, L.; Reymond, S. b.; Capdevielle, P.; Cossy, J. *Org. Lett.* **2006**, *8*, 3441-3443.

(20) Canova, S.; Bellosta, V. r.; Bigot, A.; Mailliet, P.; Mignani, S.; Cossy, J. *Org. Lett.* **2007**, *9*, 145-148.

(21) Fürstner, A.; Nevado, C.; Waser, M.; Tremblay, M.; Chevrier, C.; Teplý, F.; Aïssa, C.; Moulin, E.; Müller, O. *J. Am. Chem. Soc.* **2007**, *129*, 9150-9161.

(22) Shimizu, H.; Saito, T.; Kumobayashi, H. *Adv. Synth. Catal.* **2003**, *345*, 185-189.

(23) Jeulin, S.; Ayad, T.; Ratovelomanana-Vidal, V.; Genêt, J.-P. *Adv. Synth. Catal.* **2007**, *349*, 1592-1596.

(24) Holz, J.; Schäffner, B.; Zayas, O.; Spannenberg, A.; Börner, A. *Adv. Synth. Catal.* **2008**, *350*, 2533-2543.

(25) Pautigny, C.; Jeulin, S.; Ayad, T.; Zhang, Z.; Genêt, J.-P.; Ratovelomanana-Vidal, V. *Adv. Synth. Catal.* **2008**, *350*, 2525-2532.

(26) Wassenaar, J.; Kuil, M.; Reek, J. N. H. *Adv. Synth. Catal.* **2008**, *350*, 1610-1614.

(27) Qiu, M.; Wang, D.-Y.; Hu, X.-P.; Huang, J.-D.; Yu, S.-B.; Deng, J.; Duan, Z.-C.; Zheng, Z. *Tetrahedron: Asymmetry* **2009**, *20*, 210-213.

(28) Nielsen, L.; Skrydstrup, T. *J. Am. Chem. Soc.* **2008**, *130*, 13145-13151.

(29) Hahn, E. *J. Org. Chem.* **1973**, *38*, 2092-2093. Titanium(IV) chloride (10%) was used in place of *p*-toluene sulfonic acid.

(30) Bischofberger, N.; Waldmann, H.; Saito, T.; Simon, E. S.; Lees, W.; Bednarski, M. D.; Whitesides, G. M. *J. Org. Chem.* **1988**, *53*, 3457-3465.

(31) Marcelle L. Ferguson; Daniel J. O'Leary; Grubbs, R. H. *Org. Synth.* **2003**, *80*, 85-92.

Chapter 5

Asymmetric Hydroformylation-Wittig Olefination

Chapter 5 was submitted for publication on November 2, 2012.

5.1 Introduction

Rhodium-catalyzed hydroformylation is an atom economic, commodity-scale process for the production of linear aldehydes.[1] Asymmetric hydroformylation (AHF) is underutilized due to the limited availability of chiral ligands that demonstrate useful selectivity and activity.[2,3] Hydroformylation constitutes a potentially powerful method for synthesizing enantiopure aldehydes from readily accessible reagents.[4-6] Such chiral aldehydes are valuable intermediates in the synthesis of pharmaceuticals and other complex organic molecules. We[7-10] and others[11-20] have demonstrated effective enantioselective hydroformylation of alkenes. Previously we have reported that bisdiazaphospholane **1** (Figure 5.1) enables highly active, regio- and enantioselective rhodium-catalyzed hydroformylation of aryl alkenes,[8] 1,3-dienes,[10] vinylic and allylic amines and alcohols.[9] For example, AHF of allyl ethers using **1** and rhodium catalysts yield "Roche aldehyde" derivatives with high enantiomeric excess.[9,21] One of the many application of the Roche aldehyde concerns olefination[22-26] to form γ-chiral α,β-unsaturated carbonyl intermediates. A generalized and efficient AHF-olefination protocol would enhance emerging hydroformylation technology.

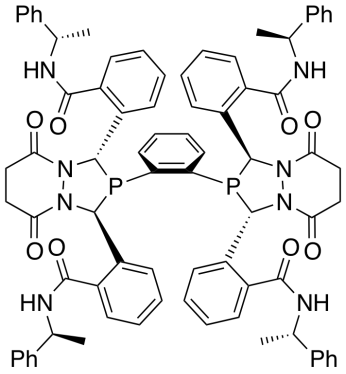

Figure 5.1 Chiral bisdiazaphospholane **1** used in this study.

There have been a few reports of one-pot hydroformylation-Wittig olefination sequences. Breit and co-workers have applied a diastereoselective hydroformylation-Wittig olefination-hydrogenation of 1,1-disubstituted allylic alcohols in which the alcohol is tethered to a phosphorus ligand to induce a diastereoselective linear hydroformylation.[27,28] Helmchen and co-workers have recently applied this to chiral homo-allylic amines to produce substituted proline analogues using a hydroformylation-Wittig olefination-aza-Michael addition sequence.[29] Burke has demonstrated the synthesis of (+)-Patulolide C[30] and the Prelog-Djerassi lactone[31] using hydroformylation reactions. Here we demonstrate general, efficient and enantioselective one-pot AHF-Wittig olefination (AHF-WO) sequences in the presence of rhodium complexes of bisdiazaphospholane **1** to produce γ-chiral α,β-unsaturated carbonyl compounds (Scheme 5.1).

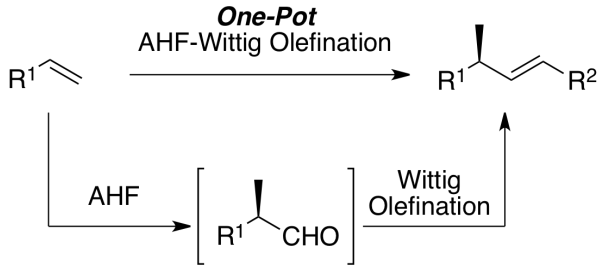

Scheme 5.1 General one-pot asymmetric hydroformylation-WO sequence with stabilized Wittig ylides resulting γ-chiral α,β-unsaturated carbonyl products.

5.2 AHF-WO of Vinyl Acetate

The enantioselective hydroformylation of vinyl acetate was conducted in the presence of various stabilized Wittig ylides (Table 5.1) in glass pressure bottles. Hydroformylation of vinyl acetate with carboethoxy-substituted Wittig ylide in a glass reaction bottle resulted in 79% yield of an α,β-unsaturated ester in 99% ee (**2a**, entry 1). Analogues of product **2** have been used in

organic synthesis.[32-36,37] The AHF-WO of vinyl acetate and Wittig ylide bearing the carbobenzyloxy group yielded **2b** (entry 2) in high enantioselectivity (99% ee) and modest yield (46%). Interestingly, **2b** was the only product observed to undergo a second hydroformylation-Wittig olefination transformation. Subsequent isomerization yielded **2b'** (equation 1). As shown in Table 1, stabilized Wittig reagents based on α-substituted esters (entries 3 and 5) and ketones (entry 4) are effective in the AHF-WO sequence. In all examples, high *E*:*Z* selectivity (>95:5), high regioselectivity, and little erosion of enantioselectivity was observed.

Table 5.1 One-pot AHF-olefination of vinyl acetate in the presence stabilized Wittig ylides.[a]

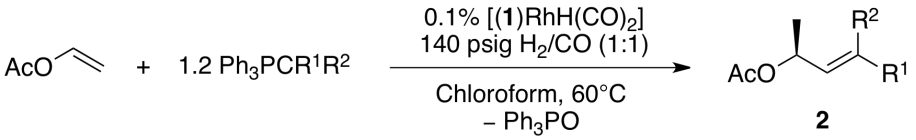

	Product	t (h)	*E*:*Z* Ratio[b]	% Yield	% ee[c]
1	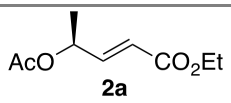 **2a**	18	>95:5	79	99
2	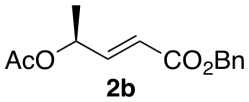 **2b**	15	>95:5	46	99
3	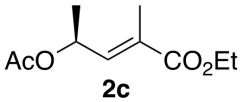 **2c**	18	>95:5	68	90
4	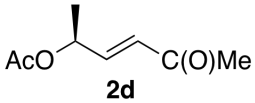 **2d**	21	>95:5	71	97
5	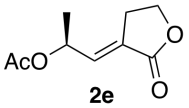 **2e**	18	>95:5	67	98

a. Pre-activation of $Rh(acac)(CO)_2$ and **1** with 140 psig (1:1) H_2/CO for 0.5 hour at 40°C followed by injection of vinyl acetate/Wittig ylide solution; [vinyl acetate] = 1.5 M, [Wittig ylide] = 1.8 M in chloroform. b. Measured by ^1H NMR spectroscopy. c. See supporting information for determination of percent enantiomeric excess.

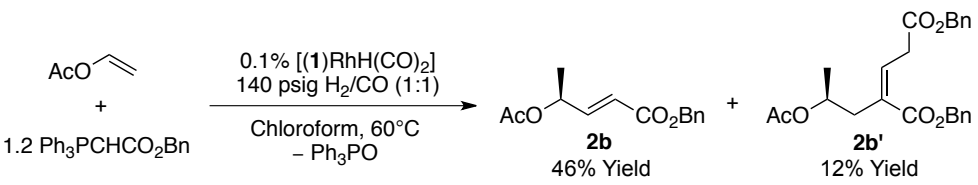

Scheme 5.2 AHF-WO of vinyl acetate and a carbobenzyloxy-substituted Wittig ylide.

5.3 AHF-WO of Diverse Alkenes

Sequential AHF-WO has been applied to alkenes of several types. Asymmetric hydroformylation-Wittig olefination of *N*-vinylphthalimide (Scheme 5.3), 6-methoxy-2-vinylnaphthalene (Scheme 5.4), CBZ-protected 3-pyrroline (Scheme 5.5), and phenyl-1,3-butadiene[10] (Scheme 5.6) proceeds with good yield and selectivities. Please note that the procedures for the vinylnaphthalene and diene involve different temperatures for the AHF and WO steps. The one-pot sequential procedure provided ca. 10% higher ee's than the tandem process, presumably because the sensitive aldehydes epimerize faster in the presence of ylide at the higher temperature. Also note that **3d'** is susceptible to isomerization to **3d''**. Reduction of the ester to the alcohol **3d** mitigates this problem.

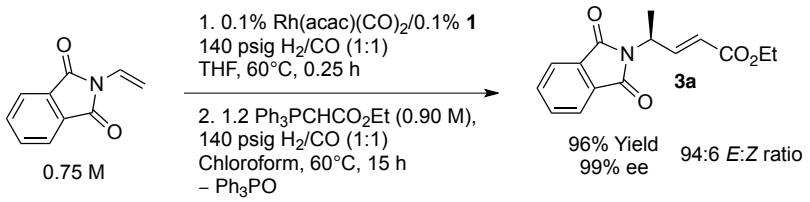

Scheme 5.3 AHF-WO of *N*-vinylphthalimide.

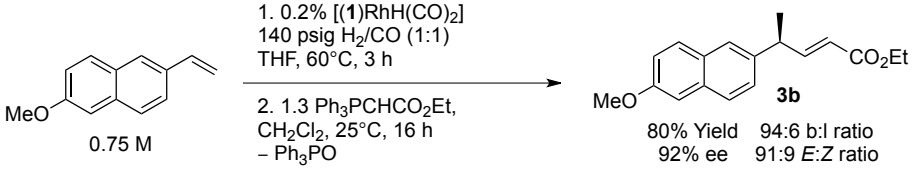

Scheme 5.4 AHF-WO of 6-methoxy-2-vinylnaphthalene.

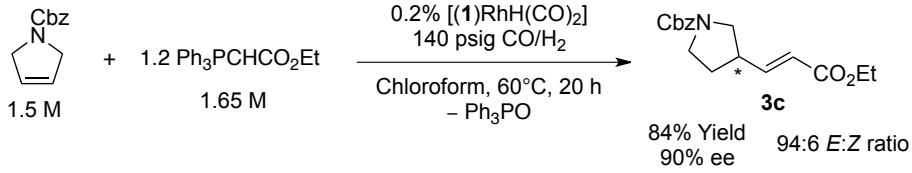

Scheme 5.5 AHF-WO of Cbz-protected 3-pyrroline.

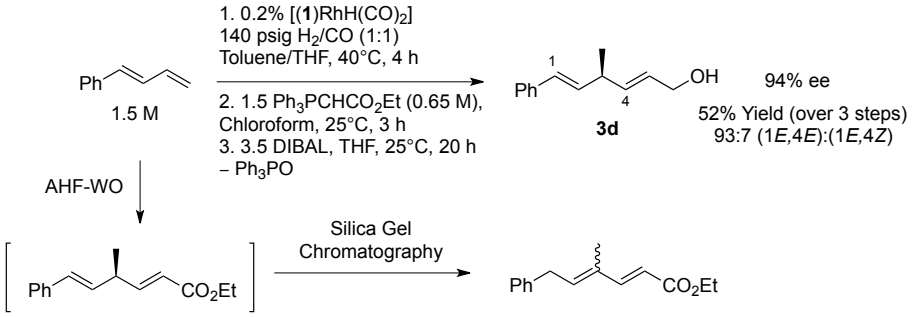

Scheme 5.6 Sequential AHF-WO of 1-phenyl-1,3-butadiene followed by a DIBAL reduction.

5.4 Iterative AHF-WO Sequences

Wittig olefination with an allyl-substituted ylide yields a 1,4-diene that can undergo subsequent hydroformylation (Table 5.2). AHF of enantiomerically-enriched samples of **4** at four different combinations of syngas (1:1 H_2/CO) pressure and temperature reveals dramatically different regioselectivities: at 140 psig of syngas and 40°C, the branched aldehyde was favored [85% **b-5** for **(*S*)-4** and 79% **b-5** for **(*R*)-4**], whereas the linear product predominates [23% **b-5** for **(*S*)-4** and 17% **b-5** for **(*R*)-4**] at 15 psig of syngas and 100°C. The combination of high pressure and high temperature (100°C and 140 psig) results in almost equal amounts of the branched and linear regioisomers [63% **b-5** for **(*S*)-4** and 52% **b-5** for **(*R*)-4**]. The low temperature and pressure (40°C and 15 psig) combination produces less branched isomer [75% **b-5** for **(*S*)-4** and 66% **b-5** for **(*R*)-4]**. Different regioselectivities for different enantiomers indicate match-mismatch effect with the enantiopure catalyst. For the reaction conditions evaluated, high diastereomeric ratios were observed for the branched product with the same enantiomer of the AHF catalyst (≥87% major diastereomer). The internal tri-substituted alkene remains unreacted in all of these experiments. Previously, interesting CO pressure effects on regio- and enantioselectivity have been observed for the AHF of conjugated alkenes (styrene and 1,3-dienes) with rhodium-diazaphospholane catalysts.[10,38] Kollár and Casey observed pressure and temperature effects on enantioselectivity in platinum hydroformylation of styrene.[39,40]

Table 5.2 AHF of **4** at various syngas pressures and temperatures.[a]

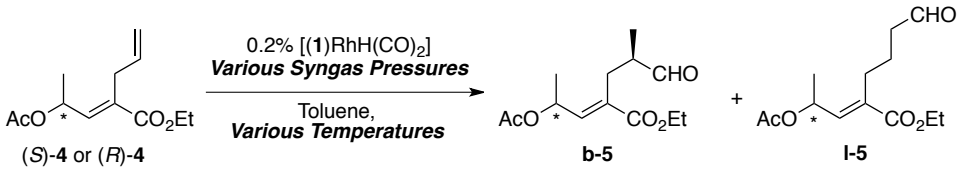

	(*S*)-**4**		(*R*)-**4**	
	140 psig 1:1 H_2/CO	15 psig 1:1 H_2/CO	140 psig 1:1 H_2/CO	15 psig 1:1 H_2/CO
	99[b,e]	99[b,e]	92[b,e]	99[b,e]
40°C, 3 h	**86:14**[c,e]	**75:25**[c,e]	**79:21**[c,e]	**69:31**[c,e]
	93:7[d,e]	*93:7*[d,e]	*4:96*[d,e]	*6:94*[d,e]
	99[b,e]	99[b,e]	99[b,e]	99[b,e]
100°C, 1h	**63:37**[c,e]	**23:77**[c,e]	**52:48**[c,e]	**17:83**[c,e]
	95:5[d,e]	*89:11*[d,e]	*6:94*[d,e]	*13:87*[d,e]

a. [Alkene] = 1.5 M and 1:1 H_2:CO. b. % Conversion. c. **b-5**:**l-5** ratio. d. dr of **b-5**. e. Determined by ^{1}H NMR spectroscopy.

Complex materials containing multiple stereocenters and various functionalities can be synthesized by sequential AHF-WO procedures. For example, olefination of aldehyde **b-5** with allyl carboethoxy-substituted Wittig ylide yielded 1,4,8-triene **6** (Scheme 5.7). Hydroformylation of triene **6** at 15 psig of syngas and 100°C gave linear (**l-7**) and branched (**b-7**) isomers with linear selectivity (12% branched aldehyde); at 140 psig of syngas and 40°C the reaction is branched selective (72% branched aldehyde). Using silica gel chromatography, each of these regioisomers can be isolated. The branched isomer **b-7**, which contains ester, acetoxy, and

aldehyde functional groups, two C=C double bonds, and three stereocenters, is obtained with high diastereometric ratio (94:6).

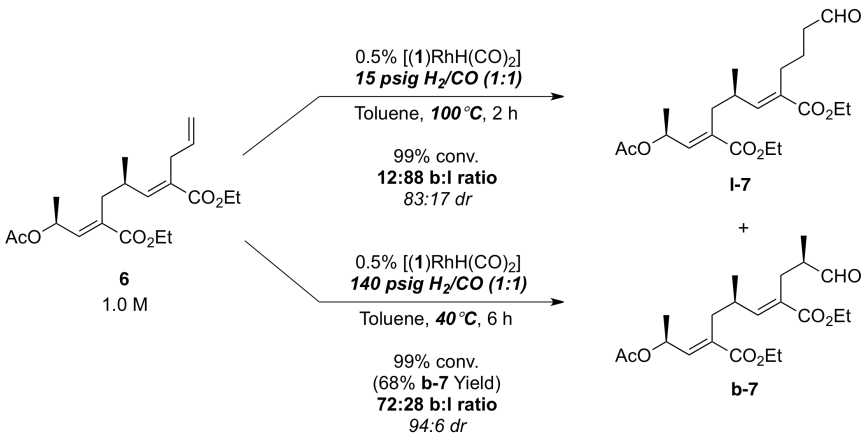

Scheme 5.7 Hydroformylation of 1,4,8-triene **6** to yield products **b-7** and **l-7**.

Multiple one-pot iterative AHF-WO sequences can be accomplished with a single catalyst loading (Schemes 5.8 and 5.9). For example, a pressure bottle charged with vinyl acetate, $Rh(acac)(CO)_2$ (0.2%), ligand **1**, and synthesis gas generated branched aldehyde in two hours. Subsequent depressurization and injection of the allyl-substituted Wittig ylide gave 1,4-diene **(*S*)-4**. This sequence was required because the allyl-substituted Wittig ylide is also capable of undergoing hydroformylation followed by an intramolecular olefination, yielding ethyl 1-cyclopentene-1-carboxylate as the major product. Repressurization with 140 psig of H_2/CO (1:1) at 40°C effected AHF of **(*S*)-4** to give aldehyde **b-5** in modest yield (56%) and in high dr (95:5).

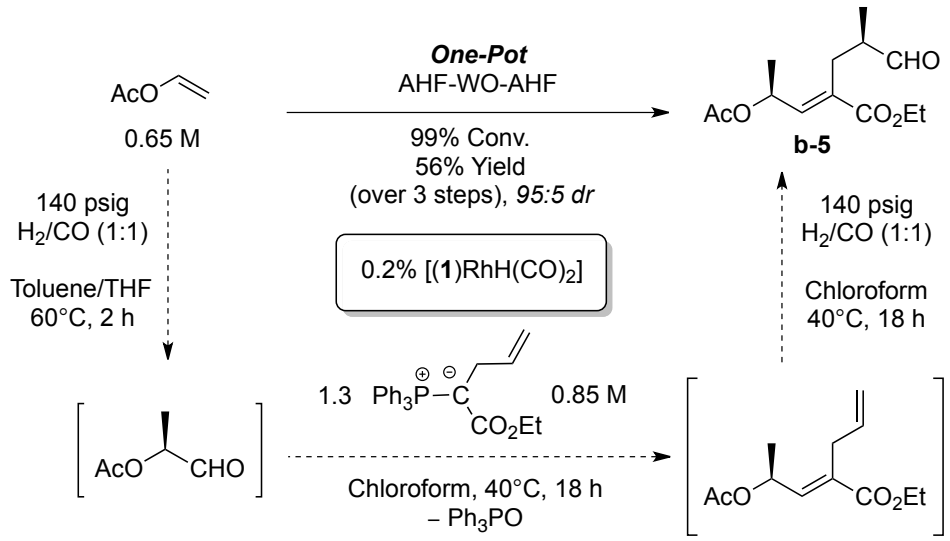

Scheme 5.8 Net one-pot AHF-WO-AHF reaction of vinyl acetate with an allyl substituted Wittig ylide (AHF and WO intermediates shown for clarity).

One-pot AHF-WO sequences with multiple iterations yield vinylogous ester oligomers with a single loading of rhodium-bis-3,4-diazaphospholane catalyst. For example, AHF-WO-AHF-WO-AHF-WO produced a substituted unsaturated trimer of 4-hydroxyvalerate (Scheme 5.9).[41] Asymmetric hydroformylation of vinyl benzoate was followed by depressurization and the first addition of a vinyl ester substituted Wittig reagent. Repressurization with syngas, hydroformylation, and depressurization was followed by injection of the second ylide. A final AHF-WO cycle yielded the trimer **8** with three unique stereocenters in 17% isolated yield. Synthesis of a monodisperse oligomer requires precise control of stoichiometric amounts of Wittig ylide at each iteration step.[42] Separation of the trimer away from smaller and larger oligomers was accomplished using silica gel chromatography. NMR spectroscopy (^{1}H, ^{13}C, COSY, HSQC) confirmed the connectivity of the trimer product, apparently with one diasteromer predominating. Mass spectrometry confirmed the presence of **8**, along with trace amounts of the dimer and tetramer. The yield and purity of the trimer appears to be limited more

by difficulties of measuring stoichiometric amounts of ylide and isolation of the product from tributylphosphine oxide than by hydroformylation conversion and selectivity.

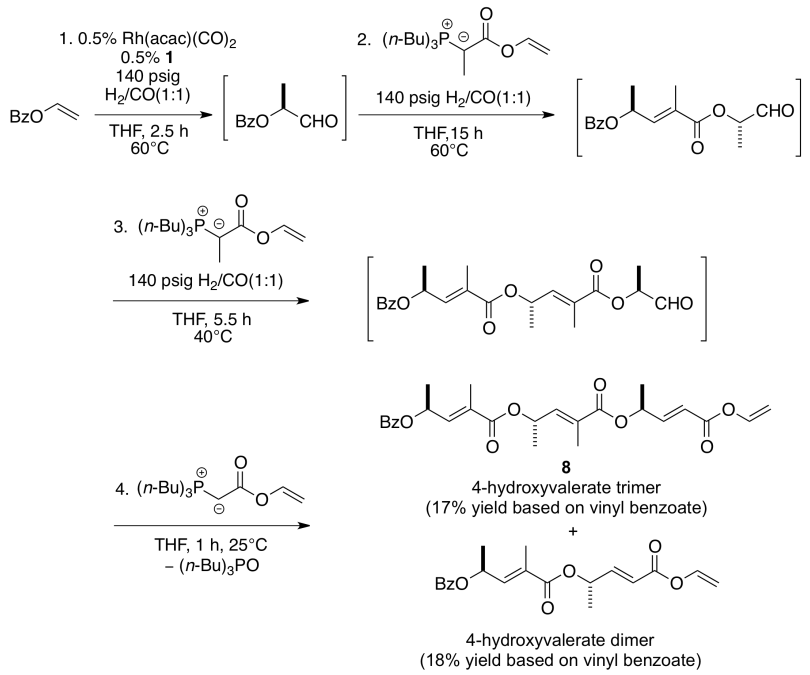

Scheme 5.9 One-pot AHF-WO-AHF-WO-AHF-WO using a single catalyst loading.

5.5 Conclusions

Iterative $(AHF\text{-}WO)_n$ sequences constitute a powerful one-pot approach to the sequence-specific construction of oligomers in which multiple stereocenters are introduced by a single charge of chiral catalyst. The success of the examples shown here rests on the remarkable activity and robustness of the Rh(bisdiazaphospholane) catalysts, their high selectivity for a variety of alkene substrates, and the ability of stabilized ylides to olefinate α-chiral aldehydes without racemization. In addition this work demonstrates that simple change in hydroformylation temperature and pressure can toggle the catalyst between linear and branched selectivity. The

α,β-unsaturated carbonyls resulting from olefination provide sites for further functionalization and creation of stereocenters.

5.6 Experimental

General Considerations

$Rh(acac)(CO)_2$ was recrystallized as green crystals from toluene and hexane. Ligand **1** was synthesized from previously reported procedure. Toluene and THF were distilled over Na/benzophenone prior to use and subjected to three freeze-pump-thaw cycles prior to use in a dinitrogen-filled glovebox. Chloroform was degassed prior to use. Vinyl acetate, *N*-vinylphthalimide, and 6-methoxy-2-vinylnaphthalene were purchased from commerial sources. A sample of vinyl acetate was degassed prior to use in the glove box. Benzyl 3-pyrroline-1-carboxylate was synthesized from olefin metathesis of benzyl diallylcarbamate. As reported previously, 1-phenyl-1,3-butadiene was synthesized from a WO of cinnamylaldehyde. 1-(Triphenylphosphoranylidene)-2-propanone was purchased from Sigma-Aldrich and was used without further manipulation. Stabilized Wittig ylides Ph_3PCHCO_2Et, Ph_3PCHCO_2Bn, $Ph_3PC(CH_2CH{=}CH_2)CO_2Et$, $Ph_3CCMeCO_2Et$, $Ph_3PC(C_3H_4O_2)$ (Wittig ylide leading to product **2e**), were synthesized as reported. All other reagents were purchased from commerical sources. Products from AHF-WO sequences (*R*)-**4**, (*S*)-**4**, and **7** were degassed and prepared samples in the glovebox for hydroformylation. Silica gel chromatography was performed using Siliaflash Å silica gel (Silicyle, particle size 40–63 μm, 230–400 mesh). Carbon monooxide and synthesis gas (custom H_2/CO 1:1 mixture) cylinders were used without further manipulation from Airgas, Inc.

Caution! Carbon monoxide is a highly toxic gas and manipulations should be conducted in a well-ventilated fume hood in the vicinity of a carbon monoxide detector. Hydrogen gas is highly flammable and explosive gas. Precautions should be taken when using synthesis gas (H_2/CO mixtures).

Branched to linear ratios, *E*:*Z* ratios, diastereomeric ratios, conversion were determined by proton (^{1}H) NMR spectroscopy on crude reaction mixtures. Proton (^{1}H) NMR spectra was collected on a Varian MercuryPlus 300 or a Bruker AC+ 300 spectrometer and referenced to tetramethylsilane (TMS). Carbon (^{13}C) NMR spectra was obtained on a Varian MercuryPlus 300 spectrometer and referenced to $CDCl_3$ (77.23 ppm). Splitting patterns from spectra were denoted as follows: single (s), doublet (d), triplet (t), quartet (q), pentet, and sextet. Non-first order splitting was denoted as (m) for a multiplet. A Varian Chrompack system using a β-Dex 225 column (30m x 0.25mm ID) was used for gas chromatography (GC) analysis. A Berger Instruments SFC system with outfitted with Chiralcel AD-H or OJ-H columns was used for Supercritical Fluid Chromatography (SFC).

General AHF-WO Procedure for Vinyl Acetate (Table 1)

In a dinitrogen-filled glovebox, an oven-dried 18 mL pressure bottle containing a magnetic stir bar was charged with solutions of $Rh(acac)(CO)_2$ (85 μL, 20 mM in toluene, 0.0017 mmols) and ligand **1** (94 μL, 20 mM in THF, 0.0019 mmols). In the glove box, prepared a chloroform solution (955 μL) of containing vinyl acetate (161 μL, 0.150 g, 1.75 mmols) and Wittig ylide (0.678 g; 1.8 mmols). The pressure bottle was attached to a reactor head and brought out of the glove box. In a well-ventilated hood, the reactor was attached to a synthesis gas source (1:1

H_2/CO) subjected to five pressurization cycles (140 psig/0 psig), followed by a final pressurization to 140 psig and heated the pressure bottle in a 40°C oil bath (pre-activation to [(**1**)RhH$(CO)_2$]). After 0.5 hour, removed the reactor from the oil bath, cooled, depressurized (0 psig), followed by injection of the vinyl acetate/Wittig ylide chloroform solution. The reactor was subjected to five pressurization/depressurization cycles and heated to 60°C in an oil bath. The reaction was conducted to the time length outlined in Table 1.

Synthesis, Characterization, and Resolution Conditions of AHF-WO Products

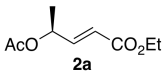

2a

70% yield, a colorless oil from silica gel chromatography (20:80 ethyl acetate: hexanes; $R_{f(\mathbf{2a})}$ = 0.41). ^{1}H NMR (300 MHz, $CDCl_3$) δ 1.30 (t, J = 7.2 Hz, 3H), δ 1.37 (d, J = 6.6 Hz, 3H), δ 2.09 (s, 3H), δ 4.21 (q, J = 7.2 Hz, 2H), δ 5.45–5.54 (m, 1H), δ 5.96 (dd, J = 15.6, 1.8 Hz, 1H), δ 6.87 (dd, J = 15.6, 5.1 Hz, 1H); ^{13}C NMR (75 MHz, $CDCl_3$) δ 14.4, δ 19.8, δ 21.3, δ 60.8, δ 69.1, δ 121.3, δ 146.4, δ 166.3, δ 170.2; HRMS: m/z (ESI) calculated $[M+Na]^+$ = 209.0785, measured 209.0790 (Δ = 2.4 ppm). GC analysis: Supelco's Beta Dex–225 column (isothermal 110°C): t = 25.9 min, t = 26.5 min.

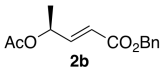

2b

46% yield, a colorless oil from silica gel chromatography (20:80 ethyl acetate: hexanes; $R_{f(\mathbf{2b})}$ = 0.37, $R_{f(\mathbf{2b'})}$ = 0.24). ^{1}H NMR (300 MHz, $CDCl_3$) δ 1.36 (d, J = 6.6 Hz, 3H), δ 2.08 (s, 3H), δ 5.19 (s, 2H), δ 5.49 (m, 1H), δ 6.01 (dd, J = 15.6, 1.8 Hz, 1H), δ 6.92 (dd, J = 15.6, 5.1 Hz, 1H),

δ 7.33–7.40 (m, 5H); ^{13}C NMR (75 MHz, $CDCl_3$) δ 19.8, δ 21.3, δ 66.7, δ 69.0, δ 120.9, δ 128.6, δ 128.8, δ 136.0, δ 147.1, δ 166.1, δ 170.2; HRMS: m/z (ESI) calculated $[M+Na]^+$ = 271.0941, measured 271.0944 (Δ = 1.1 ppm). SFC analysis: Chiracel AD–H column (40°C oven temperature, 5% MeOH, pressure = 150 bar, 2mL/min flow rate): t = 3.8 min, t = 4.2 min.

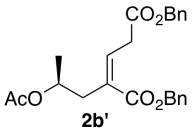

2b'

^{1}H NMR (300 MHz, $CDCl_3$) δ 1.21 (d, J = 6.3 Hz, 3H), δ 1.89 (s, 3H), δ 2.57–2.60 (m, 2H), δ 3.37 (d, J = 7.2 H, 2H), δ 4.96–5.07 (m, 1H), δ 5.15 (s, 2H), δ 5.17–5.22 (m, 2H), δ 7.11 (t, J = 7.2 Hz, 1H), δ 7.31–7.38 (m, 10H); ^{13}C NMR (75 MHz, $CDCl_3$) δ 20.2, δ 21.3, δ 33.5, δ 34.6, δ 66.9, δ 67.1, δ 70.2, δ 128.3, δ 128.4, δ 128.5, δ 128.6, δ 128.7, δ 128.8, δ 131.2, δ 135.7, δ 136.1, δ 136.2, δ 166.7, δ 170.2, δ 170.5; HRMS: m/z (ESI) calculated $[M+Na]^+$ = 433.1622, measured 433.1616 (Δ = 1.4 ppm).

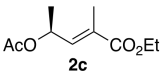

2c

91% yield, a colorless oil from silica gel chromatography (20:80 ethyl acetate: hexanes; $R_{f(\mathbf{2c})}$ = 0.28). ^{1}H NMR (300 MHz, $CDCl_3$) δ 1.30 (t, J = 7.2 Hz, 3H), δ 1.33 (d, J = 6.6, 3H), δ 1.91 (d, J = 1.2 Hz, 3H), δ 2.05 (s, 3H), δ 4.20 (q, J = 7.2 Hz, 2H), δ 5.62 (dq, J = 8.7, 6.6, 1H), δ 6.60 (dq, J = 8.7, 1.5 Hz, 1H); ^{13}C NMR (75 MHz, $CDCl_3$) δ 13.0, δ 14.4, δ 19.9, δ 21.4, δ 61.1, δ 67.8, δ 129.7, δ 139.8, δ 167.9, δ 170.5; HRMS: m/z (ESI) calculated $[M+Na]^+$ = 223.0941, measured 223.0936 (Δ = 2.2 ppm). GC analysis: Supelco's Beta Dex–225 column (isothermal 85°C for 90 minutes then 120°C at a rate of 5°C/minute for 15 minutes): t = 94.4 min, t = 94.7 min.

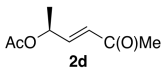

2d

71% yield, a colorless oil from silica gel chromatography (30:70 ethyl acetate: hexanes; $R_{f(\mathbf{2d})}$ = 0.36). ^{1}H NMR (300 MHz, $CDCl_3$) δ 1.37 (d, J = 6.6 Hz, 3H), δ 2.09 (s, 3H), δ 2.26 (s, 3H), δ 5.50 (m, 1H), δ 6.18 (dd, J = 16.2, 1.8 Hz, 1H), δ 6.68 (dd, J = 16.2, 4.8 Hz, 1H); ^{13}C NMR (75 MHz, $CDCl_3$) δ 19.8, δ 21.3, δ 27.5, δ 69.1, δ 129.9, δ 145.1, δ 170.2, δ 198.2; HRMS: m/z (ESI) calculated $[M+Na]^+$ = 179.0679, measured 179.0680 (Δ < 1 ppm). GC analysis: Supelco's Beta Dex–225 column (isothermal 110°C): t = 10.9 min, t = 11.6 min.

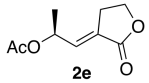

2e

67% yield, a colorless oil from silica gel chromatography (30:70 ethyl acetate: hexanes; $R_{f(\mathbf{2e})}$ = 0.36). ^{1}H NMR (300 MHz, $CDCl_3$) δ 1.38 (d, J = 6.3 Hz, 3H), δ 2.07 (s, 3H), δ 2.84–2.97 (m, 1H), δ 3.09–3.21 (m, 1H), 4.34–4.46 (m, 2H), δ 5.40–5.49 (m, 1H), δ 6.57 (dt, J = 8.1, 3.0 Hz, 1H); ^{13}C NMR (75 MHz, $CDCl_3$) δ 19.5, δ 21.3, δ 25.3, δ 65.8, δ 68.4, δ 127.3, δ 137.5, δ 170.4, δ 171.3; HRMS: m/z (ESI) calculated $[M+Na]^+$ = 207.0628, measured 207.0620 (Δ = 3.8 ppm). GC analysis: Supelco's Beta Dex–225 column (isothermal 140°C for 50 minutes then 160°C at a rate of 5°C/minute for 16 minutes): t_{minor} = 51.3 min, t_{major} = 53.4 min.

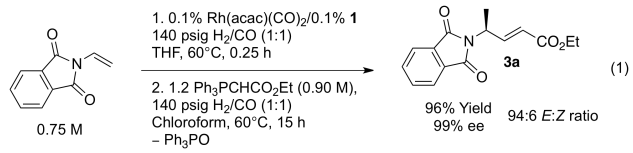

(1)

In a dinitrogen-filled glove box, charged an oven-dried glass pressure containing a magnetic stir bar with $Rh(acac)(CO)_2$ (0.00058 mmols; 29 μL of 20 mM in toluene), ligand **1** (0.00064 mmols;

32 μL of 20 mM in THF), *N*-vinylphthalimide (0.100 g; 0.57 mmols), and THF (324 μL). A reactor head was attached to the pressure bottle and removed from the glove box. In a well-ventilated fume hood, charged the reactor with 140 psig of H_2/CO (1:1) after five pressurization/depressurization cycles, and heated in an oil bath to 60°C. After 15 minutes removed from heating, cooled, depressurized the reactor, and injected a chloroform solution of Ph_3PCHCO_2Et (0.250 g in 450 μL $CHCl_3$; 0.72 mmols) prepared from the glovebox. Repressurized the reactor with 140 psig of H_2/CO and heated at 60°C for 15 hours. Reaction completion was checked by ^{1}H NMR spectroscopy and using silica gel chromatography isolated the α,β-unsaturated ester.

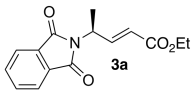

3a

96% yield, a white solid from silica gel chromatography (30:70 ethyl acetate: hexanes; $R_{f(\mathbf{3a})}$ = 0.35). ^{1}H NMR (300 MHz, $CDCl_3$) δ 1.28 (t, J = 7.2 Hz, 3H), δ 1.65 (d, J = 7.2 Hz, 3H), δ 4.19 (q, J = 7.2 Hz, 2H), δ 5.10 (m, 1H), δ 5.93 (dd, J = 15.9, 1.8 Hz, 1H), δ 7.14 (dd, J = 15.9, 5.7 Hz, 3H), δ 7.69–7.76 (m, 2H), 7.82–7.87 (m, 2H); ^{13}C NMR (75 MHz, $CDCl_3$) δ 14.4, δ 17.9, δ 47.1, δ 60.8, δ 122.6, δ 123.6, δ 132.1, δ 134.3, δ 145.6, δ 166.1, δ 167.8; HRMS: m/z (ESI) calculated $[M+Na]^+$ = 296.0894, measured 296.0894 (Δ = 0 ppm). SFC analysis: Chiracel AD–H column (40°C oven temperature, 5% MeOH, pressure = 150 bar, 2mL/min flow rate): t = 5.1 min, t = 6.1 min.

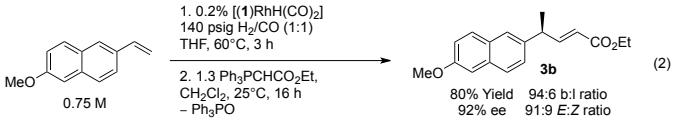

In a dinitrogen-filled glove box, charged an oven-dried glass pressure containing a magnetic stir bar with $Rh(acac)(CO)_2$ (0.0011 mmols; 54 μL of 20 mM in toluene) and ligand **1** (0.0013 mmols; 65 μL of 20 mM in THF). A reactor head was attached to the pressure bottle and removed from the glove box. In a well-ventilated fume hood, charged the reactor with 140 psig of H_2/CO (1:1) after five pressurization/depressurization cycles, and heated in an oil bath to 60°C for 0.5 hour. After cooling and depressuring to 0 psig, a solution of 6-methoxy-2-vinylnaphthalene (0.100 g; 0.35 mmols) in THF (604 μL) was injected into the reactor, cycled with syngas (10x), pressurized to 140 psig of H_2/CO (1:1) and heated to 60°C. After 3 hours removed from heating, cooled, depressurized the reactor, and added a methylene solution of Ph_3PCHCO_2Et (0.245 g in 1 mL CH_2Cl_2; 0.70 mmols). Silica gel chromatography was used to isolate the α,β-unsaturated ester.

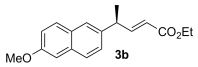

80% yield, a white solid from silica gel chromatography (15:85 ethyl acetate: hexanes; $R_{f(\mathbf{3b})}$ = 0.35). ^{1}H NMR (300 MHz, $CDCl_3$) δ 1.27 (t, J = 7.2 Hz, 3H), δ 1.50 (d, J = 7.2 Hz, 3 H), δ 3.75 (m, 1H), δ 3.91 (s, 3H), δ 4.18 (q, J = 7.2 Hz, 2H), δ 5.83 (dd, J = 15.6, 1.5 Hz, 1H), δ 7.11–7.16 (m, 2H), δ 7.18 (dd, J = 15.6, 6.6 Hz, 1H), δ 7.28 (dd, J = 8.4, 1.8 Hz, 1H), δ 7.53–5.57 (m, 1H), δ 7.65–7.71 (m, 2H). ^{13}C NMR (75 MHz, $CDCl_3$) δ 14.5, δ 20.4, δ 42.2, δ 55.5, δ 60.5, δ 105.8, δ 119.2, δ 120.5, δ 125.7, δ 126.7, δ 127.4, δ 129.3, δ 129.4, δ 133.7, δ 138.6, δ 152.9, δ 157.8, δ 167.0. HRMS: m/z (ESI) calculated $[M]^+$ = 284.1407, measured 284.1408 (Δ < 1 ppm). SFC

analysis: Chiracel AD–H column (40°C oven temperature, 4% MeOH, pressure = 150 bar, 2.0 mL/min flow rate): t = 12.6 min, t = 14.0 min.

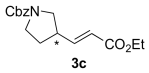

3c

64% yield, a white solid from silica gel chromatography (15:85 ethyl acetate: hexanes; $R_{f(\mathbf{3c})}$ = 0.35). ^{1}H NMR (300 MHz, $CDCl_3$) δ 1.29 (t, J = 7.2 Hz, 3H), δ 1.73–1.88 (m, 1H), δ 2.04–2.15 (m, 1H), δ 2.89–3.04 (m, 1H), δ 3.19–3.29 (m, 1H), δ 3.37–3.47 (m, 1H), δ 3.52–3.72 (m, 2H), δ 4.20 (q, J = 7.2 Hz, 2H), 5.14 (s, 2H), δ 5.89 (dd, J = 15.6, 3.3 Hz, 1H), δ 6.88 (ddd, J = 15.6, 7.5, 4.2 Hz, 1H), δ 7.30–7.39 (m, 5H); ^{13}C NMR (75 MHz, $CDCl_3$) δ 14.4, δ 30.9, δ 31.7, δ 40.6, δ 41.5, δ 45.4, δ 45.9, δ 50.3, δ 50.7, δ 60.7, δ 67.0, δ 122.3, δ 128.1, δ 128.2, δ 128.7, δ 137.0, δ 147.5, δ 147.6, δ 154.9, δ 166.4; HRMS: m/z (ESI) calculated $[M+Na]^+$ = 326.1363, measured 326.1347 (Δ = 5 ppm). SFC analysis: Chiracel AD–H column (50°C oven temperature, 10% MeOH, pressure = 150 bar, 1.5 mL/min flow rate): t = 8.9 min, t = 9.9 min.

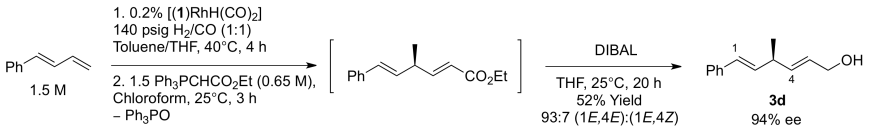

3d
94% ee

In a dinitrogen-filled glove box, charged an oven-dried glass pressure containing a magnetic stir bar with $Rh(acac)(CO)_2$ (0.0015 mmols; 77 μL of 20 mM in toluene) and ligand **1** (0.0017 mmols; 84 μL of 20 mM in THF). A reactor head was attached to the pressure bottle and removed from the glove box. In a well-ventilated fume hood, charged the reactor with 140 psig of H_2/CO (1:1) and heated in an oil bath to 40°C. After 30 minutes removed from heating, depressurized the reactor, and injected a toluene solution of 1-phenyl-1,3-butadiene (0.120 g in

0.5 mL toluene; 0.72 mmols). Repressurized the reactor with 140 psig of H_2/CO and heated at 40°C for 4 hours. The reactor was removed from heating, cooled to room temperature (25°C) and remained under synthesis gas overnight (15 hours), depressurized, followed by addition of a chloroform solution (1 mL) of Ph_3PCHCO_2Et (0.370 g; 1.1 mmols) to the pressure bottle open to atmosphere. After three hours transferred the solution to a Schlenk flask, removed the solvent, added 5 mL of THF and DIBAL (3 mL 1M in cyclohexane) to this solution under dinitrogen at room temperature. After 20 hours, quenched with water and saturated sodium bicarbonate solution and extracted with ether. Dried over $MgSO_4$, filtered, removed the solvent by rotavap, and subjected the mixture to flash chromatography.

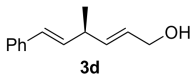

3d

52% yield, a pale yellow oil isolated from silica gel chromatography (30:70 ethyl acetate: hexanes; $R_{f(\mathbf{3d})}$ = 0.27). ^{1}H NMR (300 MHz, $CDCl_3$) δ 1.21 (d, J = 6.9 Hz, 3H), δ 1.37 (br s, 1H), δ 3.08 (sextet d, J = 6.9, 1.2 Hz, 1H), δ 4.15 (m, 2H), δ 5.64–5.79 (m, 2H), δ 6.16 (dd, J = 16.2, 7.2 Hz, 1H), δ 6.38 (d, J = 16.2, 1H), δ 7.17–7.38 (m, 5H); ^{13}C NMR (75 MHz, $CDCl_3$) δ 20.3, δ 39.6, δ 63.9, δ 101.1, δ 126.3, δ 127.3, δ 128.3, δ 128.7, δ 128.9, δ 134.3, δ 136.7, δ 137.8; HRMS: m/z (EI) calculated $[M]^+$ = 188.1196, measured 188.1196 (Δ = 0 ppm). SFC analysis: Chiracel AD–H column (50°C oven temperature, 5% MeOH, pressure = 150 bar, 2.0 mL/min flow rate): t = 6.7 min, t = 7.1 min.

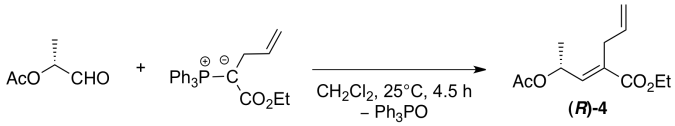

(*R*)-4

1,4–Dienes **(*R*)-4** and **(*S*)-4** were synthesized from the olefination of the corresponding lactaldehyde $Ph_3PC(CH_2CHCH_2)CO_2Et$ at room temperature. A clear colorless oil was isolated from silica gel chromatography (10:90 ethyl acetate:hexanes; $R_{f(\mathbf{R\text{-}4})} = 0.29$).

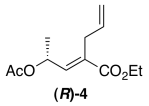

(*R*)-4

^{1}H NMR (300 MHz, $CDCl_3$) δ 1.30 (t, J = 7.2 Hz, 3H), δ 1.34 (d, J = 6.6 Hz, 3H), δ 2.04 (s, 3H), δ 3.16 (dt, J = 6.0, 1.5 Hz, 2H), δ 4.21 (q, J = 7.2 Hz, 2H), δ 4.99–5.07 (m, 2H), δ 5.63 (dq, J = 8.7, 6.6 Hz, 1H), δ 5.77–5.90 (m, 1H), δ 6.66 (d, J = 9.0, 1H); ^{13}C NMR (75 MHz, $CDCl_3$) δ 14.4, δ 20.2, δ 21.4, δ 31.5, δ 61.1, δ 67.5, δ 115.9, δ 131.9, δ 135.4, δ 140.7, δ 167.3, δ 170.4; HRMS: m/z (ESI) calculated $[M+Na]^+ = 249.1098$, measured 249.1097 ($\Delta < 1$ ppm).

AHF Procedure of (*R*)-4, (*S*)-4, and 7

In a dinitrogen-filled glove box, charged an oven-dried glass pressure containing a magnetic stir bar with solutions of $Rh(acac)(CO)_2$ (20 mM in toluene) and ligand **1** (20 mM in THF). A reactor head was attached to the pressure bottle and removed from the glove box. In a well-ventilated fume hood, charged the reactor with 140 psig of H_2/CO (1:1) and heated in an oil bath to 40°C for at least 0.5 hour. After pre-activation of $[(\mathbf{1})Rh(H)(CO)_2]$, depressurized the reactor, and injected a toluene solution of **(*R*)-4** (0.050 g, 0.22 mmols, 101 μL toluene), **(*S*)-4** (0.050 g, 0.22 mmols, 101 μL toluene), or **7** (0.057 g, 0.16 mmols, 75 μL toluene) followed by charging the reactor to the pressures (of synthesis gas) and heating the reactions to the temperatures indicated in Table 2. Conversions were determined as followed: conversion = aldehyde/(aldehyde + alkene).

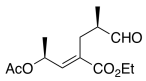

b-(*S*)-5

^{1}H NMR (300 MHz, $CDCl_3$) δ 1.12 (d, J = 7.2 Hz, 3H), δ 1.31 (t, J = 7.2, 3H), δ 1.35 (d, J = 6.6 Hz, 3H), δ 2.05 (s, 3H), δ 2.37 (dd, J = 13.8, 7.2, 1H), δ 2.65 (sextet d, J = 7.2, 1.5 Hz, 1H), δ 2.86 (dd, J = 13.8, 8.1 Hz, 1H), δ 4.21 (q, J = 7.2, 2H), δ 5.64 (dq, J = 9.3, 6.6, 1H), δ 6.67 (d, J = 9.3, 1H), δ 9.65 (d, J = 1.5 Hz, 1H); ^{13}C NMR (75 MHz, $CDCl_3$) δ 13.6, δ 14.3, δ 20.2, δ 21.3, δ 28.2, δ 45.8, δ 61.3, δ 67.5, δ 131.1, δ 141.7, δ 167.2, δ 170.4, δ 203.9; HRMS: m/z (ESI) calculated $[M+Na]^+$ = 279.1203, measured 279.1208 (Δ = 1.8 ppm).

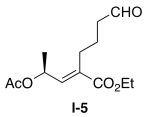

I-5

^{1}H NMR (300 MHz, $CDCl_3$) δ 1.31 (t, J = 7.2 Hz, 3H), δ 1.35 (d, J = 6.6 Hz, 3H), δ 1.70–1.87 (m, 2H), δ 2.05 (s, 3H), δ 2.31–2.51 (m, 4H), δ 4.21 (q, J = 7.2 Hz, 2H), δ 5.60 (dq, J = 9.0, 6.6 Hz, 1H), δ 6.60 (d, J = 8.7 Hz, 1H), δ 9.78 (t, J = 1.5 Hz, 1H); ^{13}C NMR (75 MHz, $CDCl_3$) δ 14.4, δ 20.4, δ 21.3, δ 21.8, δ 26.7, δ 43.5, δ 61.1, δ 67.4, δ 133.3, δ 140.5, δ 167.3, δ 170.4, δ 202.2; HRMS: m/z (ESI) calculated $[M+Na]^+$ = 279.1208, measured 279.1205 (Δ = 1.1 ppm).

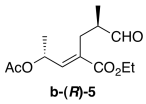

b-(*R*)-5

^{1}H NMR (300 MHz, $CDCl_3$) δ 1.08 (d, J = 7.2 Hz, 3H), δ 1.31 (t, J = 7.2 Hz, 3H), δ 1.36 (d, J = 6.6 Hz, 3H), δ 2.05 (s, 3H), δ 2.48 (dd, J = 13.2, 7.8 Hz, 1H), δ 2.56–2.67 (m, 1H), δ 2.80 (dd, J

= 13.2, 6.3 Hz, 1H), δ 4.21 (q, J = 7.2 Hz, 2H), δ 5.59 (dq, J = 9.3, 6.6 Hz, 1H), δ 6.68 (d, J = 9.3 Hz, 1H), δ 9.66 (d, J = 1.5 Hz, 1H).

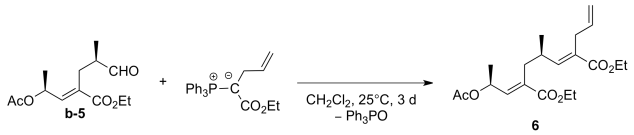

Compound **6** was synthesized from the olefination of **b-5** with $Ph_3PC(CH_2CHCH_2)CO_2Et$ at room temperature in a minimal amount of dichloromethane. A colorless oil was isolated from silica gel chromatography (20:80 ethyl acetate:hexanes). ^{1}H NMR (300 MHz, $CDCl_3$) δ 1.06 (d, J = 6.9, 3H), δ 1.25–1.33 (m, 9H), δ 2.04 (s, 3H), δ 2.41–2.54 (m, 2H), δ 2.78–2.89 (m, 1H), δ 2.92–3.05 (m, 2H), δ 4.13–4.23 (m, 4H), δ 4.92–5.01 (m, 2H), δ 5.62 (dq, J = 9.3, 6.6 Hz, 1H), δ 5.69–5.82 (m, 1H), δ 6.55 (d, J = 9.0, 1H), δ 6.58 (d, J = 8.1); HRMS: m/z (ESI) calculated $[M+Na]^+$ = 389.1935, measured 389.1932 (Δ < 1 ppm).

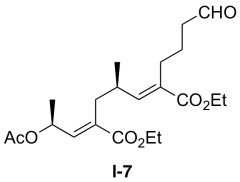

A colorless oil isolated from silica gel chromatography (25:75 ethyl acetate: hexanes; $R_{f(\mathbf{I\text{-}7})}$ = 0.24). ^{1}H NMR (300 MHz, $CDCl_3$) δ 1.08 (d, J = 6.6 Hz, 3H), δ 1.27–1.33 (m, 9H), δ 1.63–1.73 (m, 2H), δ 2.05 (s, 3H), δ 2.23–2.28 (m, 2H), δ 2.38–2.48 (m, 4H), δ 2.77–2.88 (m, 1H), δ 4.14–4.25 (m, 4H), δ 5.61 (dq, J = 9.3, 6.6 Hz, 1H), δ 6.52 (d, J = 10.8, 1H), δ 6.58 (d, J = 9.3 Hz, 1H), δ 9.75 (t, J = 1.8 Hz, 1H); ^{13}C NMR (75 MHz, $CDCl_3$) δ 14.4, δ 14.5, δ 20.3, δ 20.6, δ 21.4,

δ 22.3, δ 26.3, δ 33.1, δ 34.4, δ 43.7, δ 60.8, δ 61.2, δ 67.4, δ 131.2, δ 132.2, δ 140.6, δ 147.6, δ 167.4, δ 167.7, δ 170.4, δ 202.4; HRMS: m/z (ESI) calculated $[M+Na]^+$ = 419.2041, measured 419.2057 (Δ = 3.8 ppm).

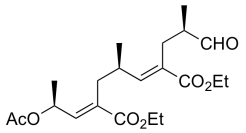

b-7

A colorless oil isolated from silica gel chromatography (25:75 ethyl acetate: hexanes; $R_{f(\mathbf{b\text{-}7})}$ = 0.32). ^{1}H NMR (300 MHz, $CDCl_3$) δ 1.03 (d, J = 6.9 Hz, 3H), δ 1.05 (d, J = 7.5, 3H) δ 1.26–1.32 (m, 9H), δ 2.04 (s, 3H), δ 2.30 (dd, J = 13.2, 6.9, 1H), δ 2.41–2.58 (m, 3H), δ 2.63 (dd, J = 13.2, 7.2 Hz, 1H), δ 2.79–2.90 (m, 1H), δ 4.14–4.23 (m, 4H), δ 5.62 (dq, J = 9.3, 6.6 Hz, 1H), δ 6.57–6.62 (m, 2H), δ 9.61 (d, J = 1.5 Hz, 1H). ^{13}C NMR (75 MHz, $CDCl_3$) δ 13.52, δ 14.4, δ 20.26, δ 20.37, δ 21.4, δ 27.9, δ 33.2, δ 34.2, δ 46.1, δ 60.9, δ 61.2, δ 67.3, δ 128.9, δ 132.1, δ 140.8, δ 148.9, δ 167.4, δ 167.5, δ 170.4, δ 204.3. HRMS: m/z (ESI) calculated $[M+H]^+$ = 397.2221, measured 397.2235 (Δ = 3.5 ppm).

AHF-WO-AHF Procedure of Vinyl Acetate with $Ph_3PC(CH_2CH{=}CH_2)CO_2Et$

In a dinitrogen-filled glovebox, an oven-dried 18 mL pressure bottle containing a magnetic stir bar was charged with solutions of $Rh(acac)(CO)_2$ (54 μL, 20 mM in toluene, 0.0011 mmols), ligand **1** (60 μL, 20 mM in THF, 0.0012 mmols), and vinyl acetate (50 μL, 0.54 mmols). In the glove box, prepared a chloroform solution (248 μL) of $Ph_3PC(CH_2CHCH_2)CO_2Et$ (0.280 g; 0.721 mmols). The pressure bottle was attached to a reactor head and brought out of the glove

box. In a well-ventilated hood, the reactor was attached to a synthesis gas source (1:1 H_2/CO) subjected to five pressurization cycles (140 psig/0 psig), followed by a final pressurization to 140 psig and heated the pressure bottle in a 40°C oil bath. After two hours, removed the reactor from the oil bath, cooled, depressurized (0 psig), followed by injection of the chloroform solution containing the Wittig ylide followed by an adding 0.5 mL of chloroform using the same syringe. The reactor was subjected to five pressurization/depressurization cycles and heated to 40°C in an oil bath for 18 hours. The reaction was checked by ^{1}H NMR spectroscopy and **b-5** was isolated from silica gel chromatography.

Synthesis of (nBu)$_3$PCHCO$_2$CH=CH$_2$

In a 100 mL Schlenk flask, combined 50 mL of diethyl ether, 6.2 mL (5 g, 0.0247 mols) of tri-*n*-butylphosphine, and 2.8 mL (3.3 g, 0.0273 mols) of vinyl chloroacetate, and stirred at room temperature. A white solid began to precipitate from solution after stirring for a few minutes. [(nBu)$_3$PCH$_2$CO$_2$CHCH$_2$]Cl was filtered using a filter cannula after stirring overnight (22.5 hours) as 5.04 g of a white solid (63% isolated yield). ^{31}P{^{1}H} NMR (121 MHz, $CDCl_3$) δ 33.5 (s). ^{1}H NMR (300 MHz, $CDCl_3$) δ 0.98 (t, J = 7.2 Hz, 9H), δ 1.47–1.66 (m, 12H), δ 2.59–2.69 (m, 6H), δ 4.57 (d, J = 13.8 Hz, 2H), δ 4.73 (dd, J = 6.0, 2.1 Hz, 1H), δ 5.01 (dd, J = 14.1, 2.1 Hz, 1H), δ 7.18 (dd, J = 14.1, 6.0, 1H).

In a 250 mL round bottom flask, 4.0 g of [(nBu)$_3$PCH$_2$CO$_2$CHCH$_2$]Cl was dissolved in 50 mL of CH_2Cl_2 and 40 mL of a 0.4 M NaOH(aq) was added and stirred vigorously for 1 hour. The organic layer was separated from the aqueous solution, dried over $MgSO_4$, and the

dichloromethane was removed to quantitatively yield a pale yellow oil. $^{31}P\{^{1}H\}$ NMR (121 MHz, $CDCl_3$) δ 20.3 (br s), δ 22.9 (br s). ^{1}H NMR (300 MHz, $CDCl_3$) δ 0.94 (t, J = 7.2 Hz, 9H), δ 1.37–1.54 (m, 12H), δ 1.83–1.93 (m, 6H), δ 2.18–2.32 (br s, 1H), δ 4.18 (d, J = 6.6 Hz 1H), δ 4.54 (br d, J = 14.1 Hz 1H), δ 7.38 (dd, J = 14.1, 6.3 Hz 1H). $^{13}C\{^{1}H\}$ NMR (75 MHz, $CDCl_3$) δ 13.8 (s), δ 22.1 (d, J = 55.6 Hz), δ 24.2 (d, J = 14.8 Hz), δ 24.2 (d, J = 3.7 Hz), δ 27.9 (d, J = 65.6 Hz), δ 27.5 (d, J = 117.1 Hz), δ 90.8 (s), δ 143.0 (s), δ 168 (d, J = 14.5 Hz).

Note: samples of $(n\text{Bu})_3\text{PCHCO}_2\text{CH=CH}_2$ browned over time while stored in a nitrogen-filled glovebox freezer (−22°C).

Synthesis of Vinyl 2-bromopropanoate

A synthesis of vinyl 2-bromopropanoate has been reported.[43] The following procedure was used to achieve a higher yield of product: In a 50 mL Schlenk flask, combined 0.074 g of $Pd(OAc)_2$ (0.32 mmols) 0.108 g of bathophenanthroline (0.32 mmols), 5.0 g of 2-bromopropanoic acid (0.033 mols), and 30 mL of vinyl acetate (0.325 mols) and heated to reflux open to air (using a needle vent on the reflux condenser). After ~18 hours of reflux, removed the flask from heating, cooled, filtered the yellow mixture over a plug of silica and Celite, and rinsed with pentane (3 x 5 mL). Rovaped off the excess vinyl acetate and subjected the resulting oil to column chromatography (5% ether/pentane, v/v) to yield 3.75 g of a colorless oil (64% isolated yield). ^{1}H NMR (300 MHz, $CDCl_3$) δ 1.87 (d, J = 6.9 Hz, 3H), δ 4.42 (q, J = 6.9 Hz, 1H), δ 4.69 (dd, J = 6.3, 2.1 Hz, 1H), 5.01 (dd, J = 13.8, 2.1 Hz, 1H), δ 7.26 (dd, J = 13.8, 6.3 Hz, 1H). $^{13}C\{^{1}H\}$ NMR (75 MHz, $CDCl_3$) δ 21.6, δ 39.3, δ 99.4, δ 141.4, δ 167.6.

Synthesis of (nBu)$_3$PC(CH$_3$)CO$_2$CH=CH$_2$

In a nitrogen-filled glovebox, charged 5.75 mL (0.023 mols) of tri-*n*-butylphosphine into a 50 mL Schlenk flask. Transferred the sample to an Schlenk line, added 25 mL of hexane and 4.1 g (0.023 mols) of vinyl 2-bromopropanoate, and stirred at 50°C. The reaction was stirred for 9.5 hours resulting in two phases. The hexane layer was decented off to leave behind a pale yellow oil, [(nBu)$_3$PCH$_2$CO$_2$CH=CH$_2$]Br. ^{31}P{^{1}H} NMR (121 MHz, CDCl$_3$) δ 37.4 (s). ^{1}H NMR (300 MHz, CDCl$_3$) δ 0.98 (t, J = 7.2 Hz, 9H), δ 1.37–1.73 (m, 15H), δ 2.46–2.77 (m, 6H), δ 4.79 (dd, J = 6.3, 2.4 Hz, 1H), δ 4.86 (dq, J = 15.9, 7.2 Hz, 1H), 5.05 (dd, J = 13.8, 2.4 Hz, 1H), 7.23 (dd, J = 13.8, 6.3 Hz, 1H). ^{13}C{^{1}H} NMR (75 MHz, CDCl$_3$) δ 11.9 (d, J = 3.5 Hz), δ 13.5 (s), δ 19.0 (d, J = 45.1 Hz), δ 24.0 (d, J = 2.0 Hz), δ 24.2 (d, J = 7.5 Hz), δ 34.2 (d, J = 46.4 Hz), δ 100.7 (s), δ 140.5 (s), δ 166.4 (d, J = 2.3 Hz).

In a 250 mL round bottom flask, combined [(nBu)$_3$PCH(CH$_3$)CO$_2$CH=CH$_2$]Br, 30 mL of methylene chloride, and 75 mL of a 0.4 M solution of NaOH (aq) and stirred vigorously in air for 10 minutes. Separated the organic layer, dried over MgSO$_4$, and rotavaped off the solvent to isolate 6.3 g of an orange oil (~71% purity by ^{1}H NMR). ^{31}P{^{1}H} NMR (121 MHz, CDCl$_3$) δ 37.4 (s). ^{1}H NMR (400 MHz, CDCl$_3$) δ 0.94 (t, J = 7.2 Hz), δ 1.38–1.45 (m), δ 1.50–1.60 (m), δ 1.70 (d, J = 12 Hz), δ 1.83–2.01 (br s), δ 4.15 (d, J = 6.4 Hz), δ 4.37–4.64 (br s), δ 7.43 (dd, J = 14.0, 6.4 Hz).

Note: (nBu)$_3$PC(CH$_3$)CO$_2$CH=CH$_2$ is air-sensitive and samples were stored in a nitrogen-filled glovebox freezer (−22°C).

AHF-WO-AHF-WO-AHF-WO Procedure of Vinyl Benzoate with (nBu)$_3$PC*(CH$_3$)*CO$_2$CH=CH$_2$ and (nBu)$_3$PC*H*CO$_2$CH=CH$_2$

In a dinitrogen-filled glovebox, an oven-dried 18 mL pressure bottle containing a magnetic stir bar was charged with solutions of Rh(acac)(CO)$_2$ (337 μL, 20 mM in toluene, 0.0067 mmols), ligand **1** (371μL, 20 mM in THF, 0.0074 mmols), and vinyl benzoate (187 μL, 1.34 mmols). In the glove box, prepared two THF solutions (192 μL) of Ph$_3$PC(CH$_3$)CO$_2$(CH=CH$_2$) (0.408 and 0.401 g; 1.4 and 1.3 mmols respectively) and one THF solution (192 μL) of Ph$_3$PCHCO$_2$(CH=CH$_2$) (0.384 g, 1.3 mmols) in culture tubes fixed with septa. The pressure bottle was attached to a reactor head, brought out of the glove box and in a well-ventilated hood, the reactor was subjected to five pressurization cycles of syngas (140 psig/0 psig; 1:1 H$_2$:CO), followed by a final pressurization to 140 psig, and heated the pressure bottle in a 60°C oil bath. After 2.5 hours, removed the reactor from the oil bath, cooled, depressurized (0 psig), followed by injection of Ph$_3$PC(CH$_3$)CO$_2$(CH=CH$_2$) (0.408 g sample) and was subjected to ten pressurization/depressurization cycles, and heated again to 60°C in an oil bath for 15 hours. The same operational sequence was performed to add 0.401 g of Ph$_3$PC(CH$_3$)CO$_2$(CH=CH$_2$) followed by ten syngas cycles, and heated reactor back to 60°C in an oil bath. After 5.5 hours, the reaction was removed from heating, cooled, depressurized, an aliquote was removed for ^{1}H and COSY NMR spectroscopy, and last addition of Wittig ylide, Ph$_3$PCHCO$_2$(CH=CH$_2$) was added at room temperature. Using silica gel chromatography (2x; 15:85 ethyl acetate: hexanes, R_f = 0.38), isolated 0.089 g of the dimer and 0.110 g of the trimer (18% and 17% respectively, based on vinyl benzoate).

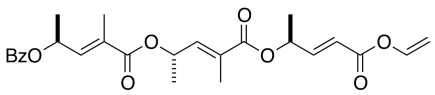

8
4-hydroxyvalerate trimer

A colorless oil isolated from silica gel chromatography. ^{1}H NMR (300 MHz, $CDCl_3$) δ 1.40 (d, J = 6.4 Hz), δ 1.42 (d, J = 6.8 Hz), δ 1.43 (d, J = 6.8 Hz), δ 1.48 (d, J = 6.8 Hz), δ 1.96 (s), δ 1.99 (s), δ 4.59–4.64 (m), δ 4.91–4.97 (m), δ 5.54–5.62 (m), δ 5.69 (dq, J = 8.4, 6.4 Hz), δ 5.84–5.91 (m), δ 5.96–6.05 (m), δ 6.67–6.72 (m), δ 6.74–6.78 (m), δ 7.00–7.08 (m), δ 7.30–7.37 (m), δ 7.426–7.46 (m), δ 7.55–7.58 (m), δ 8.02–8.06 (m). $^{13}C\{^{1}H\}$ NMR (75 MHz, $CDCl_3$) δ 13.06, δ 13.12, δ 19.76, δ 19.8, δ 20.0, δ 68.29, δ 68.33, δ 68.37, δ 68.38, δ 68.41, δ 69.55, δ 69.56, δ 98.4, δ 119.9, δ 120.0, δ 128.5, δ 128.6, δ 129.22, δ 129.25, δ 129.58, δ 129.61, δ 129.63, δ 129.75, δ 129.85, δ 130.31, δ 133.3, δ 140.38, δ 140.74, δ 140.80, δ 141.26, δ 148.72, δ 148.77, δ 163.2, δ 166.0, δ 166.7, δ 167.0, δ 167.1. HRMS: m/z (ESI) calculated $[M+NH_4]^+$ = 488.2279, measured 488.2286 (Δ = 1.4 ppm).

5.7 References

(1) Claver, C.; van Leeuwen, P. W. N. M. *Rhodium Catalyzed Hydroformylation*; Kluwer Academic Publishers: Dordrecht, The Netherlands, 2000.

(2) Klosin, J.; Landis, C. R. *Acc. Chem. Res.* **2007**, *40*, 1251-1259.

(3) Gual, A.; Godard, C.; Castillón, S.; Claver, C. *Tetrahedron: Asymmetry* **2010**, *21*, 1135-1146.

(4) Eilbracht, P.; Bärfacker, L.; Buss, C.; Hollmann, C.; Kitsos-Rzychon, B. E.; Kranemann, C. L.; Rische, T.; Roggenbuck, R.; Schmidt, A. *Chem. Rev.* **1999**, *99*, 3329-3366.

(5) Breit, B.; Seiche, W. *Synthesis* **2001**, *2001*, 0001-0036.

(6) Breit, B. In *Metal Catalyzed Reductive C–C Bond Formation*; Krische, M., Ed.; Springer Berlin / Heidelberg: 2007; Vol. 279, p 139-172.

(7) Clark, T. P.; Landis, C. R.; Freed, S. L.; Klosin, J.; Abboud, K. A. *J. Am. Chem. Soc.* **2005**, *127*, 5040-5042.

(8) Watkins, A. L.; Hashiguchi, B. G.; Landis, C. R. *Org. Lett.* **2008**, *10*, 4553-4556.

(9) McDonald, R. I.; Wong, G. W.; Neupane, R. P.; Stahl, S. S.; Landis, C. R. *J. Am. Chem. Soc.* **2010**, *132*, 14027-14029.

(10) Watkins, A. L.; Landis, C. R. *Org. Lett.* **2011**, *13*, 164-167.

(11) Axtell, A. T.; Cobley, C. J.; Klosin, J.; Whiteker, G. T.; Zanotti-Gerosa, A.; Abboud, K. A. *Angew. Chem. Int. Ed.* **2005**, *44*, 5834-5838.

(12) Yan, Y.; Zhang, X. *J. Am. Chem. Soc.* **2006**, *128*, 7198-7202.

(13) Thomas, P. J.; Axtell, A. T.; Klosin, J.; Peng, W.; Rand, C. L.; Clark, T. P.; Landis, C. R.; Abboud, K. A. *Org. Lett.* **2007**, *9*, 2665-2668.

(14) Worthy, A. D.; Joe, C. L.; Lightburn, T. E.; Tan, K. L. *J. Am. Chem. Soc.* **2010**, *132*, 14757-14759.

(15) Zhang, X.; Cao, B.; Yu, S.; Zhang, X. *Angew. Chem. Int. Ed.* **2010**, *49*, 4047-4050.

(16) Joe, C. L.; Tan, K. L. *J. Org. Chem.* **2011**, *76*, 7590-7596.

(17) Wang, X.; Buchwald, S. L. *J. Am. Chem. Soc.* **2011**, *133*, 19080-19083.

(18) Chikkali, S. H.; Bellini, R.; de Bruin, B.; van der Vlugt, J. I.; Reek, J. N. H. *J. Am. Chem. Soc.* **2012**, *134*, 6607-6616.

(19) Clemens, A. J. L.; Burke, S. D. *J. Org. Chem.* **2012**, *77*, 2983-2985.

(20) Noonan, G. M.; Fuentes, J. A.; Cobley, C. J.; Clarke, M. L. *Angew. Chem. Int. Ed.* **2012**, *51*, 2477-2480.

(21) Wong, G. W.; Adint, T. A.; Landis, C. R. *Org. Synth.* **2012**, *89*, 243-254.

(22) Marshall, J. A.; Yanik, M. M. *J. Org. Chem.* **2001**, *66*, 1373-1379.

(23) Ehrlich, G.; Kalesse, M. *Synlett* **2005**, *2005*, 655,657.

(24) Canova, S.; Bellosta, V. r.; Bigot, A.; Mailliet, P.; Mignani, S.; Cossy, J. *Org. Lett.* **2006**, *9*, 145-148.

(25) Chandrasekhar, S.; Yaragorla, S. R.; Sreelakshmi, L.; Reddy, C. R. *Tetrahedron* **2008**, *64*, 5174-5183.

(26) Dunetz, J. R.; Julian, L. D.; Newcom, J. S.; Roush, W. R. *J. Am. Chem. Soc.* **2008**, *130*, 16407-16416.

(27) Breit, B.; Zahn, S. K. *Angew. Chem. Int. Ed.* **1999**, *38*, 969-971.

(28) Breit, B.; Zahn, S. K. *Tetrahedron* **2005**, *61*, 6171-6179.

(29) Farwick, A.; Helmchen, G. *Adv. Synth. Catal.* **2010**, *352*, 1023-1032.

(30) Risi, R. M.; Burke, S. D. *Org. Lett.* **2012**, *14*, 1180-1182.

(31) Risi, R. M.; Burke, S. D. *Org. Lett.* **2012**, *14*, 2572-2575.

(32) Trost, B. M.; Surivet, J.-P.; Toste, F. D. *J. Am. Chem. Soc.* **2004**, *126*, 15592-15602.

(33) Duvall, J. R.; Wu, F.; Snider, B. B. *J. Org. Chem.* **2006**, *71*, 8579-8590.

(34) López, I.; Rodríguez, S.; Izquierdo, J.; Gonzáez, F. V. *J. Org. Chem.* **2007**, *72*, 6614-6617.

(35) Crimmins, M. T.; Jacobs, D. L. *Org. Lett.* **2009**, *11*, 2695-2698.

(36) Ichikawa, Y.; Matsuda, Y.; Okumura, K.; Nakamura, M.; Masuda, T.; Kotsuki, H.; Nakano, K. *Org. Lett.* **2011**, *13*, 2520-2523.

(37) One-pot AHF-Wittig olefination experiments in which the reagents, catalyst precursor, and diazaphospholane were combined in a pressure bottle followed by pressurization yielded partial hydrogenation of the α,β-unsaturated ester C=C bond and lowered ee. However, preformation of Rh(**1**)H$(CO)_2$ followed by addition of the hydroformylation substrate, Wittig reagent, and synthesis gas led to high ee and no hydrogenation of the olefination product.

(38) Watkins, A. L.; Landis, C. R. *J. Am. Chem. Soc.* **2010**, *132*, 10306-10317.

(39) Kollár, L.; Bakos, J.; Tóth, I.; Heil, B. *J. Organomet. Chem.* **1988**, *350*, 277-284.

(40) Casey, C. P.; Martins, S. C.; Fagan, M. A. *J. Am. Chem. Soc.* **2004**, *126*, 5585-5592.

(41) Vinyl ester substituted Wittig ylides were accessed from tributylphosphine and an α-halogenated vinyl ester (synthesized from Pd-catalyzed transvinylation with various substituted bromoacetic acids).

(42) The experiment was performed with 1.3 mmols (0.2g) of vinyl benzoate. Because the tributylphosphine ylides are viscous oils, addition of precise stoichiometric amounts iwas difficult. It is anticipated that larger scale experiments would improved polydispersity.

(43) Schmitt, J.; Blanchard, N.; Poly, J. *Polym. Chem.* **2011**, *2*, 2231-2238.

Chapter 6

Appendix

Table of Contents

[1]Structure determined by Ilia Guzei

6.1 NMR Spectra from Chapter 3

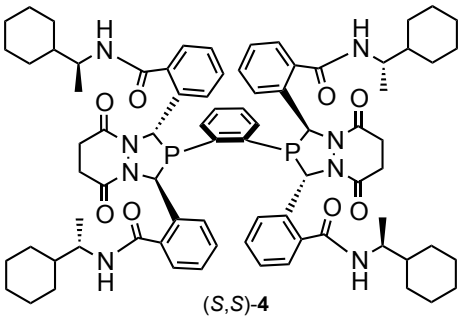

(*S*,*S*)-**4**

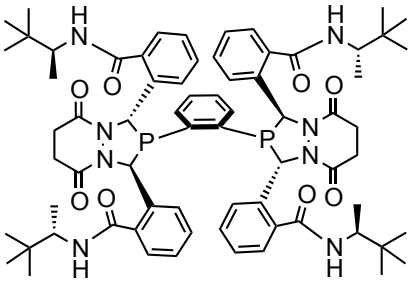

(*S*,*S*)-**5**

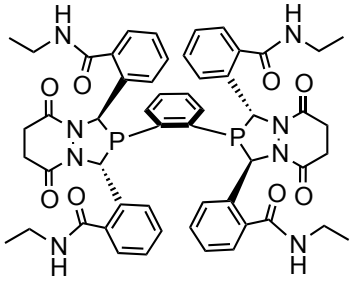

(*R*,*R*)-**6**

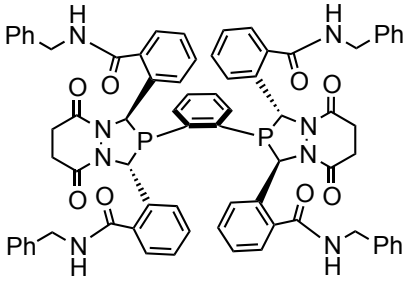

(*R*,*R*)-**7**

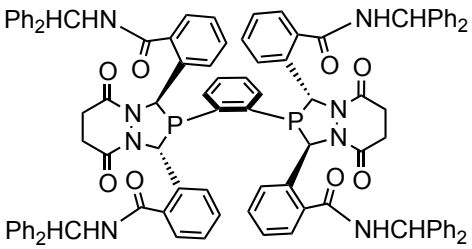

(*S*,*S*)-**8**

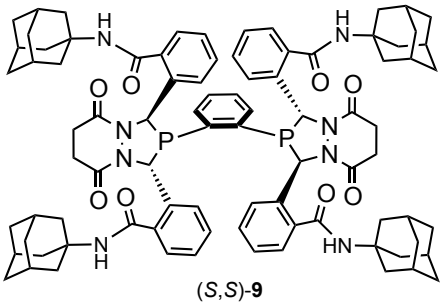

(*S*,*S*)-**9**

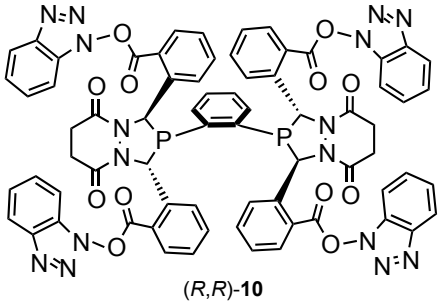

(*R*,*R*)-**10**

$^{31}P\{^{1}H\}$ NMR of (*S*,*S*)-**4** (contains a small amount of a hexafluorophosphate salt, not shown):

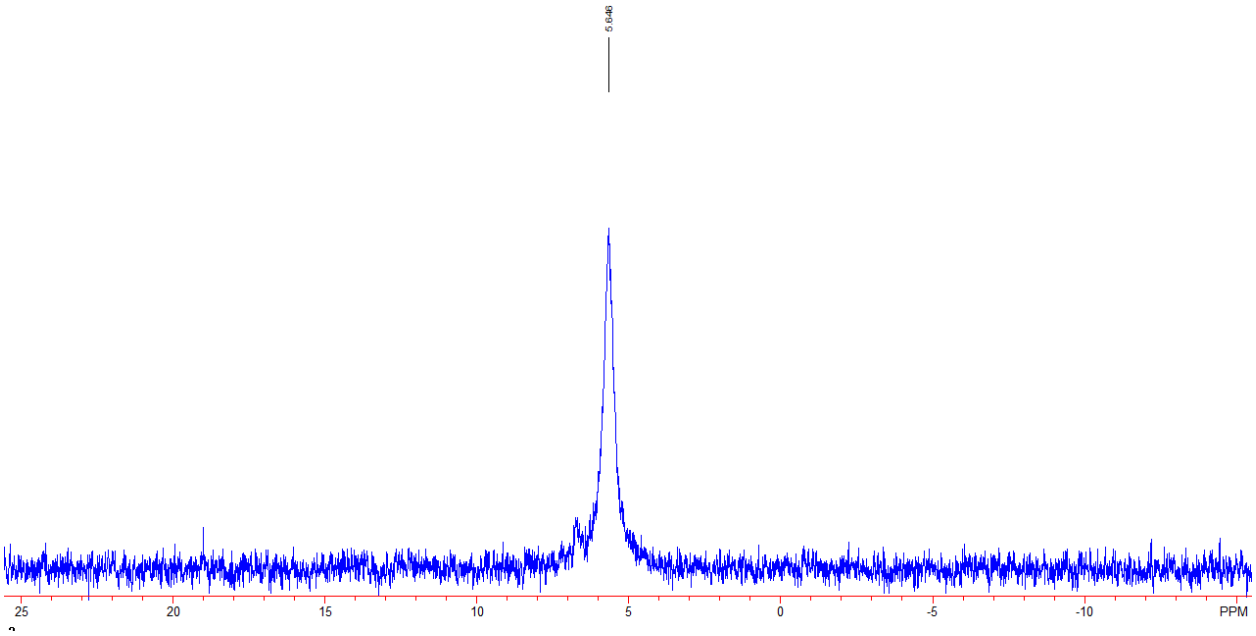

^{1}H NMR of (*S*,*S*)-**4**:

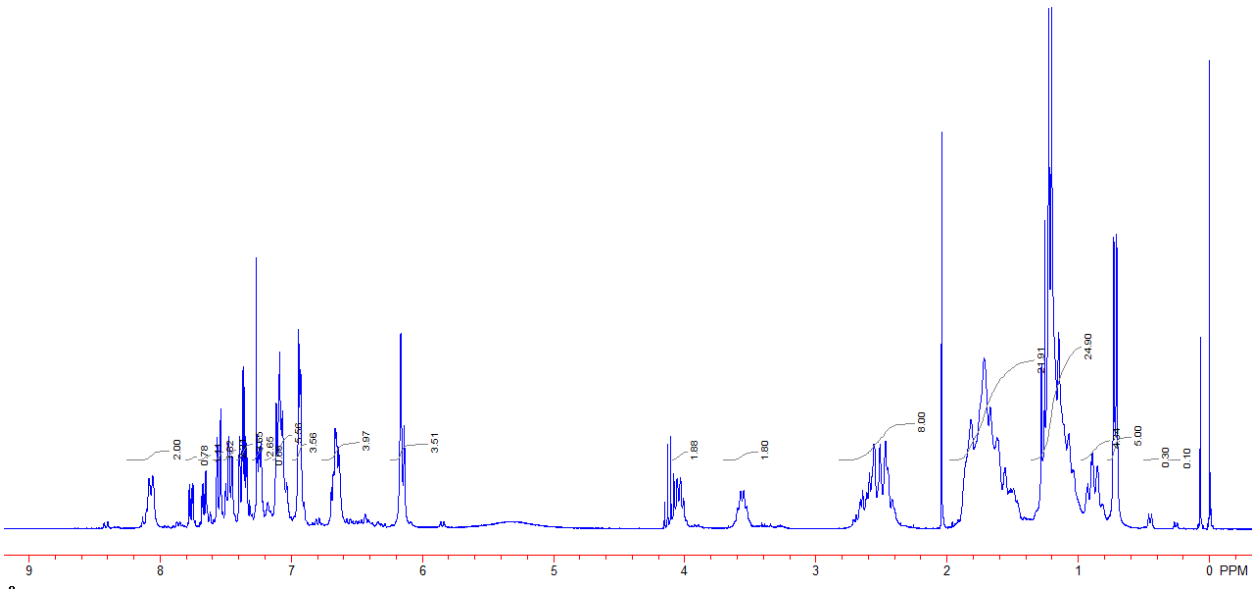

^{1}H NMR of (*S*,*S*)-**4**:

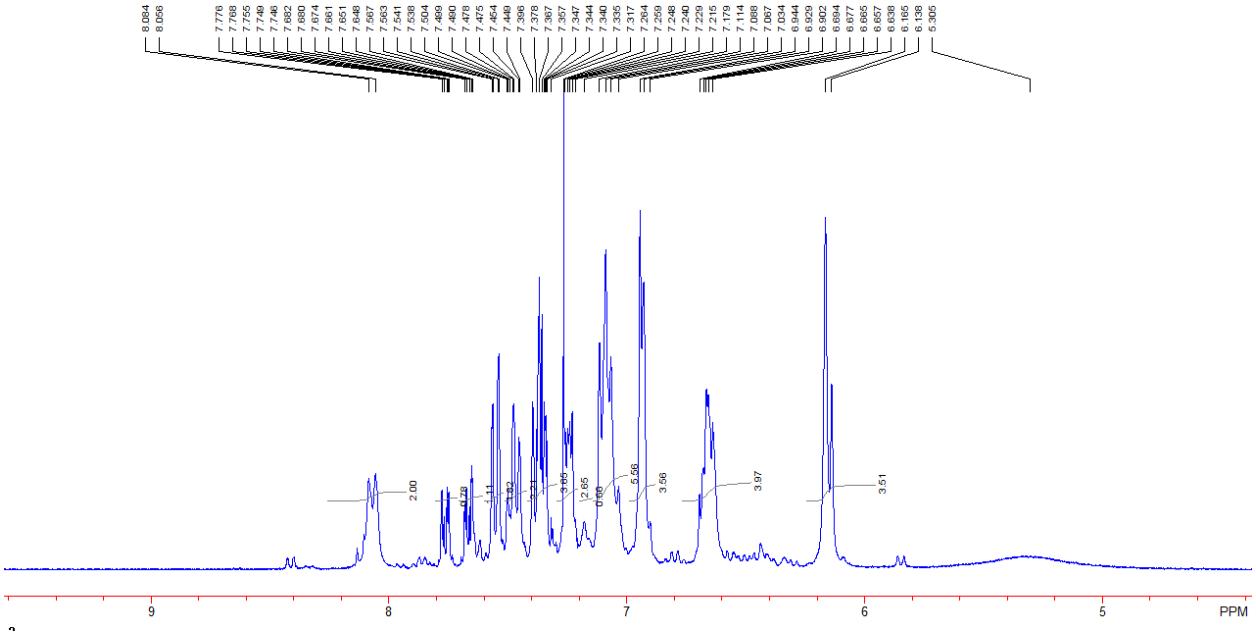

^{1}H NMR of (*S*,*S*)-**4**:

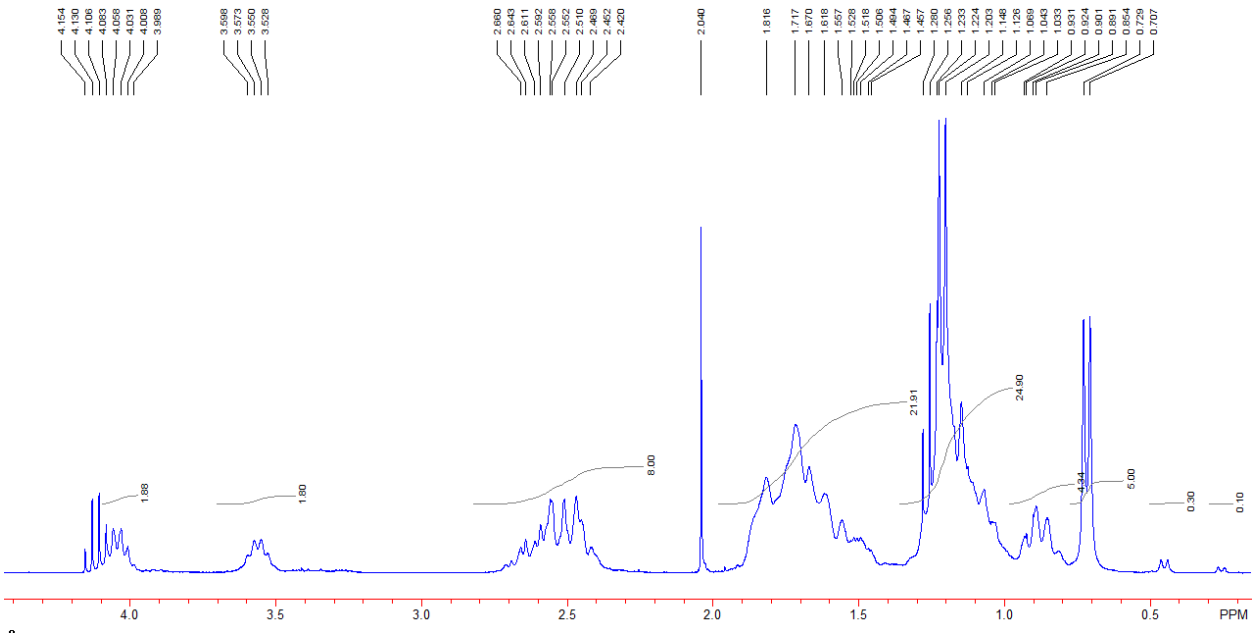

^{13}C NMR of (*S*,*S*)-**4**:

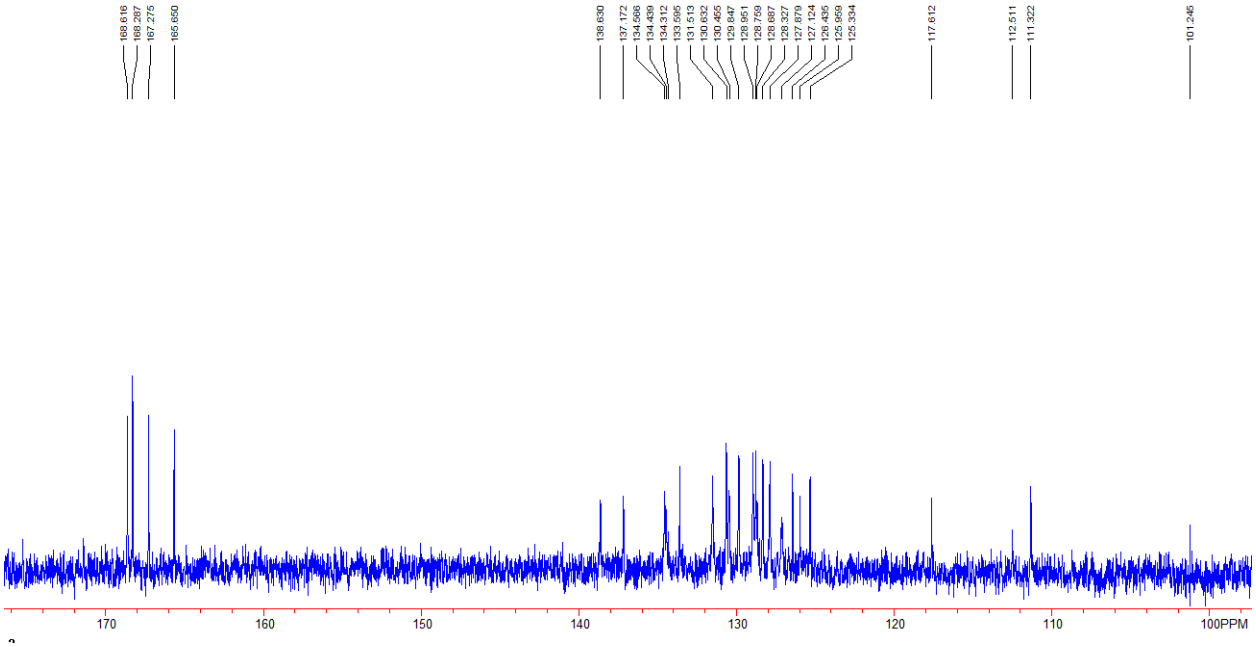

^{13}C NMR of (*S*,*S*)-**4**:

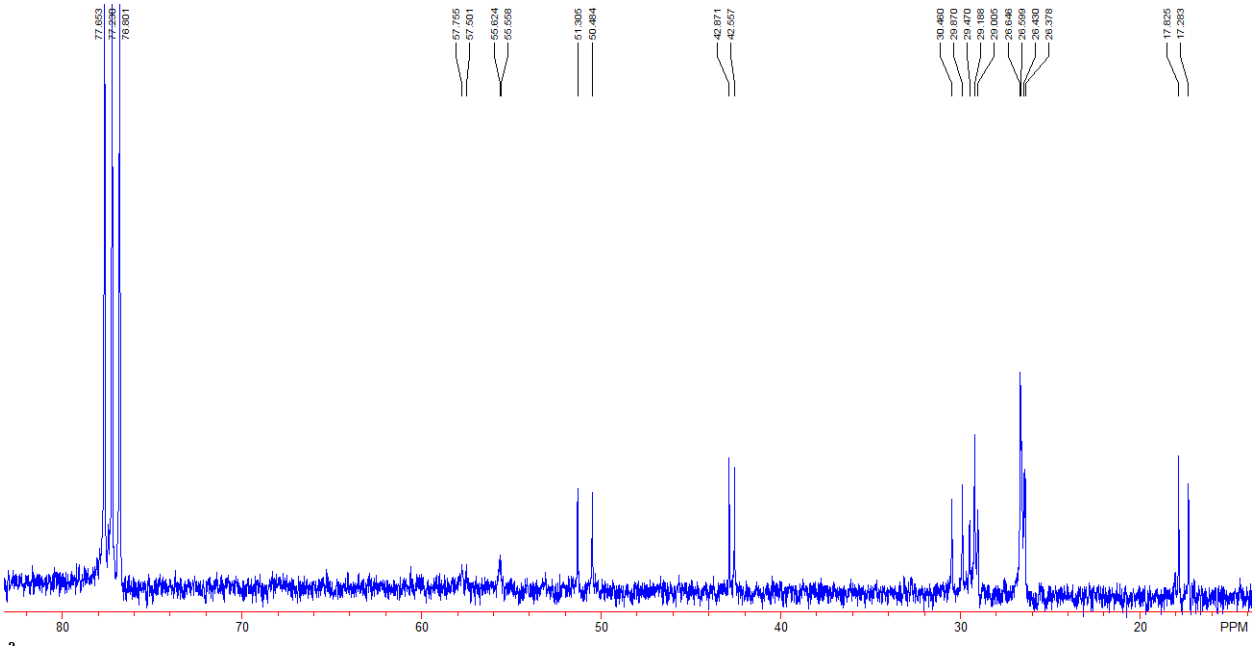

$^{31}P\{^{1}H\}$ NMR of (*S*,*S*)-**5** (contains a small amount of a hexafluorophosphate salt, not shown):

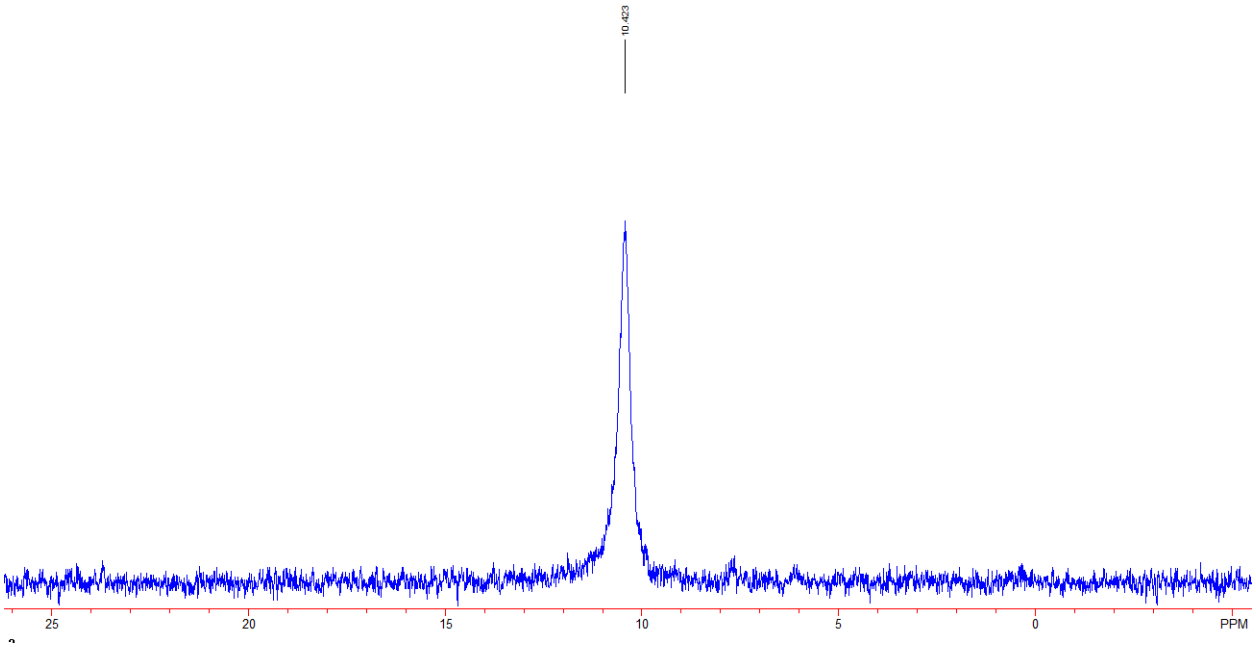

^{1}H NMR of (*S*,*S*)-**5**:

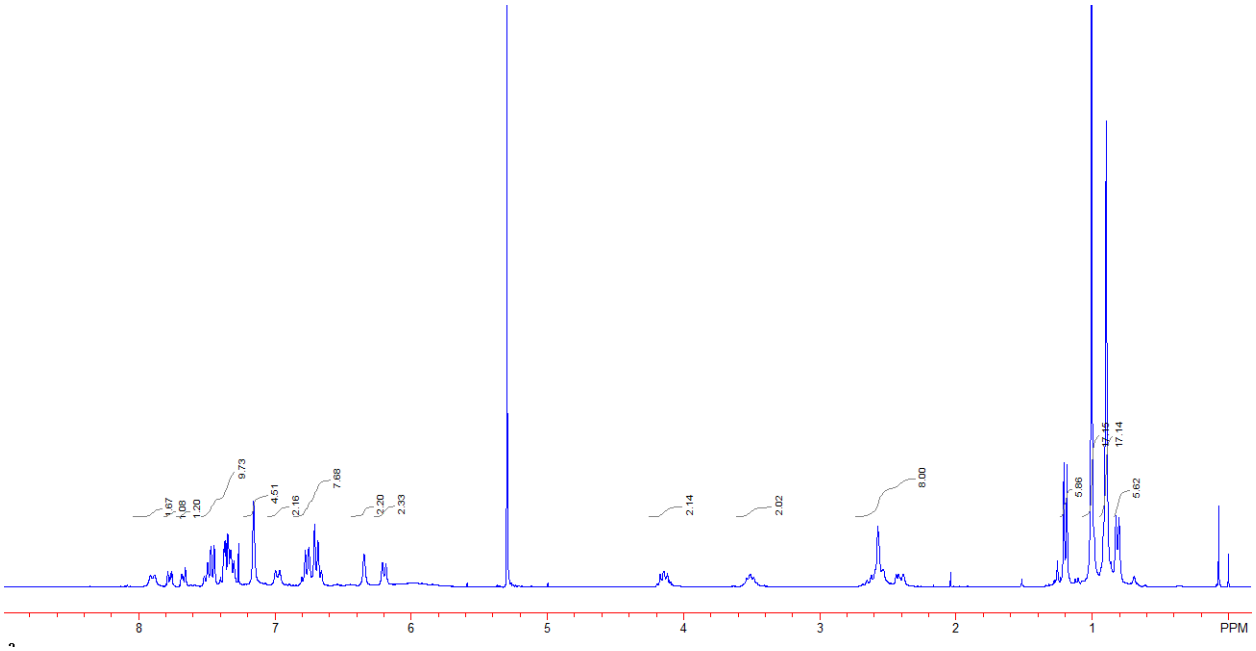

^{1}H NMR of (*S*,*S*)-**5**:

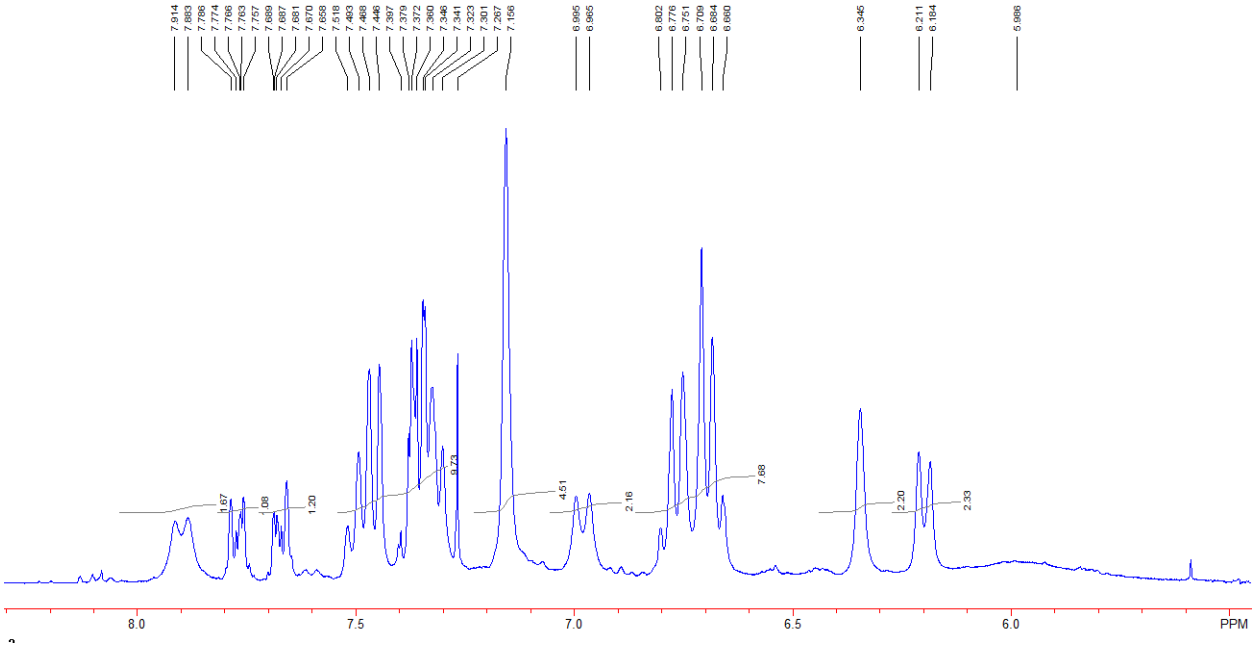

^{1}H NMR of (*S*,*S*)-**5**:

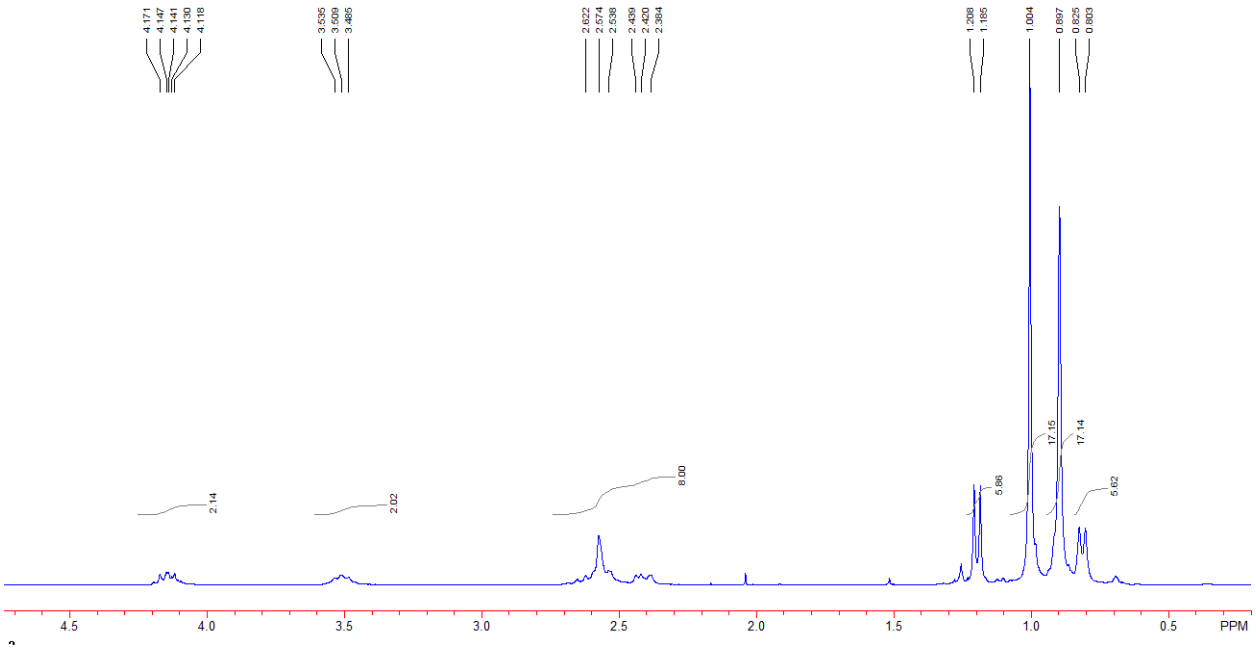

^{13}C NMR of (*S*,*S*)-**5**:

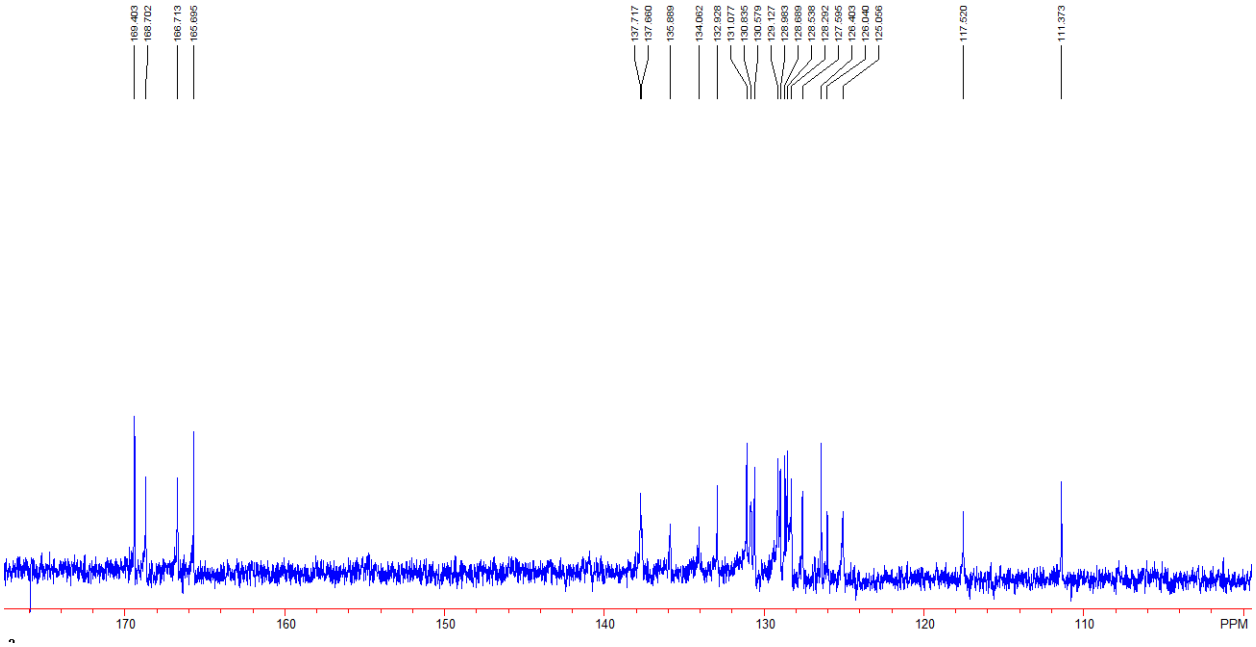

^{13}C NMR of (*S*,*S*)-**5**:

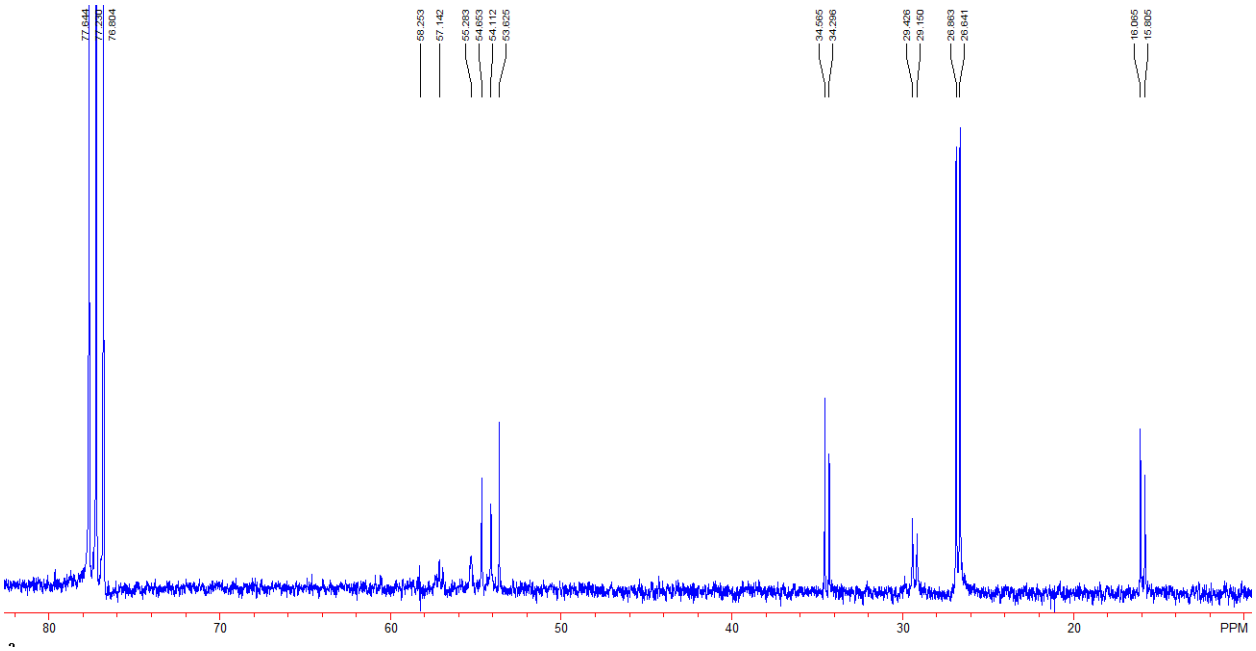

$^{31}P\{^{1}H\}$ NMR of (*R*,*R*)-**6**:

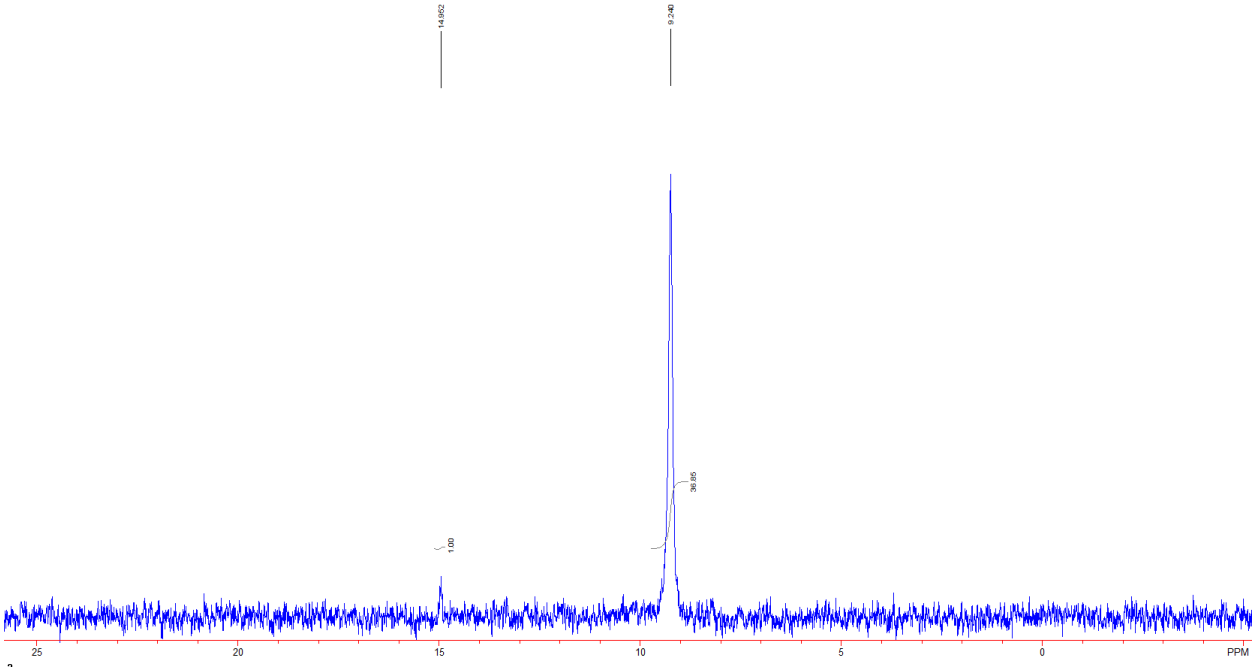

^{1}H NMR of (*R*,*R*)-**6**:

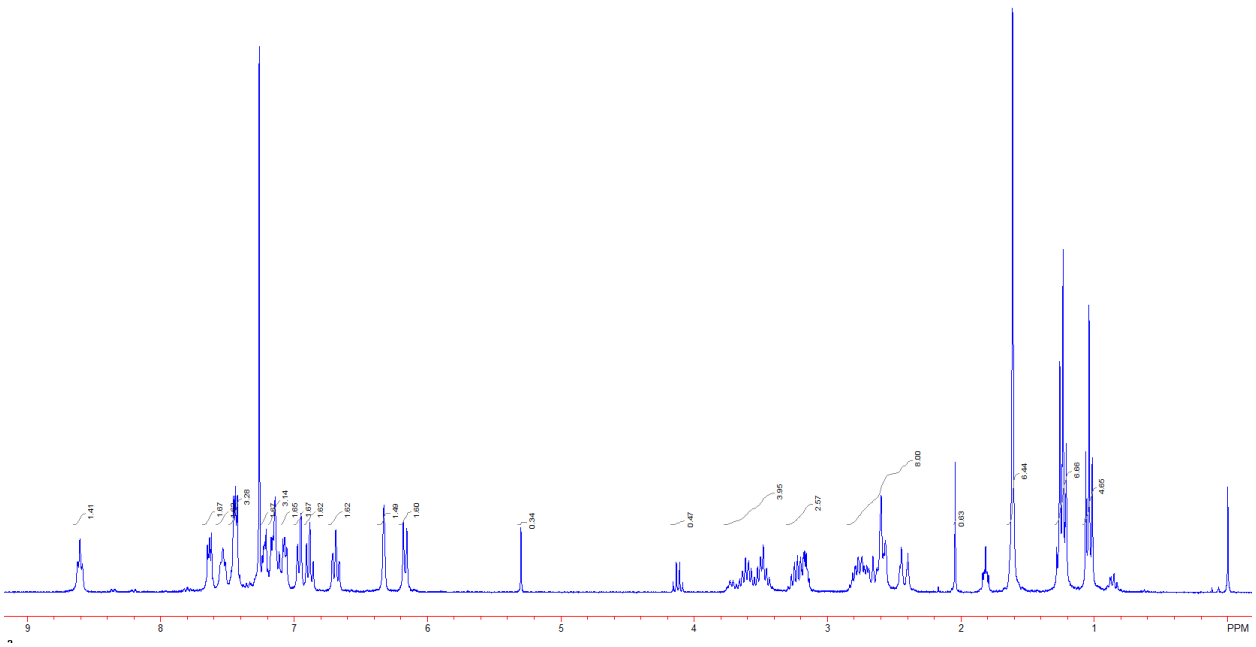

^{1}H NMR of (*R*,*R*)-**6**:

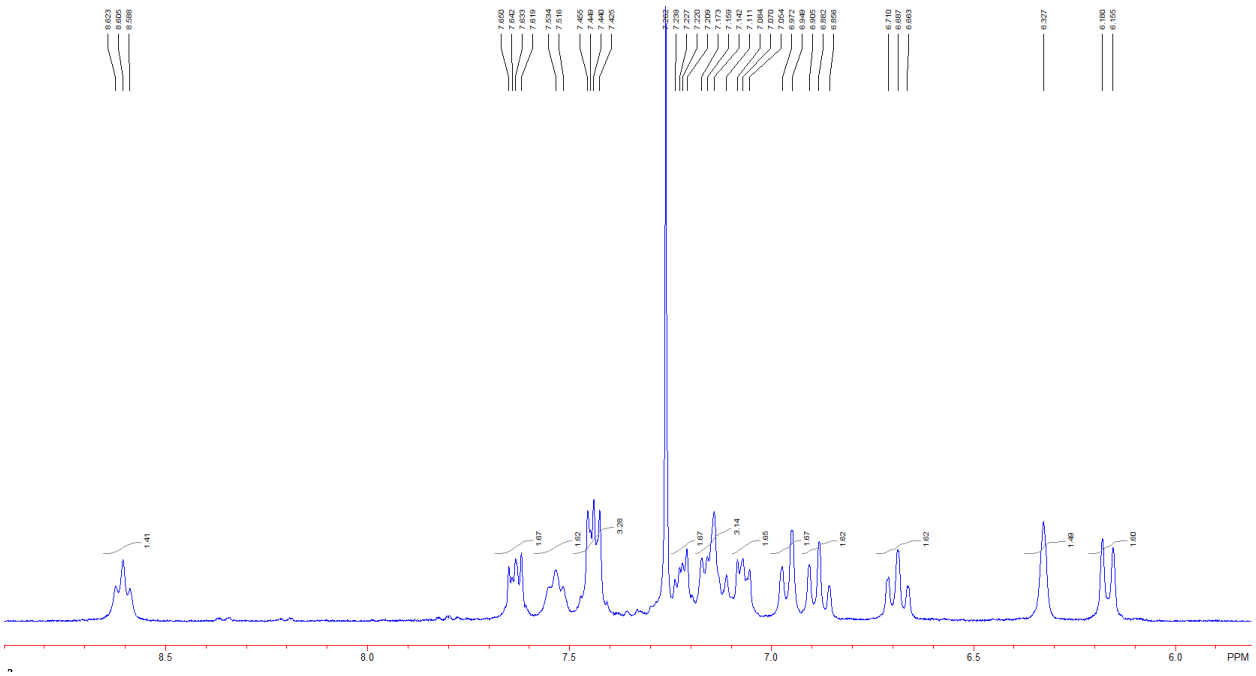

^{1}H NMR of (*R*,*R*)-**6** (contains a small amount of ethylacetate):

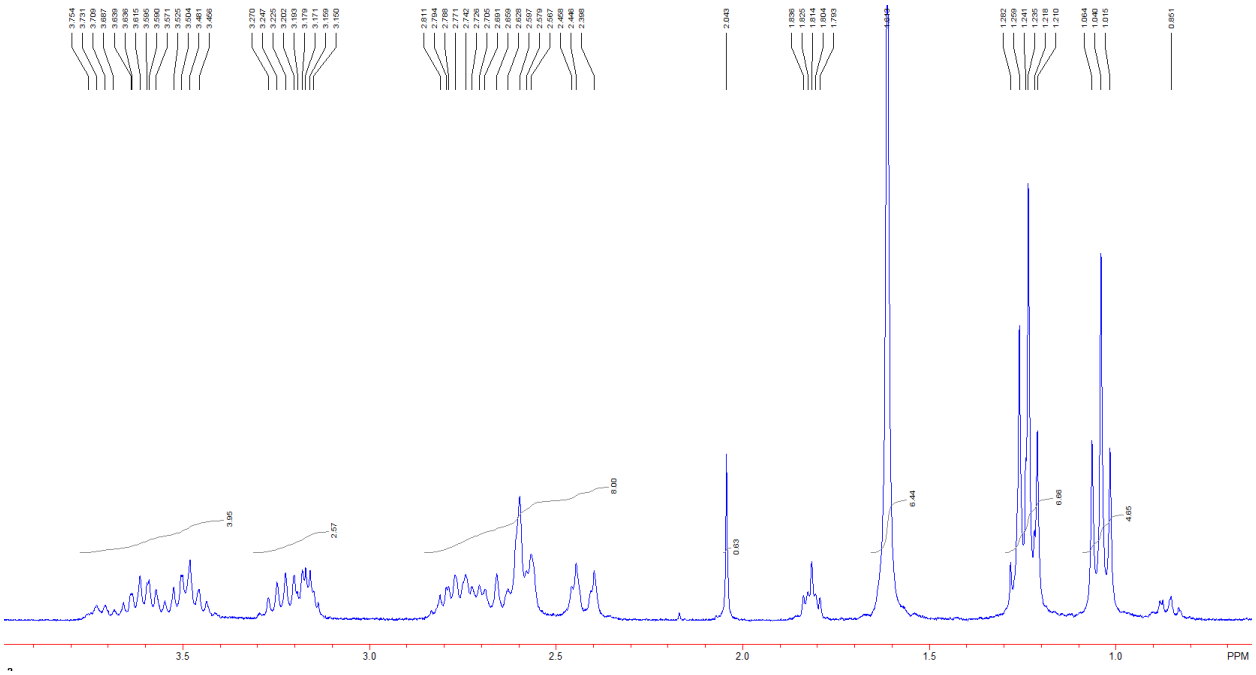

^{13}C NMR of (*R*,*R*)-**6**:

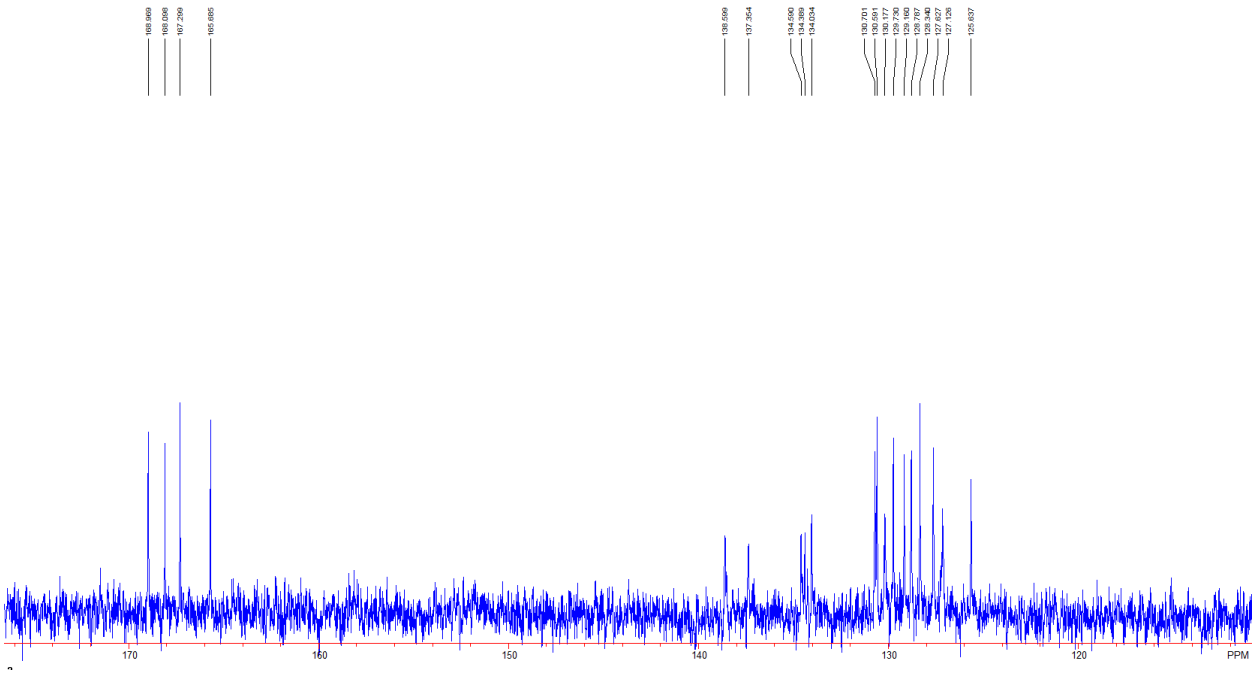

^{13}C NMR of (*R*,*R*)-**6**:

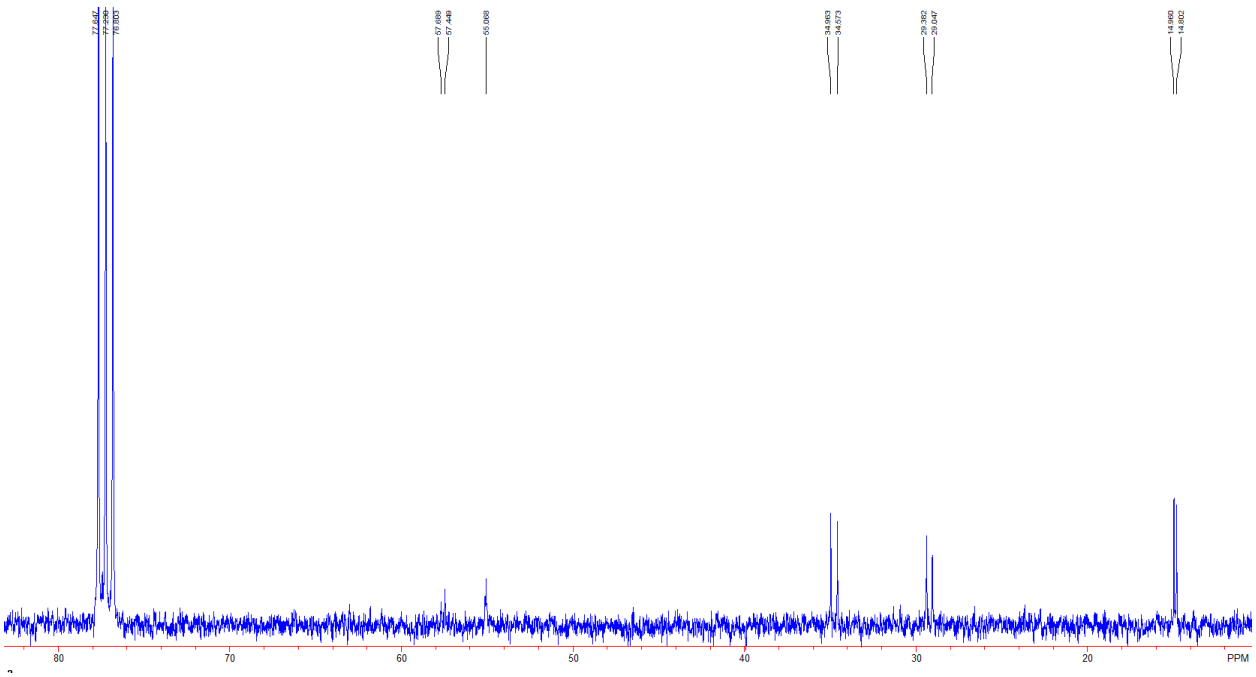

$^{31}P\{^{1}H\}$ NMR of (*R*,*R*)-**7** (contains a small amount of a hexafluorophosphate salt, not shown):

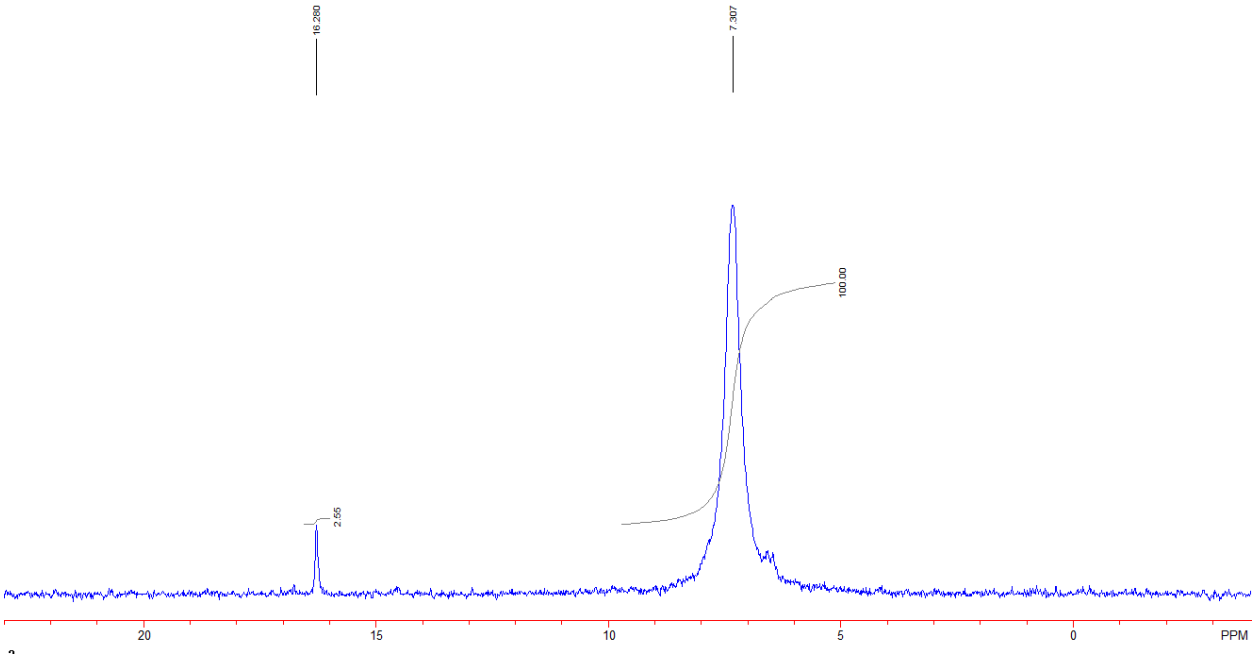

^{1}H NMR of (*R*,*R*)-**7**:

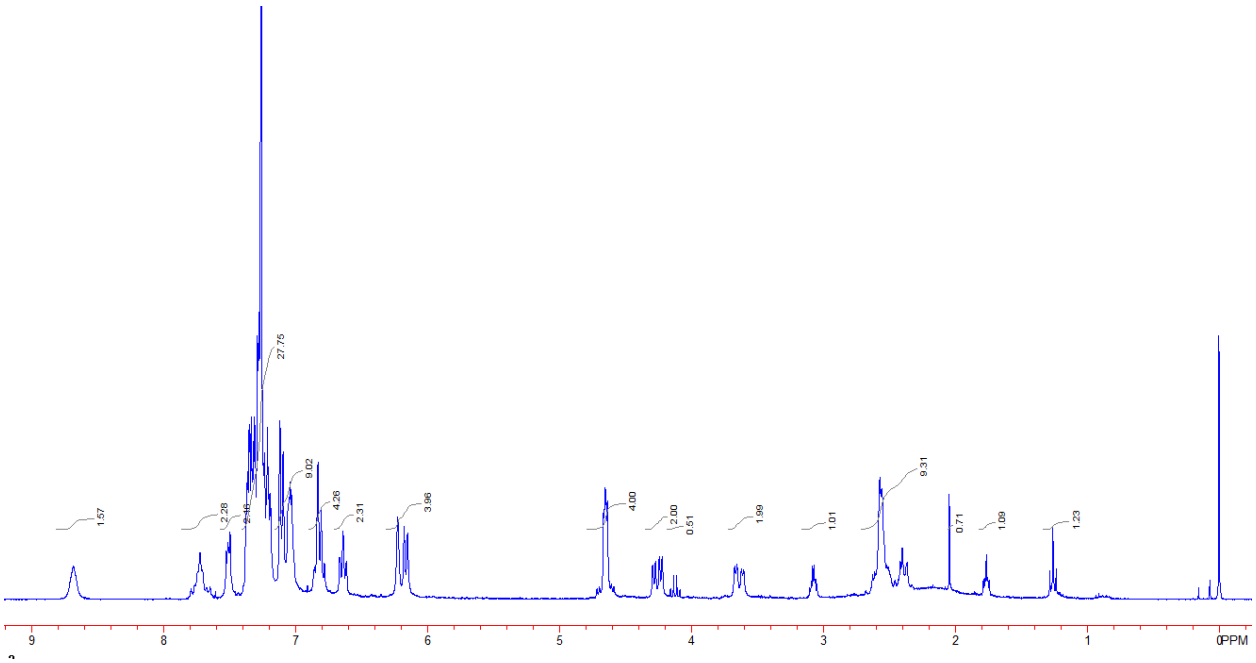

^{1}H NMR of (*R*,*R*)-**7**:

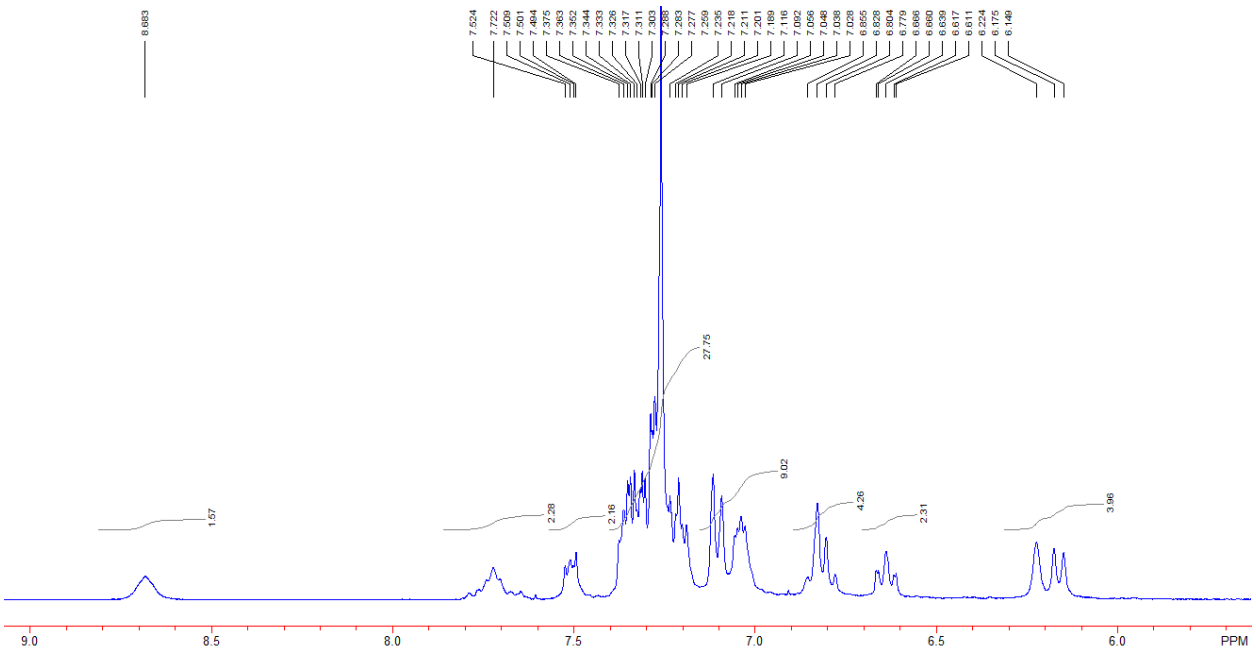

^{1}H NMR of (*R*,*R*)-**7** (contains a small amount of THF and ethyl acetate):

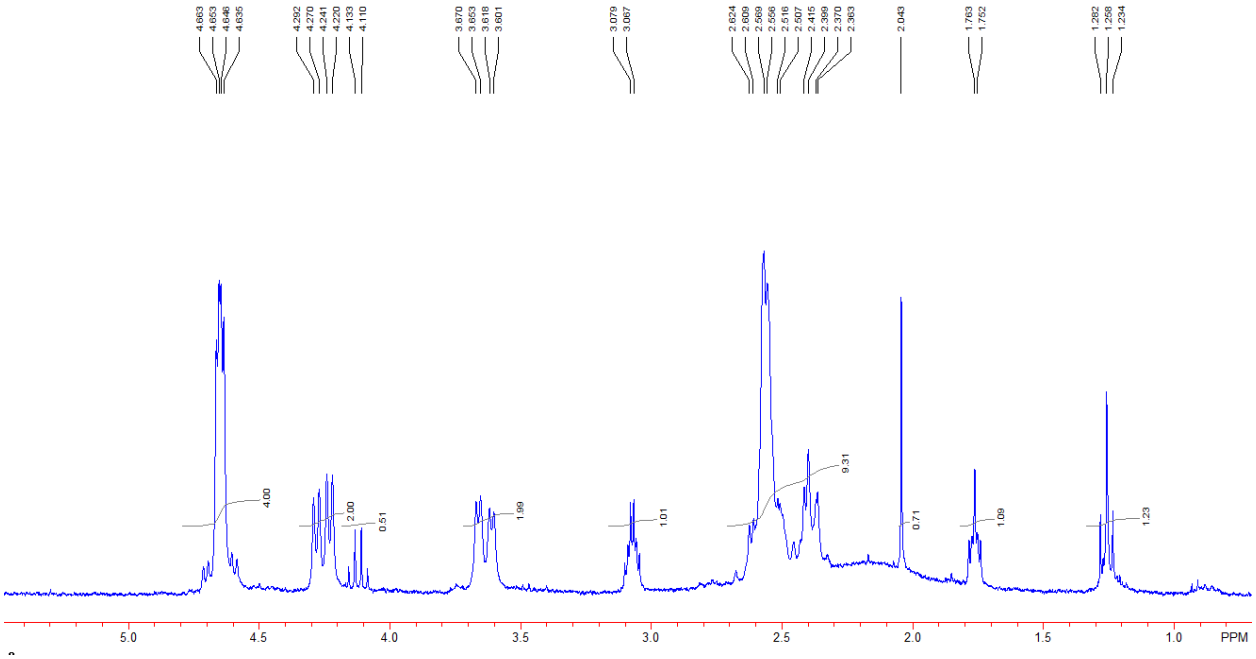

^{13}C NMR of (*R*,*R*)-**7**:

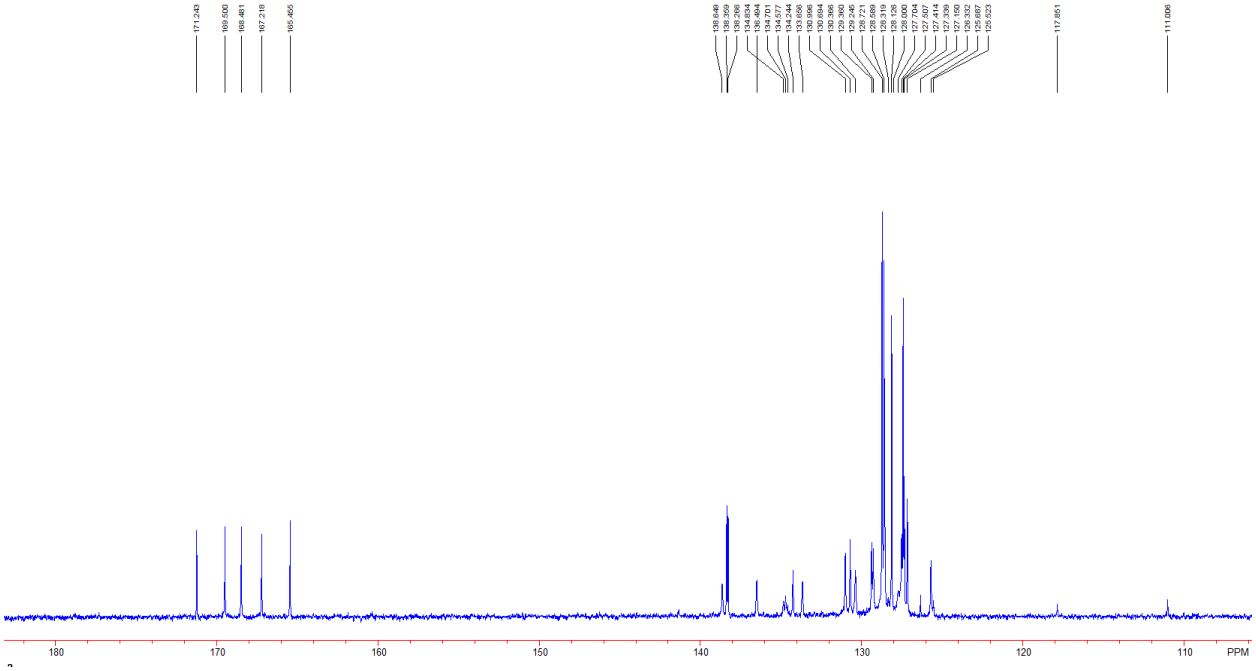

^{13}C NMR of (*R*,*R*)-**7** (contains a small amount of ethyl acetate):

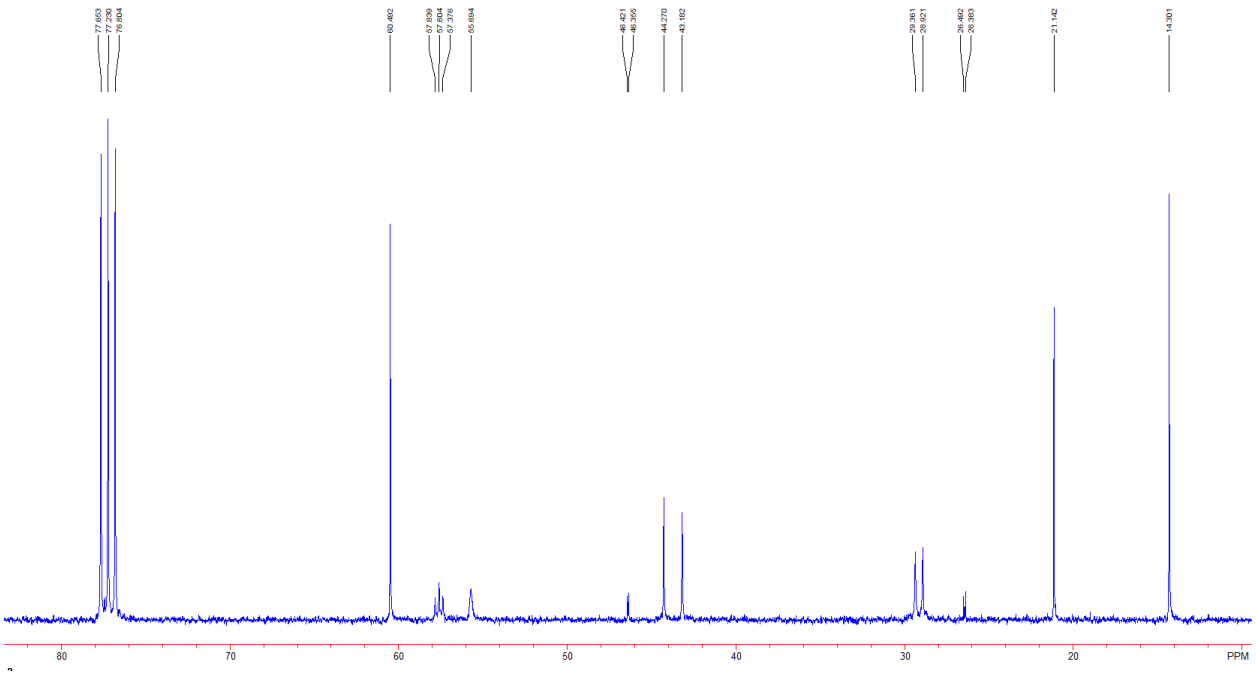

$^{31}P\{^{1}H\}$ NMR of (*R*,*R*)-**8** (contains a small amount of a hexafluorophosphate salt, not shown):

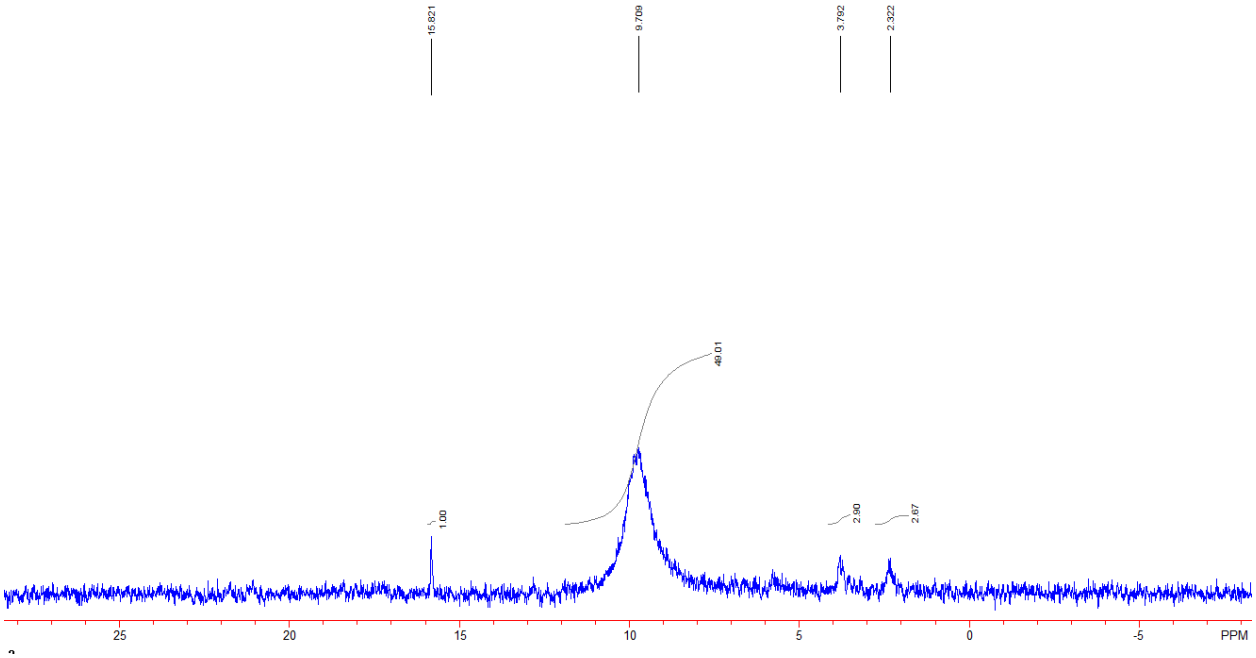

^{1}H NMR of (*R*,*R*)-**8**:

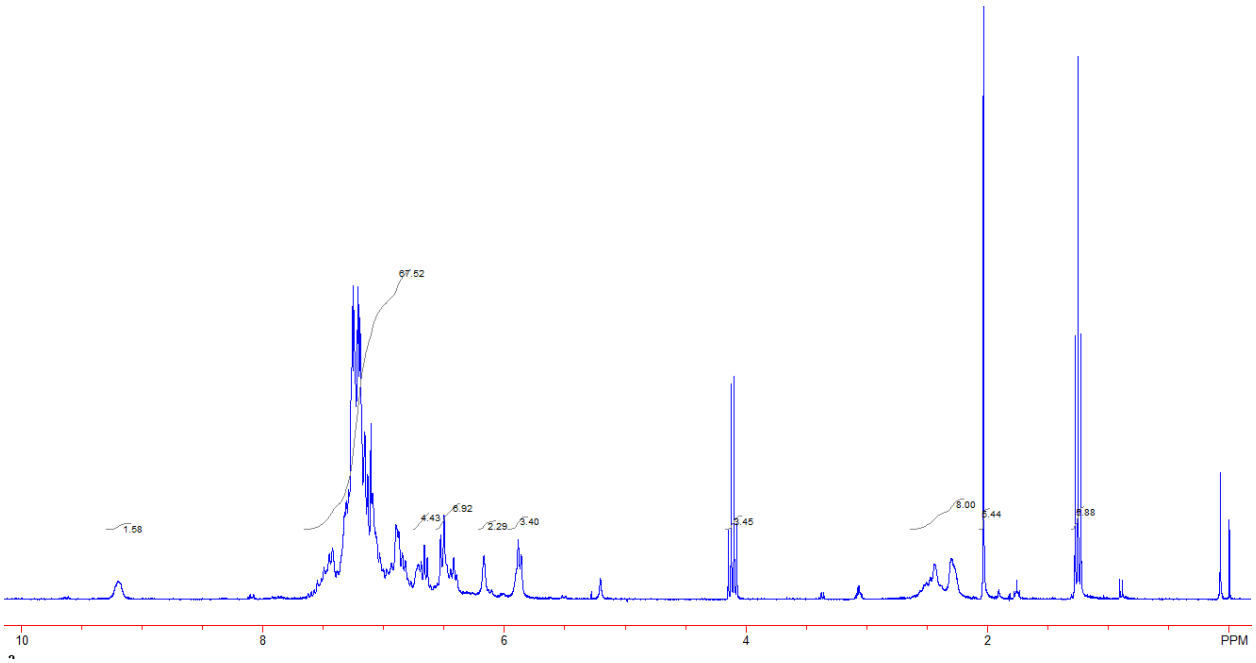

^{1}H NMR of (*R*,*R*)-**8**:

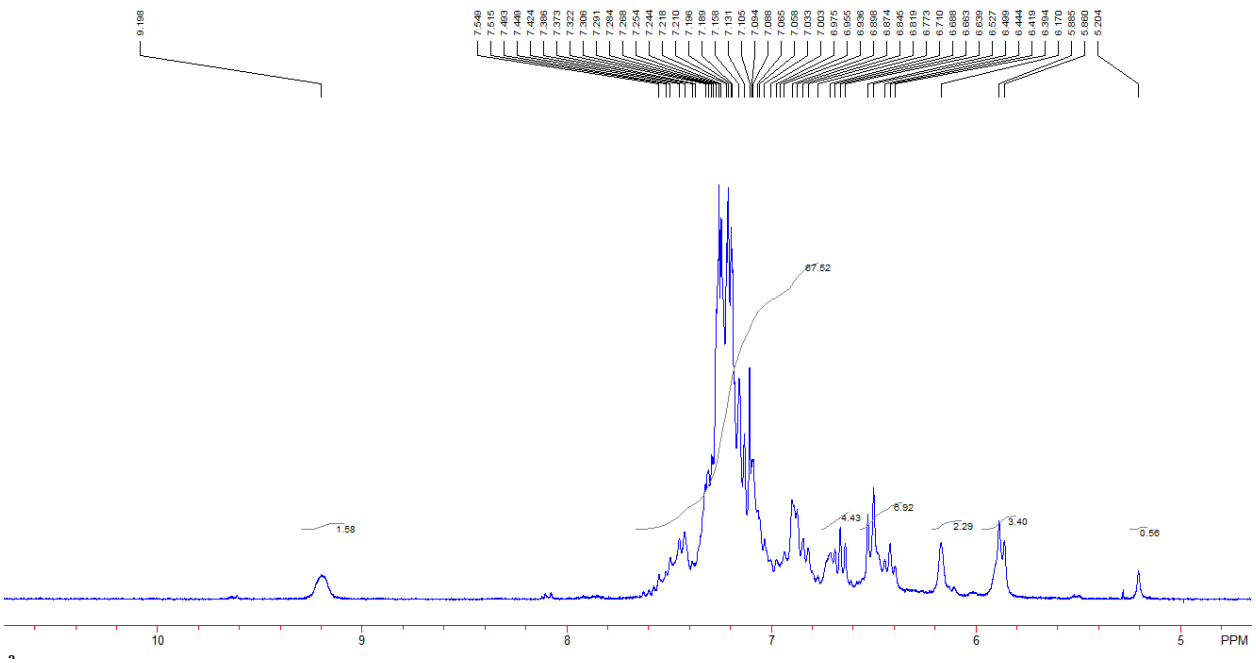

^{1}H NMR of (*R*,*R*)-**8** (contains ethyl acetate):

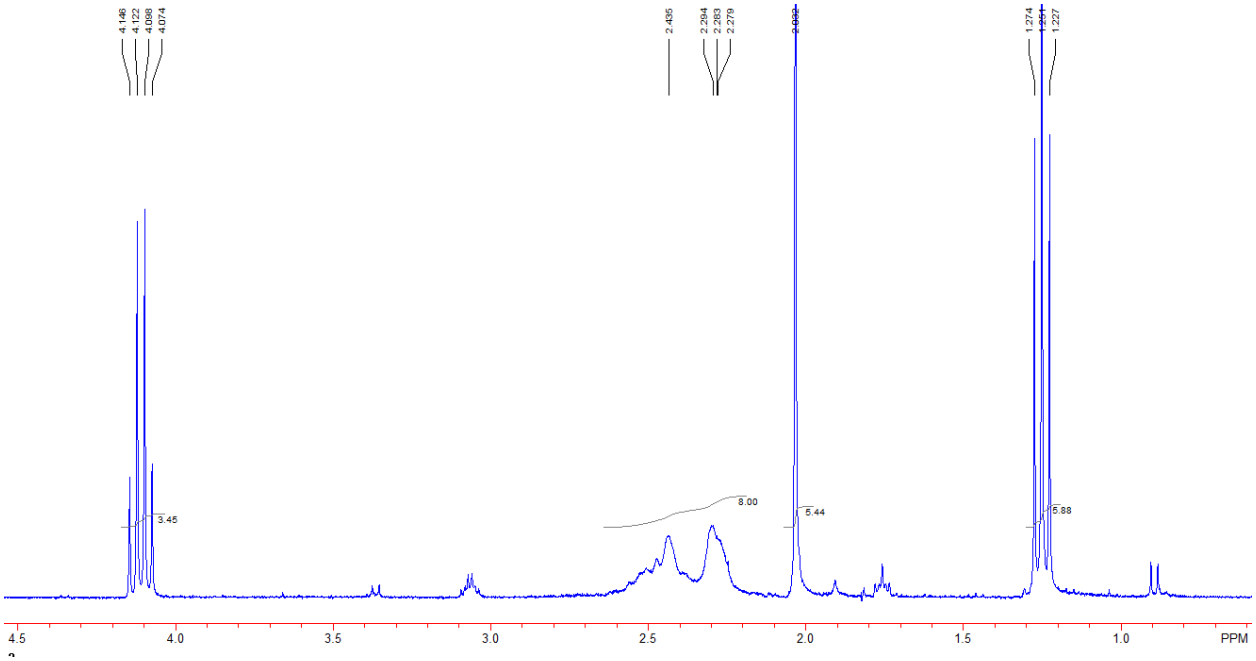

^{13}C NMR of (*R*,*R*)-**8**:

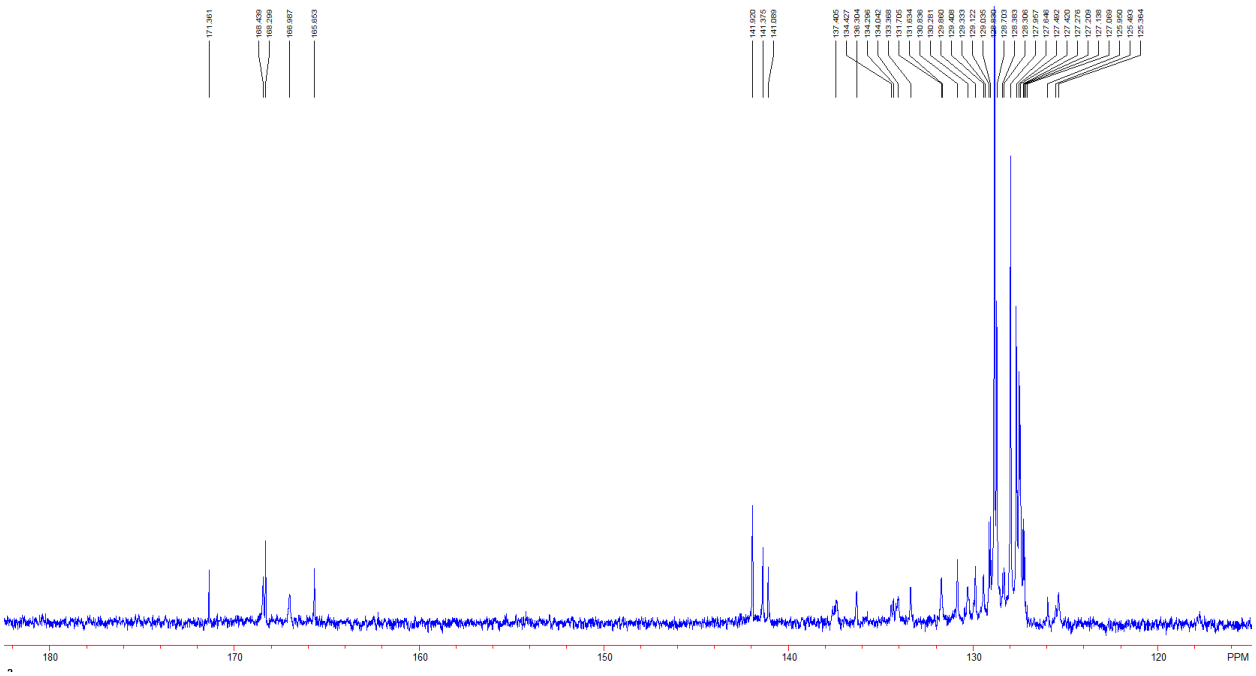

^{13}C NMR of (*R*,*R*)-**8** (contains ethyl acetate):

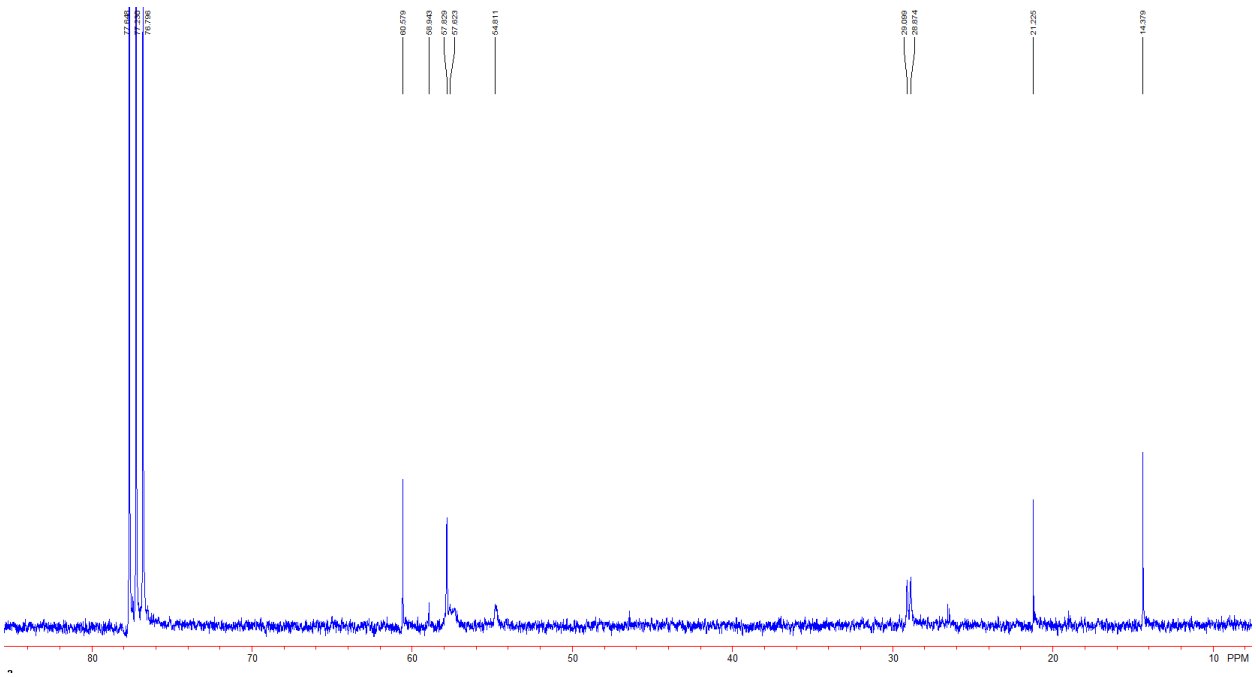

$^{31}P\{^{1}H\}$ NMR of (*R*,*R*)-**9** (contains a small amount of a hexafluorophosphate salt, not shown):

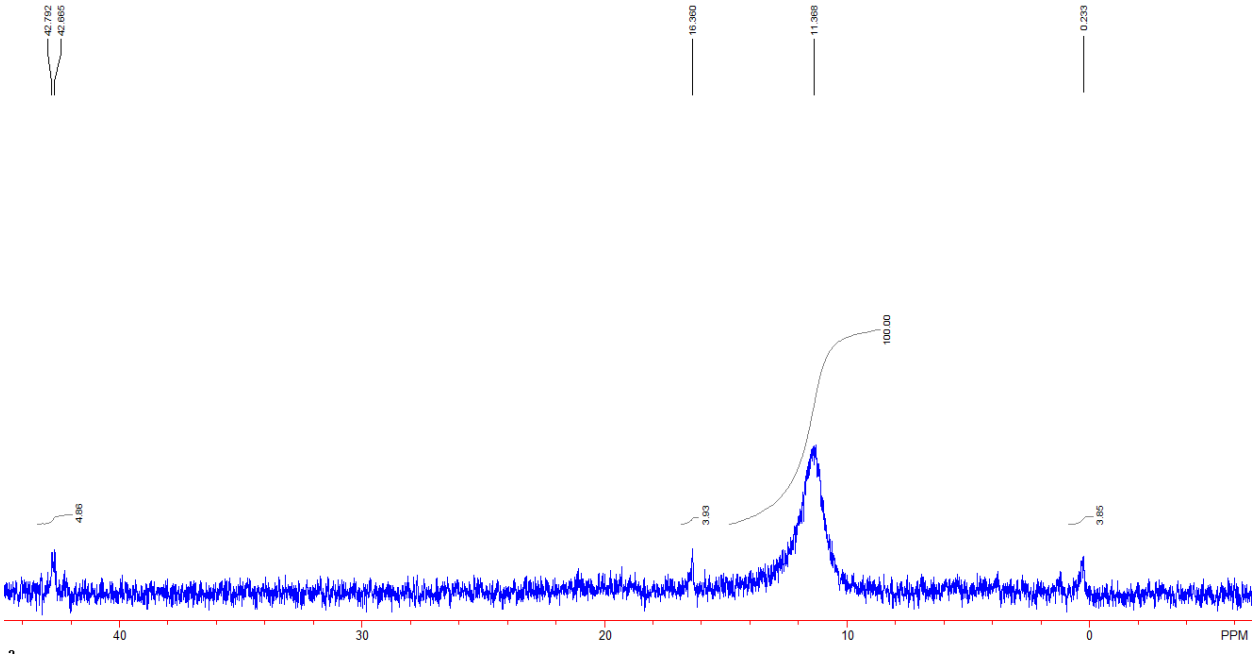

^{1}H NMR of (*R*,*R*)-**9** (contains ethyl acetate):

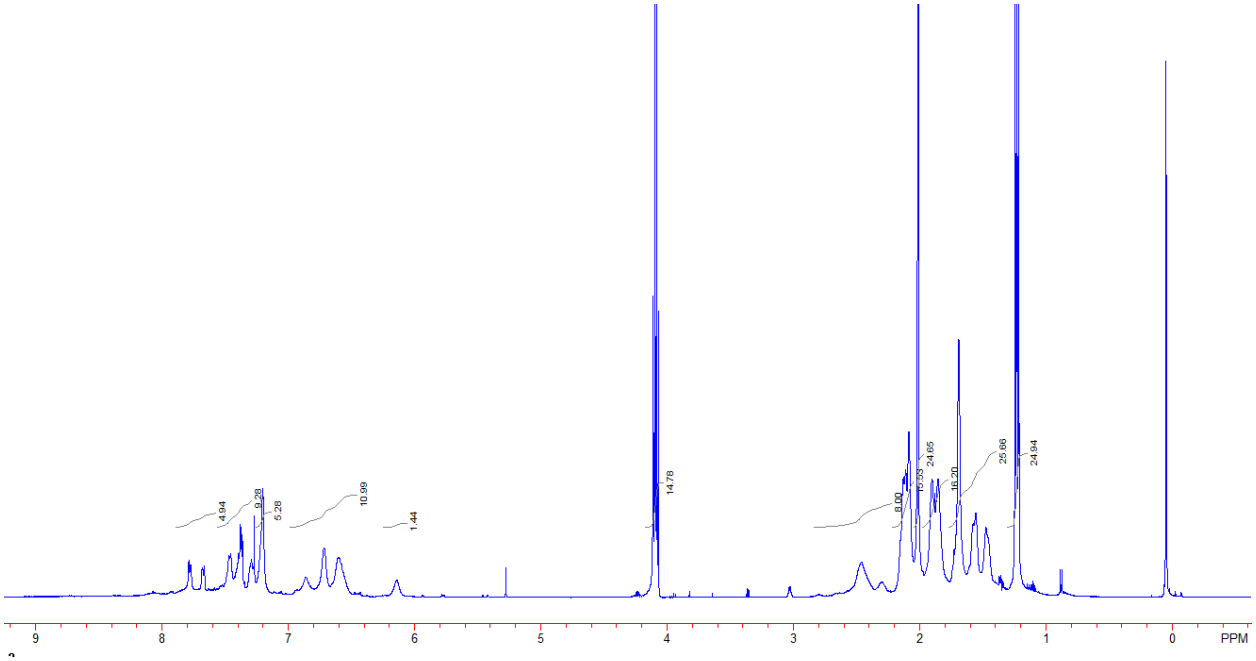

^{1}H NMR of (*R*,*R*)-**9** (contains ethyl acetate):

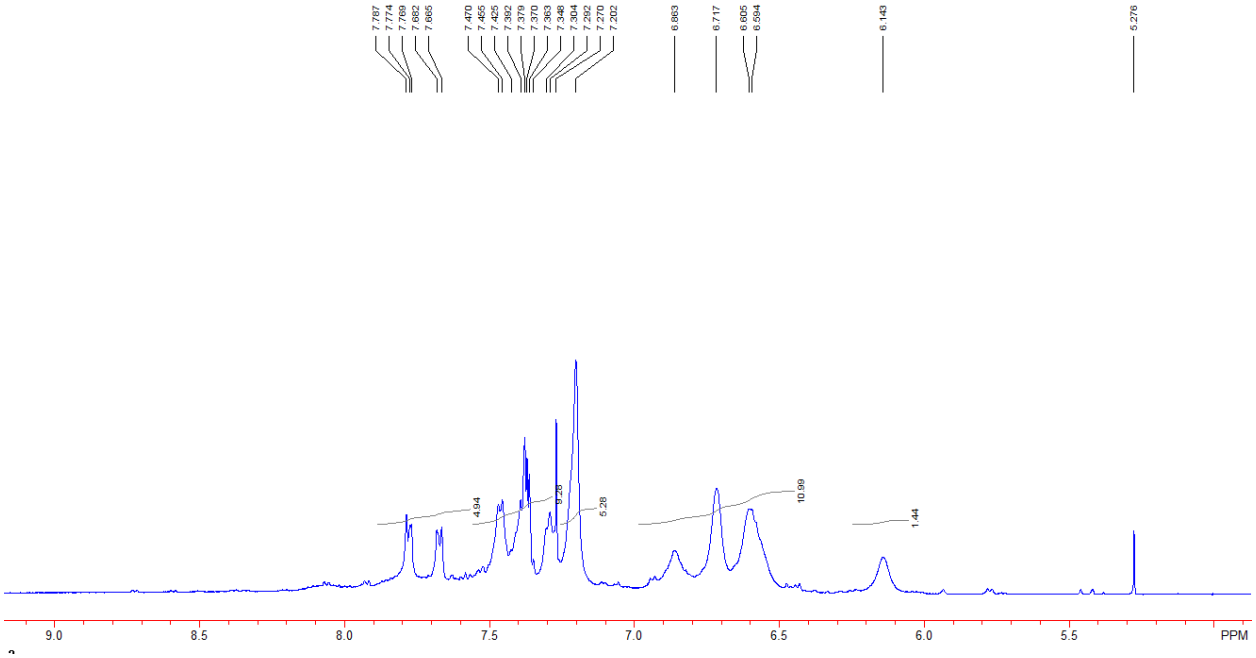

^{1}H NMR of (*R*,*R*)-**9** (contains ethyl acetate):

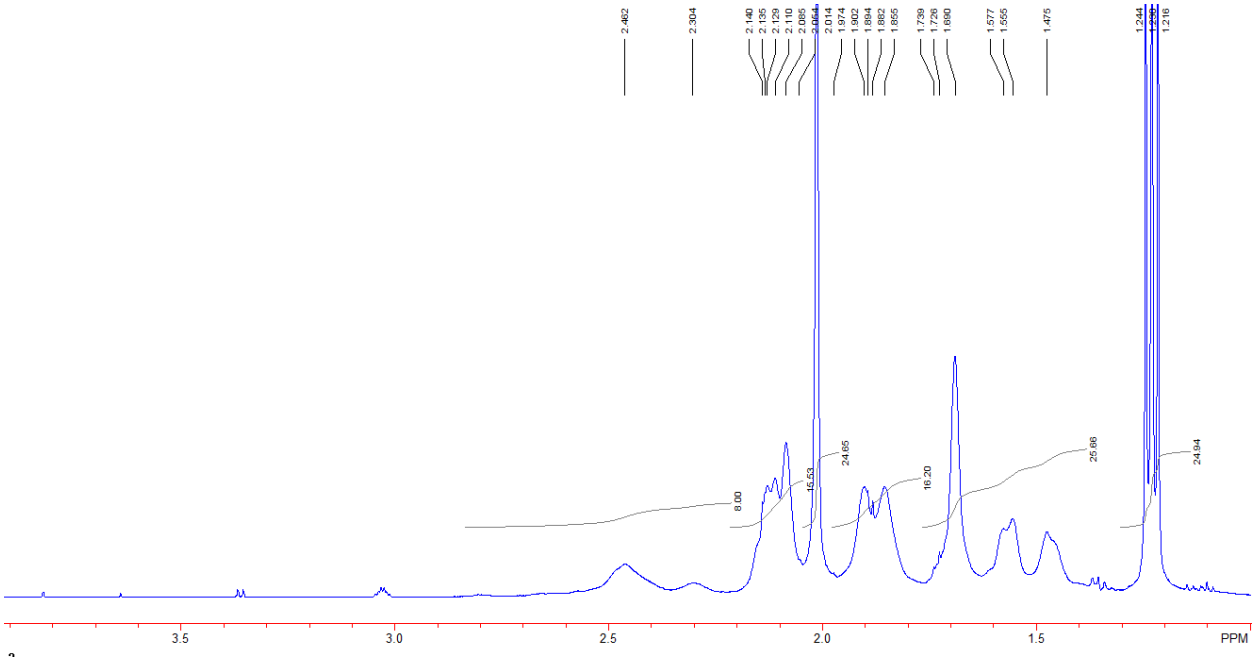

^{13}C NMR of (*R*,*R*)-**9** (contains ethyl acetate):

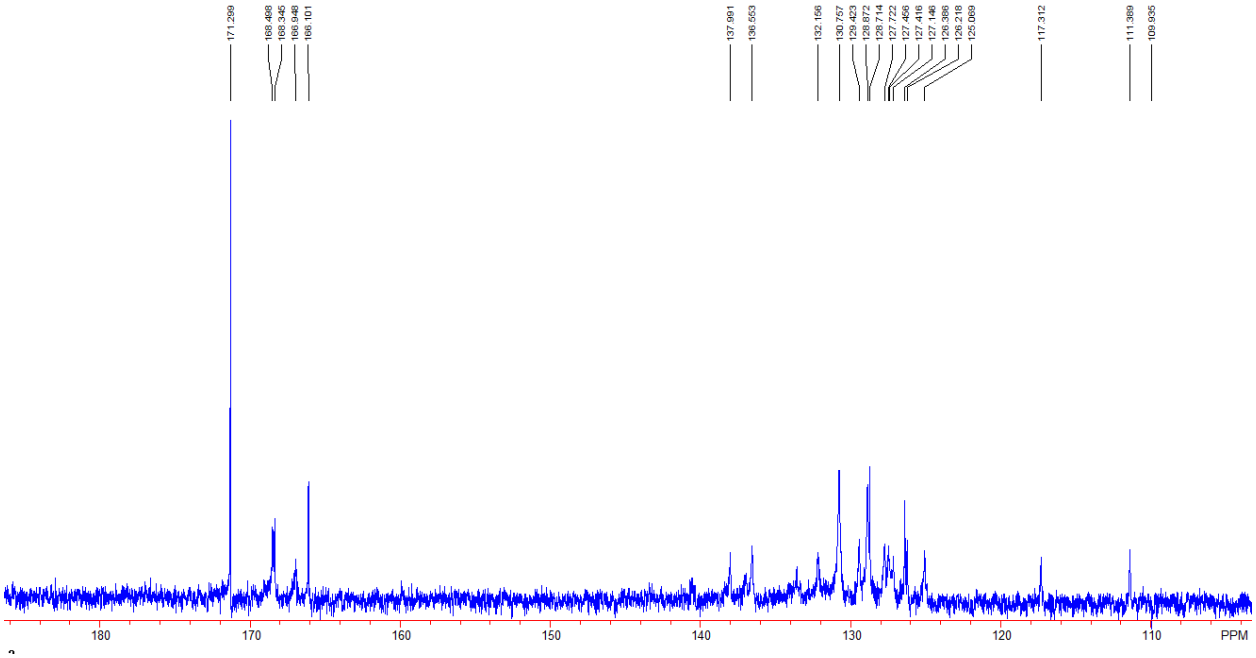

^{13}C NMR of (*R*,*R*)-**9** (contains ethyl acetate):

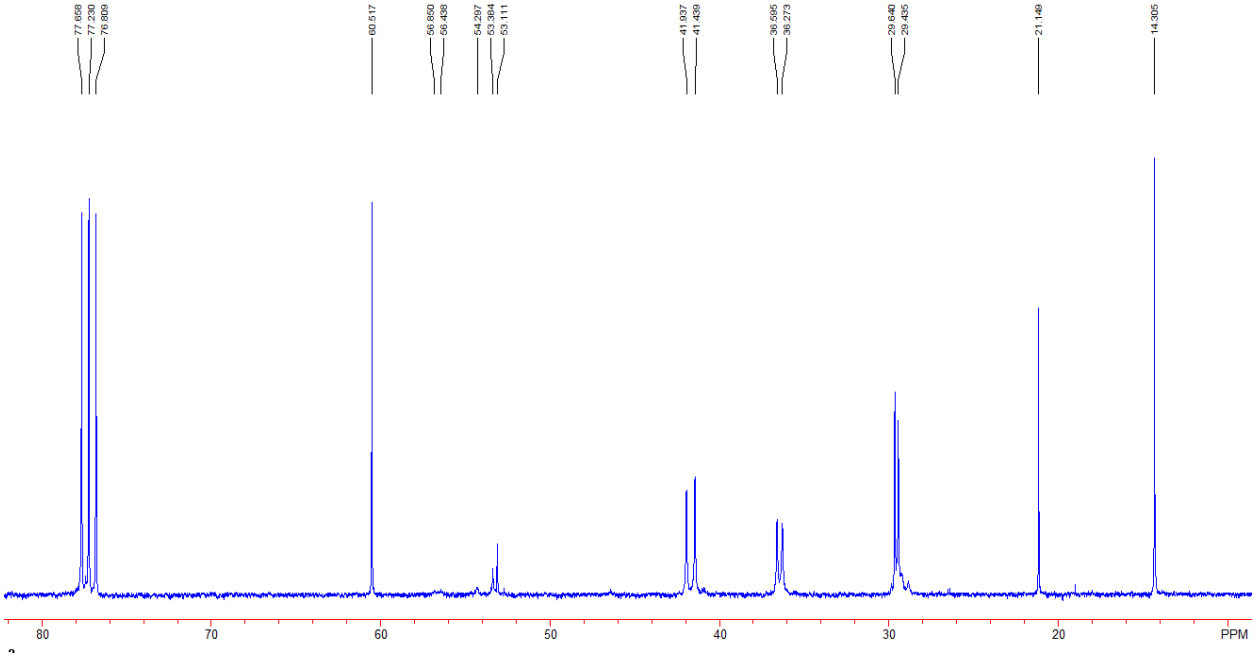

$^{31}P\{^{1}H\}$ NMR of (*R*,*R*)-**10** (contains analogous bisdiazaphospholane monoxide):

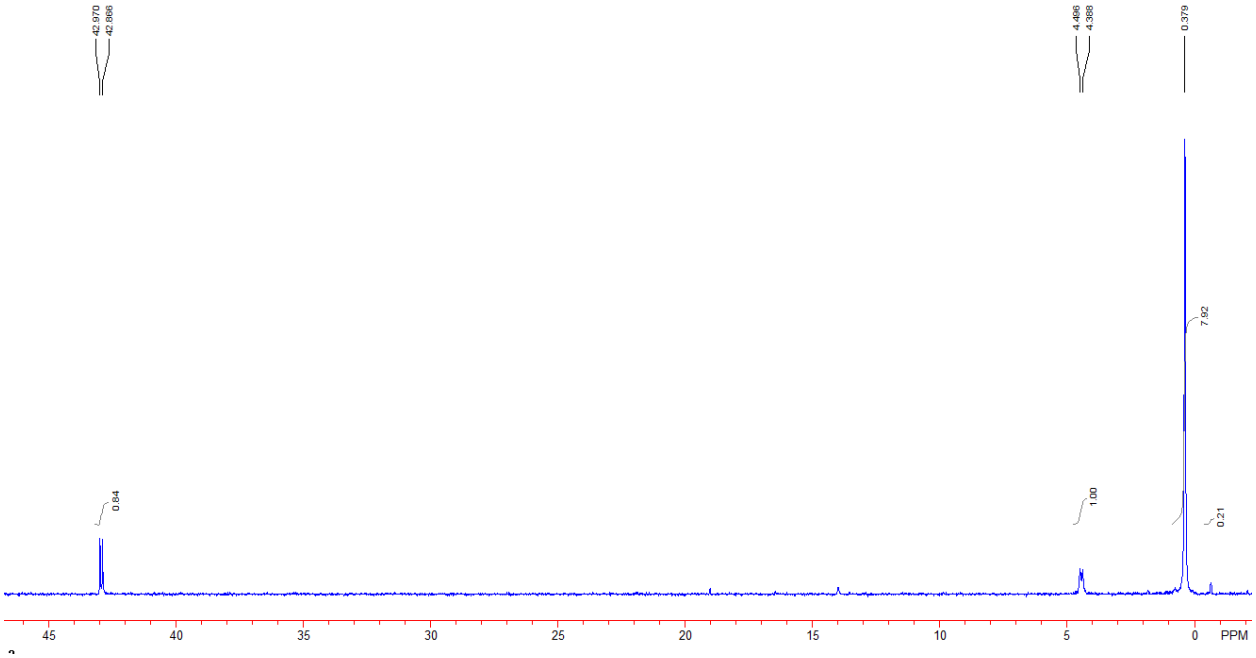

^{1}H NMR of (*R*,*R*)-**10**:

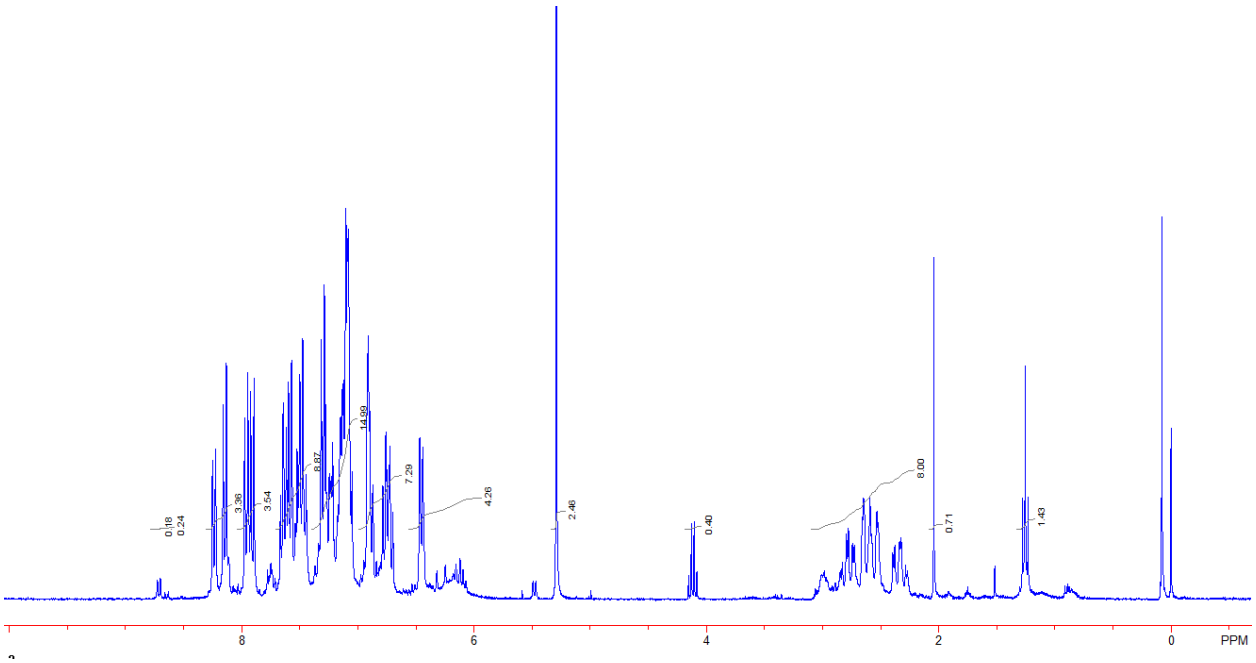

^{1}H NMR of (*R*,*R*)-**10**:

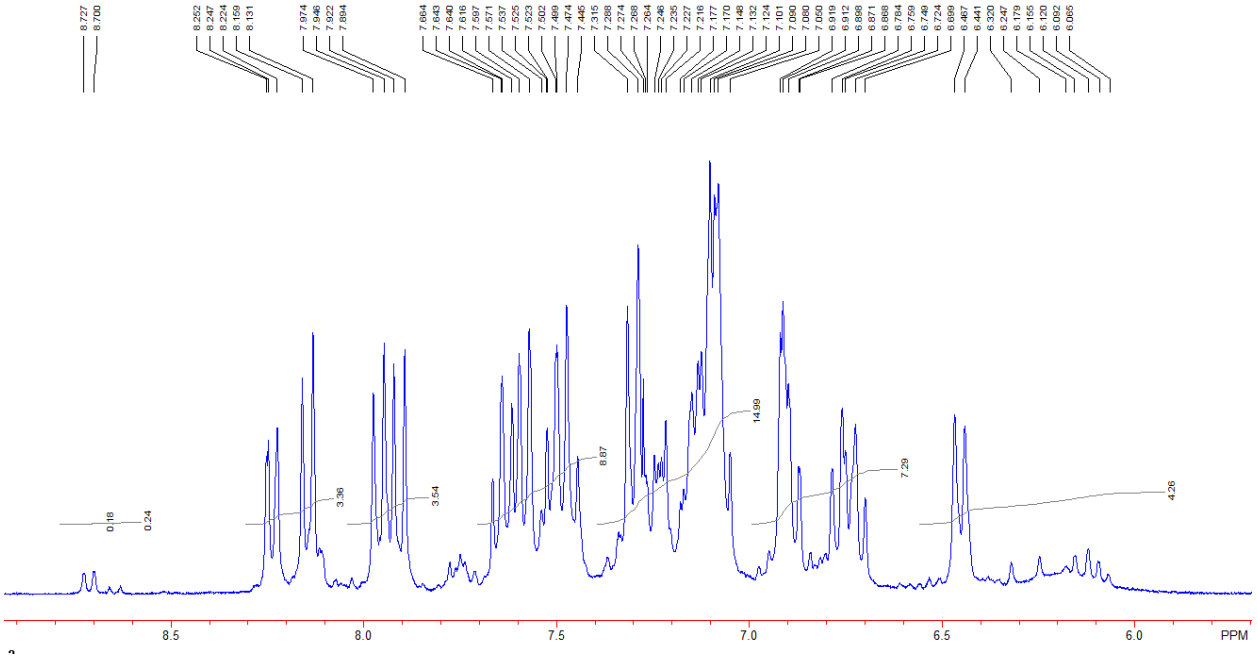

^{1}H NMR of (*R*,*R*)-**10** (contains a small amount of ethyl acetate):

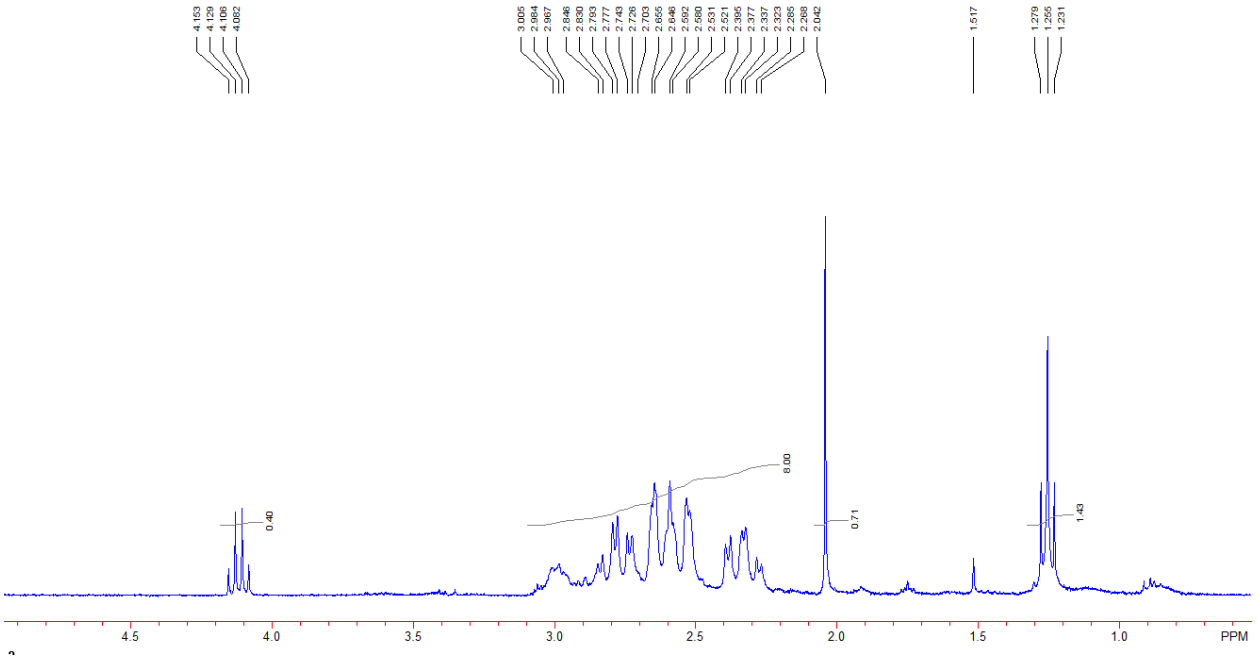

^{13}C NMR of (*R*,*R*)-**10** (contains a small amount of ethyl acetate):

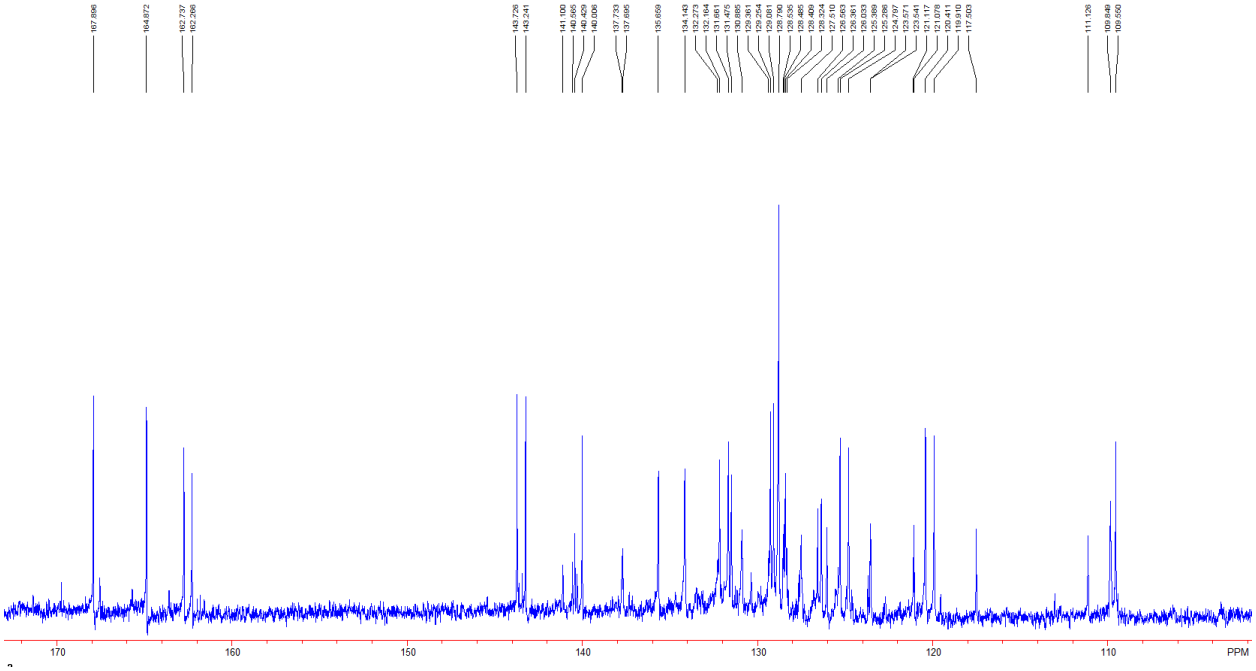

^{13}C NMR of (*R*,*R*)-**10** (contains a small amount of ethyl acetate):

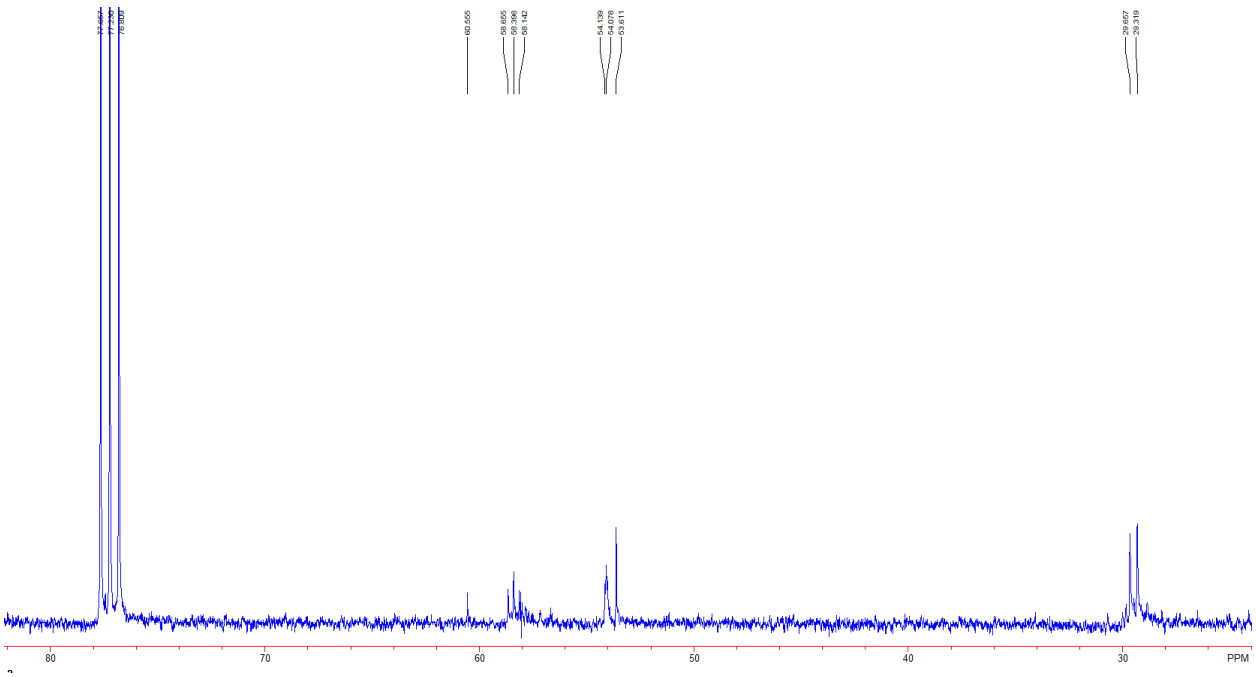

6.2 NMR Spectra from Chapter 4

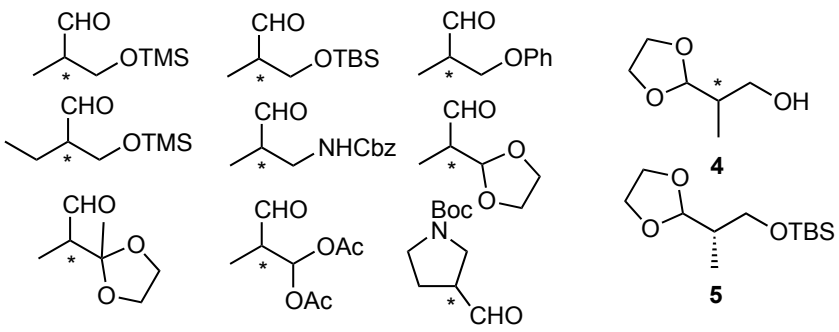

^{1}H NMR:

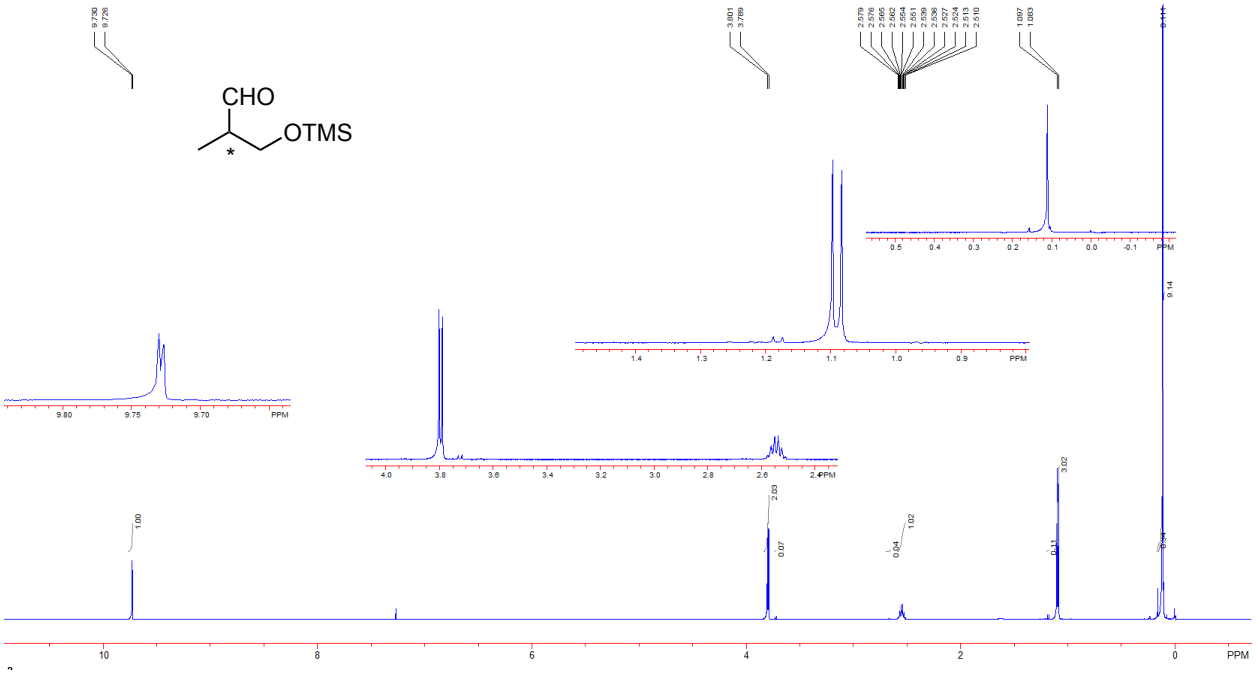

^{13}C NMR:

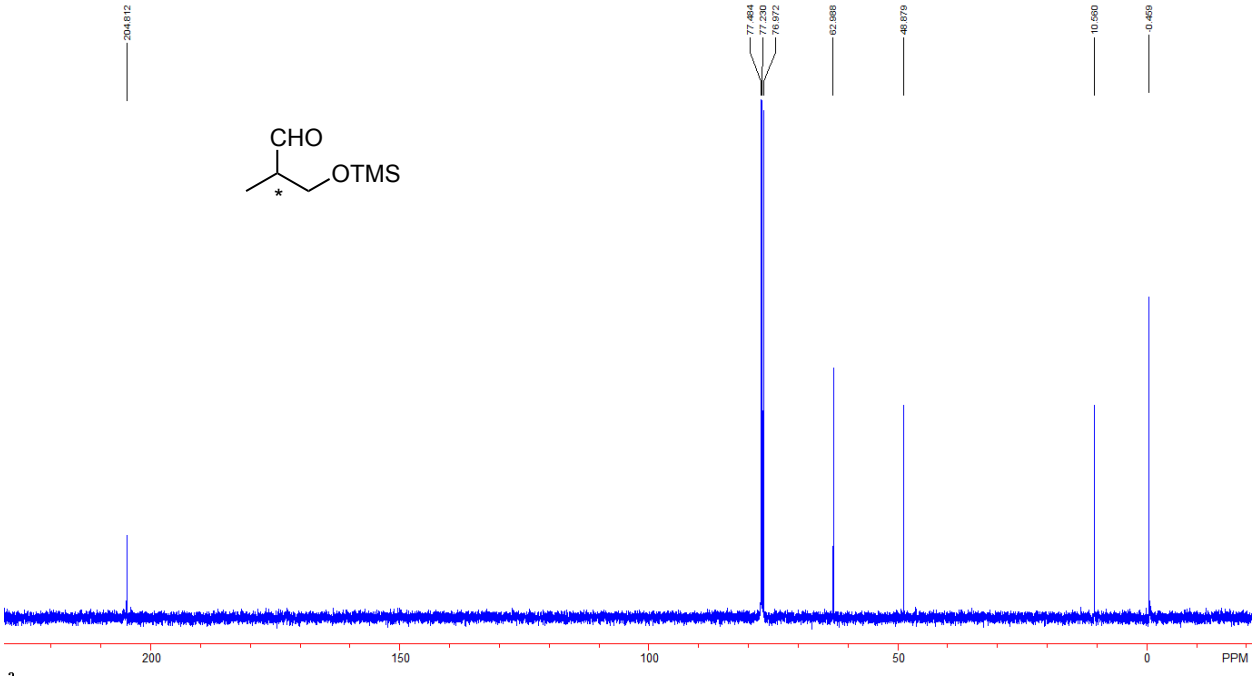

^{1}H NMR:

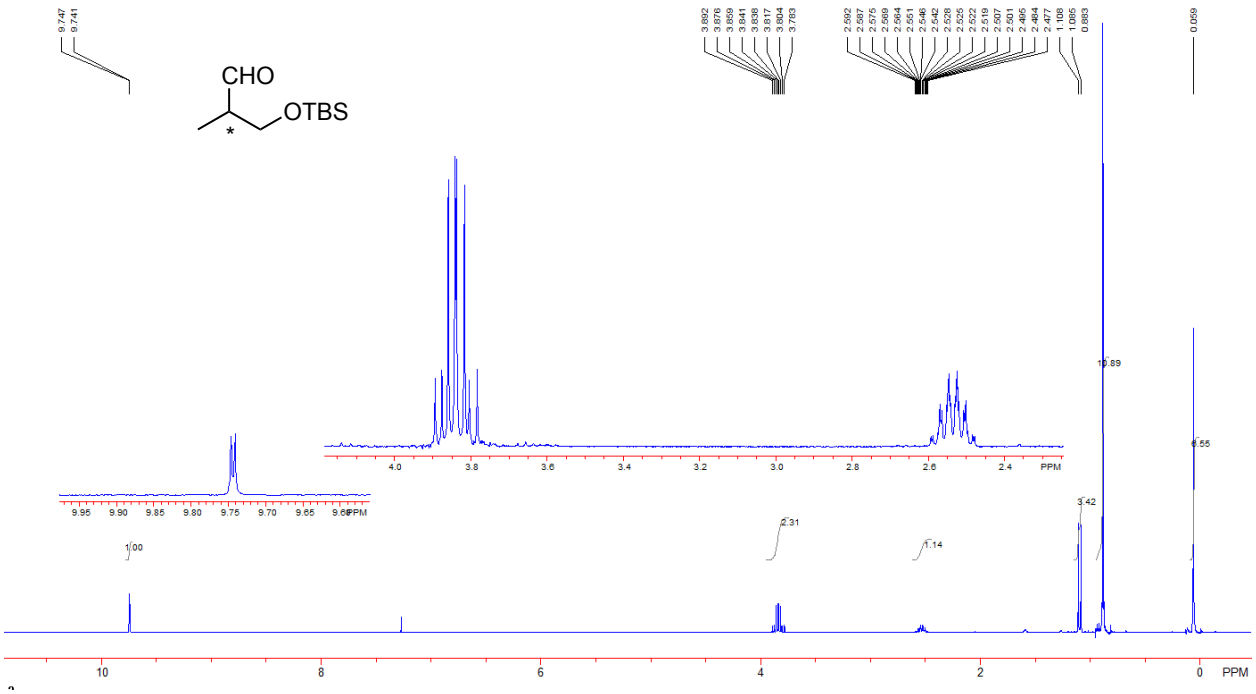

^{13}C NMR:

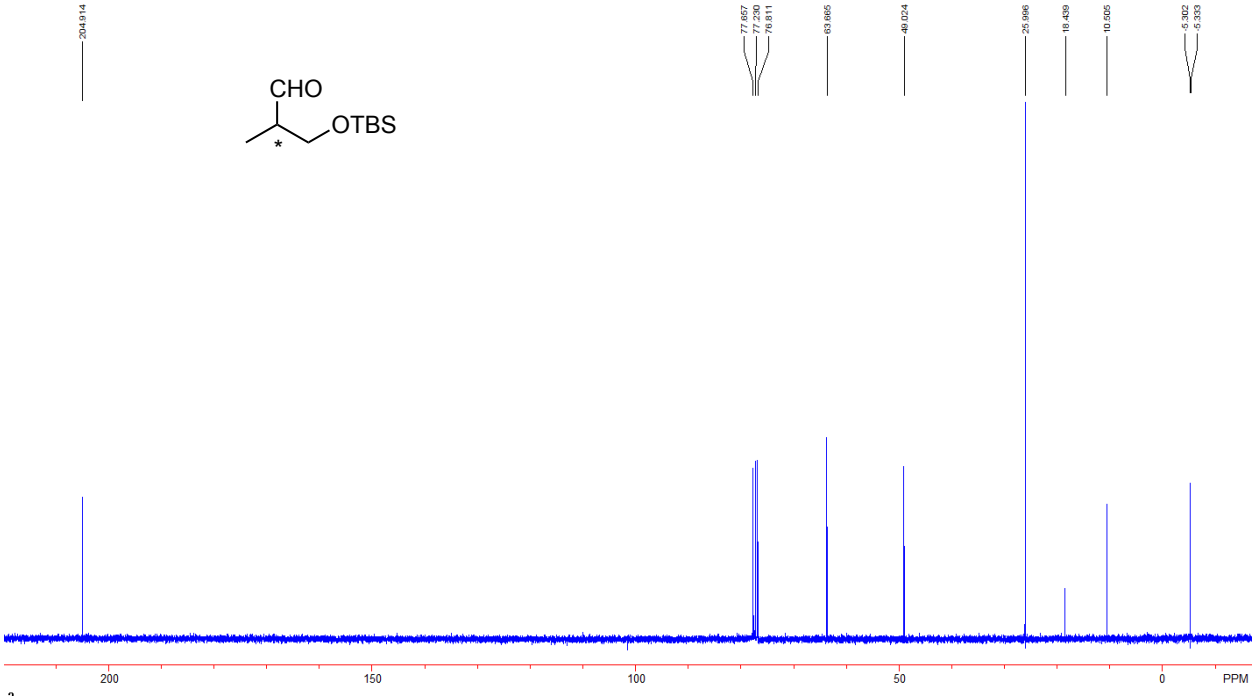

^{1}H NMR:

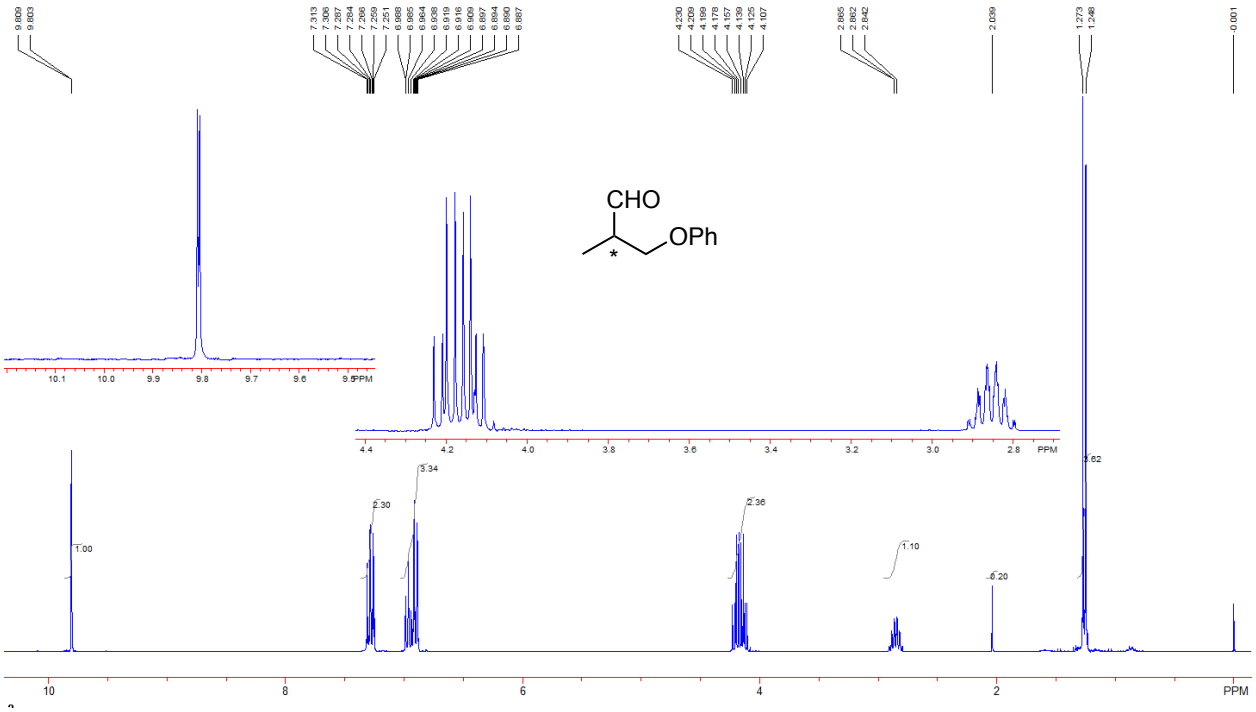

^{13}C NMR:

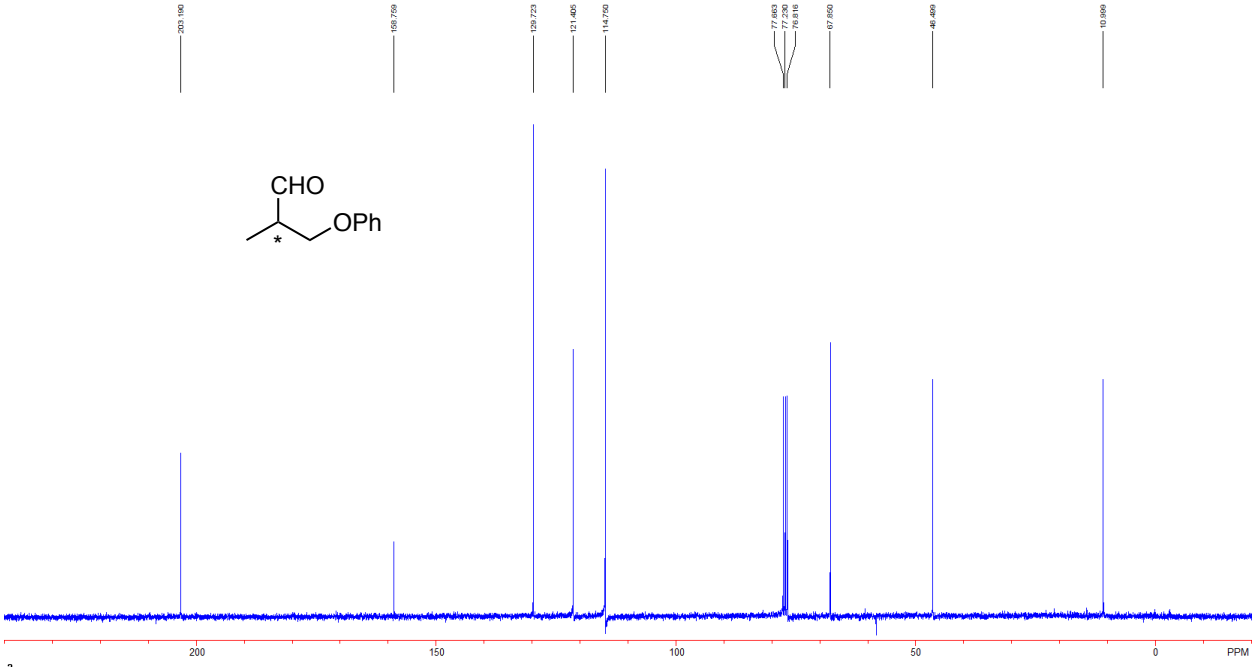

^{1}H NMR:

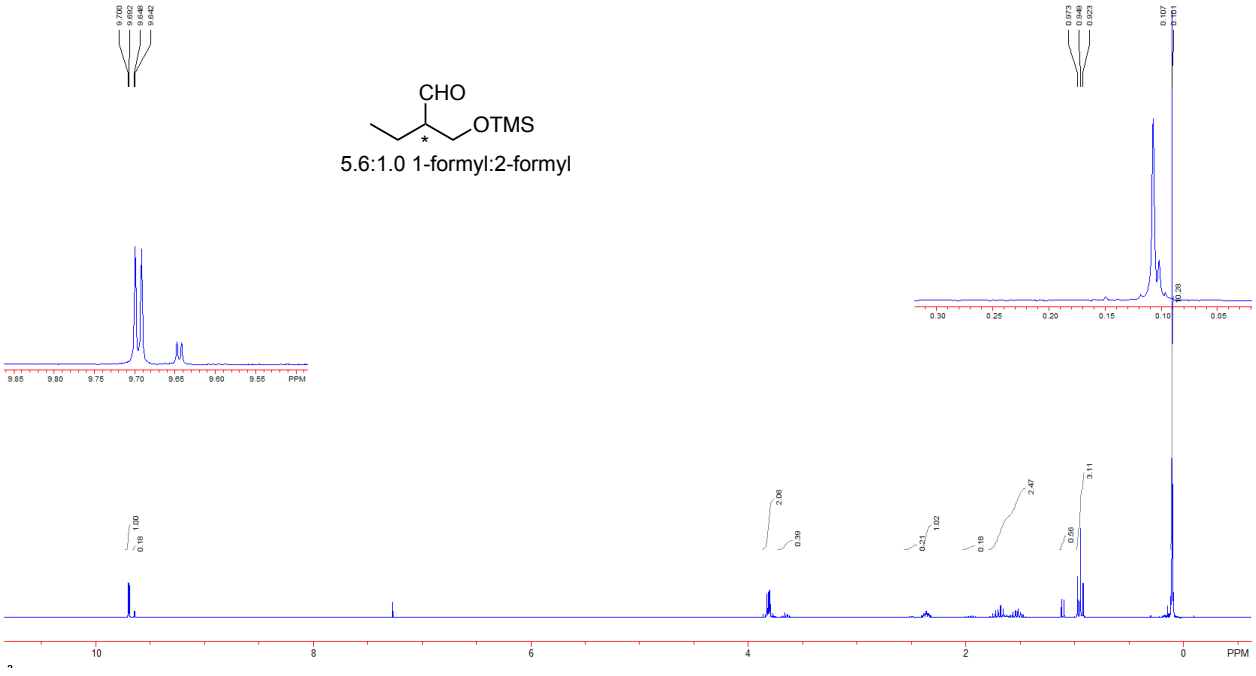

^{1}H NMR:

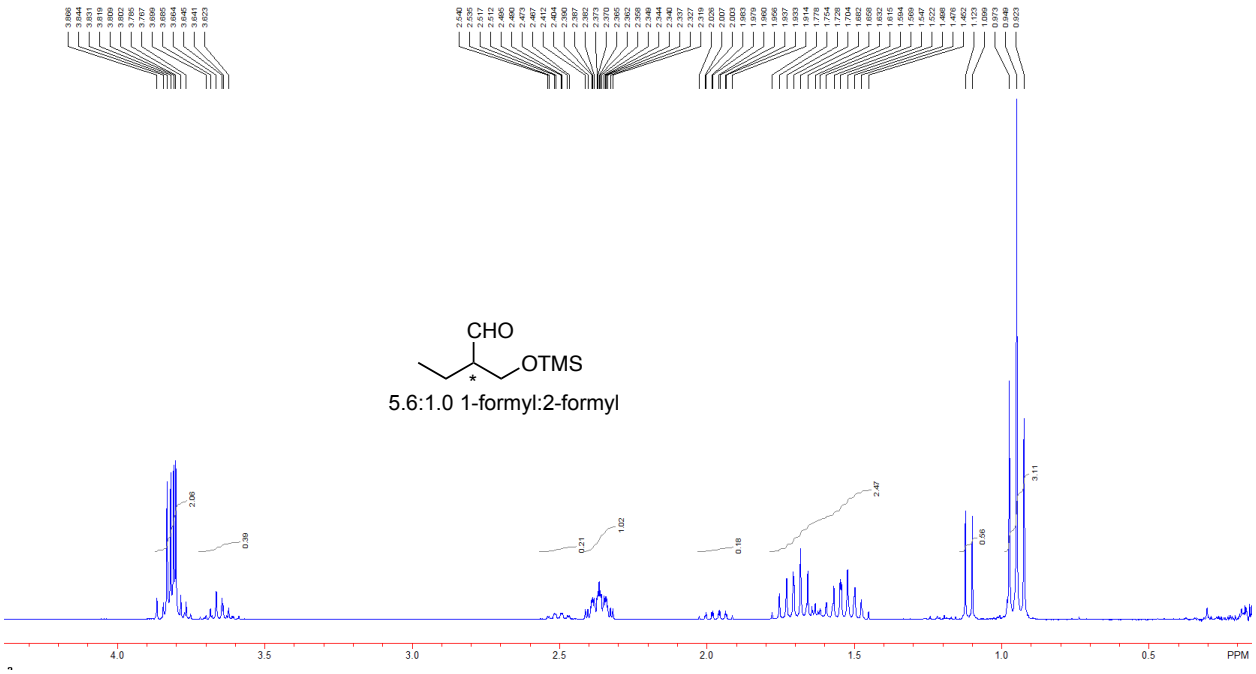

^{13}C NMR:

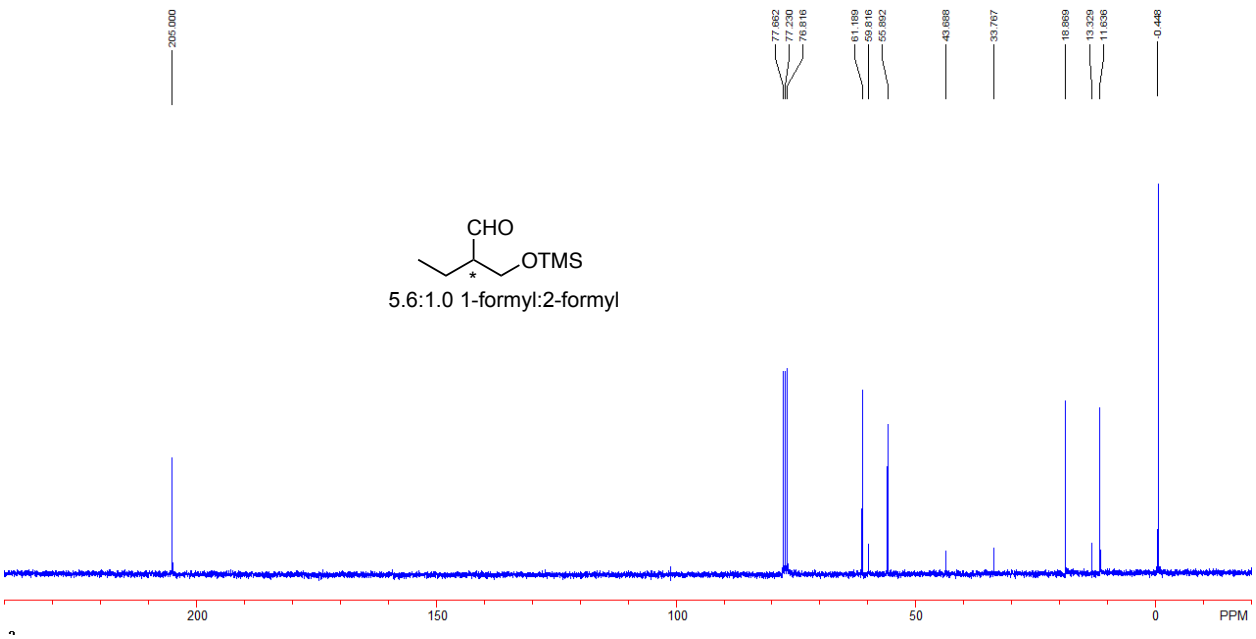

^{1}H NMR:

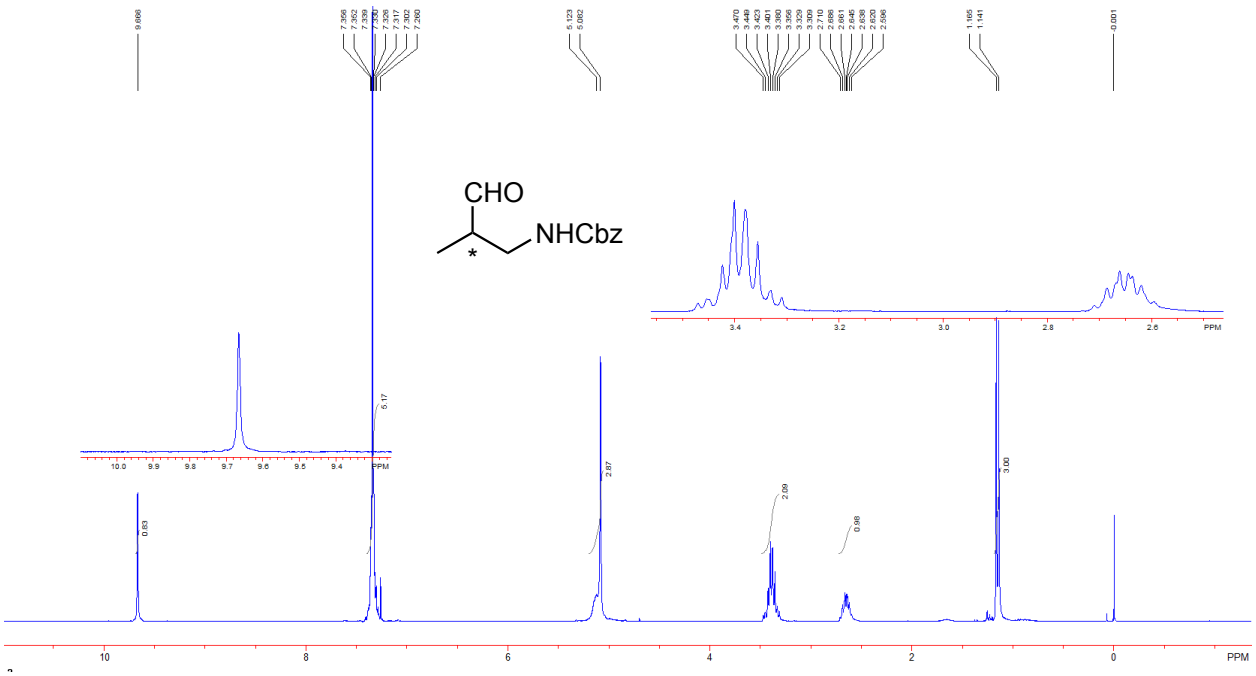

^{13}C NMR:

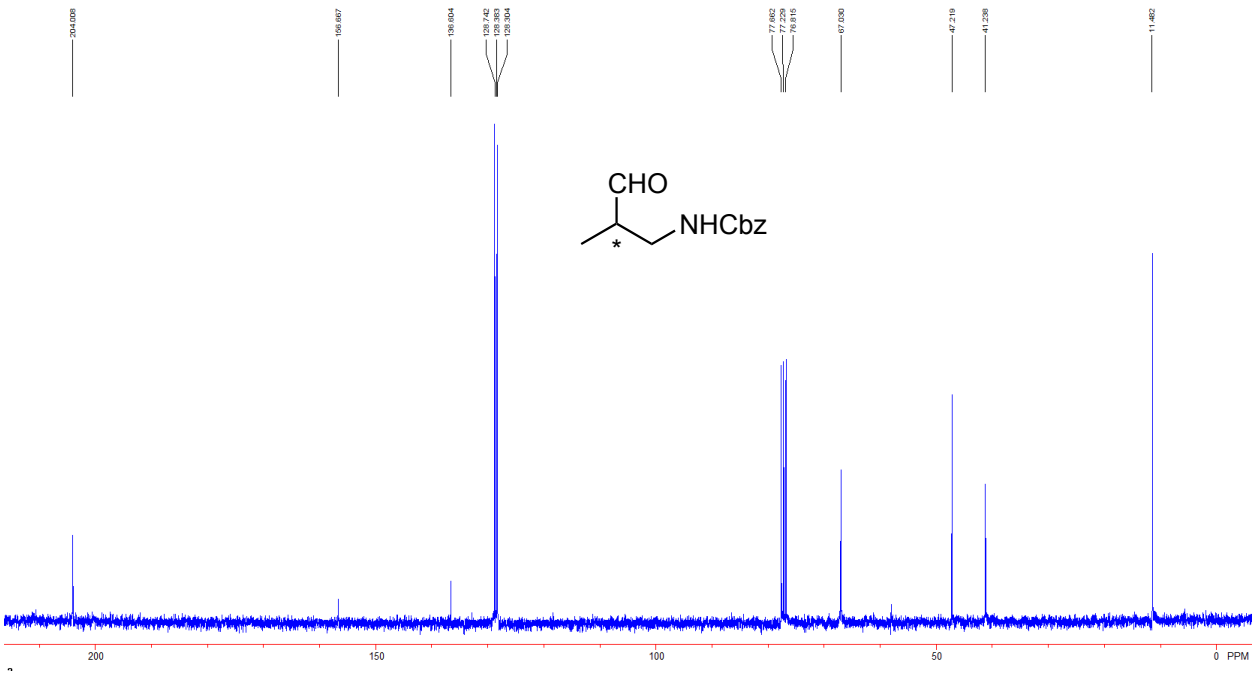

^{1}H NMR:

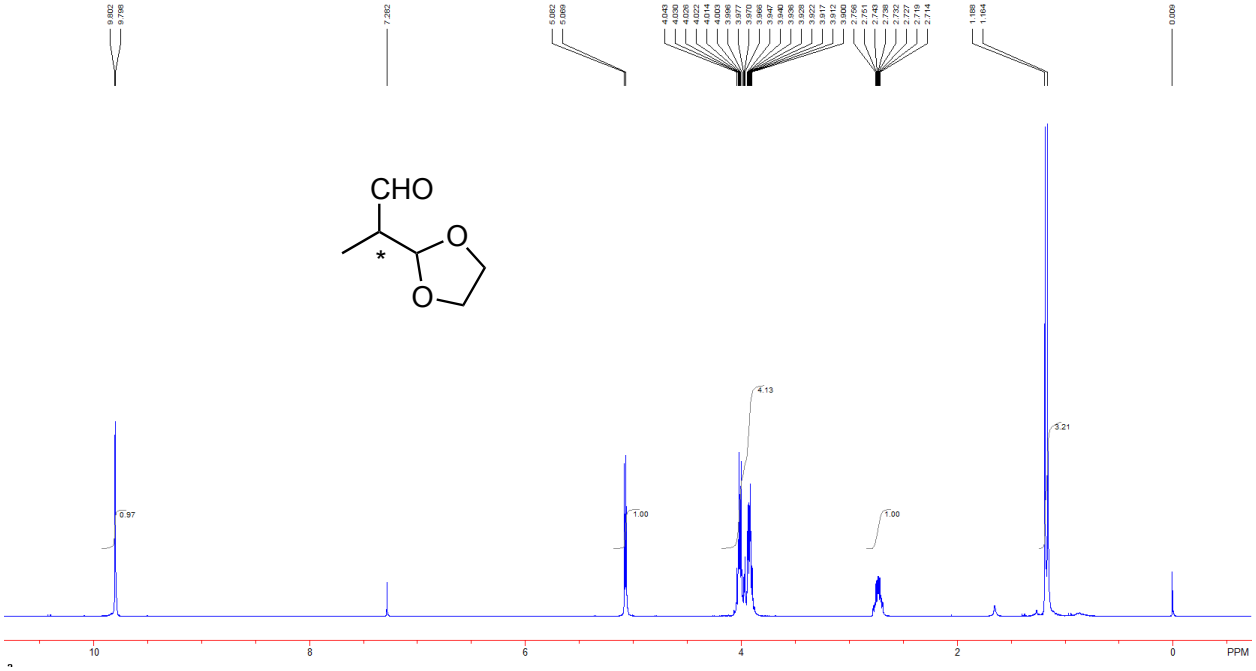

^{13}C NMR:

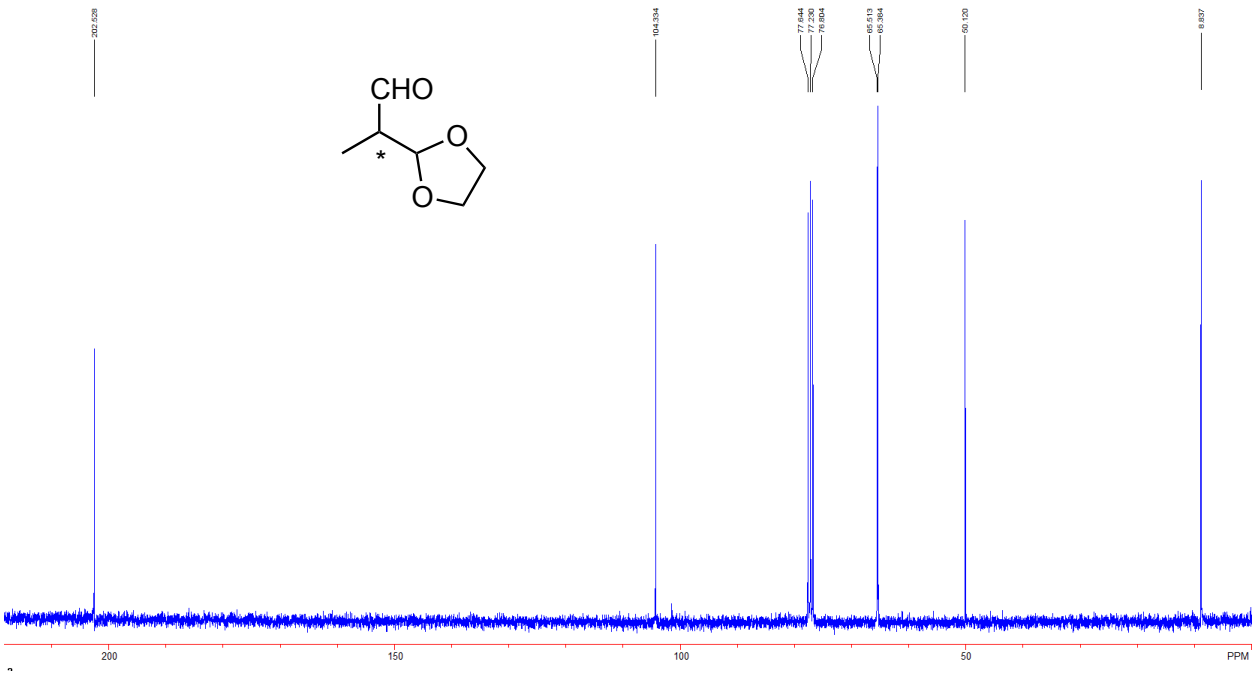

^{1}H NMR:

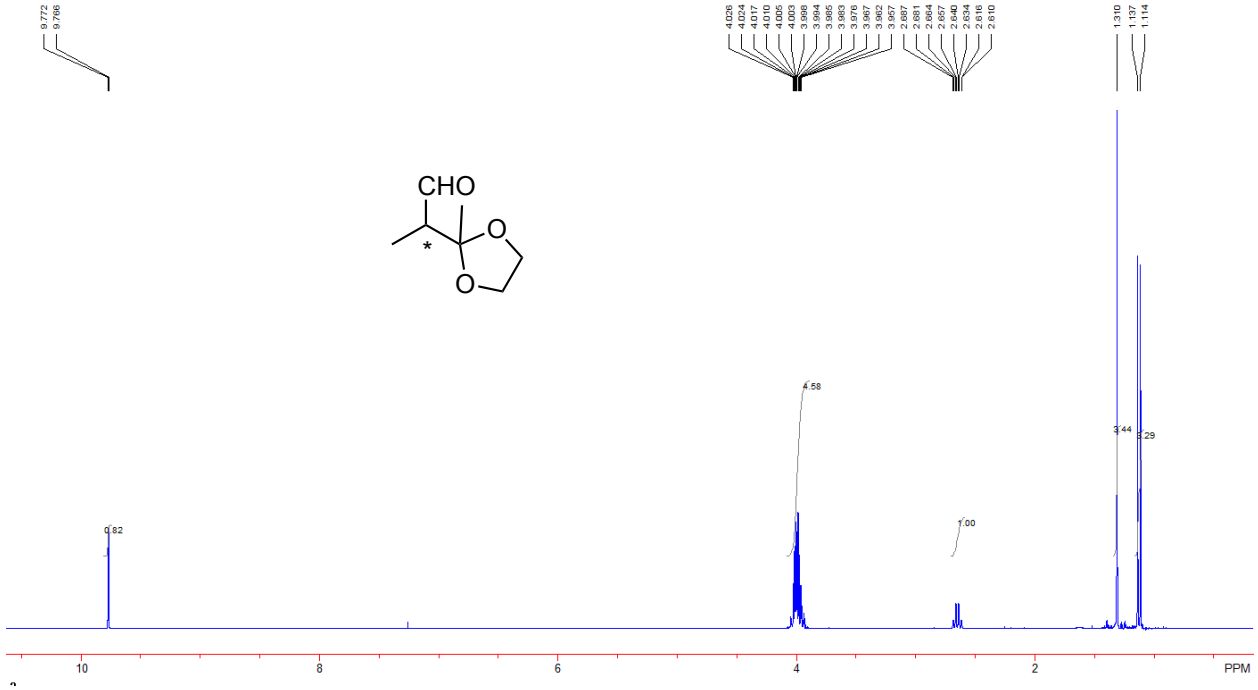

^{13}C NMR:

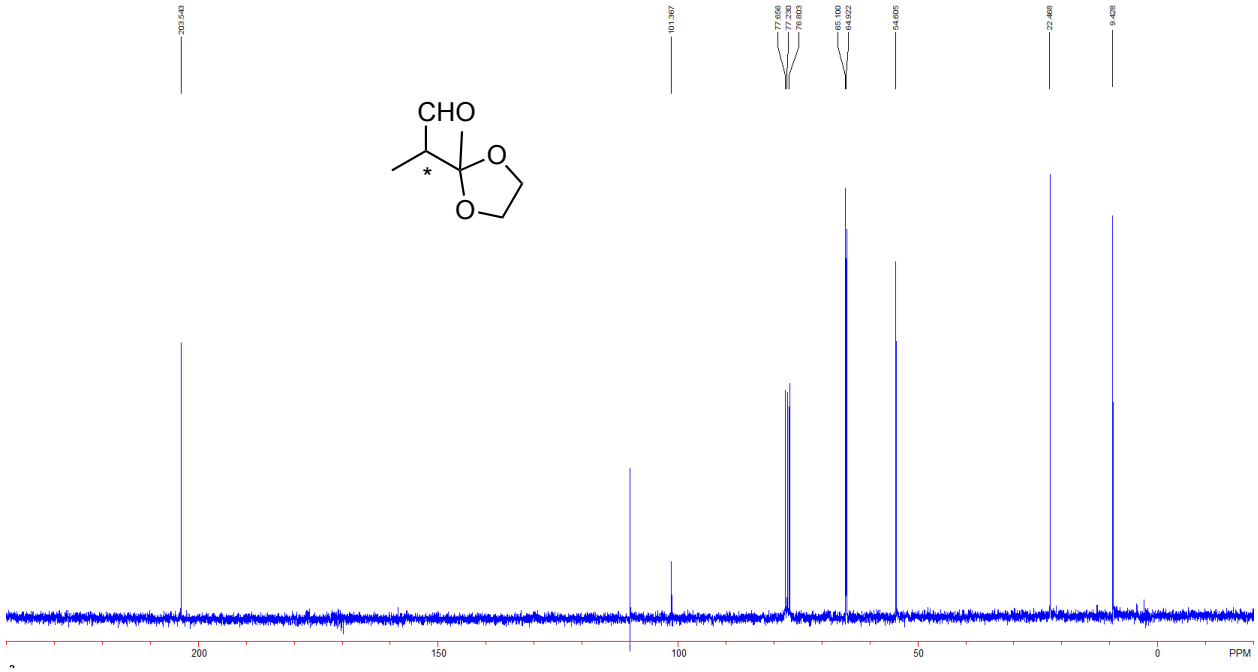

^{1}H NMR:

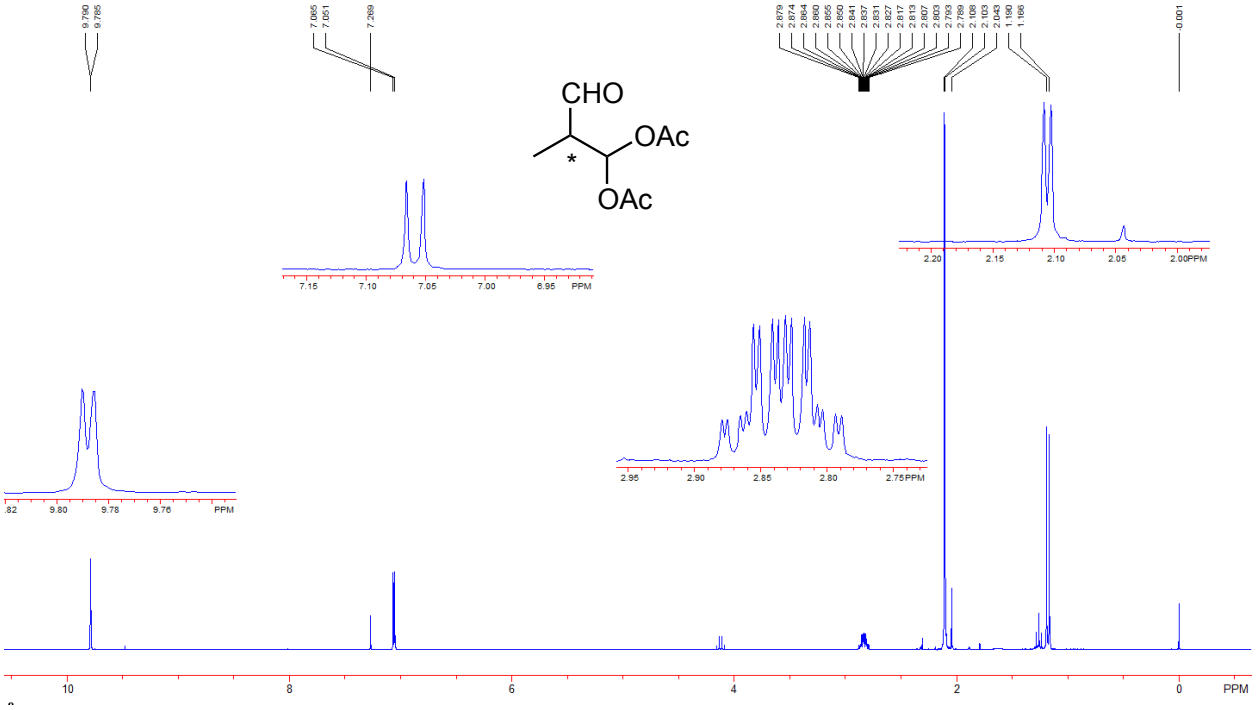

^{13}C NMR:

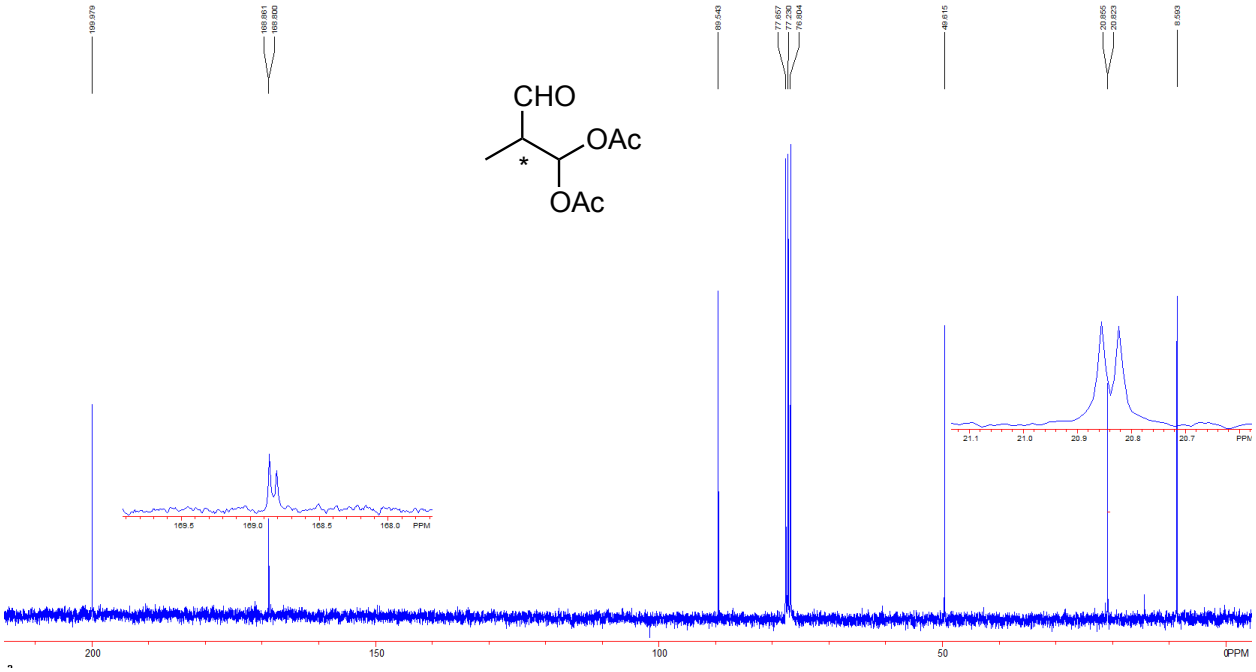

^{1}H NMR:

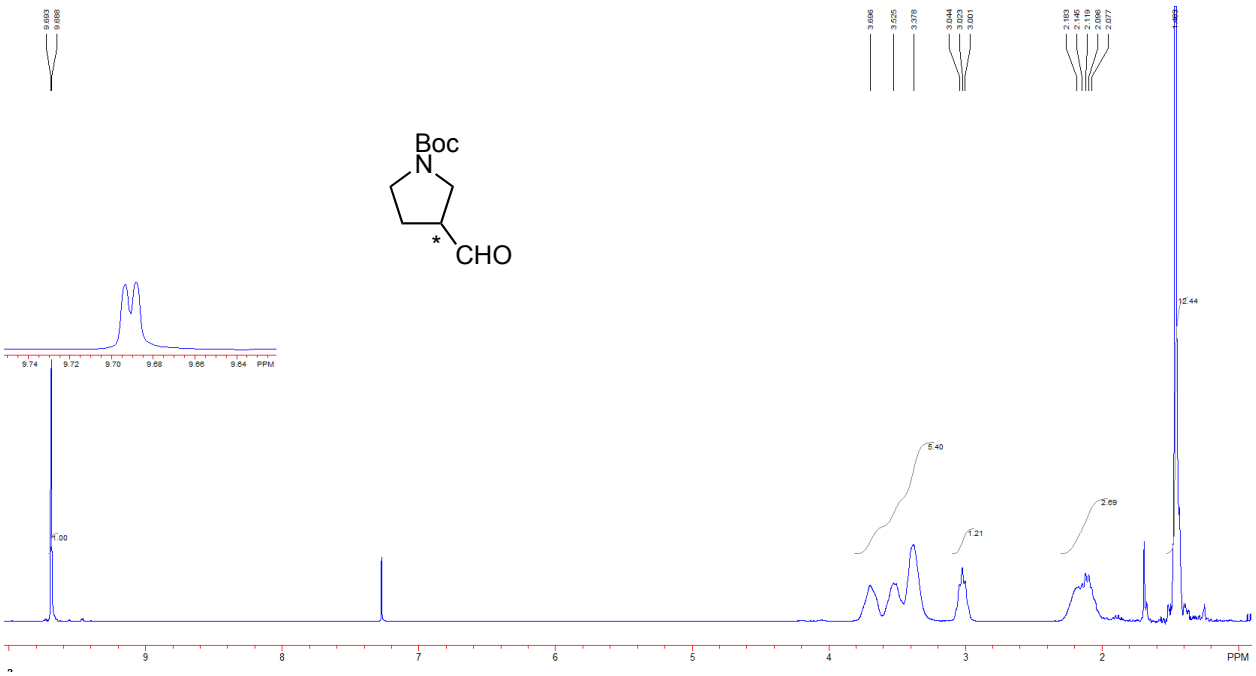

^{13}C NMR:

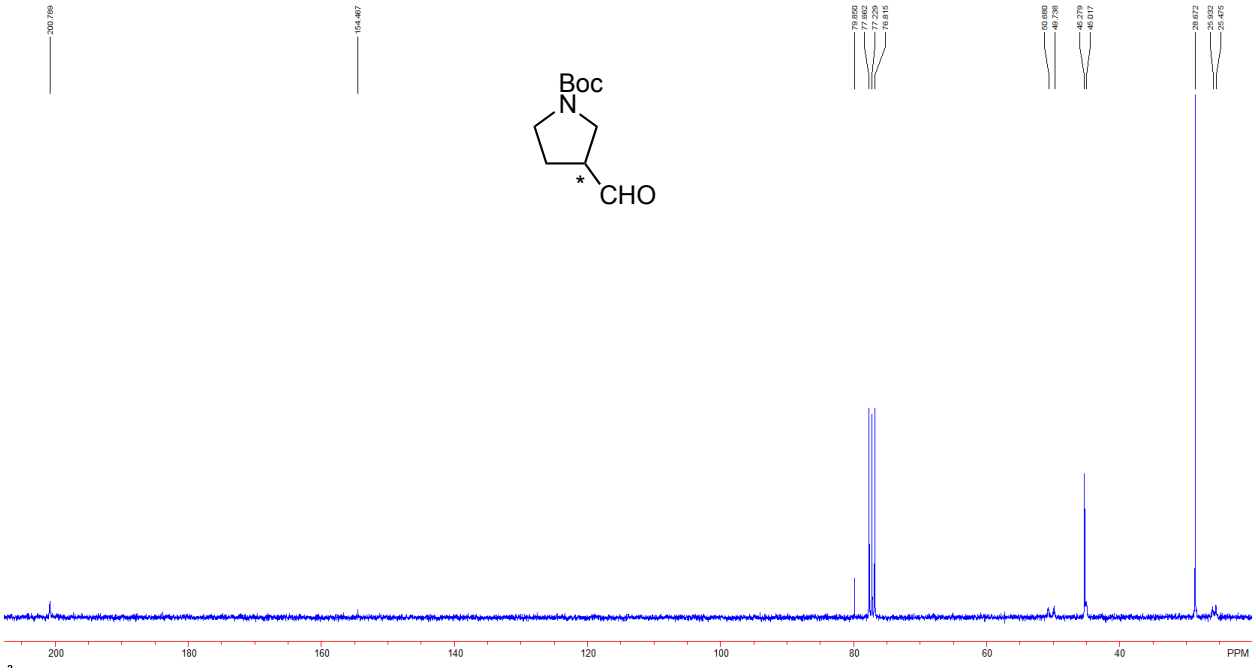

^{1}H NMR:

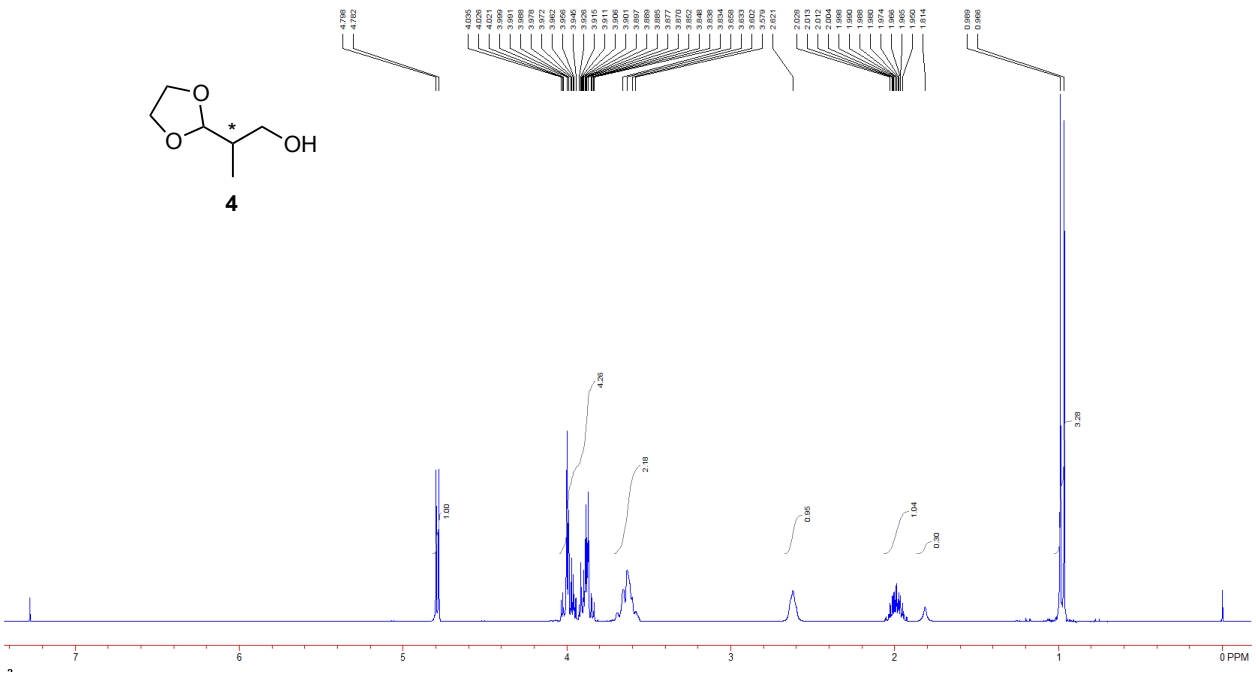

^{13}C NMR:

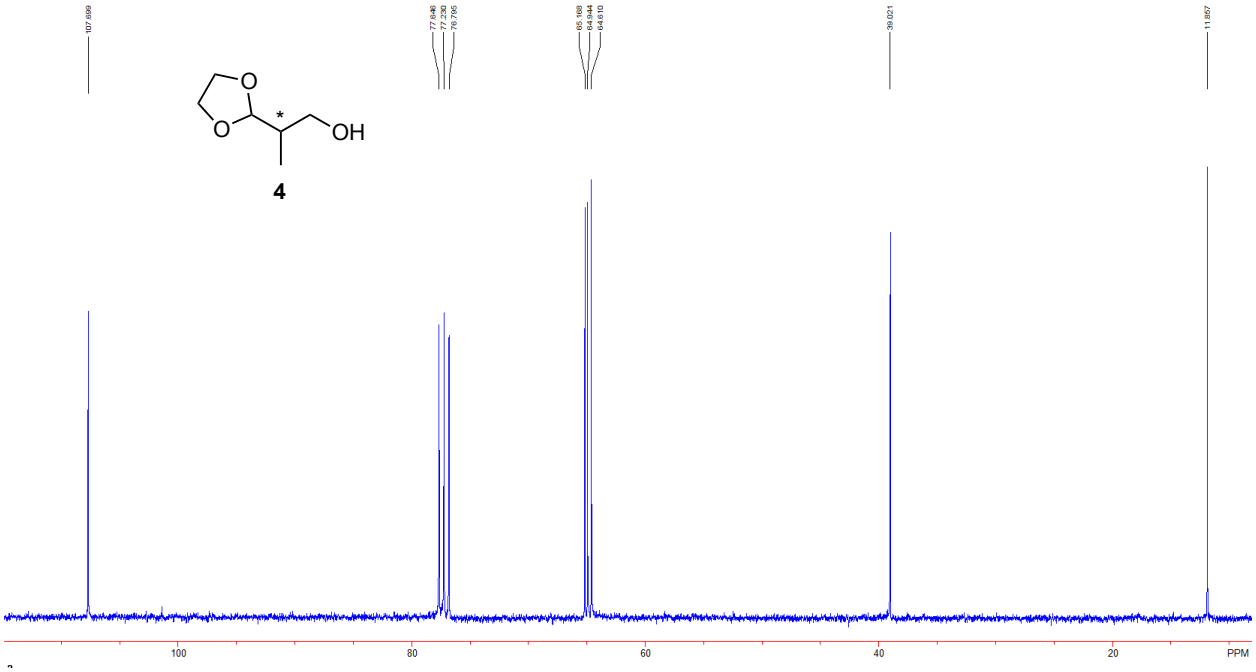

^{1}H NMR:

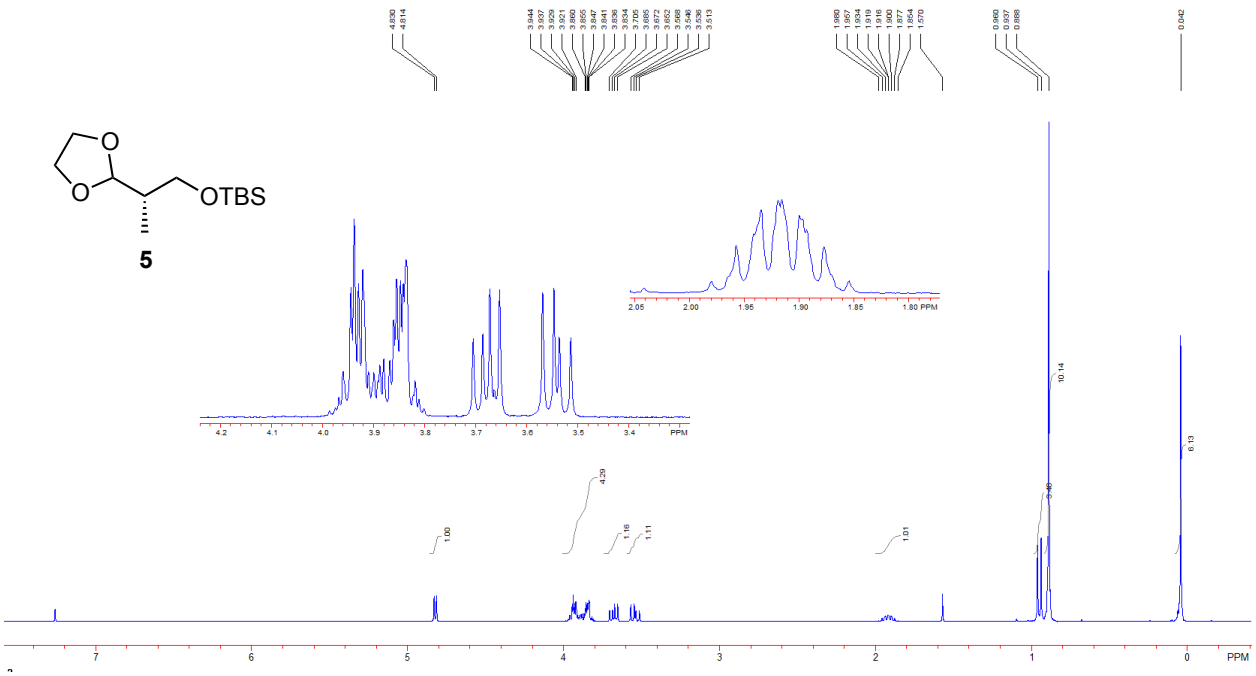

^{13}C NMR:

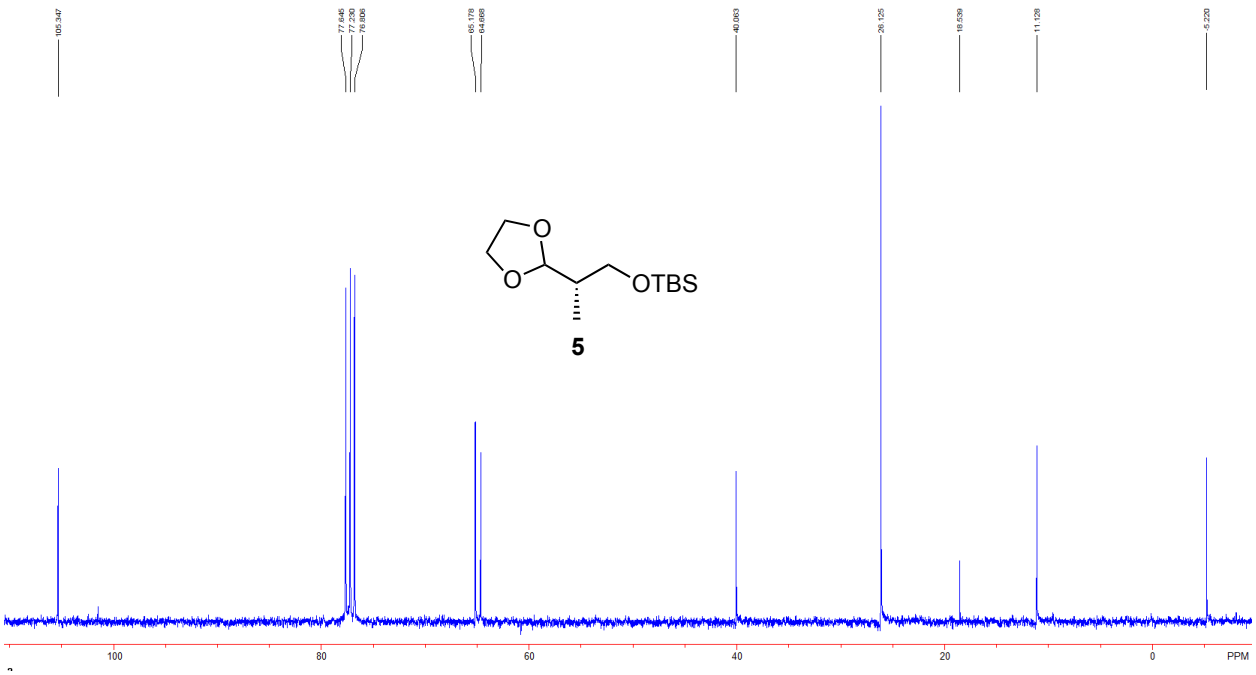

6.3 NMR Spectra, GC and SFC Chromatograms from Chapter 5

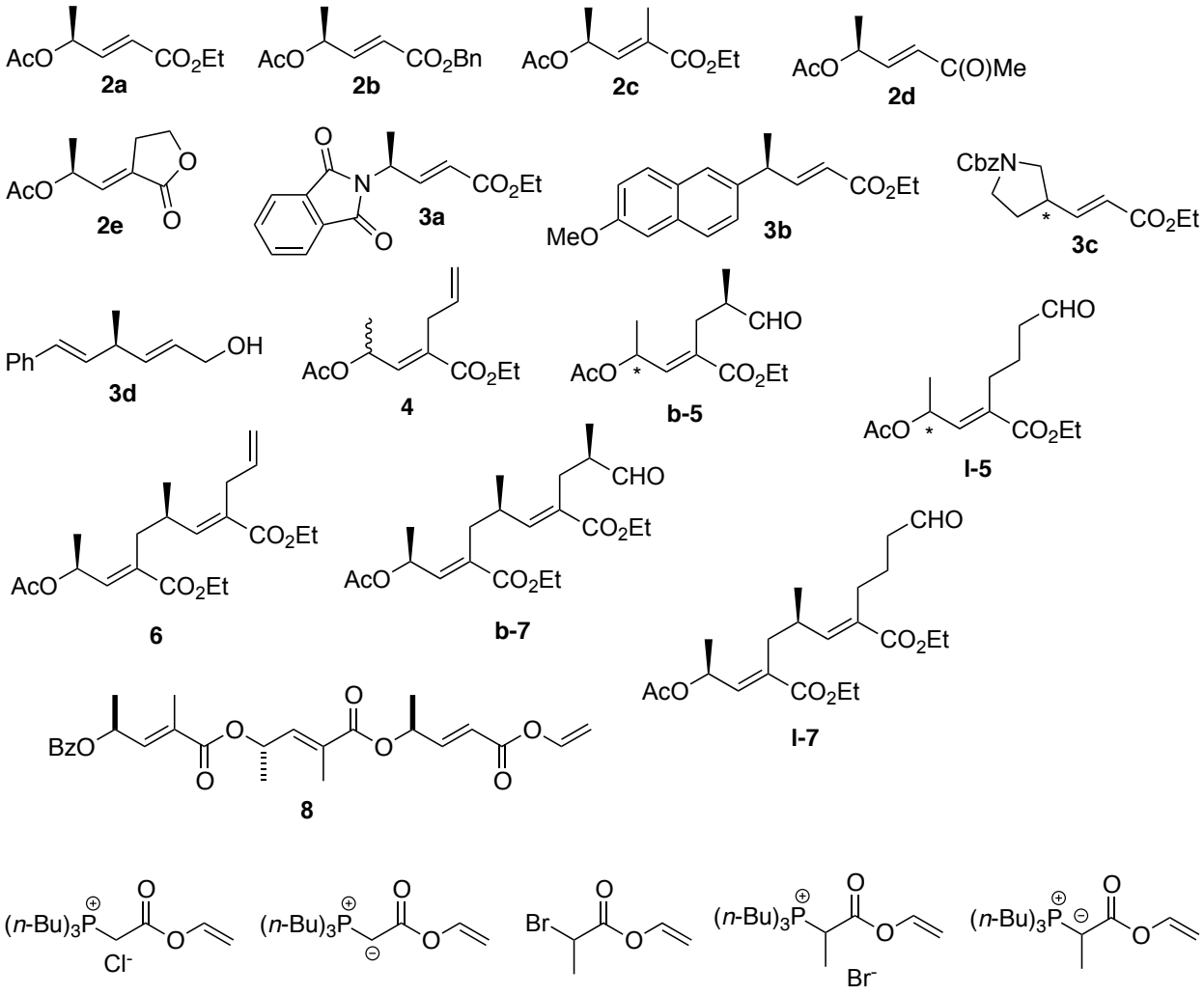

^{1}H NMR for **2a**:

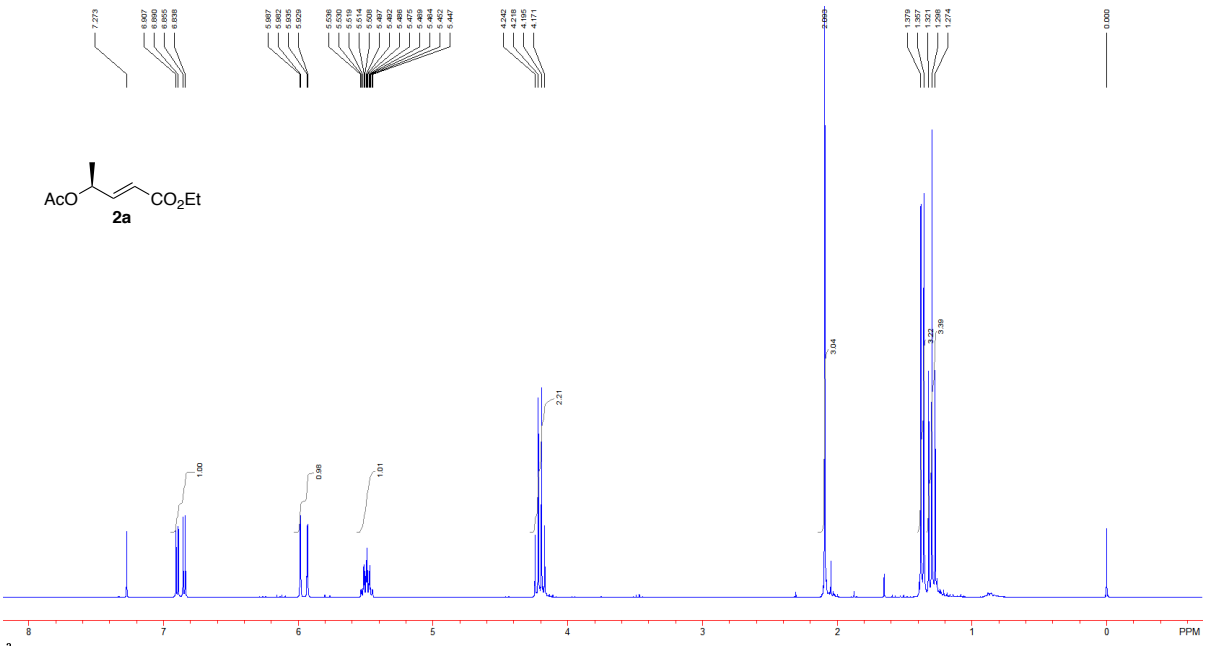

^{13}C NMR for **2a**:

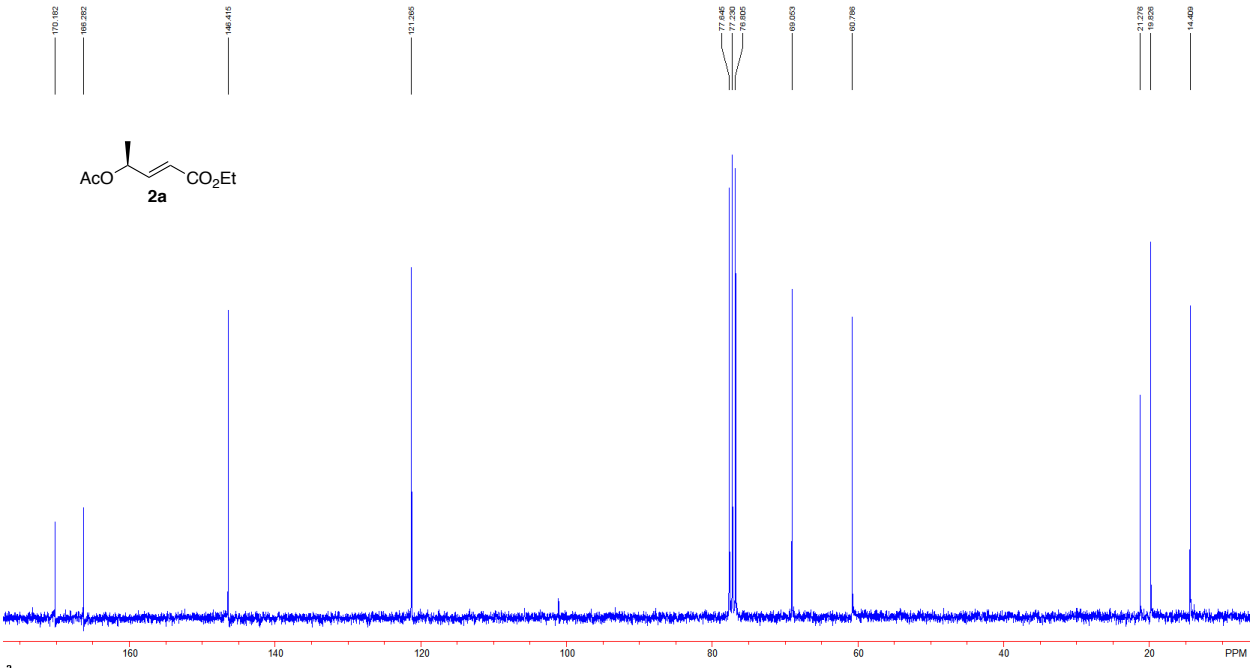

^{1}H NMR for **2b**:

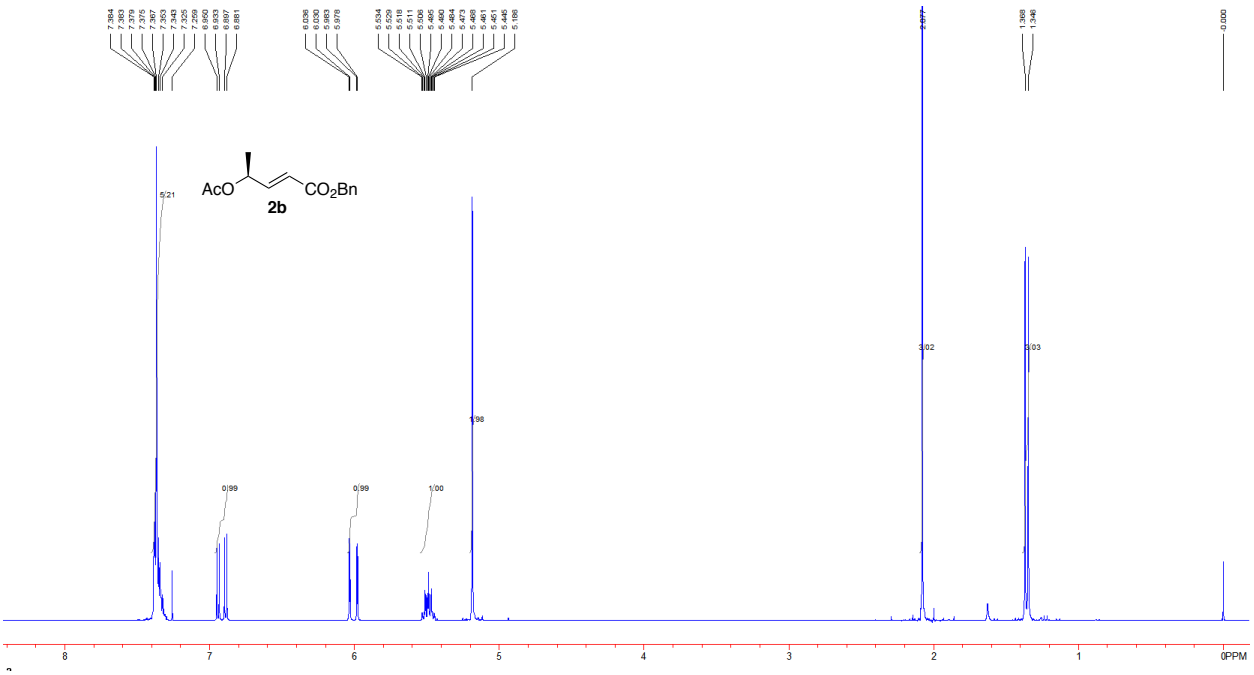

^{13}C NMR for **2b**:

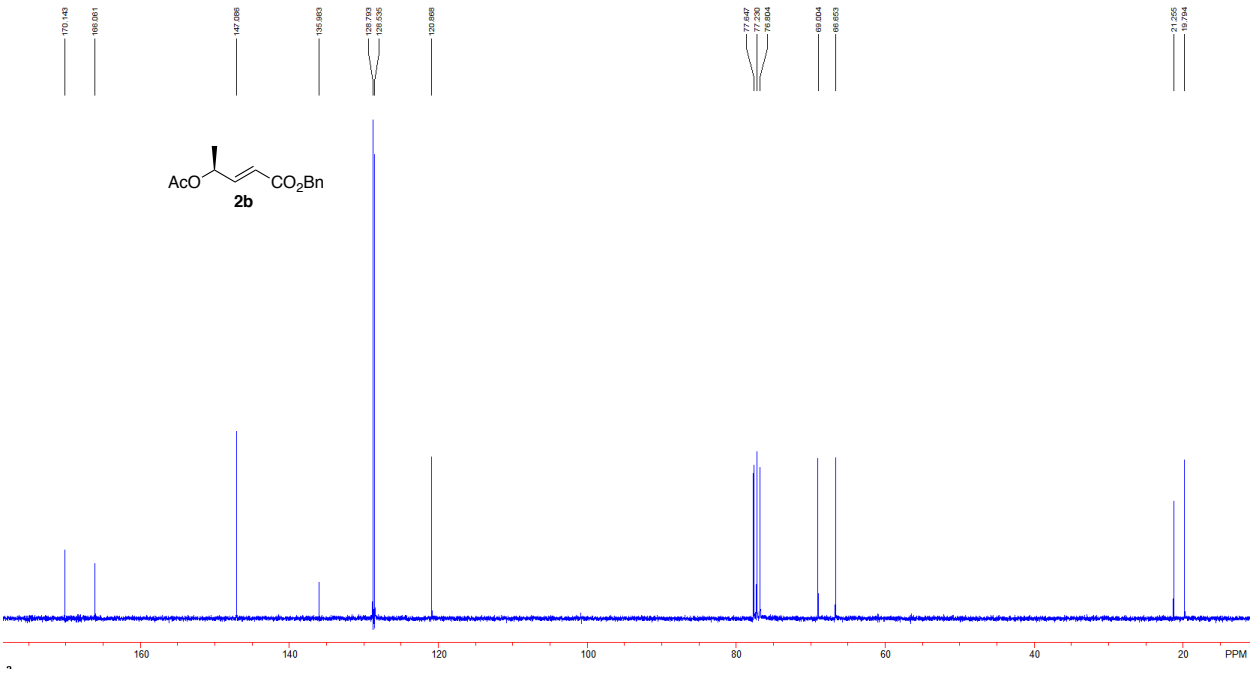

SFC chromatogram of enantioenriched **2b** (AD-H 5% MeOH 2mL/min flow 40°C):

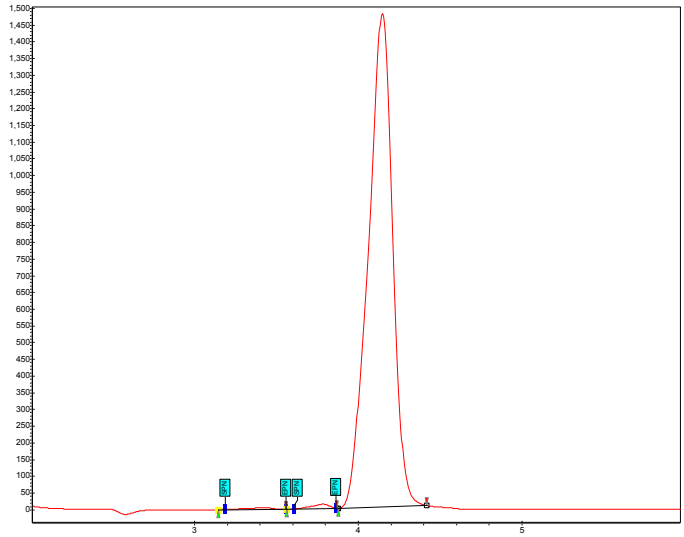

#	Name	Start [Min]	Time [Min]	End [Min]	RT Offset [Min]	Quantity [% Area]	Height [µV]	Area [µV.Min]	Area [%]
1	UNKNOWN	3.15	3.42	3.56	0.00	0.41	6.0	1.0	0.410
2	UNKNOWN	3.57	3.78	3.87	0.00	0.69	13.3	1.8	0.687
3	UNKNOWN	3.88	4.15	4.42	0.00	98.90	1475.1	252.8	98.903
Total					100.00	1494.5	255.6	100.000	

SFC chromatogram of a *mixture* of **2b** enantiomers (AD-H 5% MeOH 2mL/min flow 40°C):

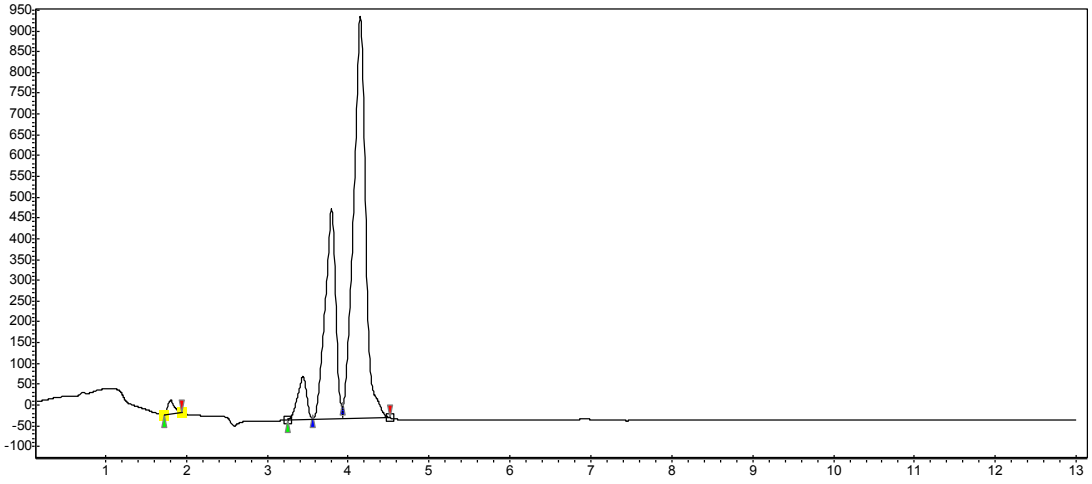

#	Name	Start [Min]	Time [Min]	End [Min]	RT Offset [Min]	Quantity [% Area]	Height [µV]	Area [µV.Min]	Area [%]
1	UNKNOWN	1.73	1.81	1.94	0.00	1.18	32.7	3.1	1.182
2	UNKNOWN	3.25	3.44	3.56	0.00	5.06	102.8	13.2	5.065
3	UNKNOWN	3.56	3.79	3.93	0.00	29.49	504.5	76.8	29.489
4	UNKNOWN	3.93	4.15	4.52	0.00	64.26	966.0	167.3	64.264
Total					100.00	1605.9	260.4	100.000	

^{1}H NMR for **2b'**:

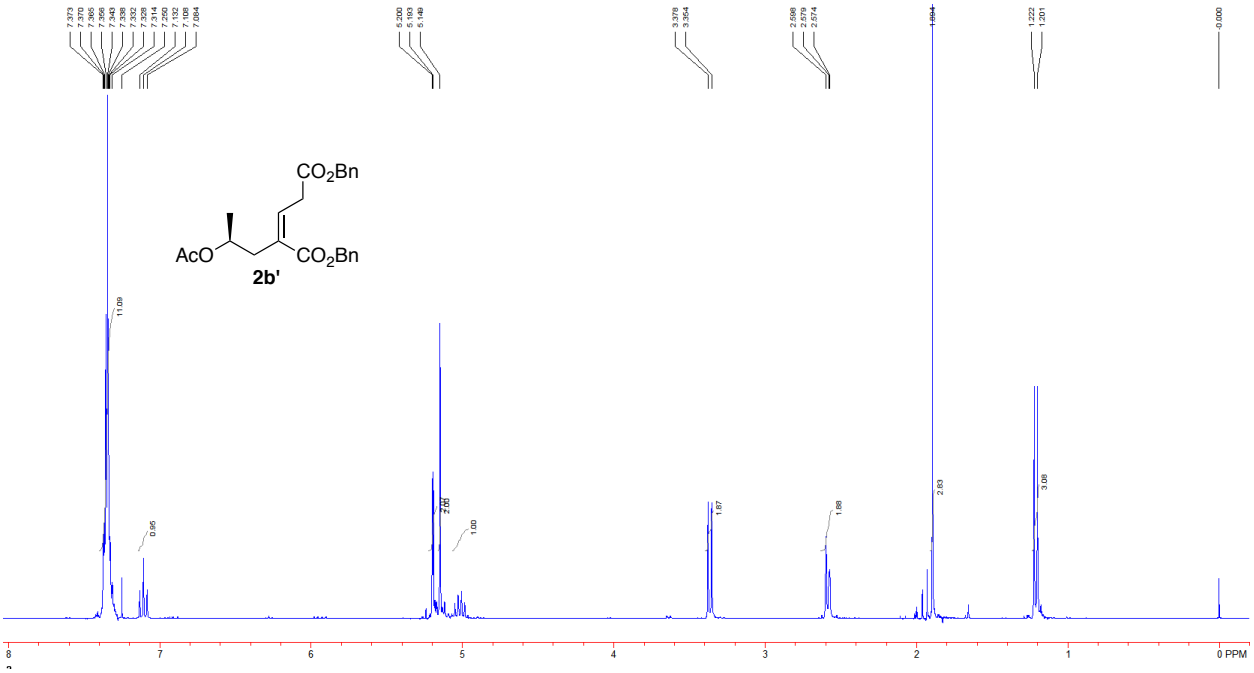

^{13}C NMR for **2b'**:

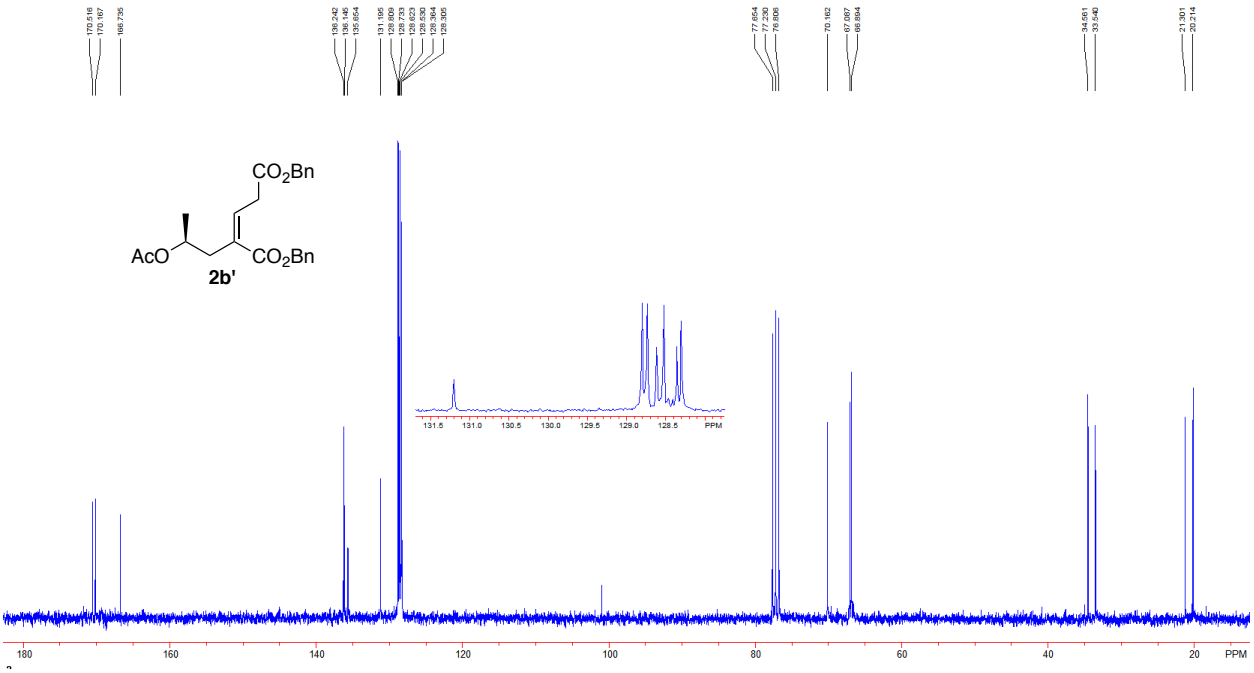

^{1}H NMR for **2c**:

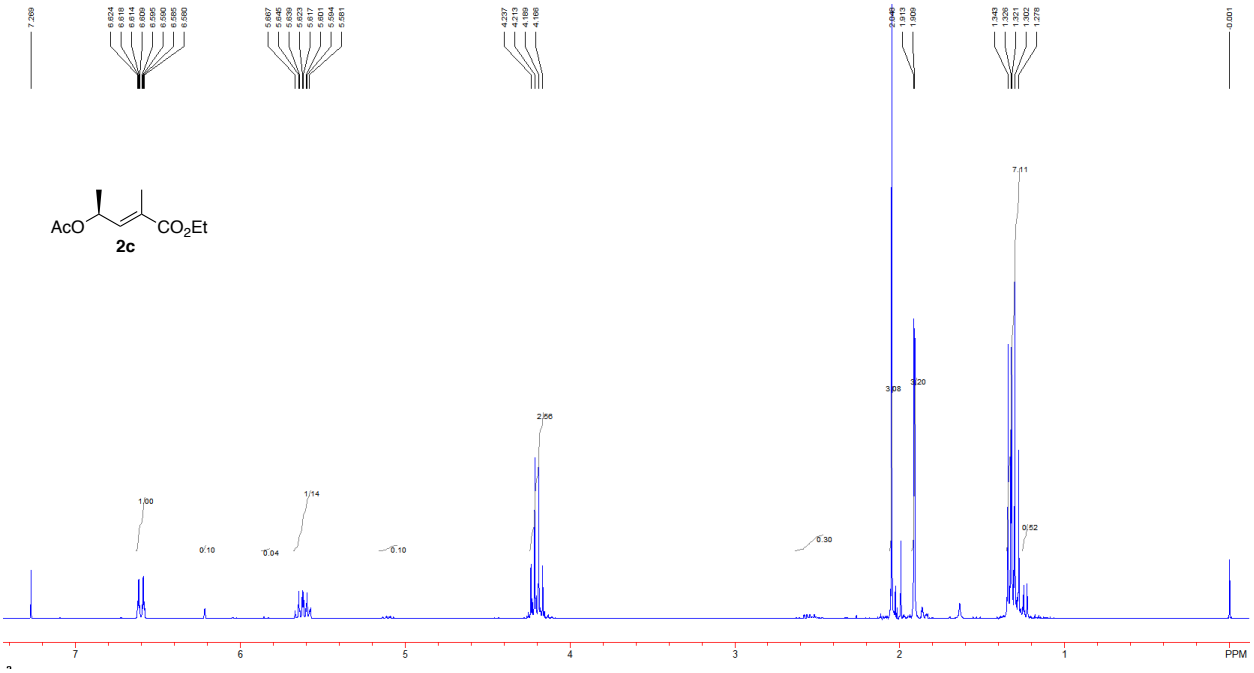

^{13}C NMR for **2c**:

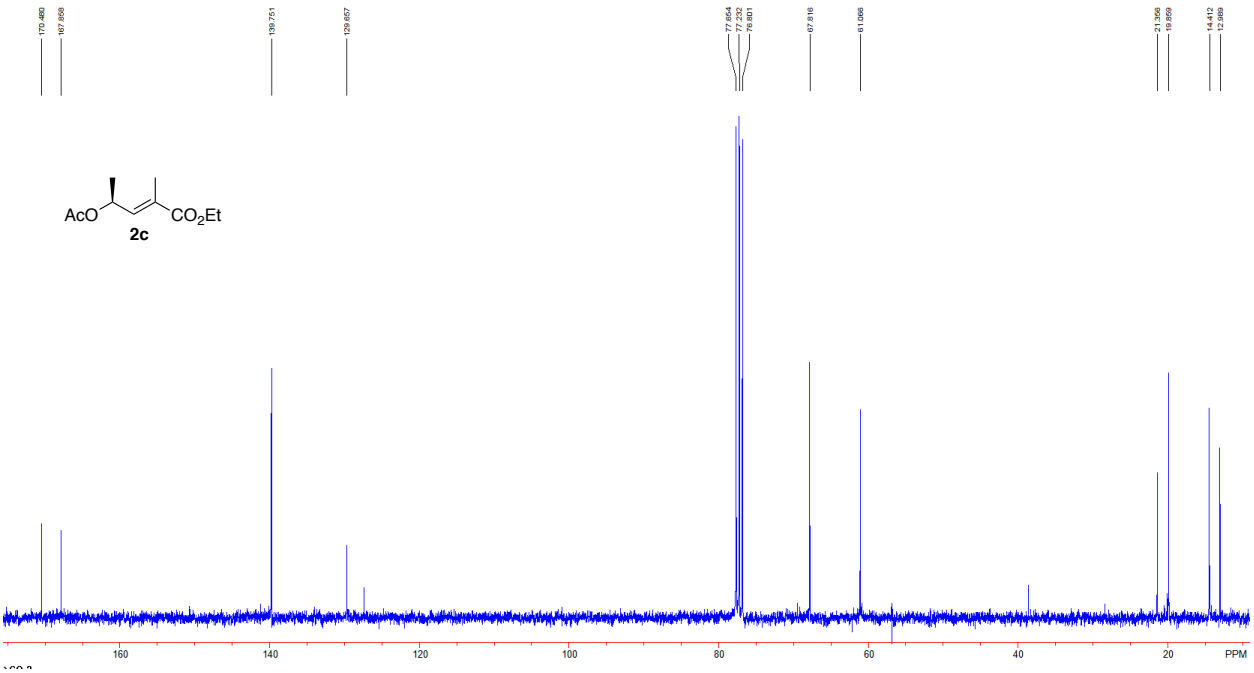

GC chromatogram of enantioenriched **2c** (85°C hold for 90 min. then 120°C 5C/min and hold for 15min.):

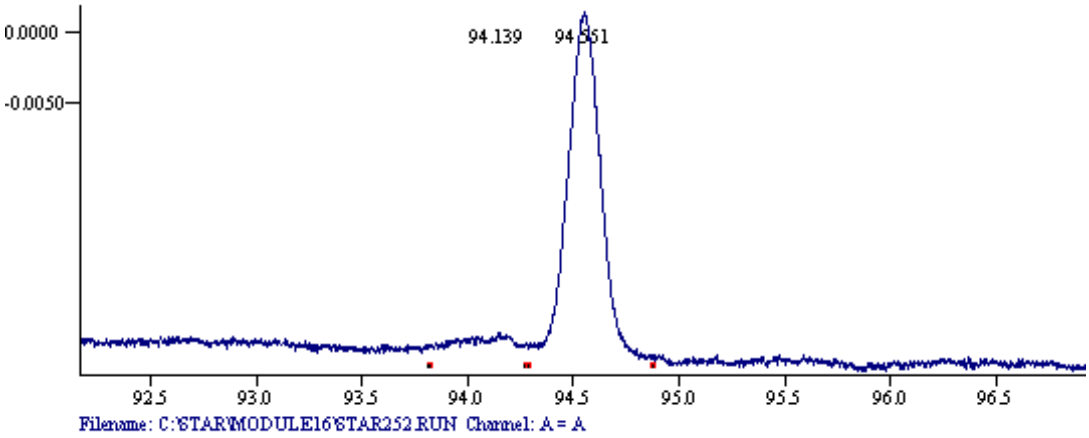

4.2963 94.139 0.000 11577 BB 6.4
89.4833 94.551 0.000 241116 BB 9.4

GC chromatogram of (*rac*)-**2c** (85°C hold for 90 min. then 120°C 5C/min and hold for 15min.):

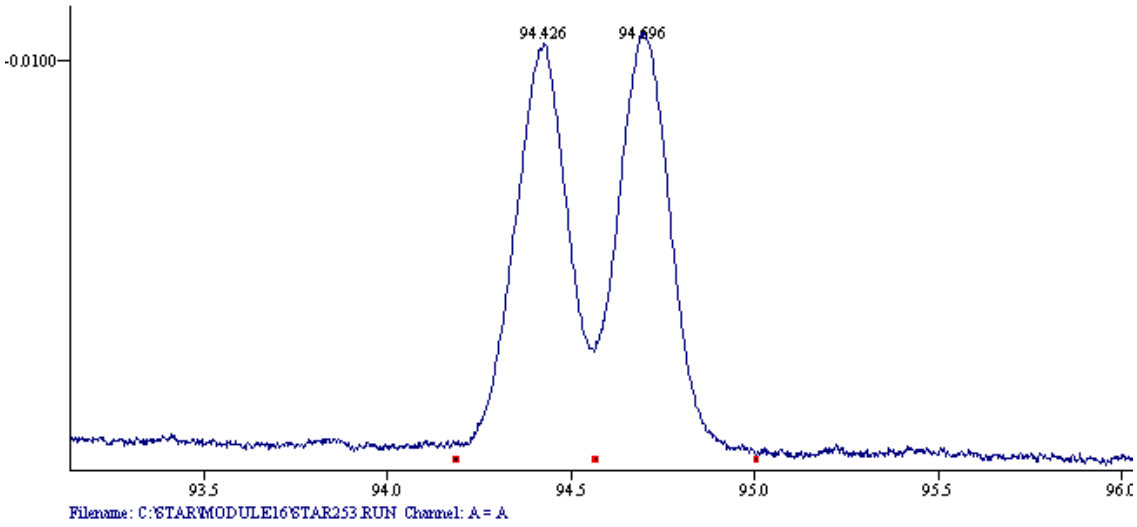

22.9029 94.426 0.000 195203 BB 9.4
23.2441 94.696 0.000 198112 BB 7.9

^{1}H NMR for **2d**:

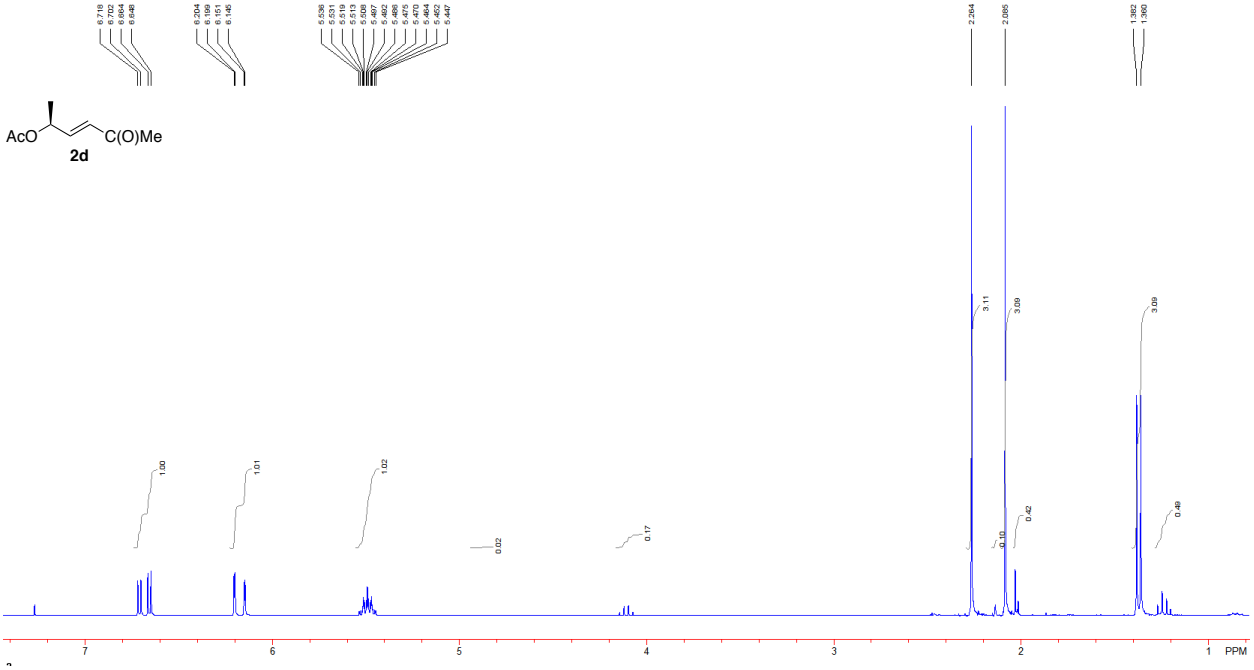

^{13}C NMR for **2d**:

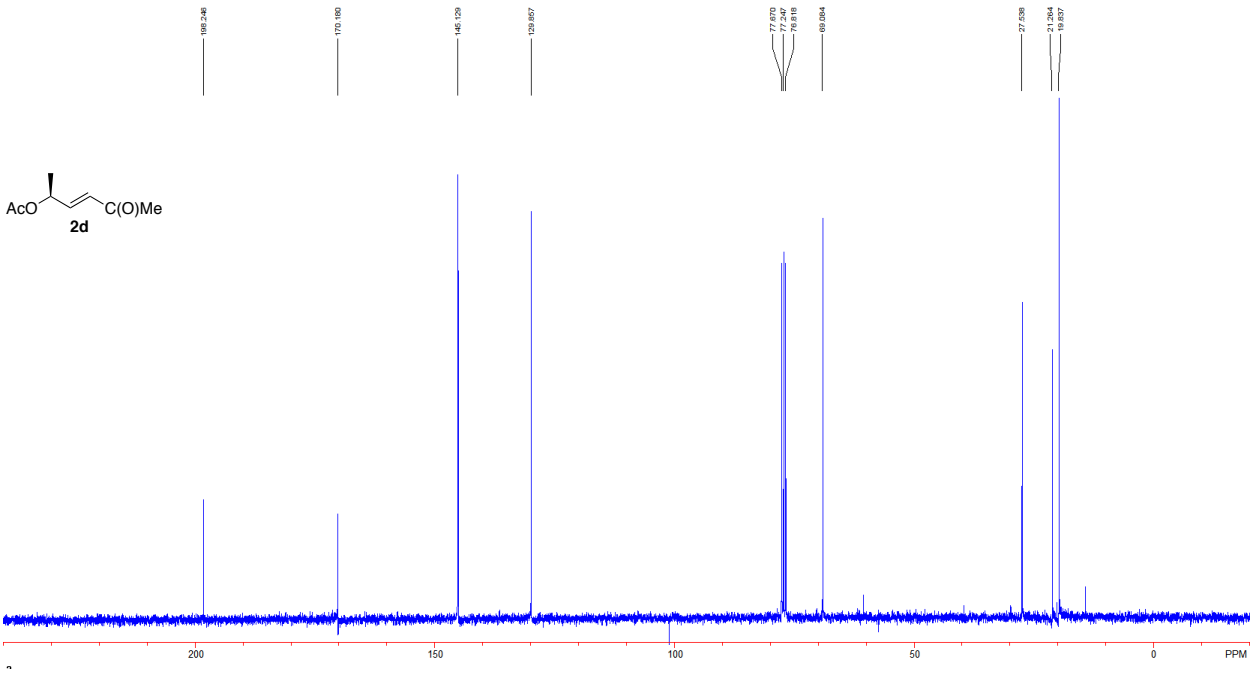

GC chromatogram of enantioenriched **2d** (110°C hold for 15 min.):

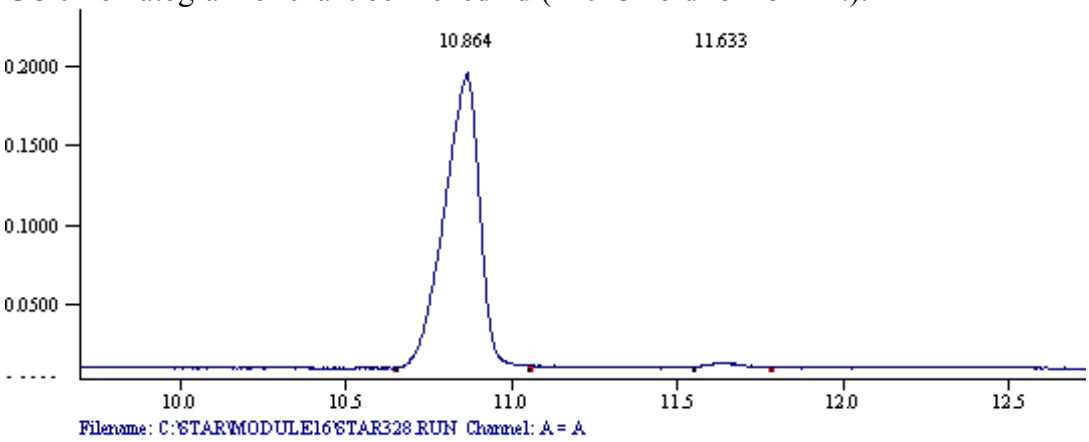

22.4986 10.864 0.000 1346460 BB 6.9
0.3485 11.632 0.000 20855 BB 7.2

GC chromatogram of (*rac*)-**2d** (110°C hold for 15 min.):

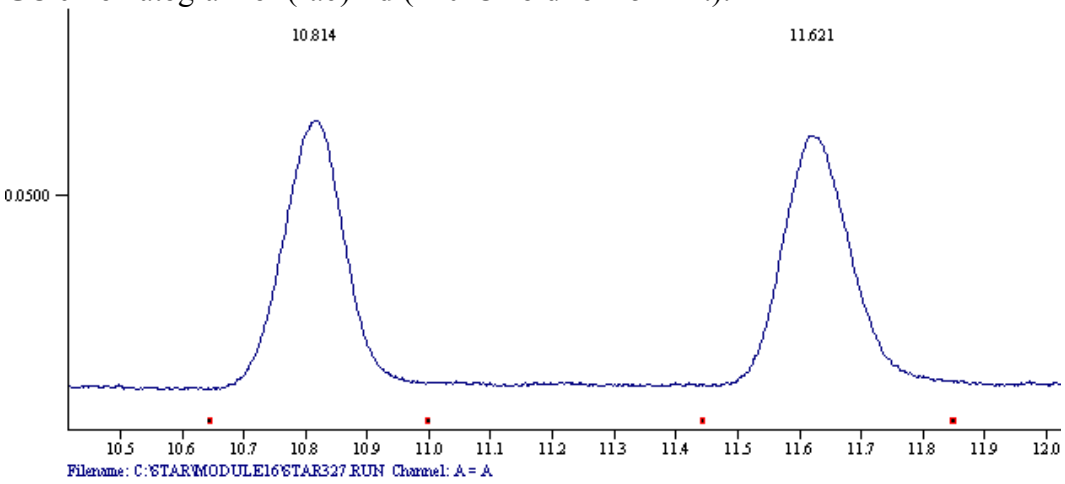

Overlay chromatograms of enantioenriched **2d** and (*rac*)-**2d**:

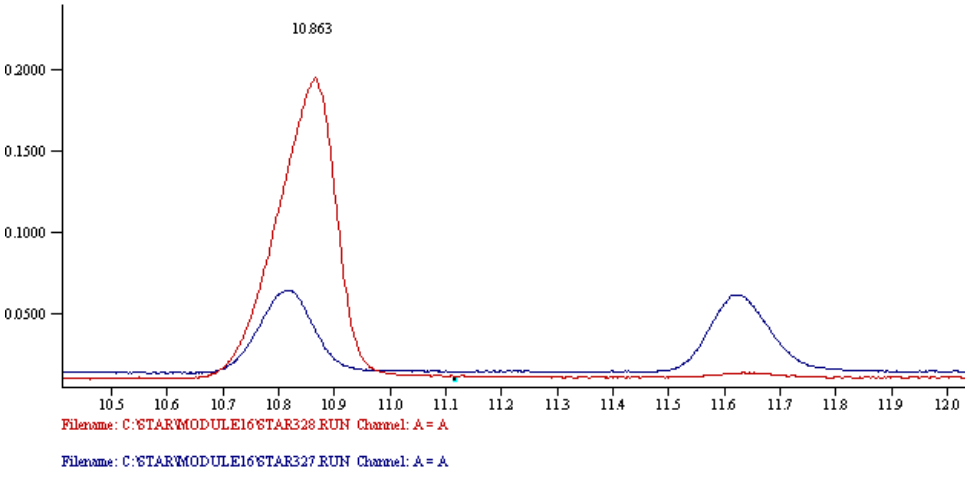

^{1}H NMR for **2e**:

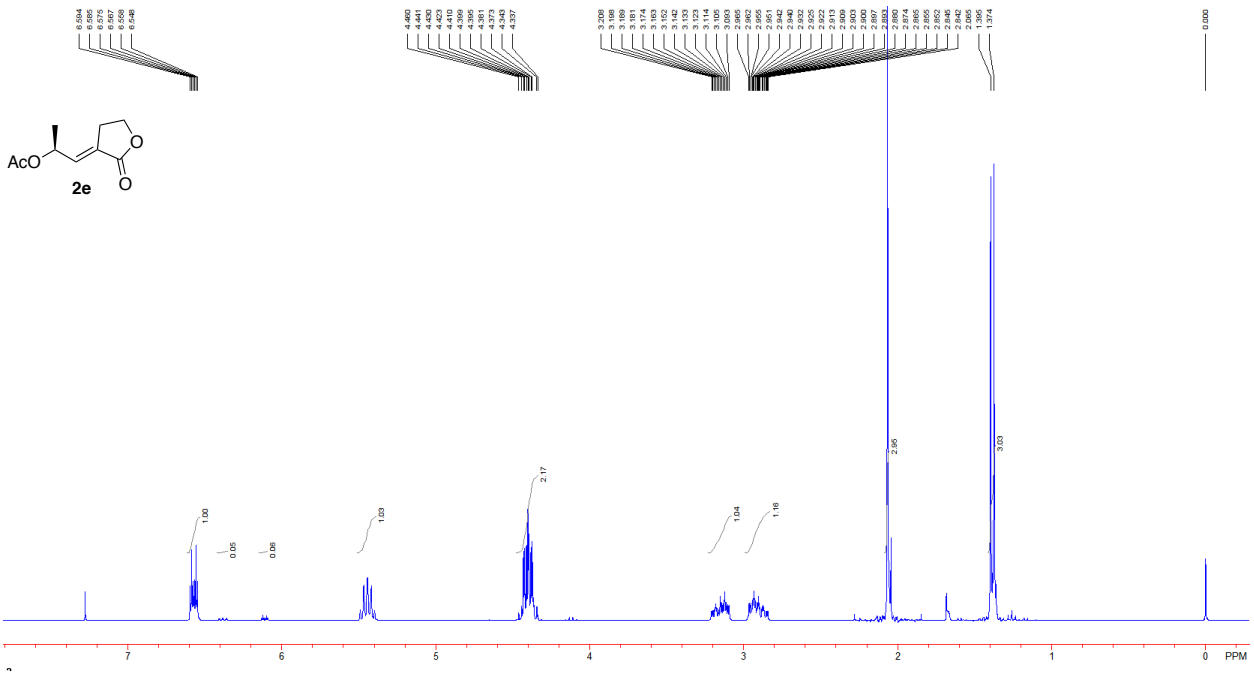

^{13}C NMR for **2e**:

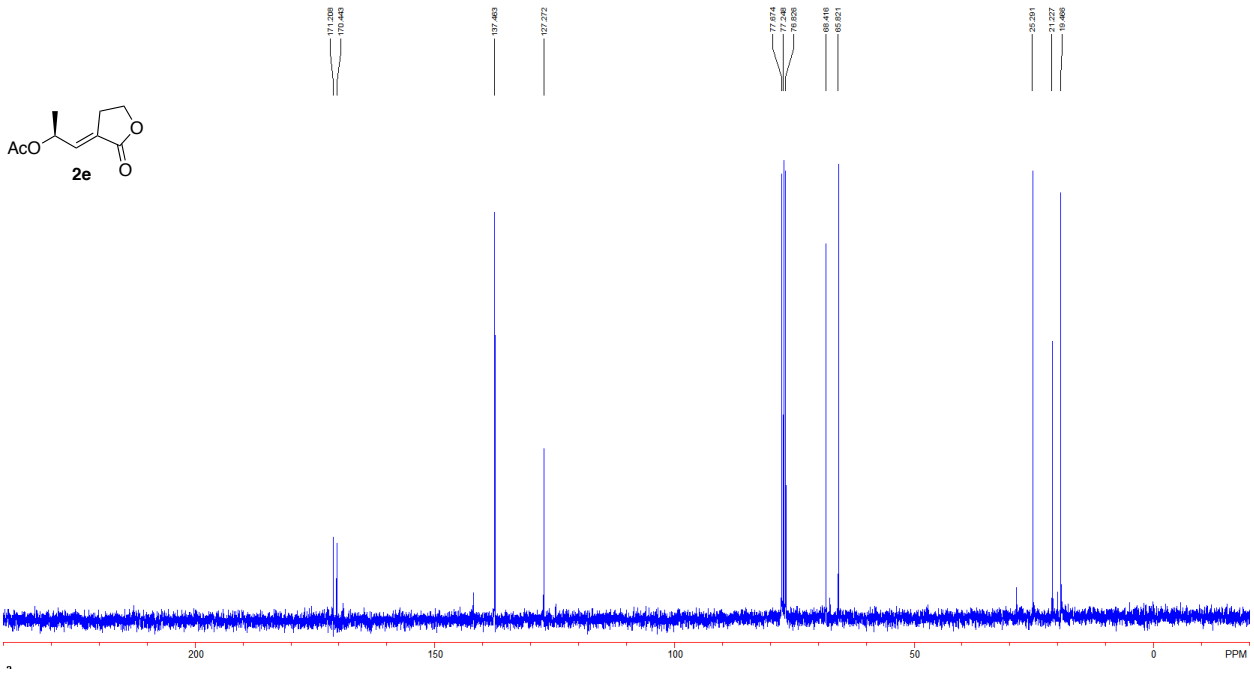

^{1}H NMR for **3a**:

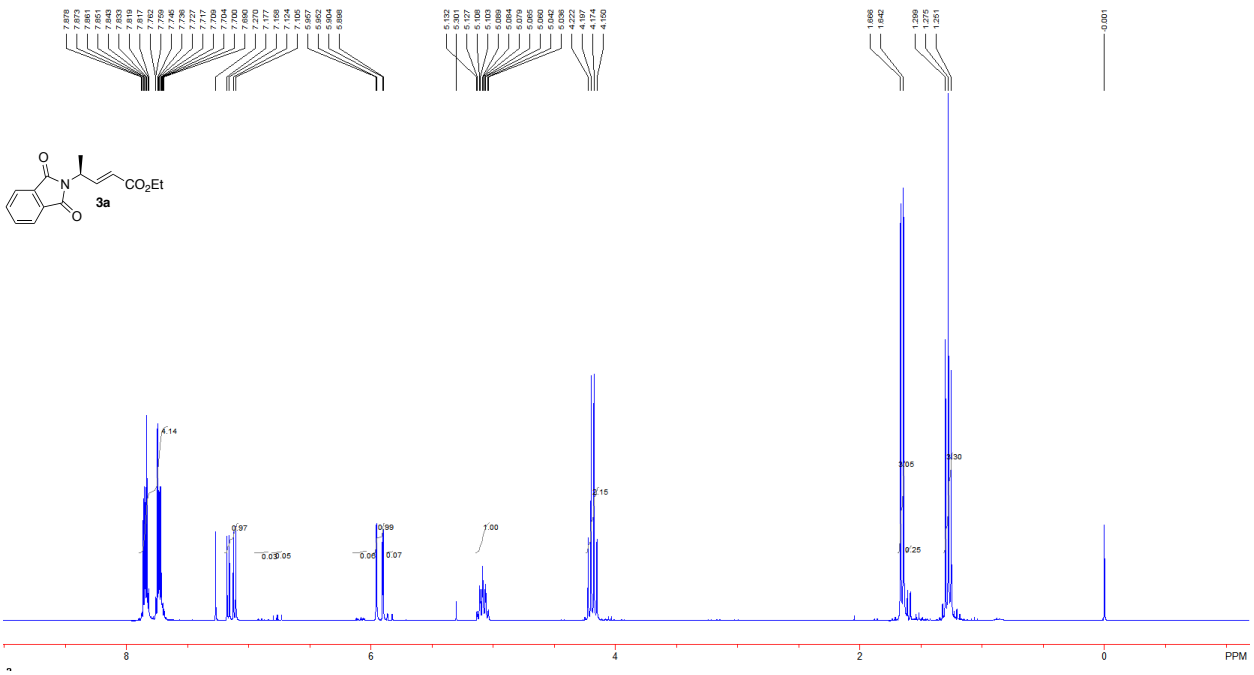

^{13}C NMR for **3a**:

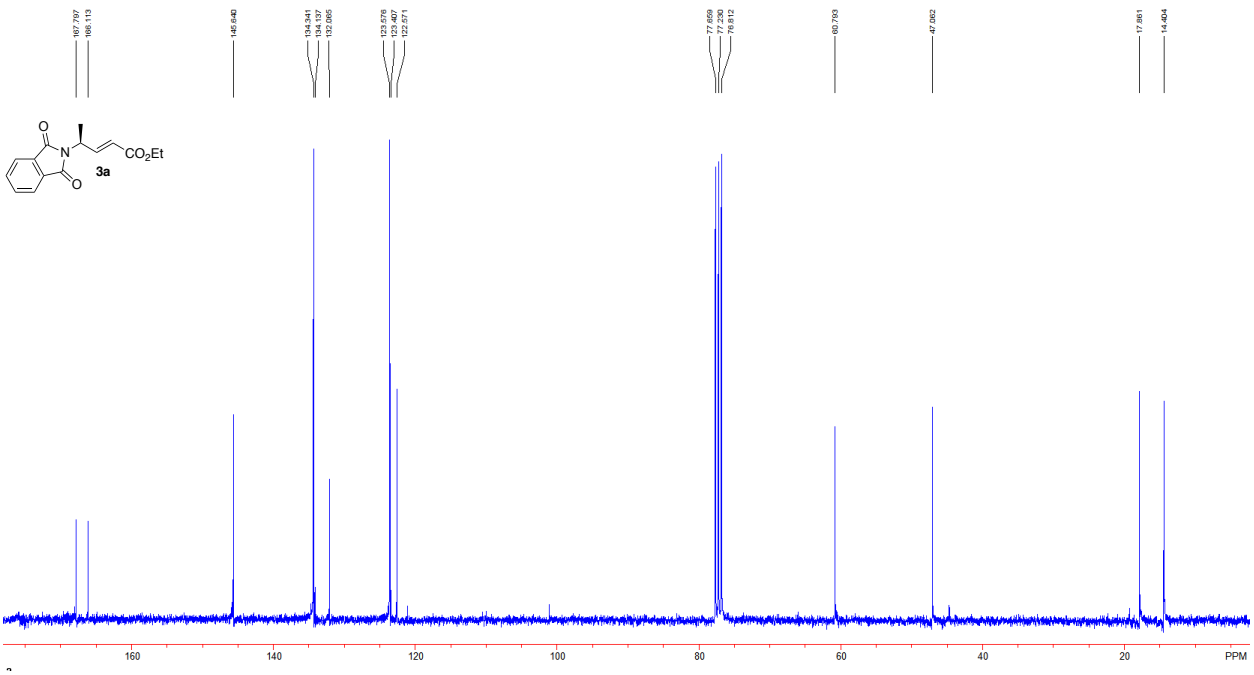

SFC chromatogram of enantioenriched **3a** (AD-H 5% methanol 2.0 mL/min 40°C):

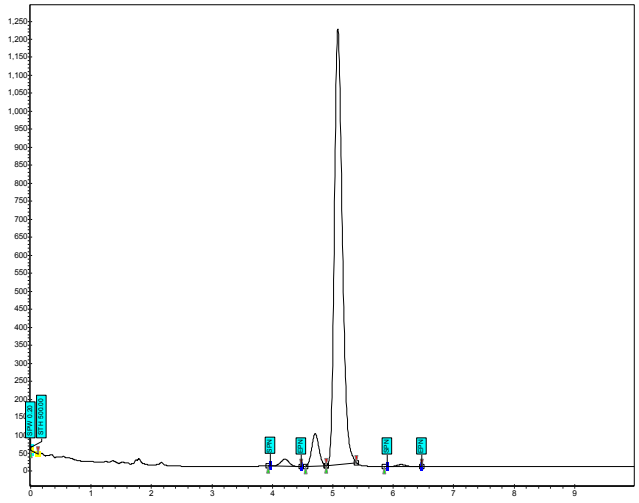

#Name	Start [Min]	Time [Min]	End [Min]	RT Offset [Min]	Quantity [% Area]	Height [µV]	Area [µV.Min]	Area [%]
1	UNKNOWN	0.00	0.02	0.12	0.00	0.04	1.1	0.1	0.039
2	UNKNOWN	3.93	4.21	4.48	0.00	1.55	19.3	3.1	1.552
3	UNKNOWN	4.55	4.71	4.89	0.00	6.13	90.0	12.3	6.134
4	UNKNOWN	4.89	5.08	5.39	0.00	91.81	1210.3	183.9	91.807
5	UNKNOWN	5.86	6.13	6.47	0.00	0.47	5.5	0.9	0.468
Total					100.00	1326.1	200.4	100.000	

SFC chromatogram of (*rac*)-**3a** (AD-H 5% methanol 2.0 mL/min 40°C):

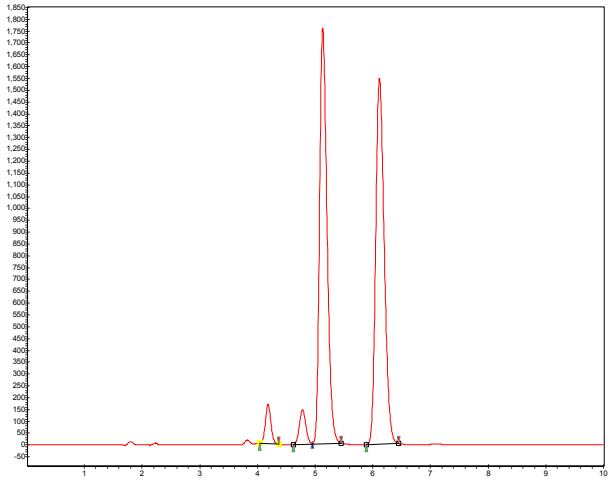

#	Name	Start [Min]	Time [Min]	End [Min]	RT Offset [Min]	Quantity [% Area]	Height [µV]	Area [µV.Min]	Area [%]
1	UNKNOWN	4.04	4.18	4.37	0.00	3.32	167.0	18.8	3.324
2	UNKNOWN	4.62	4.78	4.95	0.00	3.35	145.8	18.9	3.347
3	UNKNOWN	4.95	5.13	5.45	0.00	46.46	1758.8	262.2	46.461
4	UNKNOWN	5.89	6.12	6.44	0.00	46.87	1546.0	264.5	46.868
Total					100.00	3617.5	564.4	100.000	

^{1}H NMR for **3b**:

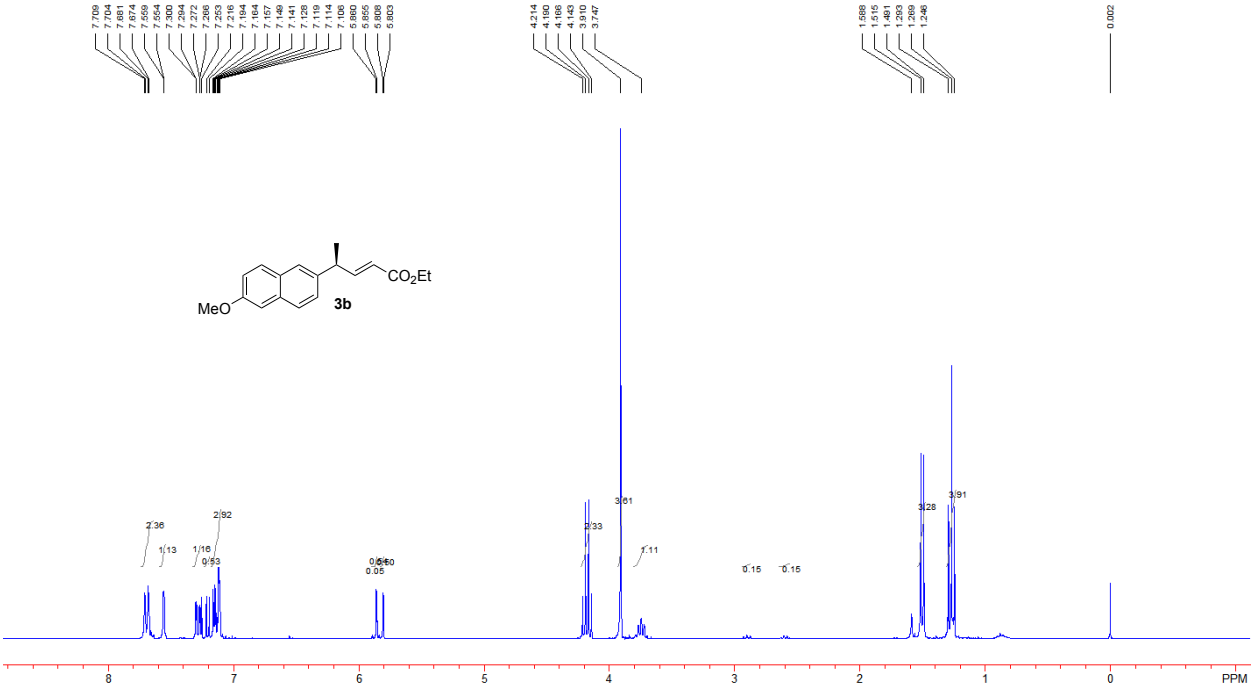

^{13}C NMR for **3b**:

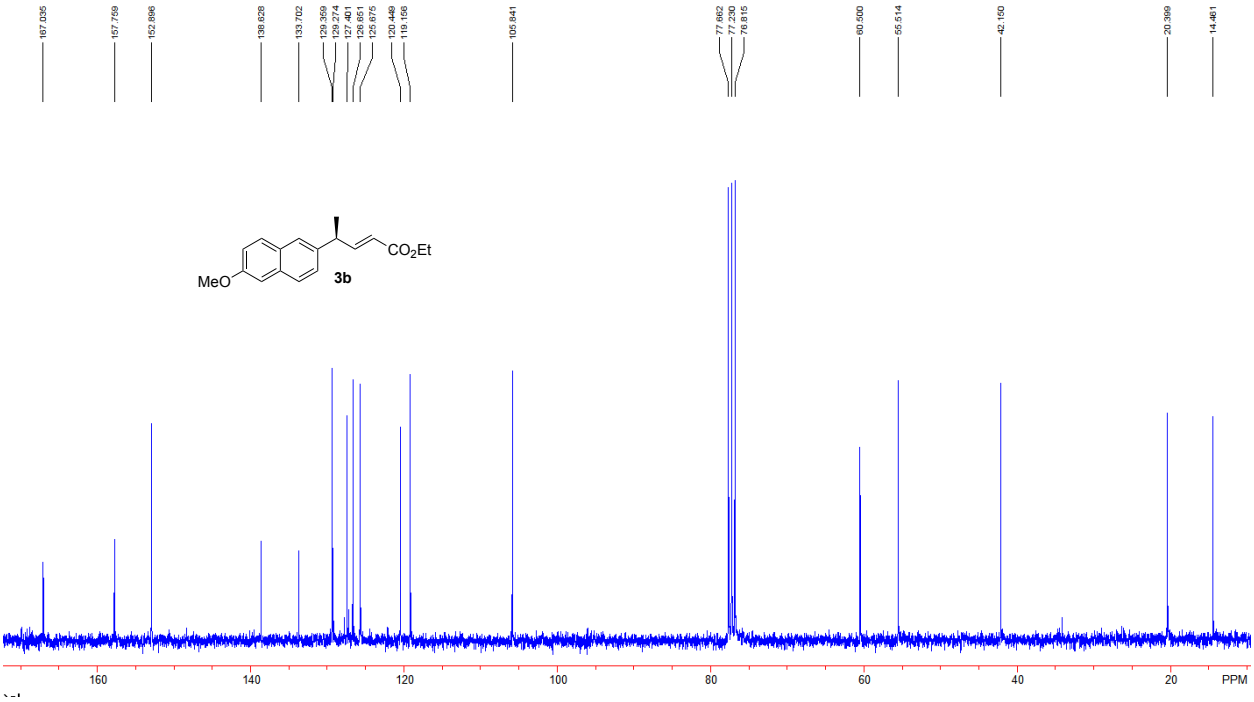

SFC chromatogram of enantioenriched **3b** (AD-H 4% MeOH 2mL/min 40°C 150 bar):

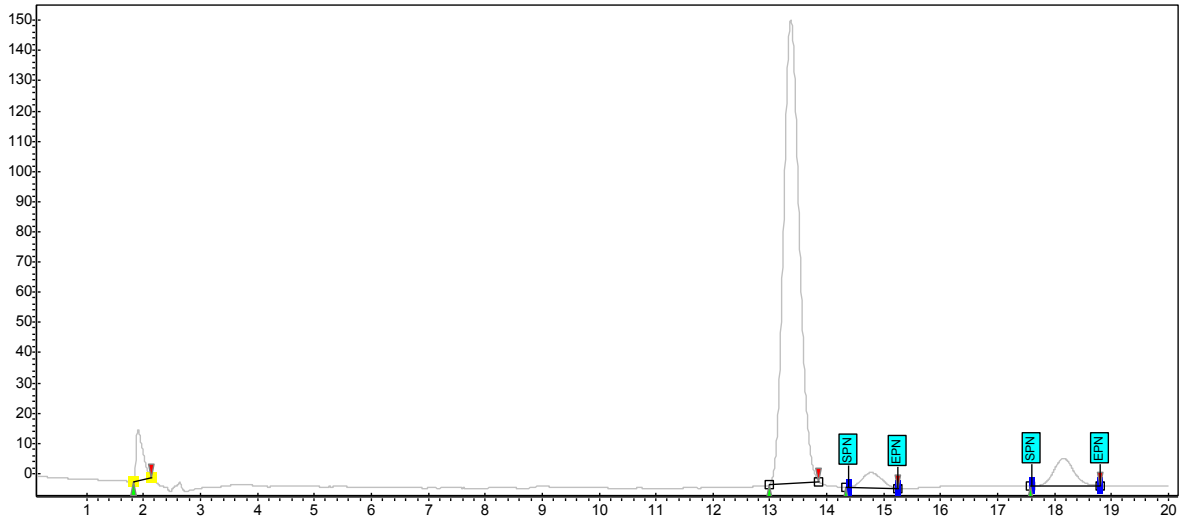

#	Name	Start [Min]	Time [Min]	End [Min]	RT Offset [Min]	Quantity [% Area]	Height [µV]	Area [µV.Min]	Area [%]
1	UNKNOWN	1.83	1.90	2.14	0.00	4.16	17.1	2.4	4.156
2	UNKNOWN	12.99	13.37	13.86	0.00	85.79	153.3	49.3	85.791
3	UNKNOWN	14.34	14.78	15.25	0.00	3.41	5.0	2.0	3.411
4	UNKNOWN	17.57	18.15	18.79	0.00	6.64	9.1	3.8	6.642
Total					100.00	184.5	57.5	100.000	

SFC chromatogram of (*rac*)-**3b** (AD-H 4% MeOH 2mL/min 40°C 150 bar):

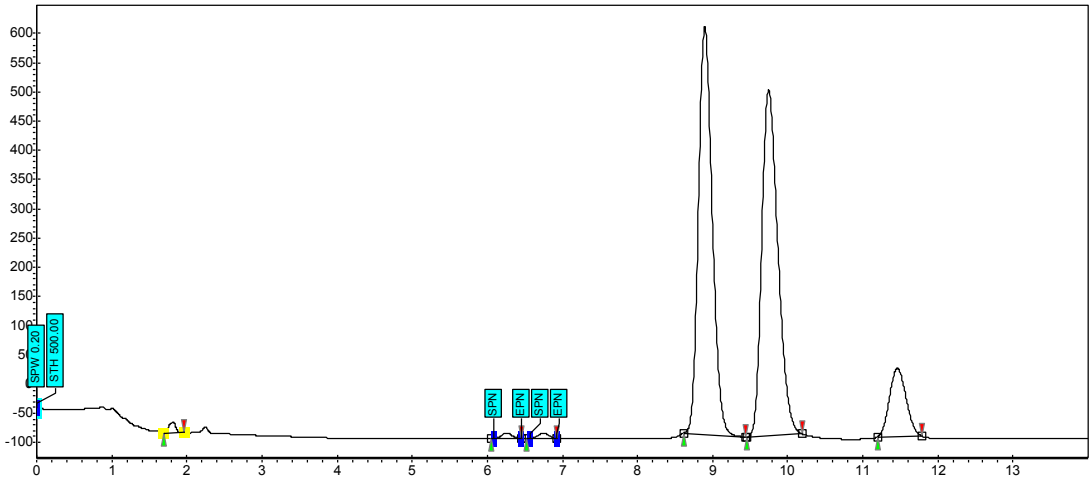

#	Name	Start [Min]	Time [Min]	End [Min]	RT Offset [Min]	Quantity [% Area]	Height [µV]	Area [µV.Min]	Area [%]
1	UNKNOWN	1.70	1.82	1.95	0.00	0.58	17.9	1.9	0.578
2	UNKNOWN	6.05	6.26	6.45	0.00	0.42	9.2	1.4	0.419
3	UNKNOWN	6.53	6.74	6.93	0.00	0.42	8.7	1.4	0.416
4	UNKNOWN	8.62	8.89	9.43	0.00	44.96	696.3	148.5	44.958
5	UNKNOWN	9.45	9.74	10.19	0.00	44.61	592.1	147.3	44.607
6	UNKNOWN	11.20	11.46	11.78	0.00	9.02	116.6	29.8	9.023
Total					100.00	1440.8	330.3	100.000	

^{1}H NMR for **3c**:

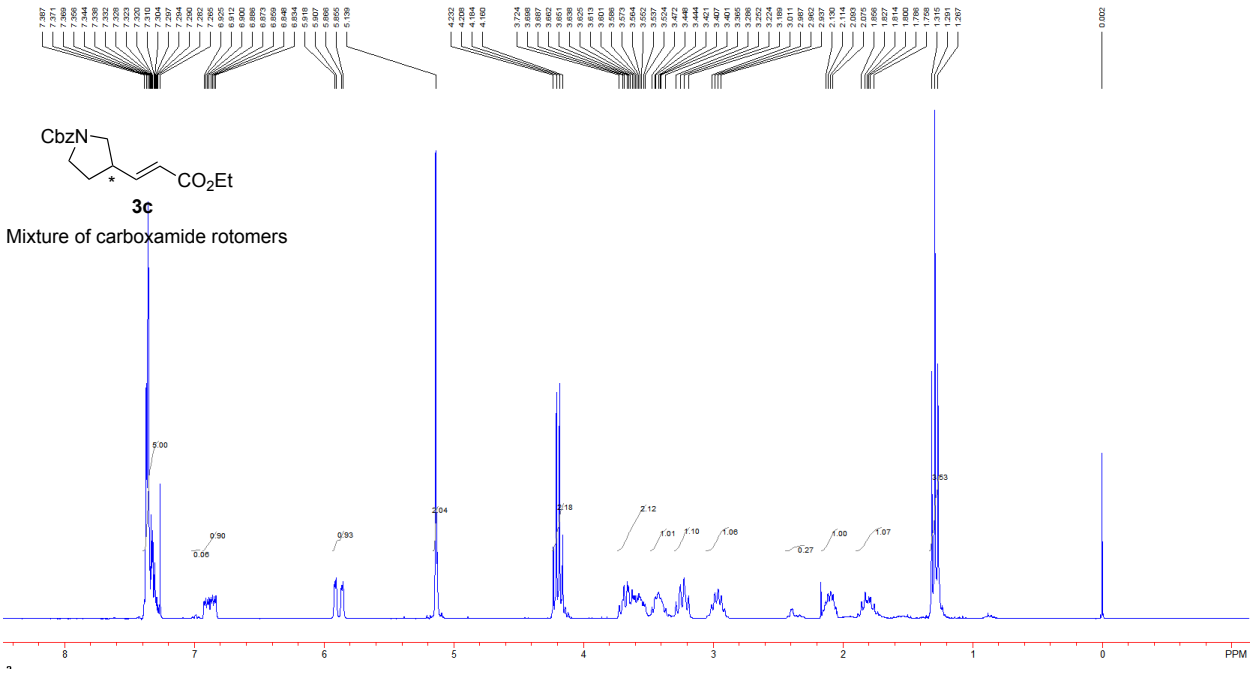

^{1}H NMR for **3c**:

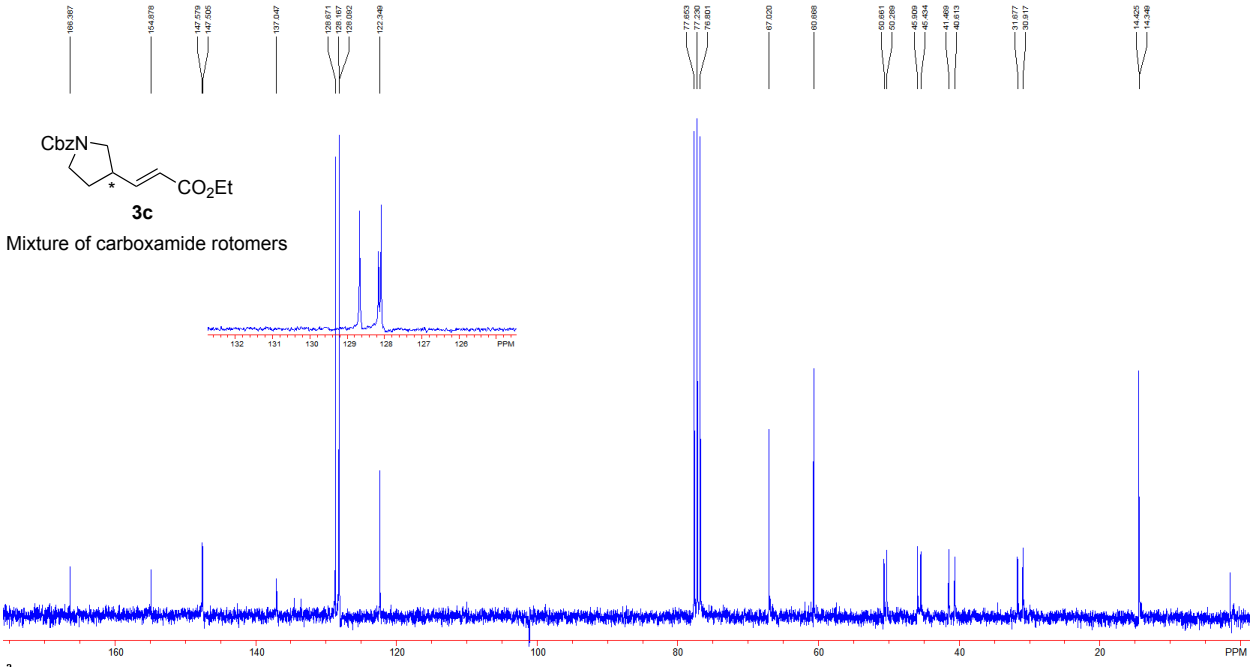

SFC chromatogram of enantioenriched **3c** (AD-H 10% methanol 1.5 mL/min flow 50°C):

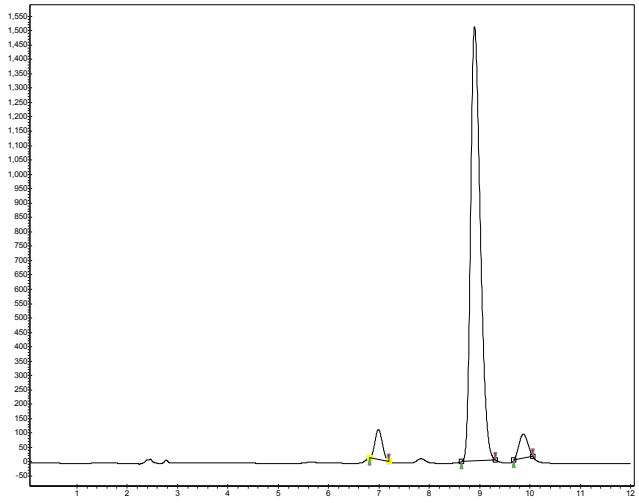

#	Name	Start [Min]	Time [Min]	End [Min]	RT Offset [Min]	Quantity [% Area]	Height [µV]	Area [µV.Min]	Area [%]
1	UNKNOWN	6.82	6.99	7.20	0.00	4.74	104.2	17.6	4.745
2	UNKNOWN	8.64	8.90	9.31	0.00	90.64	1511.5	336.7	90.645
3	UNKNOWN	9.68	9.86	10.06	0.00	4.61	84.9	17.1	4.610
Total					100.00	1700.6	371.5	100.000	

SFC chromatogram of (*rac*)-**3c** (AD-H 10% methanol 1.5 mL/min flow 50°C):

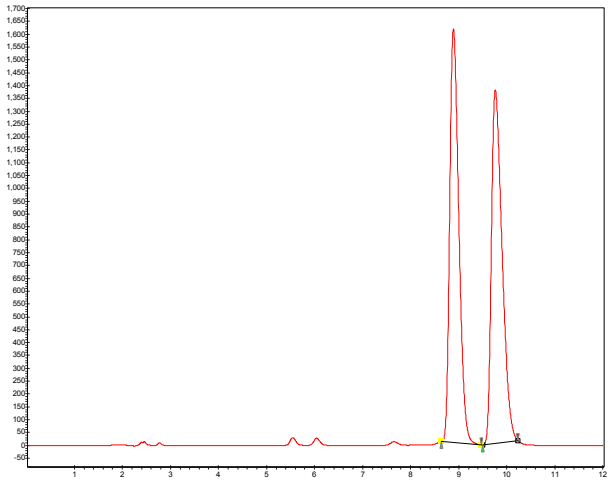

#	Name	Start [Min]	Time [Min]	End [Min]	RT Offset [Min]	Quantity [% Area]	Height [µV]	Area [µV.Min]	Area [%]
1	UNKNOWN	8.64	8.89	9.47	0.00	49.88	1611.0	353.1	49.882
2	UNKNOWN	9.50	9.76	10.23	0.00	50.12	1375.6	354.8	50.118
Total					100.00	2986.6	707.9	100.000	

^{1}H NMR for **3d**:

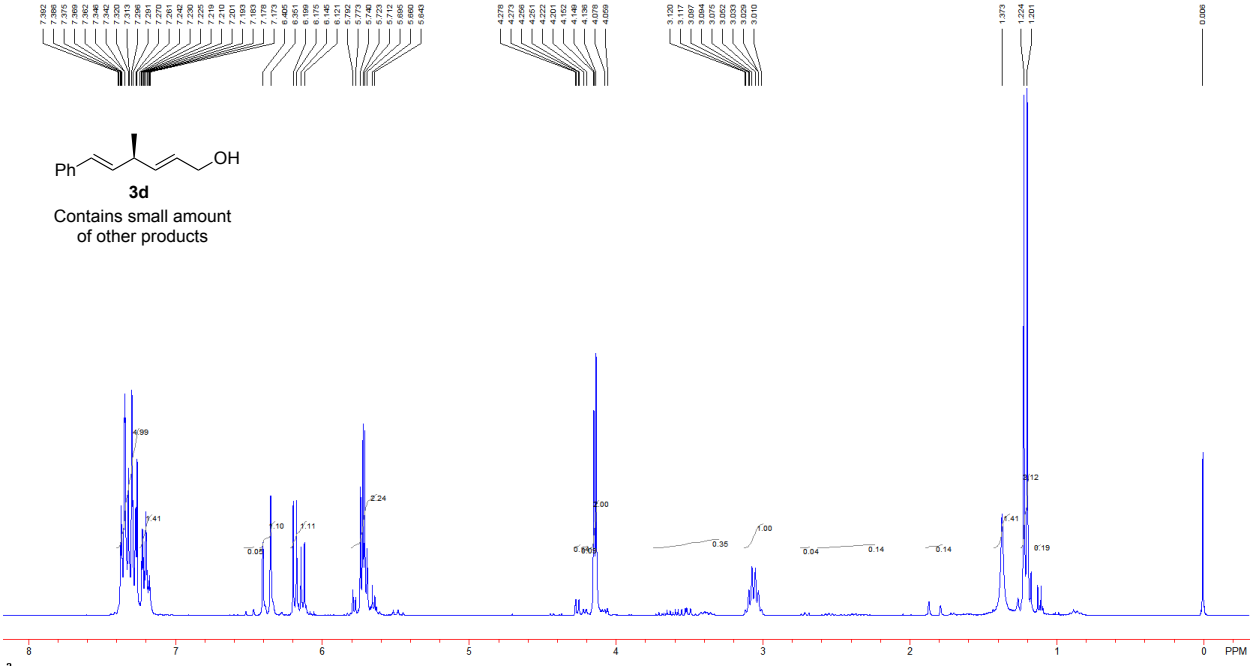

^{1}H NMR for **3d**:

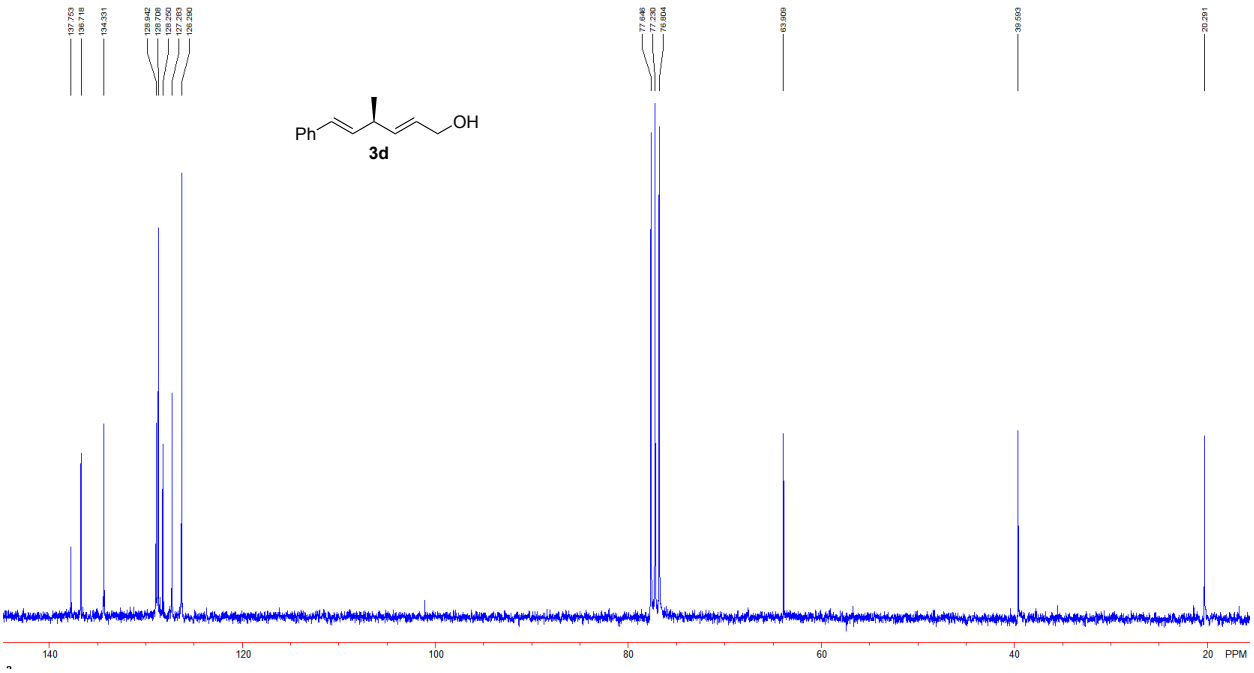

SFC chromatogram of enantioenriched **3d** (5% MeOH AD-H 40C flow rate 2 ml/min):

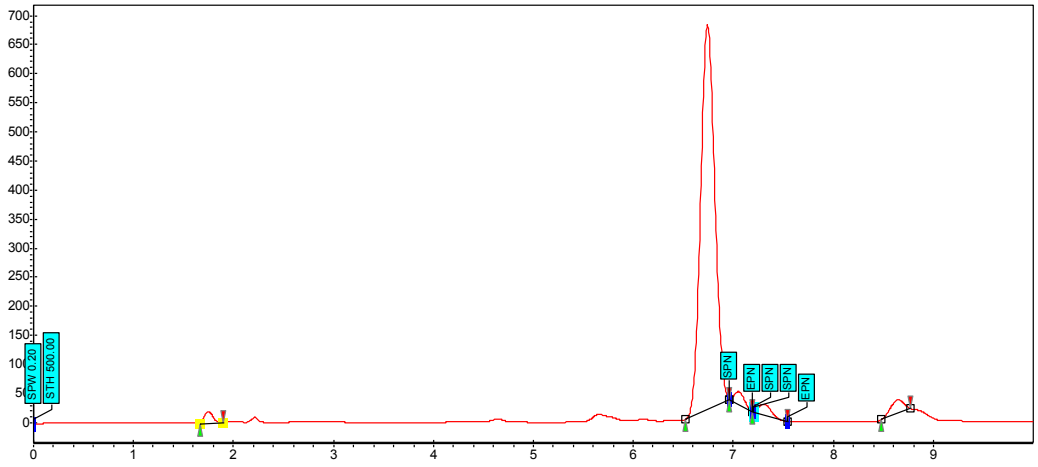

#Name	Start [Min]	Time [Min]	End [Min]	RT Offset [Min]	Quantity [% Area]	Height [µV]	Area [µV.Min]	Area [%]
1	UNKNOWN	1.66	1.74	1.90	0.00	1.60	19.4	1.9	1.596
2	UNKNOWN	6.52	6.74	6.96	0.00	91.19	661.0	108.2	91.192
3	UNKNOWN	6.96	7.06	7.19	0.00	2.04	21.9	2.4	2.042
4	UNKNOWN	7.19	7.31	7.55	0.00	2.10	18.9	2.5	2.096
5	UNKNOWN	8.48	8.63	8.78	0.00	3.07	23.6	3.6	3.074
Total					100.00	744.8	118.7	100.000	

SFC chromatogram of (*rac*)-**3d** (5% MeOH AD-H 40C flow rate 2 ml/min):

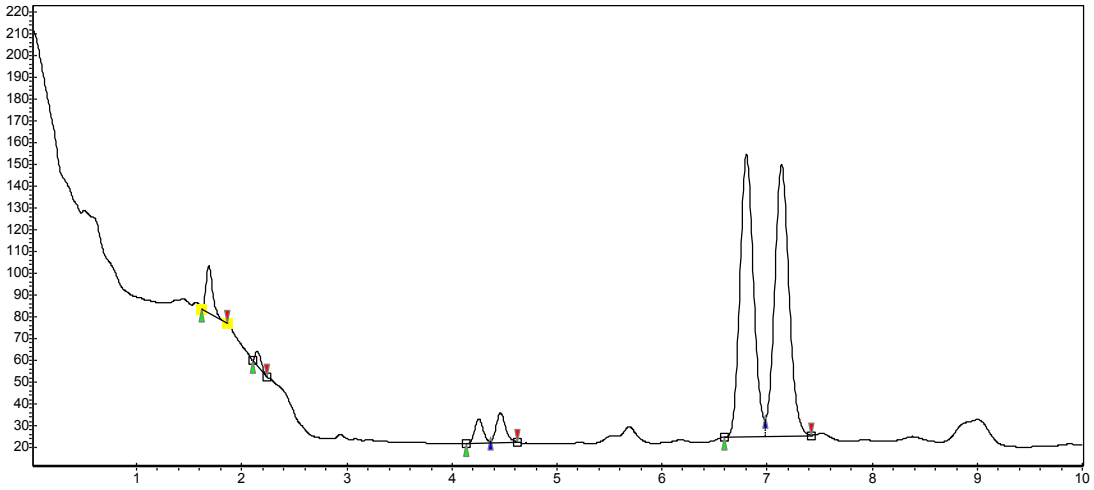

#Name	Start [Min]	Time [Min]	End [Min]	RT Offset [Min]	Quantity [% Area]	Height [µV]	Area [µV.Min]	Area [%]
1	UNKNOWN	1.62	1.69	1.87	0.00	3.67	21.9	1.6	3.666
2	UNKNOWN	2.10	2.15	2.24	0.00	1.08	7.1	0.5	1.082
3	UNKNOWN	4.14	4.26	4.36	0.00	2.42	11.2	1.0	2.415
4	UNKNOWN	4.36	4.46	4.62	0.00	3.25	13.6	1.4	3.253
5	UNKNOWN	6.59	6.80	6.98	0.00	44.29	129.3	19.2	44.292
6	UNKNOWN	6.98	7.14	7.42	0.00	45.29	124.3	19.7	45.291
Total					100.00	307.4	43.4	100.000	

^{1}H NMR for **4**:

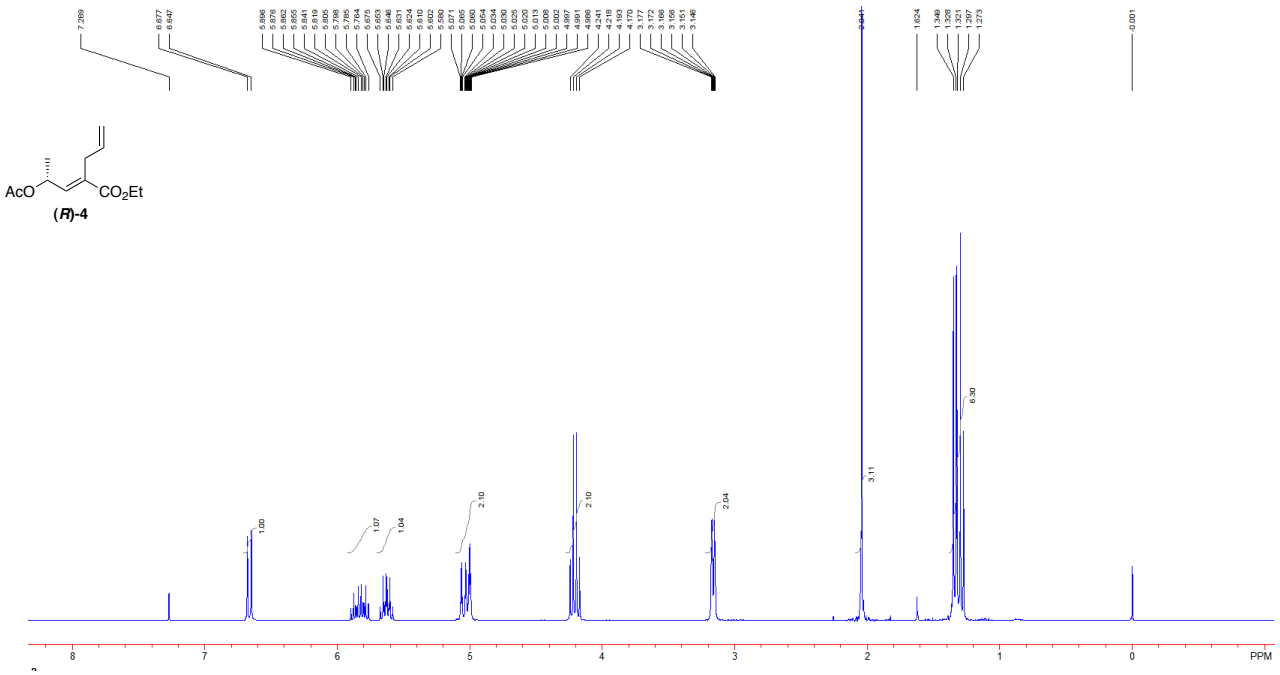

^{13}C NMR for **4**:

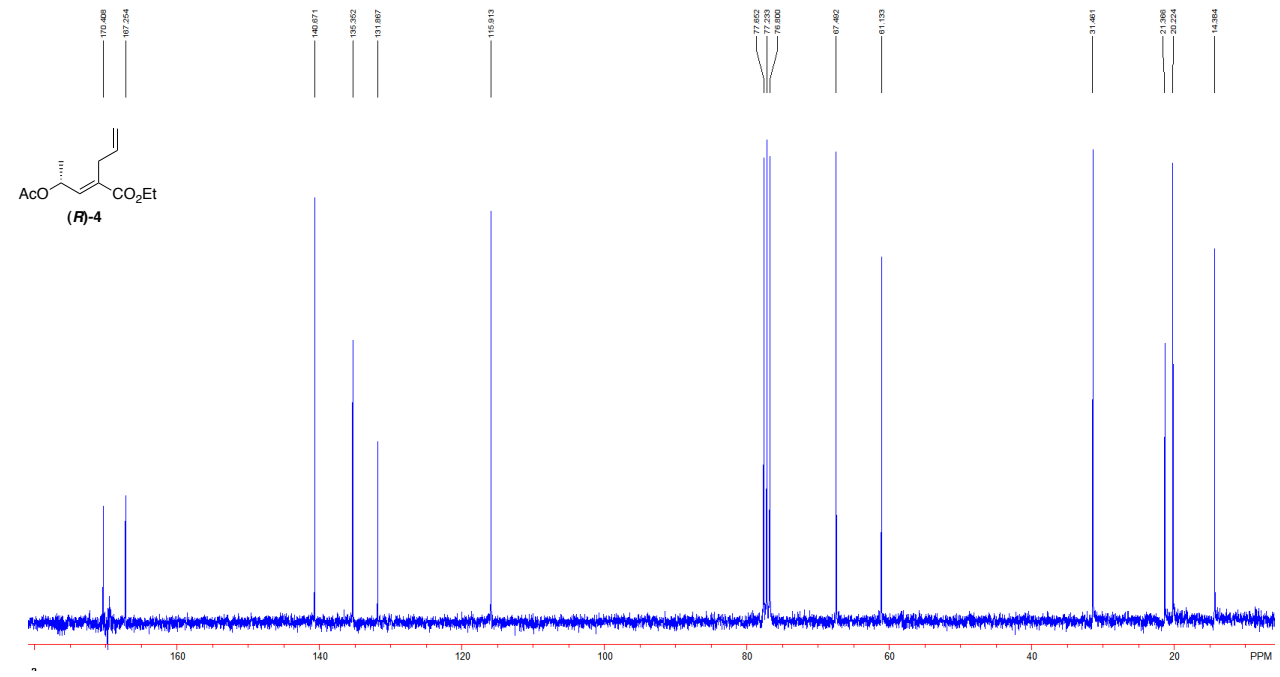

^{1}H NMR for **b-(*S*)-5**:

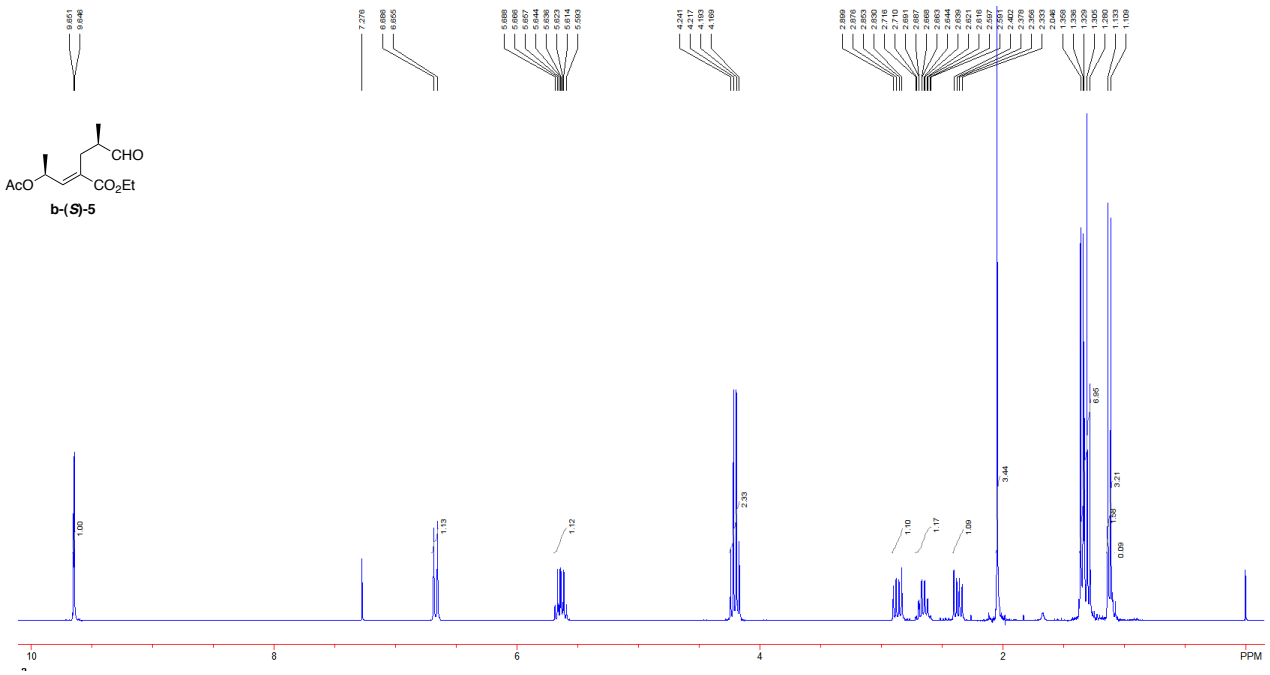

^{13}C NMR for **b-(*S*)-5**:

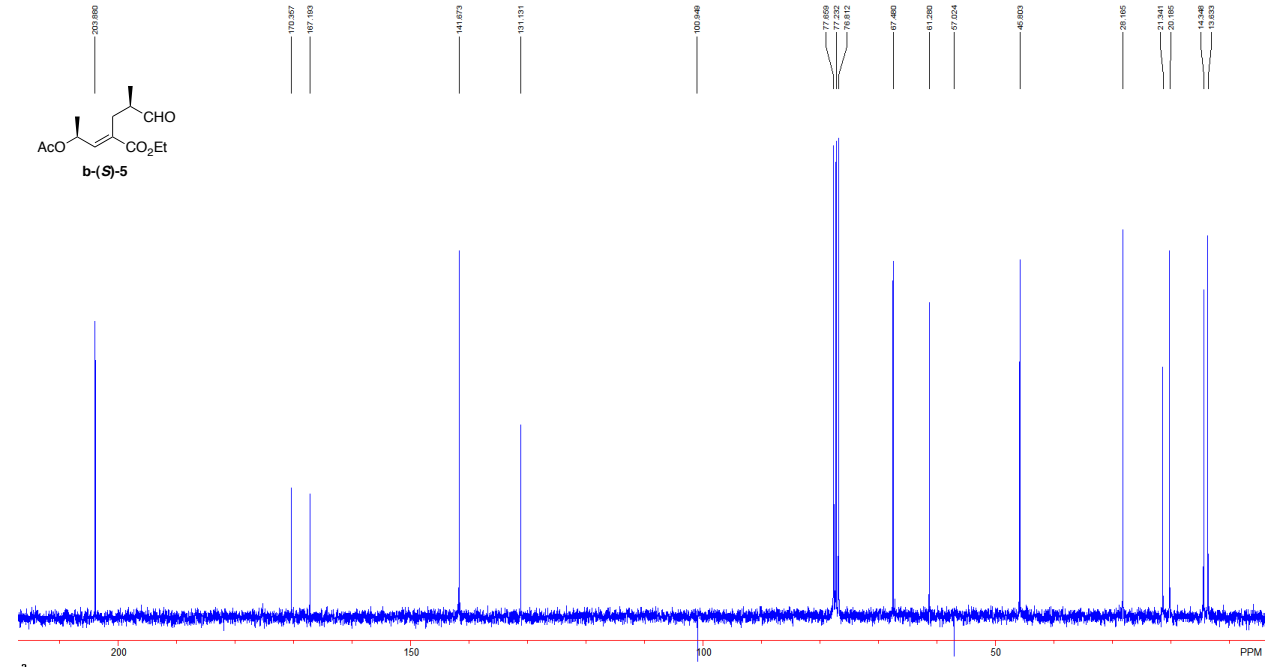

^{1}H NMR for **I-5**:

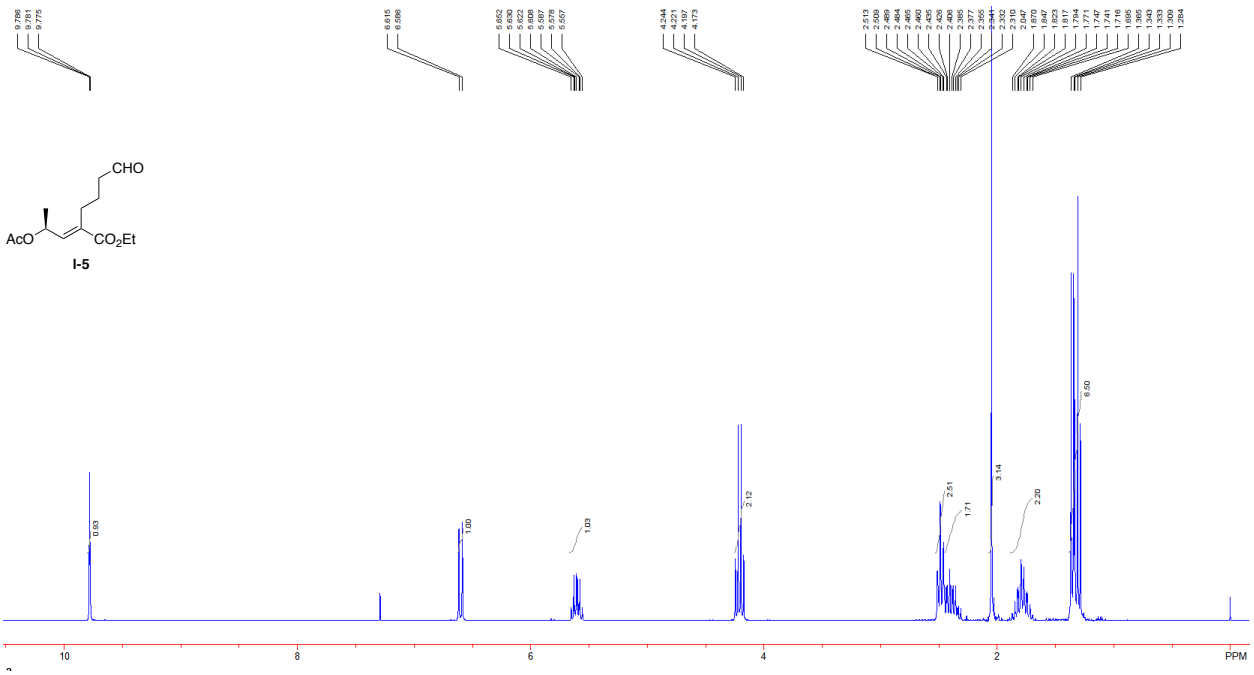

^{13}C NMR for **I-5**:

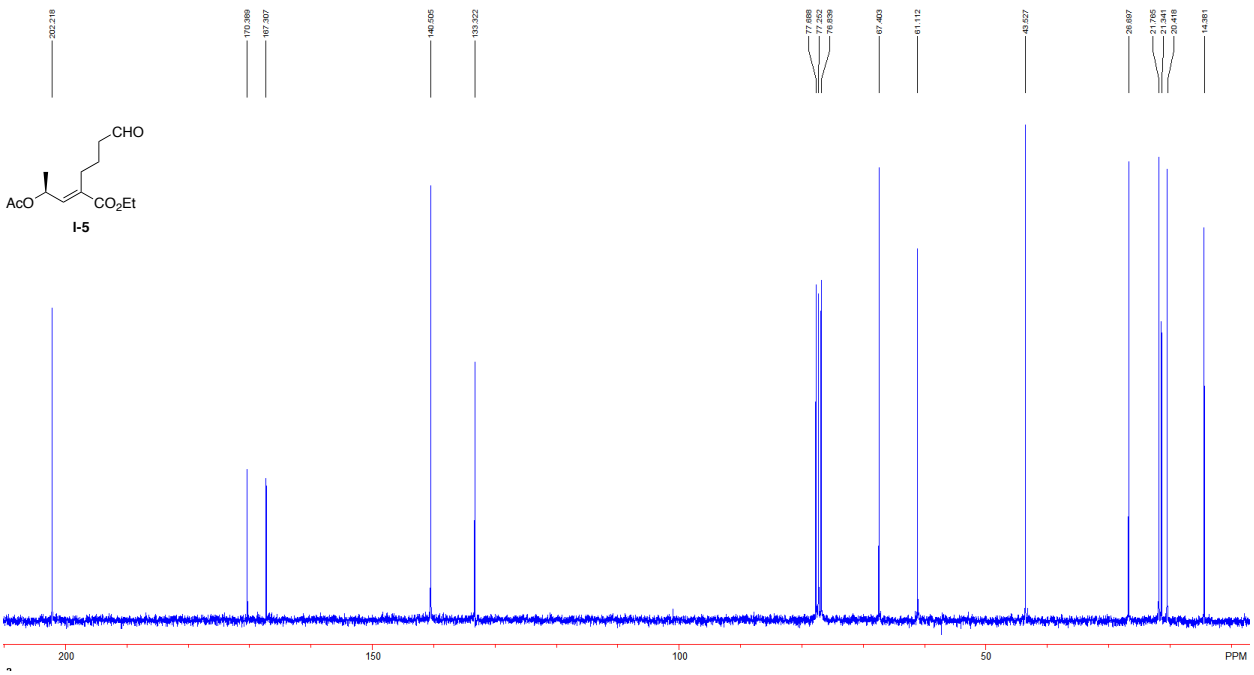

^{1}H NMR for **b-(*R*)-5**:

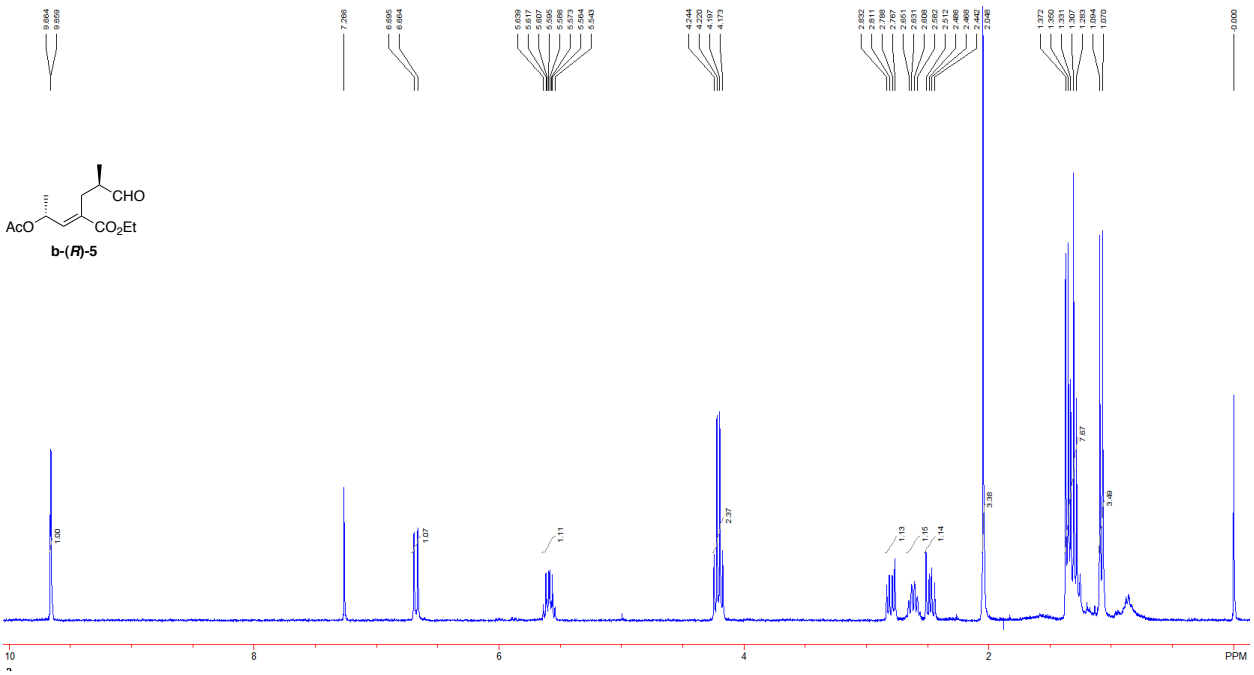

^{1}H NMR for **6**:

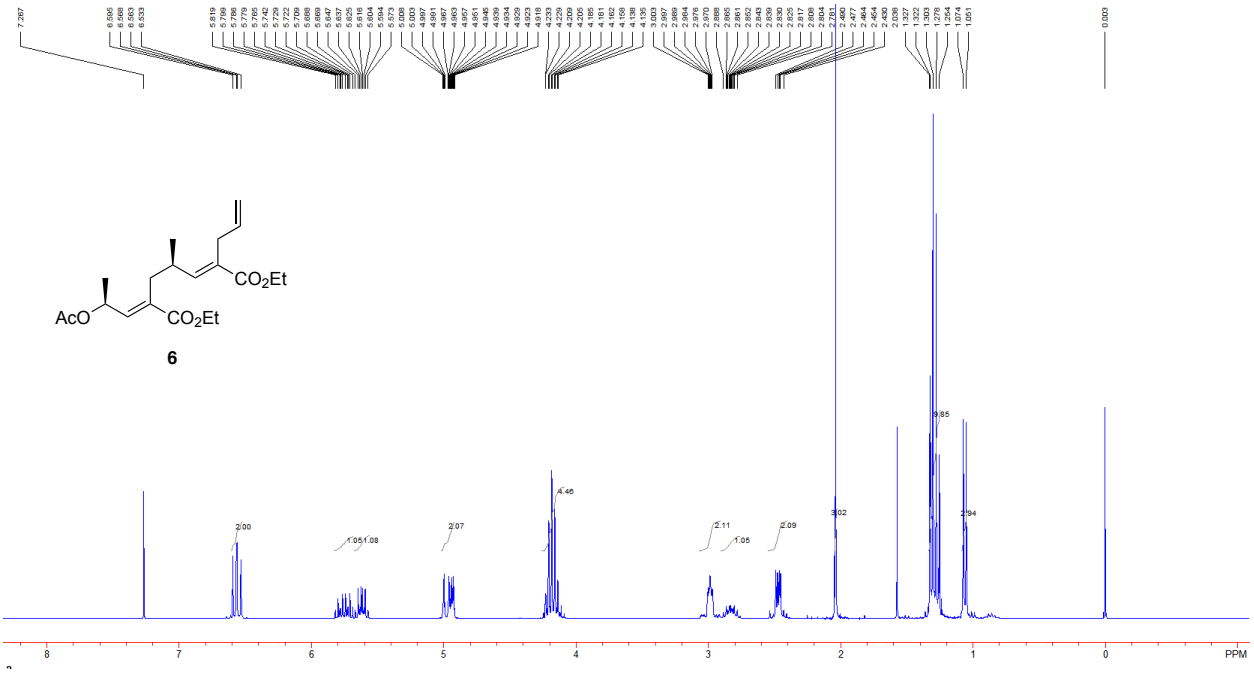

^{1}H NMR for **I-7**:

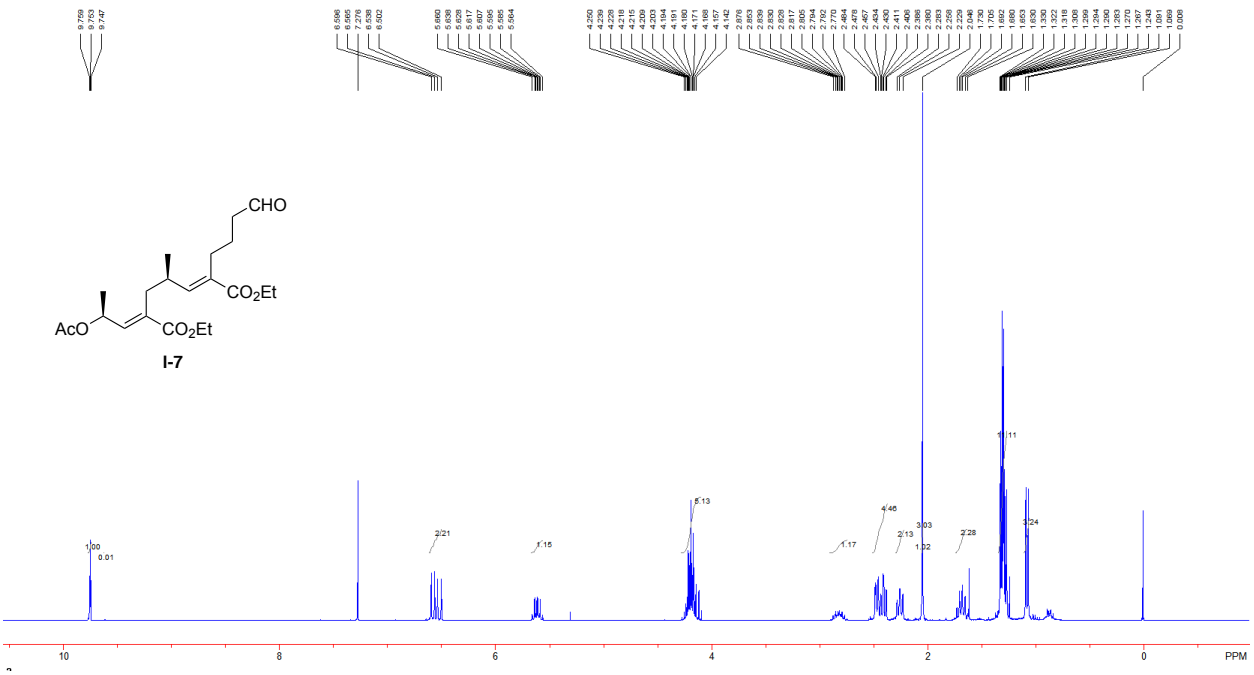

^{13}C NMR for **I-7**:

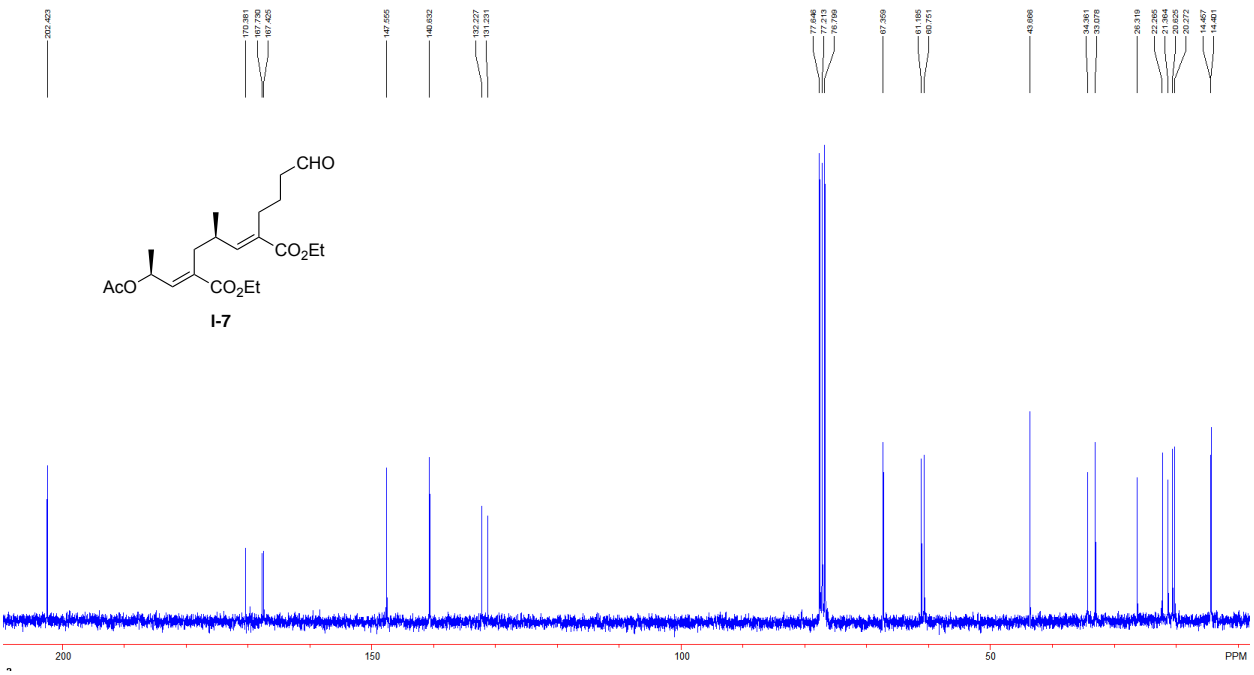

^{1}H NMR for **b-7**:

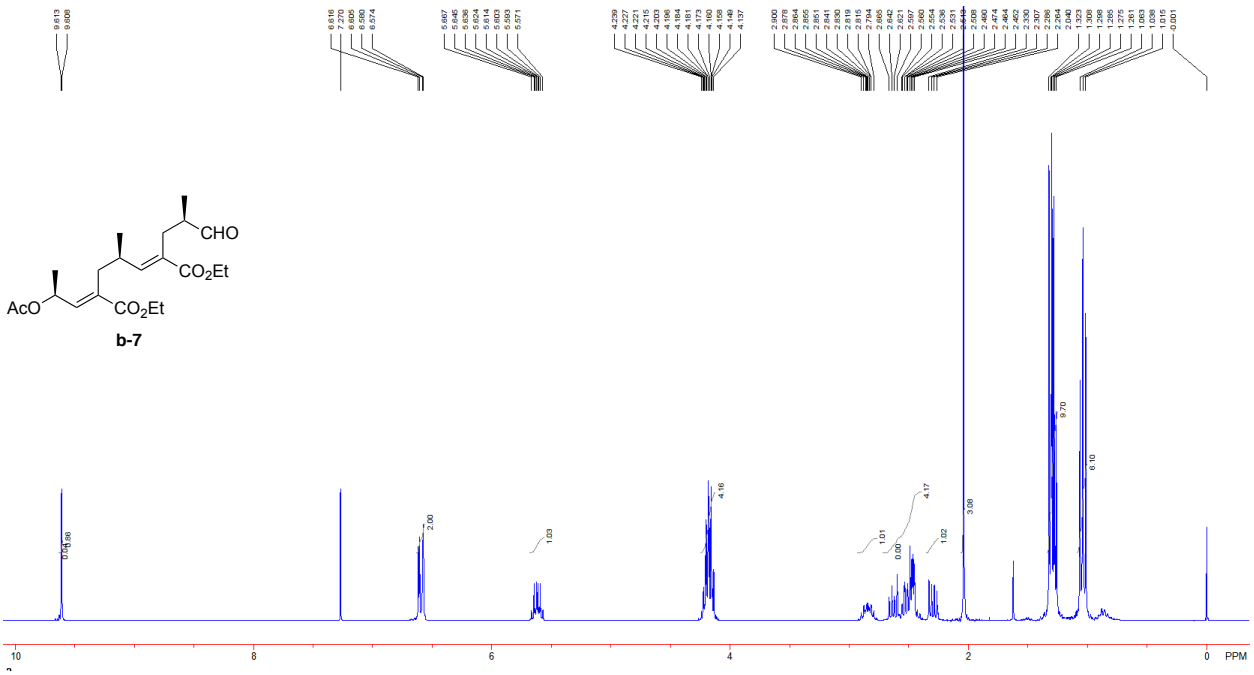

^{13}C NMR for **b-7**:

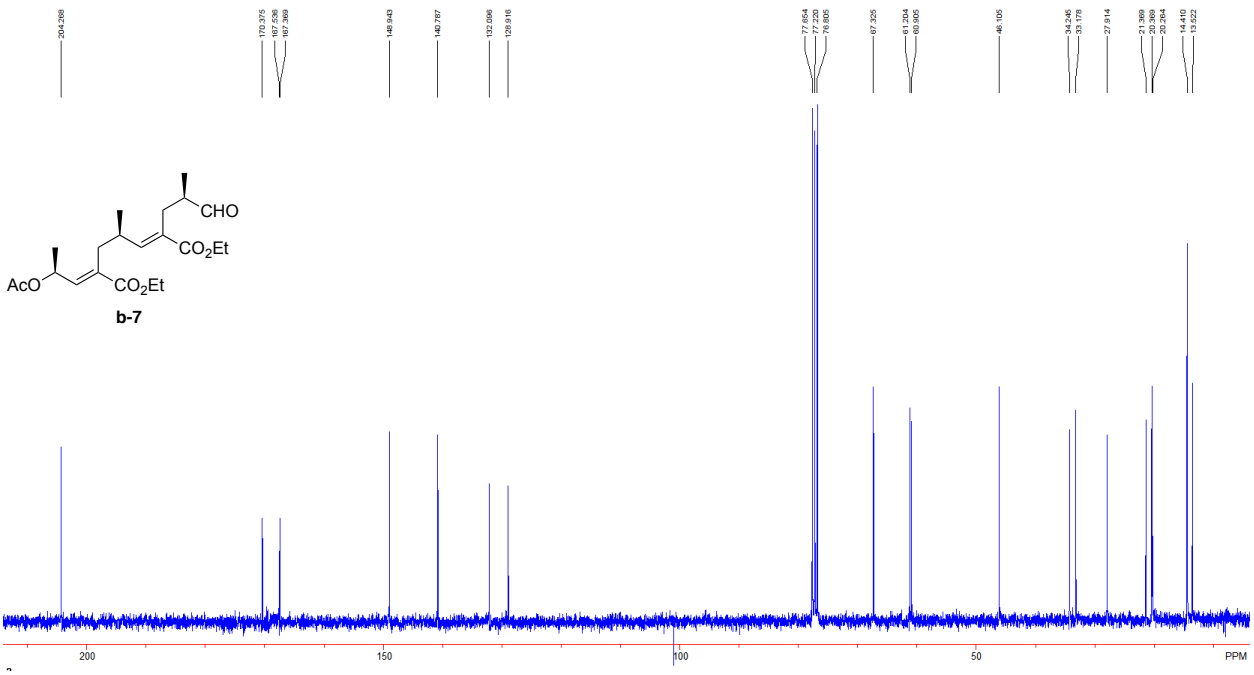

$^{31}P\{^{1}H\}$ NMR:

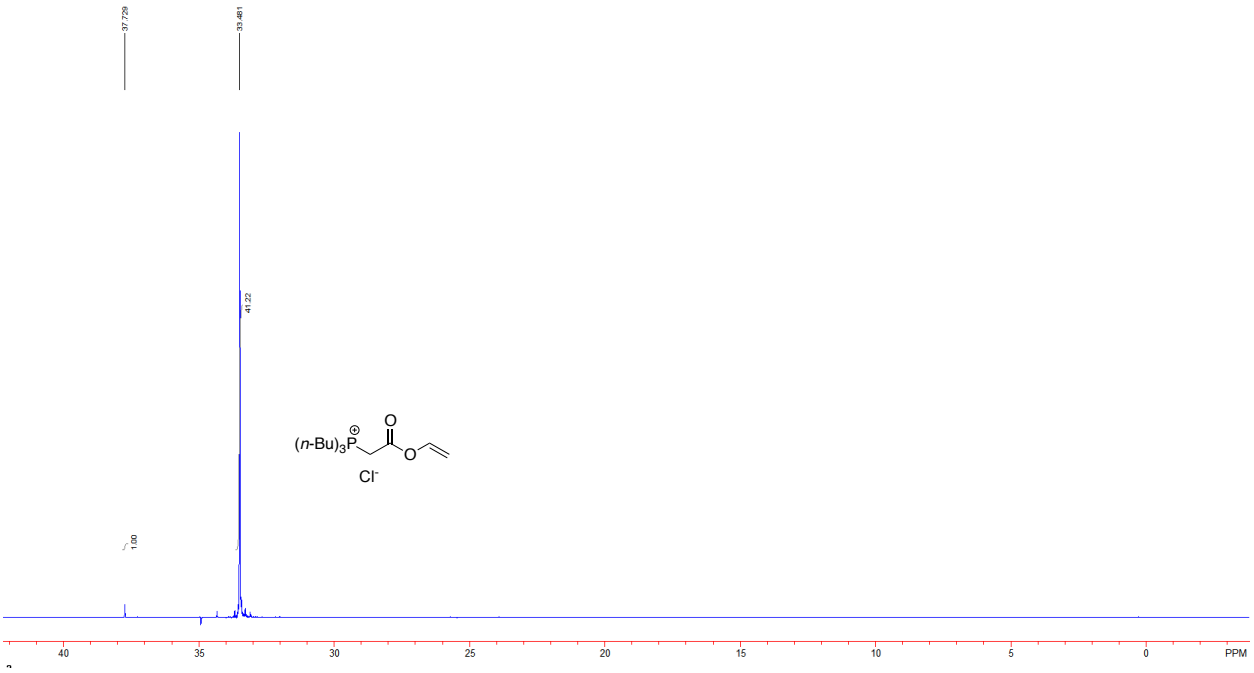

^{1}H NMR:

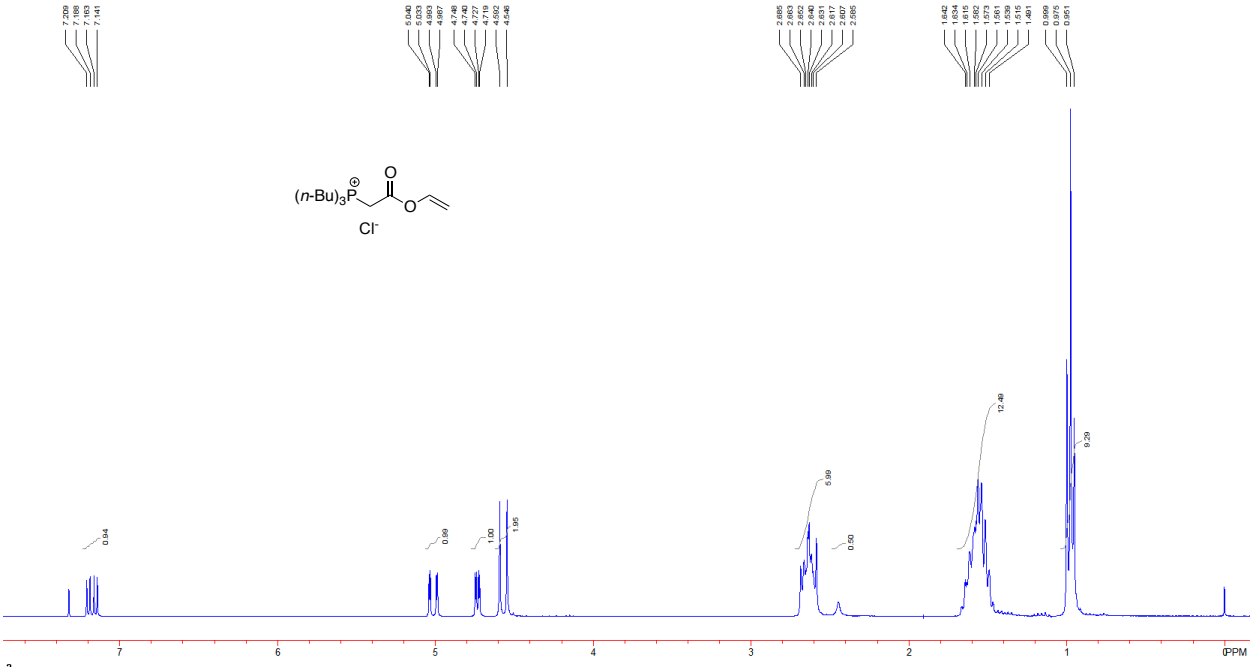

$^{31}P\{^{1}H\}$ NMR:

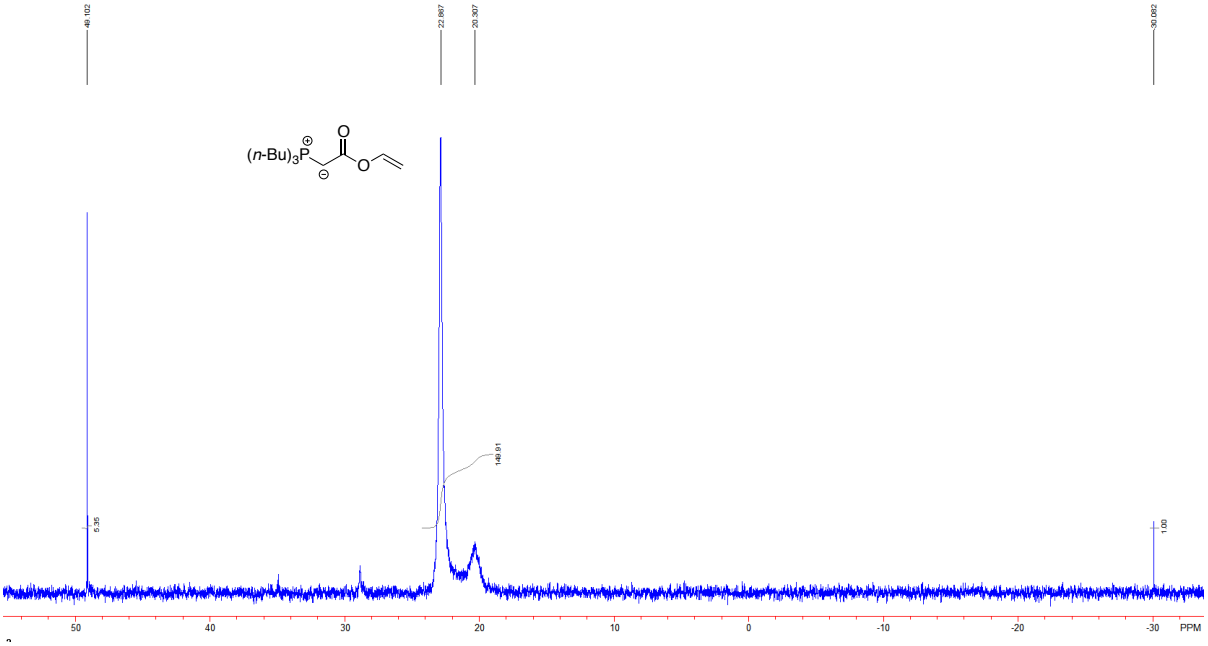

^{1}H NMR:

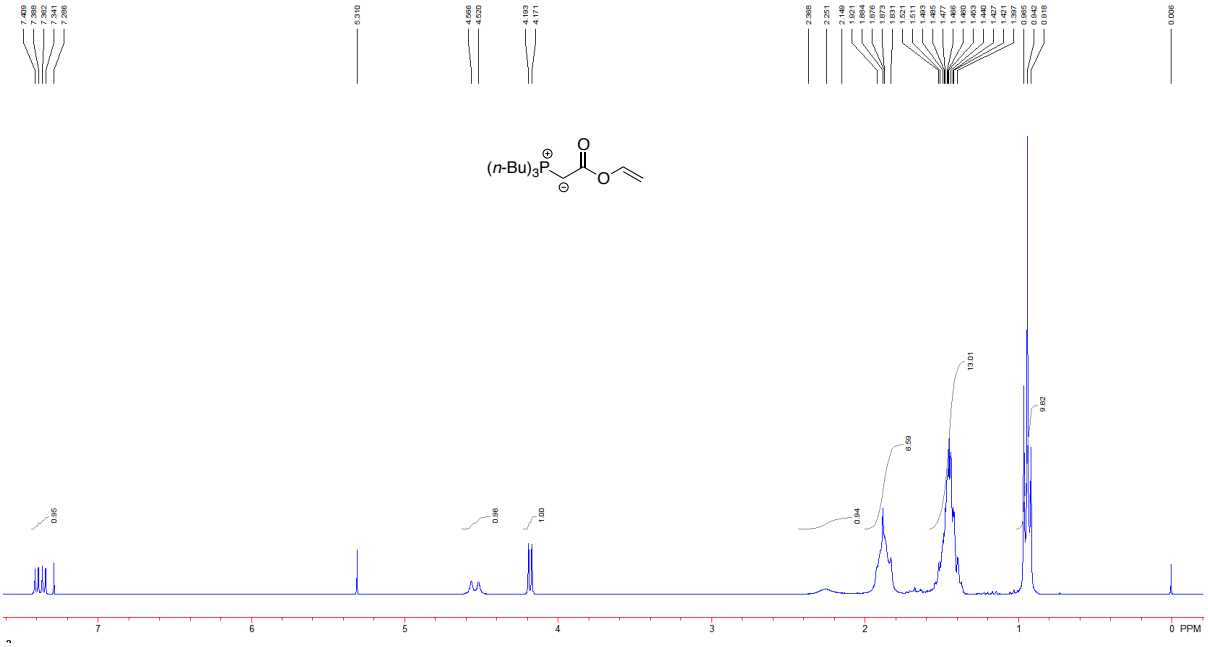

^{13}C NMR:

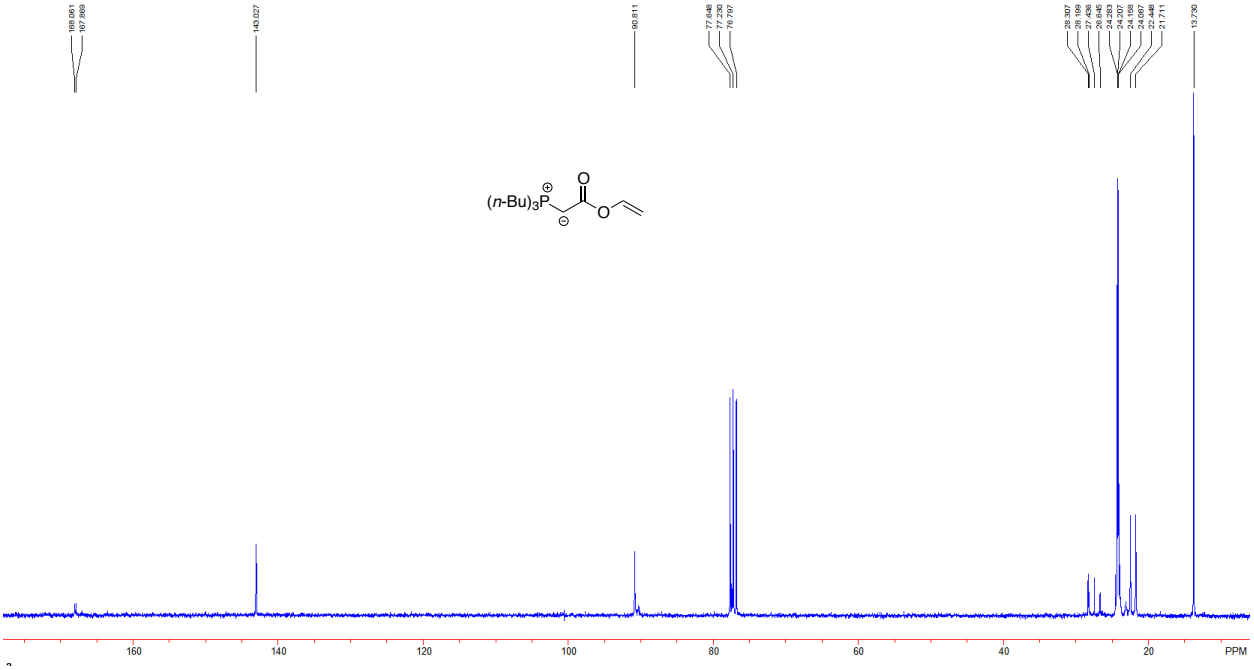

^{1}H NMR:

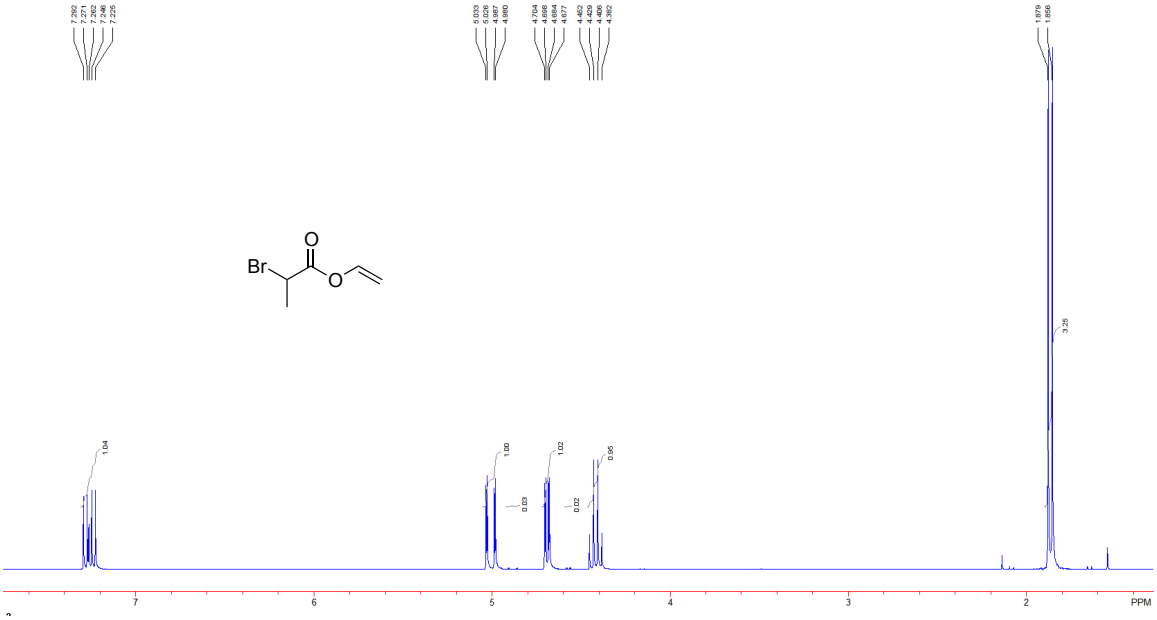

^{13}C NMR:

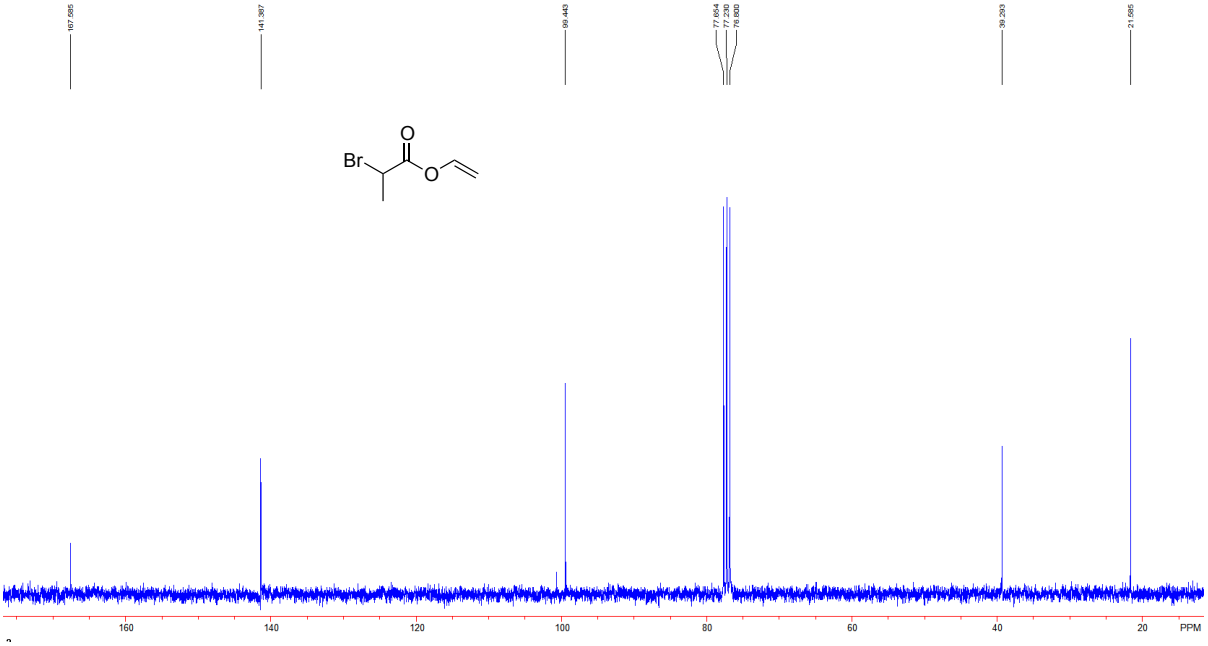

^{1}H NMR:

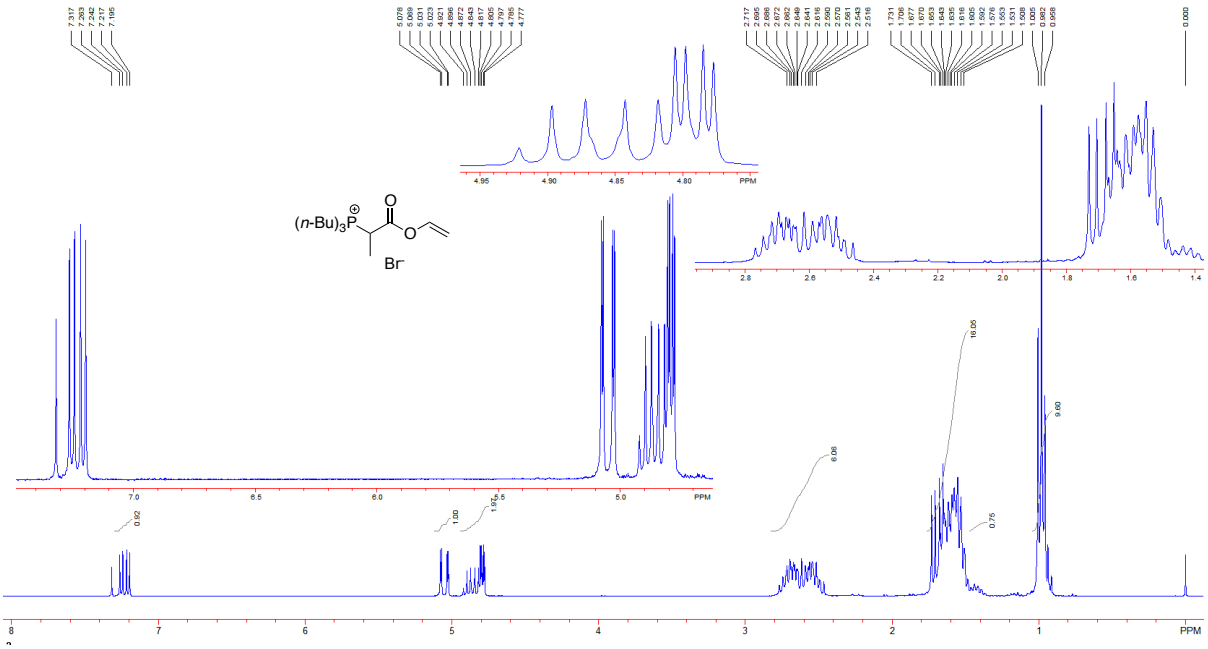

$^{31}P\{^{1}H\}$ NMR

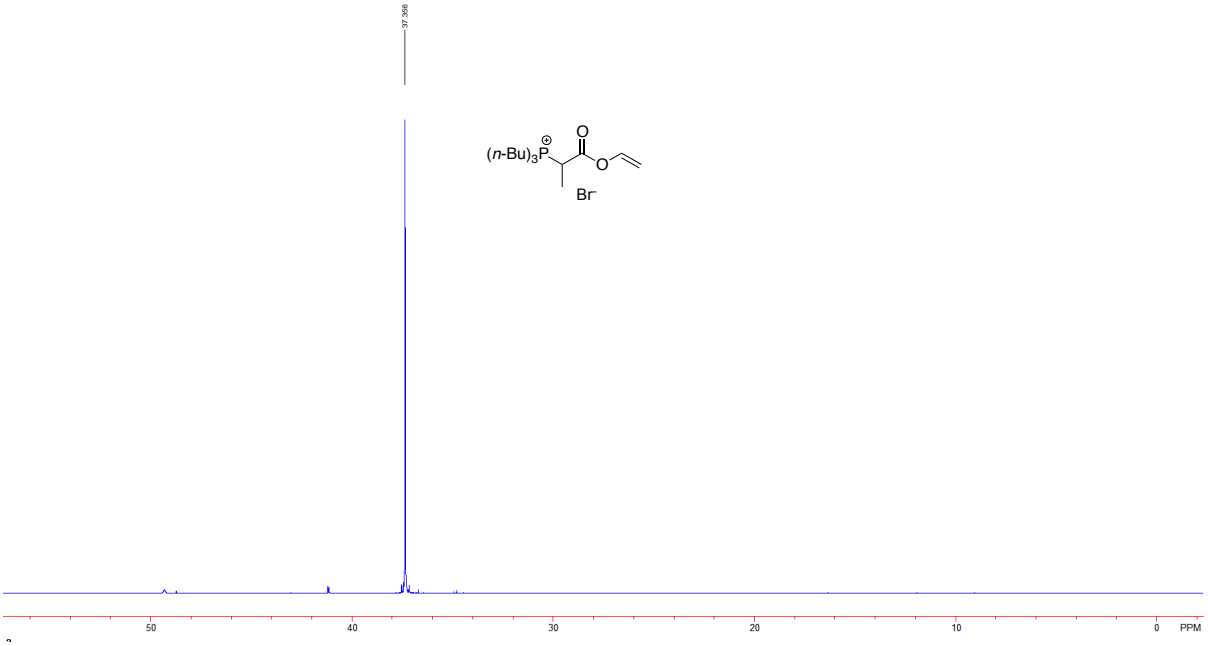

^{13}C NMR:

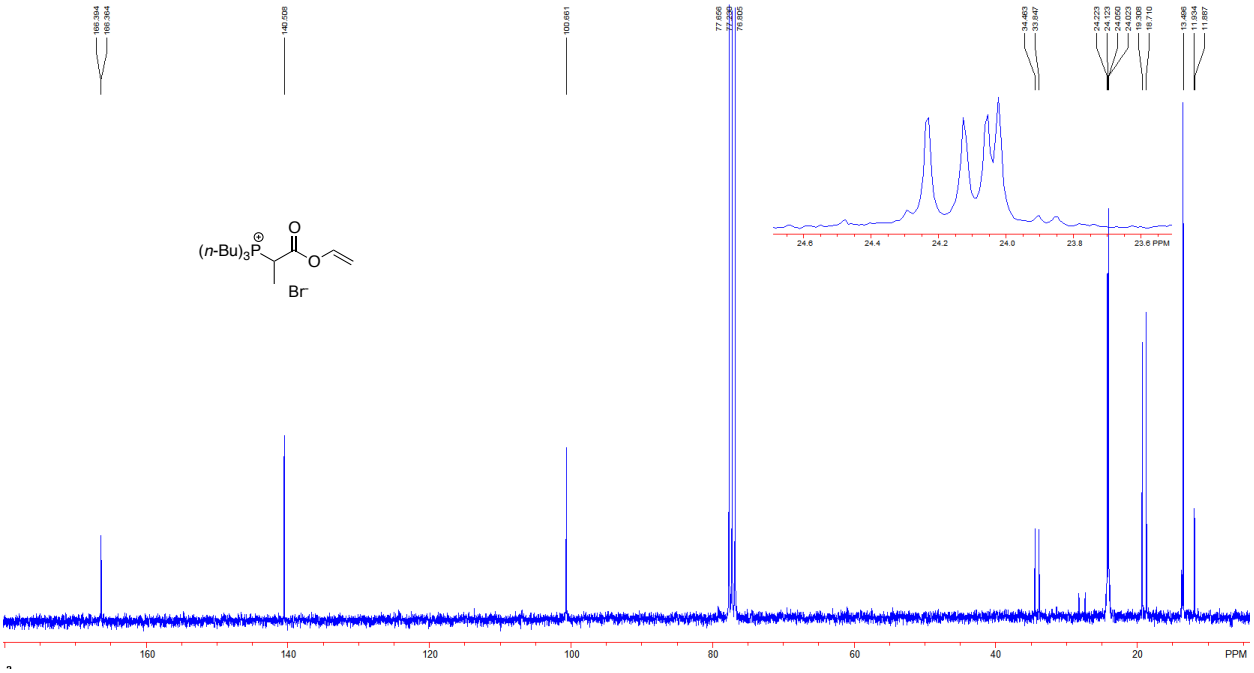

$^{31}P\{^{1}H\}$ NMR:

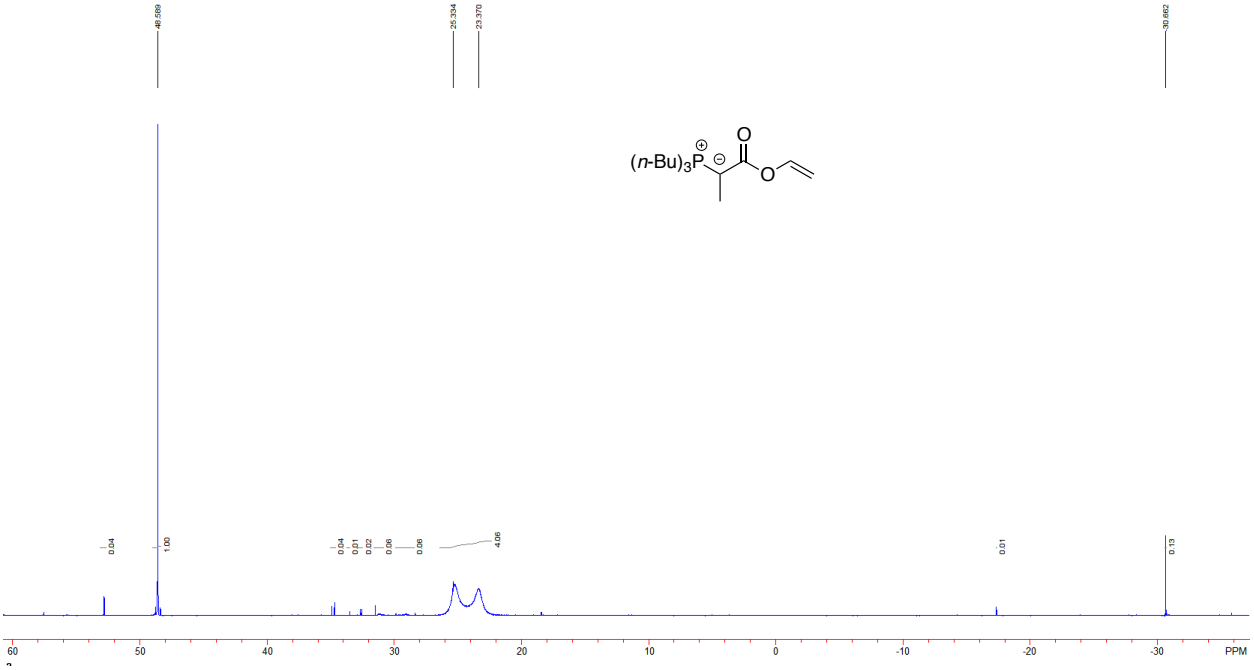

^{1}H NMR of **8**:

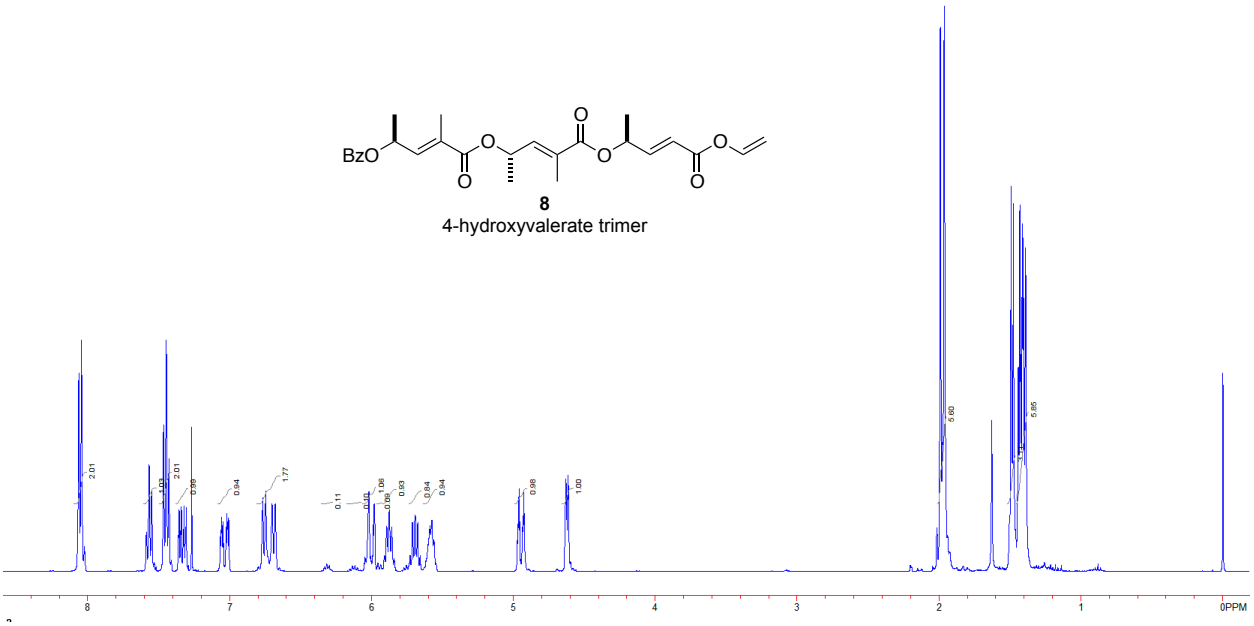

^{1}H NMR of **8**:

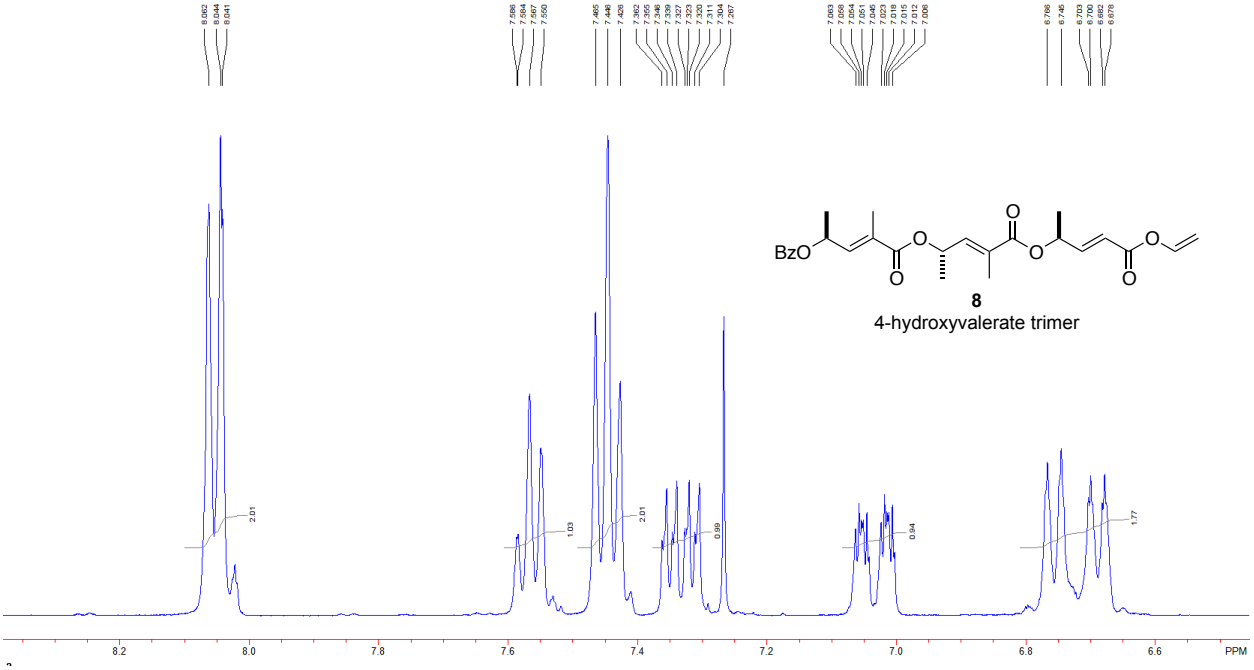

^{1}H NMR of **8**:

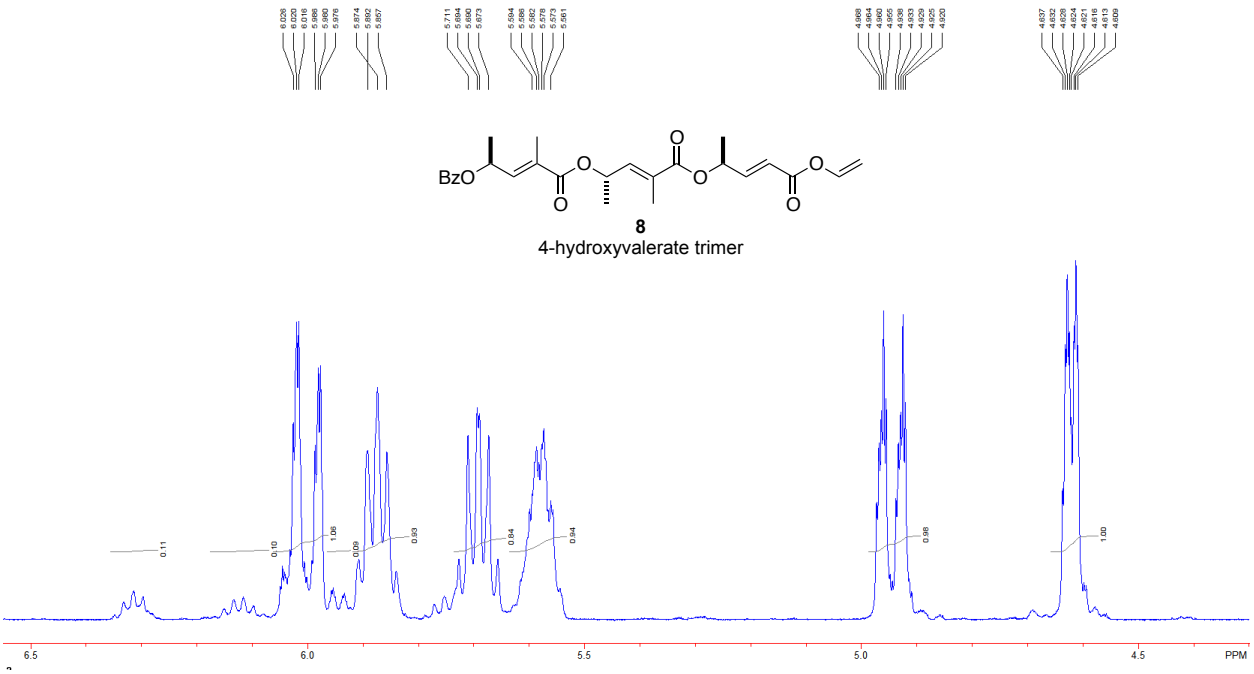

^{1}H NMR of **8**:

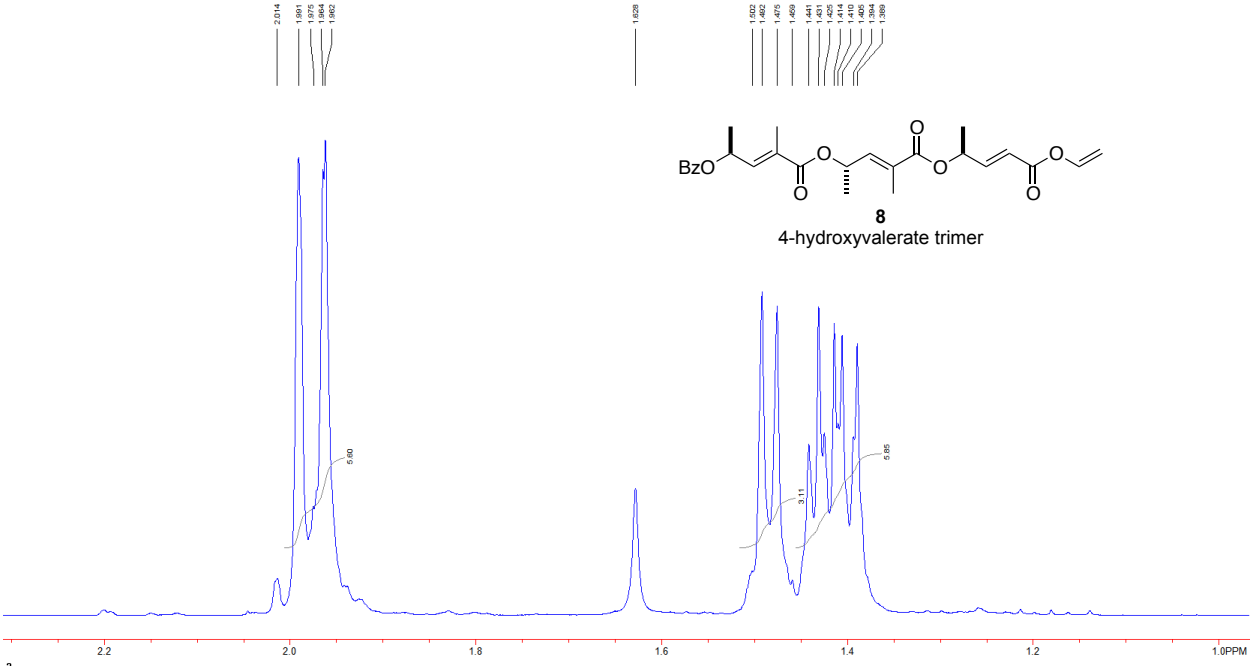

^{13}C NMR of **8**:

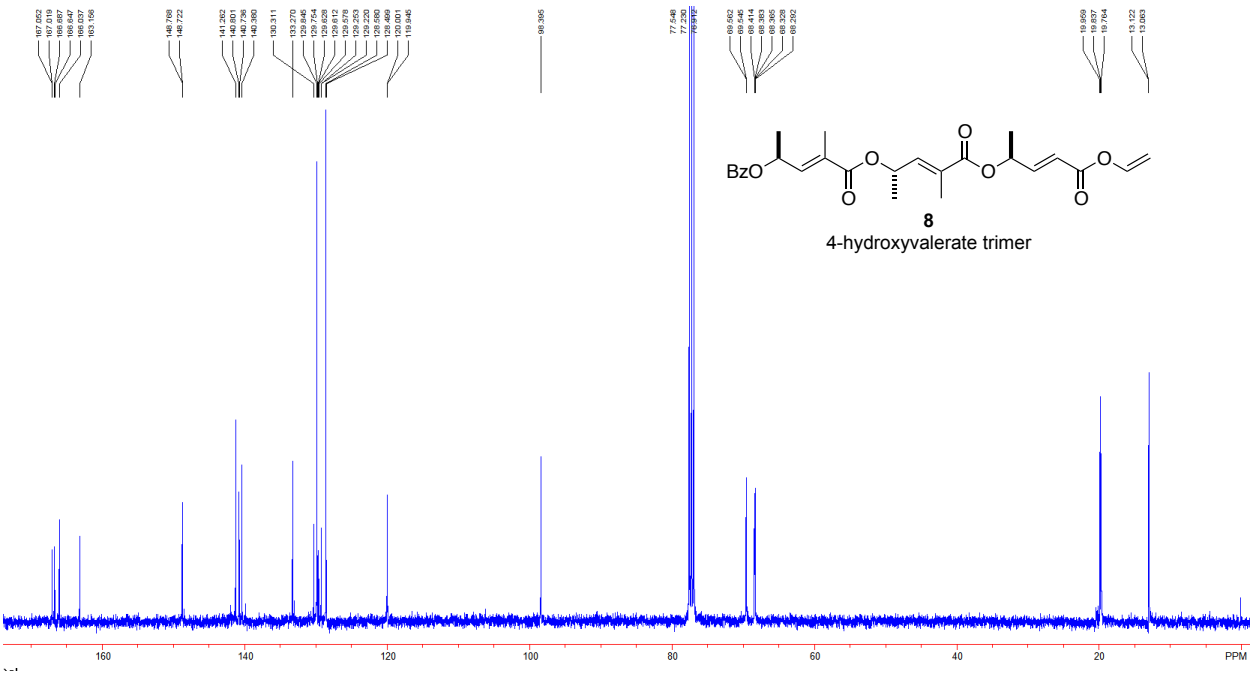

^{13}C NMR of **8**:

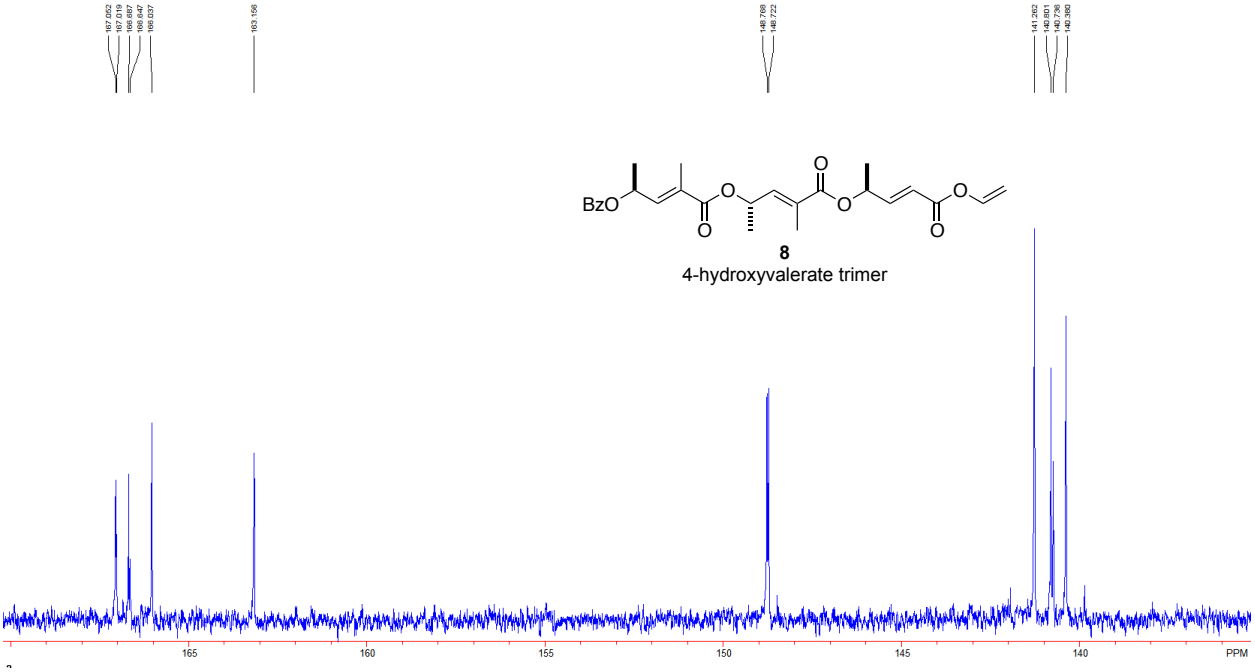

8
4-hydroxyvalerate trimer

^{13}C NMR of **8**:

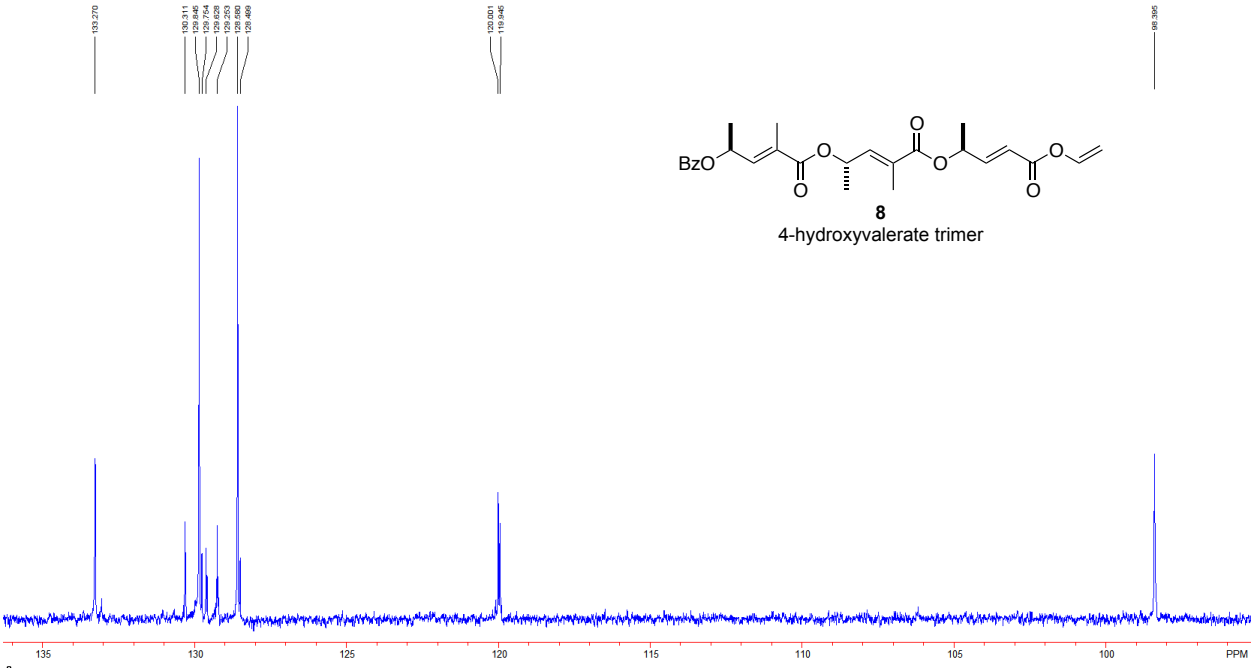

8
4-hydroxyvalerate trimer

^{13}C NMR of **8**:

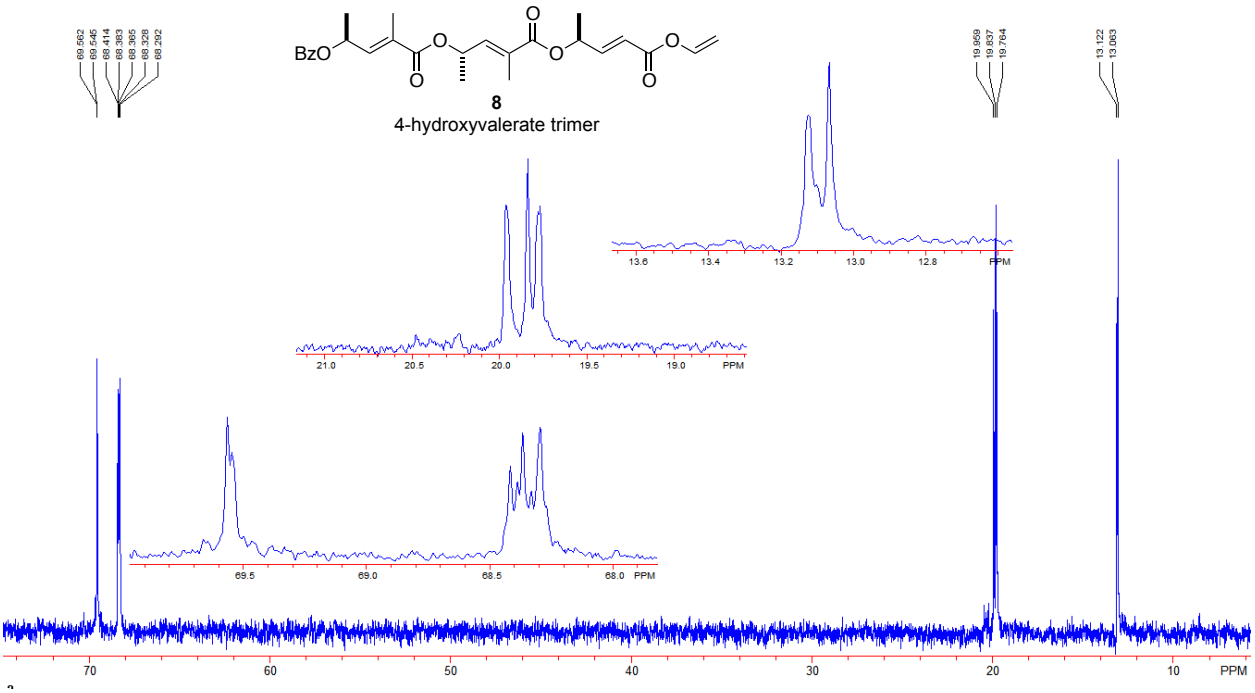
69.562
69.545
69.414
69.363
69.305
69.328
69.292
BzO
O
O
O
O
O
8
4-hydroxyvalerate trimer
19.969
19.837
19.764
13.122
13.083
13.6
13.4
13.2
13.0
12.8
PPM
21.0
20.5
20.0
19.5
19.0
PPM
69.5
69.0
68.5
68.0
PPM
70
60
50
40
30
20
10
PPM

COSY of **8**:

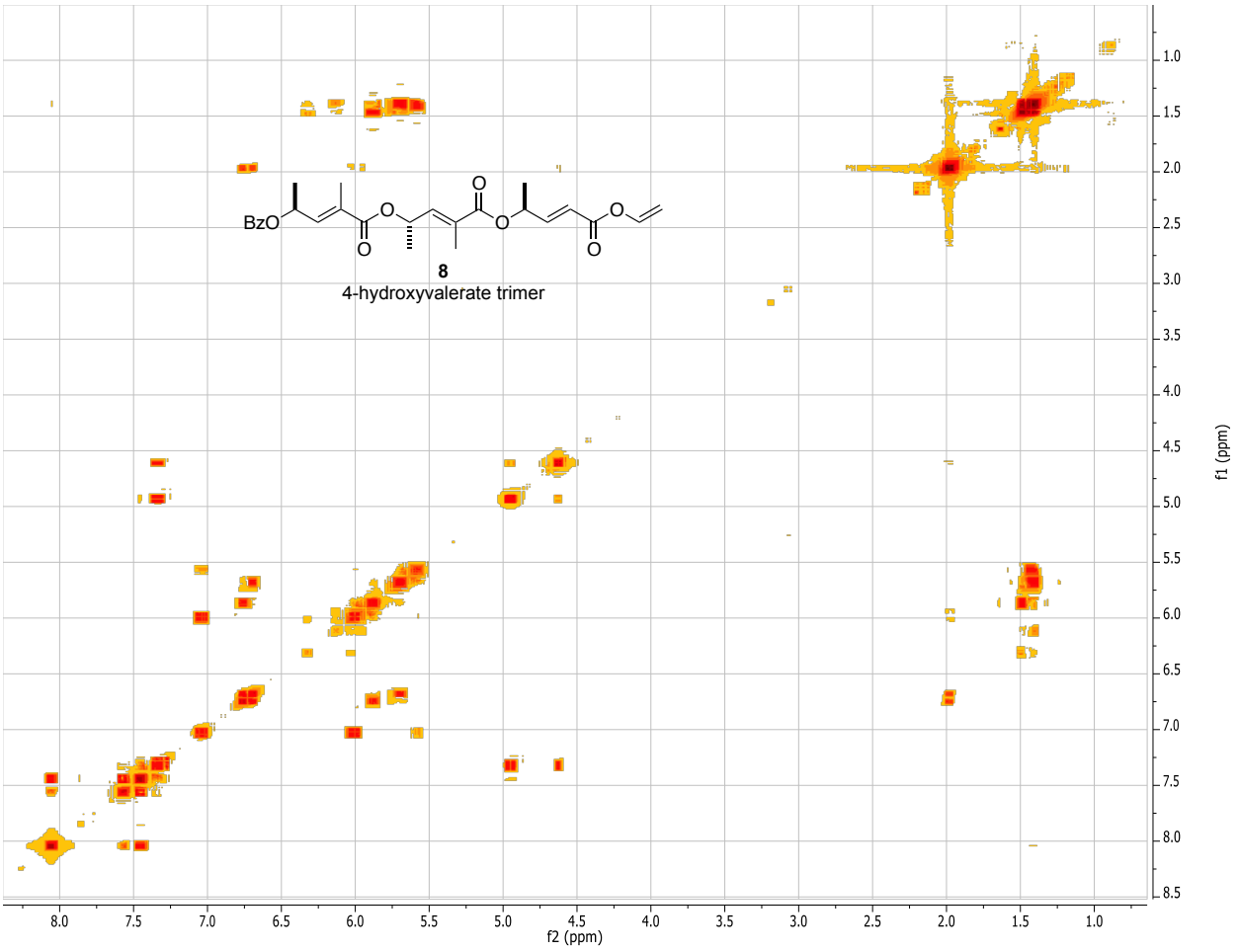

HSQC of **8**:

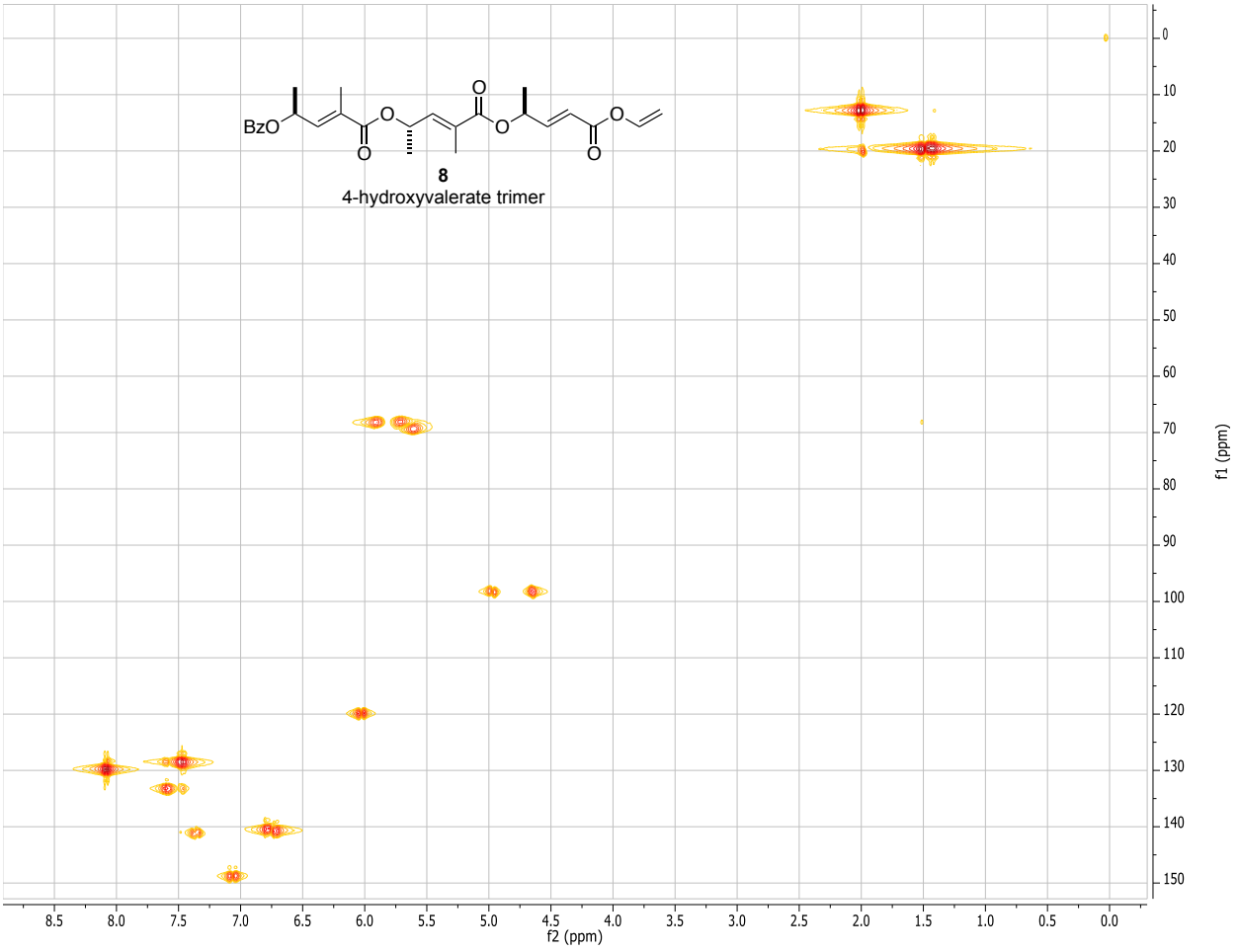

Mass spectrum of **8**:

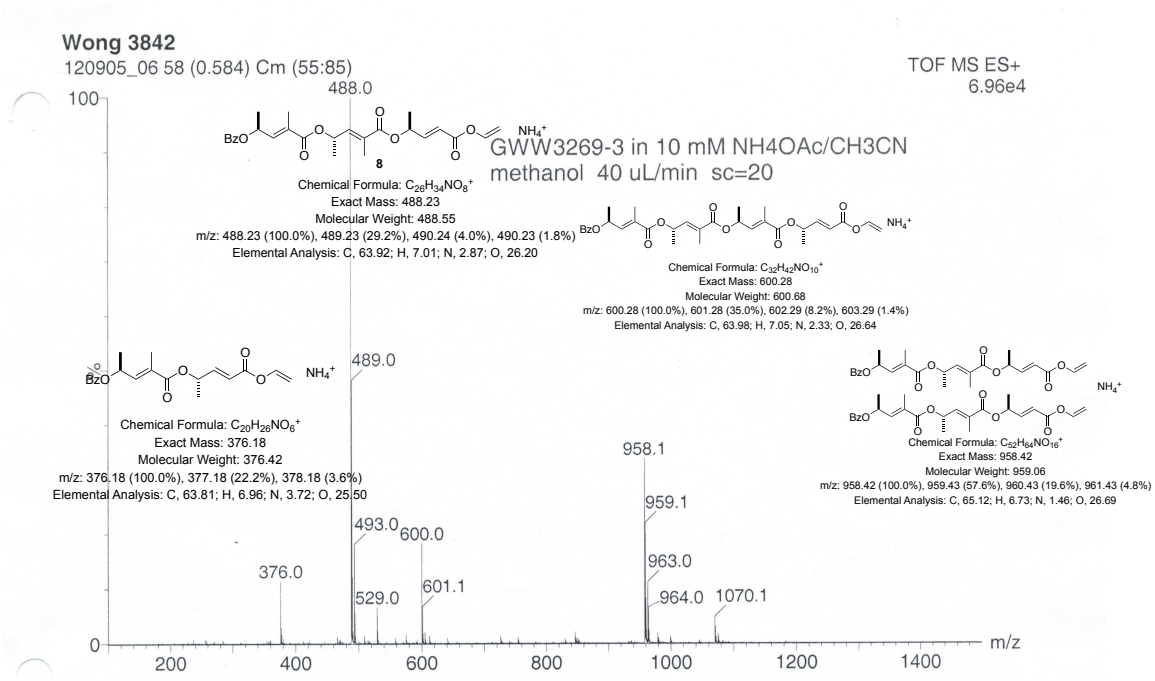

6.4 Crystallography Data for Tetraacid Bisdiazaphos 1 (Chapter 3)

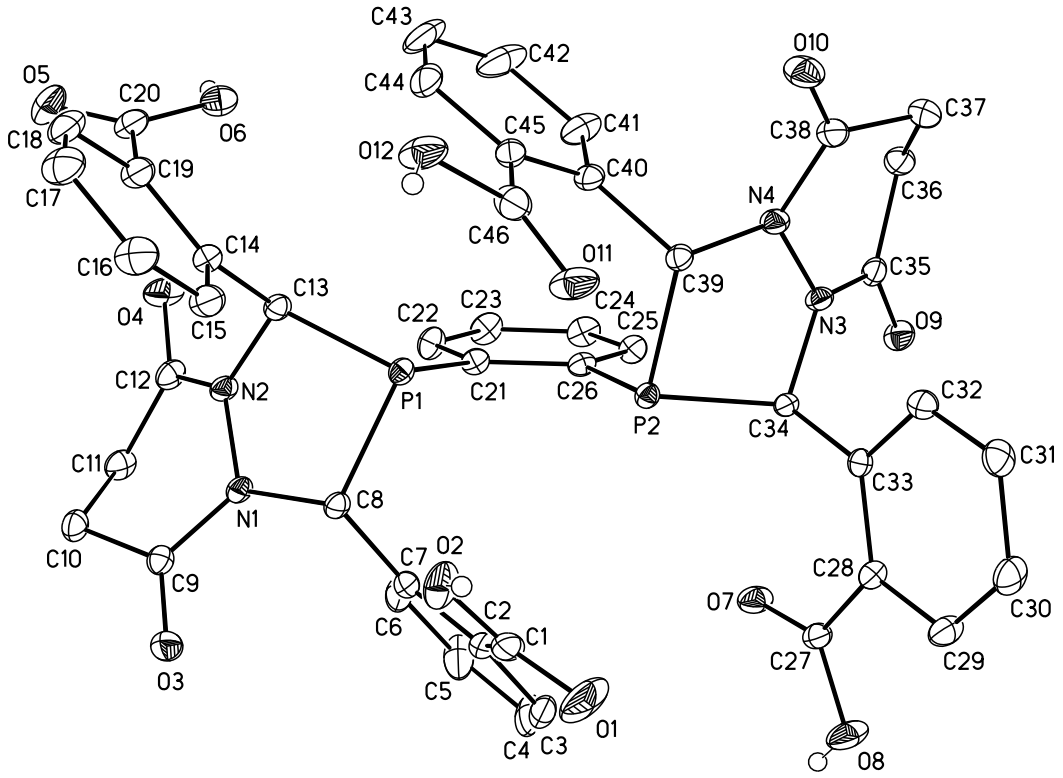

Figure 6.1 ORTEP drawing of tetraacid bisdiazaphos **1**. Thermal ellipsoids are drawn at the 30% probability level. All hydrogens, except for the four carboxylic acids moieties, are omitted for clarity. Only the (*S*,*S*) stereoisomer is shown; however, both exist in the structure.

Data Collection

A colorless crystal with approximate dimensions 0.40 x 0.38 x 0.32 mm^3 was selected under oil under ambient conditions and attached to the tip of a MiTeGen MicroMount©. The crystal was mounted in a stream of cold nitrogen at 102(1) K and centered in the X-ray beam by using a video camera.

The crystal evaluation and data collection were performed on a Bruker SMART APEXII diffractometer with Cu K_α (λ = 1.54178 Å) radiation and the diffractometer to crystal distance of 4.03 cm.

The initial cell constants were obtained from three series of ω scans at different starting angles. Each series consisted of 50 frames collected at intervals of 0.5º in a 25º range about ω with the exposure time of 5 seconds per frame. The reflections were successfully indexed by an automated indexing routine built in the SMART program. The final cell constants were calculated from a set of 9032 strong reflections from the actual data collection.

The data were collected by using the full sphere data collection routine to survey the reciprocal space to the extent of a full sphere to a resolution of 0.82 Å. A total of 77061 data were harvested by collecting 18 sets of frames with 0.5º scans in ω with an exposure time 5 sec per frame. These highly redundant datasets were corrected for Lorentz and polarization effects. The absorption correction was based on fitting a function to the empirical transmission surface as sampled by multiple equivalent measurements. [1]

Structure Solution and Refinement

The systematic absences in the diffraction data and the E-statistics were uniquely consistent for the space group $P2_1/c$ that yielded chemically reasonable and computationally stable results of refinement [2].

A successful solution by the direct methods provided most non-hydrogen atoms from the *E*-map. The remaining non-hydrogen atoms were located in an alternating series of least-squares cycles and difference Fourier maps. All non-hydrogen atoms were refined with anisotropic displacement coefficients. All hydrogen atoms were included in the structure factor calculation at idealized positions and were allowed to ride on the neighboring atoms with relative isotropic displacement coefficients. Atoms O11 and O12 are disordered over two positions each in a 51.0(5):49.0(5) ratio. The disorder was modeled with restraints.

There were three partially or fully occupied solvate molecules of methanol and/or ethanol present in the asymmetric unit. A significant amount of time was invested in identifying and refining the disordered molecules. Bond length restraints were applied to model the molecules but the resulting isotropic displacement coefficients suggested the molecules were mobile. In addition, the refinement was computationally unstable. Option SQUEEZE of program PLATON [3] was used to correct the diffraction data for diffuse scattering effects and to identify the solvate molecule. PLATON calculated the upper limit of volume that can be occupied by the solvent to be 974 $Å^3$, or 20% of the unit cell volume. The program calculated 234 electrons in the unit cell for the diffuse species. This approximately corresponds to one molecule of EtOH and two molecules of MeOH in the asymmetric unit (248 electrons). It is very likely that this solvate molecules are disordered over several positions forming hydrogen bonds. Please note that all derived results in the following tables are based on the known contents. No data are given for the diffusely scattering species.

The final least-squares refinement of 584 parameters against 8980 data resulted in residuals R (based on F^2 for $I \geq 2\sigma$) and wR (based on F^2 for all data) of 0.0512 and 0.1392, respectively. The final difference Fourier map was featureless.

The molecular diagrams is drawn with 30% probability ellipsoids.

References

[1] Bruker-AXS. (2007) APEX2, SADABS, and SAINT Software Reference Manuals. Bruker-AXS, Madison, Wisconsin, USA.

[2] Sheldrick, G. M. (2008) SHELXL. *Acta Cryst.* **A64**, 112-122.

[3] A.L. Spek (1990) Acta Cryst. A46, C34.

Table 6.1 Crystal data and structure refinement for tetraacid bisdiazaphos **1**.

Empirical formula	$C_{50} H_{50} N_4 O_{15} P_2$. 2 MeOH . EtOH	
Formula weight	1008.88	
Temperature	102(1) K	
Wavelength	1.54178 Å	
Crystal system	Monoclinic	
Space group	$P2_1/c$	
Unit cell dimensions	a = 21.5297(4) Å	α= 90°.
	b = 12.2669(3) Å	β= 95.2000(10)°.
	c = 18.5384(4) Å	γ = 90°.
Volume	4875.89(18) $Å^3$	
Z	4	
Density (calculated)	1.374 Mg/m^3	
Absorption coefficient	1.439 mm^{-1}	
F(000)	2112	
Crystal size	0.40 x 0.38 x 0.32 mm^3	
Theta range for data collection	2.06 to 69.94°.	
Index ranges	-26<=h<=25, -14<=k<=14, -22<=l<=22	
Reflections collected	77061	
Independent reflections	8980 [R(int) = 0.0211]	
Completeness to theta = 69.94°	97.3 %	
Absorption correction	Empirical with SADABS	
Max. and min. transmission	0.6560 and 0.5968	
Refinement method	Full-matrix least-squares on F^2	
Data / restraints / parameters	8980 / 18 / 584	
Goodness-of-fit on F^2	1.049	
Final R indices [I>2sigma(I)]	R1 = 0.0512, wR2 = 0.1375	
R indices (all data)	R1 = 0.0531, wR2 = 0.1392	
Largest diff. peak and hole	1.939 and -0.562 $e.Å^{-3}$	

Table 6.2 Atomic coordinates (x 10^4) and equivalent isotropic displacement parameters ($Å^2$x 10^3) for tetraacid bisdiazaphos **1**. U(eq) is defined as one third of the trace of the orthogonalized U^{ij} tensor.

	x	y	z	U(eq)
P(1)	2173(1)	1391(1)	3389(1)	19(1)
P(2)	2990(1)	-83(1)	2468(1)	18(1)
O(1)	3260(1)	2801(2)	1333(1)	67(1)
O(2)	2416(1)	2899(2)	1924(1)	40(1)
O(3)	2419(1)	5094(1)	3694(1)	30(1)
O(4)	1817(1)	2196(1)	5651(1)	38(1)
O(9)	4340(1)	-2775(1)	2748(1)	30(1)
O(10)	1924(1)	-3237(1)	1882(1)	36(1)
N(1)	2277(1)	3366(1)	4051(1)	21(1)
N(2)	1989(1)	2652(1)	4520(1)	22(1)
N(3)	3400(1)	-2133(1)	2363(1)	20(1)
N(4)	2744(1)	-2252(1)	2310(1)	23(1)
C(1)	3023(1)	2870(2)	1898(1)	36(1)
C(2)	3396(1)	2937(2)	2620(1)	32(1)
C(3)	4041(1)	2993(2)	2592(2)	46(1)
C(4)	4445(1)	3043(2)	3215(2)	54(1)
C(5)	4207(1)	3040(2)	3878(2)	49(1)
C(6)	3567(1)	2990(2)	3922(1)	34(1)
C(7)	3153(1)	2943(2)	3302(1)	25(1)
C(8)	2461(1)	2851(2)	3389(1)	20(1)
C(9)	2254(1)	4467(2)	4149(1)	23(1)
C(10)	2066(1)	4783(2)	4886(1)	28(1)
C(11)	2315(1)	3940(2)	5447(1)	29(1)
C(12)	2031(1)	2854(2)	5234(1)	27(1)
C(13)	1686(1)	1698(2)	4154(1)	21(1)
C(14)	1000(1)	1914(2)	3909(1)	25(1)
C(15)	829(1)	2339(2)	3225(1)	30(1)
C(16)	208(1)	2556(2)	2983(1)	37(1)
C(17)	-254(1)	2371(2)	3432(2)	40(1)
C(18)	-98(1)	1965(2)	4113(1)	38(1)
C(19)	524(1)	1721(2)	4361(1)	30(1)
C(20)	623(1)	1260(2)	5107(1)	31(1)
O(5)	371(1)	1652(2)	5612(1)	41(1)
O(6)	969(1)	388(1)	5168(1)	32(1)
C(21)	2814(1)	616(2)	3879(1)	21(1)
C(22)	2942(1)	636(2)	4633(1)	28(1)
C(23)	3389(1)	-39(2)	4979(1)	30(1)
C(24)	3722(1)	-744(2)	4580(1)	29(1)
C(25)	3606(1)	-777(2)	3830(1)	25(1)

C(26)	3152(1)	-111(2)	3467(1)	20(1)
C(27)	4530(1)	530(2)	1654(1)	24(1)
C(28)	4120(1)	-156(2)	1141(1)	22(1)
O(7)	4498(1)	567(1)	2301(1)	33(1)
O(8)	4943(1)	1103(2)	1326(1)	41(1)
C(29)	4184(1)	-65(2)	402(1)	30(1)
C(30)	3836(1)	-703(2)	-101(1)	32(1)
C(31)	3425(1)	-1461(2)	139(1)	29(1)
C(32)	3357(1)	-1562(2)	871(1)	25(1)
C(33)	3697(1)	-914(2)	1388(1)	19(1)
C(34)	3606(1)	-1041(2)	2187(1)	18(1)
C(35)	3772(1)	-2937(2)	2631(1)	23(1)
C(36)	3442(1)	-3996(2)	2743(1)	29(1)
C(37)	2921(1)	-4167(2)	2134(1)	32(1)
C(38)	2483(1)	-3206(2)	2083(1)	27(1)
C(39)	2396(1)	-1217(2)	2292(1)	20(1)
C(40)	1894(1)	-1250(2)	2810(1)	25(1)
C(41)	2021(1)	-1788(2)	3470(1)	36(1)
C(42)	1587(1)	-1811(3)	3978(1)	54(1)
C(43)	1020(1)	-1288(3)	3836(2)	58(1)
C(44)	888(1)	-762(2)	3188(2)	45(1)
C(45)	1314(1)	-732(2)	2664(1)	31(1)
C(46)	1132(1)	-165(2)	1962(2)	38(1)
O(11)	1491(2)	59(4)	1516(2)	43(1)
O(12)	547(1)	150(4)	2010(3)	43(1)
O(11A)	1373(2)	-345(4)	1401(2)	43(1)
O(12A)	639(2)	487(4)	1880(3)	43(1)

Table 6.3 Bond lengths [Å] and angles [°] for tetraacid bisdiazaphos **1**.

P(1)-C(21)	1.8464(19)	C(13)-H(13)	1.0000
P(1)-C(13)	1.8767(19)	C(14)-C(15)	1.390(3)
P(1)-C(8)	1.8955(19)	C(14)-C(19)	1.402(3)
P(2)-C(26)	1.8534(19)	C(15)-C(16)	1.396(3)
P(2)-C(34)	1.8805(19)	C(15)-H(15)	0.9500
P(2)-C(39)	1.8983(19)	C(16)-C(17)	1.372(4)
O(1)-C(1)	1.209(3)	C(16)-H(16)	0.9500
O(2)-C(1)	1.313(3)	C(17)-C(18)	1.369(4)
O(2)-H(2O)	0.8400	C(17)-H(17)	0.9500
O(3)-C(9)	1.217(3)	C(18)-C(19)	1.408(3)
O(4)-C(12)	1.235(3)	C(18)-H(18)	0.9500
O(9)-C(35)	1.238(2)	C(19)-C(20)	1.492(3)
O(10)-C(38)	1.229(3)	C(20)-O(5)	1.222(3)
N(1)-C(9)	1.364(3)	C(20)-O(6)	1.302(3)
N(1)-N(2)	1.417(2)	O(6)-H(6O)	0.8400
N(1)-C(8)	1.466(2)	C(21)-C(22)	1.400(3)
N(2)-C(12)	1.342(3)	C(21)-C(26)	1.416(3)
N(2)-C(13)	1.475(2)	C(22)-C(23)	1.382(3)
N(3)-C(35)	1.337(3)	C(22)-H(22)	0.9500
N(3)-N(4)	1.414(2)	C(23)-C(24)	1.381(3)
N(3)-C(34)	1.457(2)	C(23)-H(23)	0.9500
N(4)-C(38)	1.350(3)	C(24)-C(25)	1.391(3)
N(4)-C(39)	1.472(2)	C(24)-H(24)	0.9500
C(1)-C(2)	1.500(4)	C(25)-C(26)	1.398(3)
C(2)-C(3)	1.397(3)	C(25)-H(25)	0.9500
C(2)-C(7)	1.410(3)	C(27)-O(7)	1.209(2)
C(3)-C(4)	1.382(5)	C(27)-O(8)	1.323(2)
C(3)-H(3)	0.9500	C(27)-C(28)	1.497(3)
C(4)-C(5)	1.375(4)	C(28)-C(29)	1.394(3)
C(4)-H(4)	0.9500	C(28)-C(33)	1.407(3)
C(5)-C(6)	1.389(3)	O(8)-H(8O)	0.8400
C(5)-H(5)	0.9500	C(29)-C(30)	1.383(3)
C(6)-C(7)	1.390(3)	C(29)-H(29)	0.9500
C(6)-H(6A)	0.9500	C(30)-C(31)	1.386(3)
C(7)-C(8)	1.517(3)	C(30)-H(30)	0.9500
C(8)-H(8)	1.0000	C(31)-C(32)	1.384(3)
C(9)-C(10)	1.510(3)	C(31)-H(31)	0.9500
C(10)-C(11)	1.529(3)	C(32)-C(33)	1.399(3)
C(10)-H(10A)	0.9900	C(32)-H(32)	0.9500
C(10)-H(10B)	0.9900	C(33)-C(34)	1.520(3)
C(11)-C(12)	1.503(3)	C(34)-H(34)	1.0000
C(11)-H(11A)	0.9900	C(35)-C(36)	1.505(3)
C(11)-H(11B)	0.9900	C(36)-C(37)	1.531(3)
C(13)-C(14)	1.528(3)	C(36)-H(36A)	0.9900

C(36)-H(36B)	0.9900	C(43)-C(44)	1.370(5)
C(37)-C(38)	1.507(3)	C(43)-H(43)	0.9500
C(37)-H(37A)	0.9900	C(44)-C(45)	1.397(3)
C(37)-H(37B)	0.9900	C(44)-H(44)	0.9500
C(39)-C(40)	1.511(3)	C(45)-C(46)	1.497(4)
C(39)-H(39)	1.0000	C(46)-O(11)	1.213(3)
C(40)-C(41)	1.394(3)	C(46)-O(11A)	1.225(3)
C(40)-C(45)	1.404(3)	C(46)-O(12A)	1.326(3)
C(41)-C(42)	1.386(4)	C(46)-O(12)	1.329(3)
C(41)-H(41)	0.9500	O(12)-H(12O)	0.8400
C(42)-C(43)	1.383(5)	O(12A)-H(12)	0.8400
C(42)-H(42)	0.9500		

C(21)-P(1)-C(13)	100.15(9)	C(6)-C(5)-H(5)	119.9
C(21)-P(1)-C(8)	104.86(9)	C(5)-C(6)-C(7)	121.3(2)
C(13)-P(1)-C(8)	90.89(8)	C(5)-C(6)-H(6A)	119.4
C(26)-P(2)-C(34)	101.08(8)	C(7)-C(6)-H(6A)	119.4
C(26)-P(2)-C(39)	102.78(8)	C(6)-C(7)-C(2)	118.6(2)
C(34)-P(2)-C(39)	88.58(8)	C(6)-C(7)-C(8)	118.52(18)
C(1)-O(2)-H(2O)	109.5	C(2)-C(7)-C(8)	122.80(19)
C(9)-N(1)-N(2)	120.50(16)	N(1)-C(8)-C(7)	113.52(15)
C(9)-N(1)-C(8)	123.62(16)	N(1)-C(8)-P(1)	107.10(12)
N(2)-N(1)-C(8)	114.42(15)	C(7)-C(8)-P(1)	113.24(13)
C(12)-N(2)-N(1)	119.76(16)	N(1)-C(8)-H(8)	107.6
C(12)-N(2)-C(13)	126.08(16)	C(7)-C(8)-H(8)	107.6
N(1)-N(2)-C(13)	114.10(14)	P(1)-C(8)-H(8)	107.6
C(35)-N(3)-N(4)	120.73(16)	O(3)-C(9)-N(1)	121.16(18)
C(35)-N(3)-C(34)	125.18(16)	O(3)-C(9)-C(10)	125.63(19)
N(4)-N(3)-C(34)	113.68(14)	N(1)-C(9)-C(10)	112.97(17)
C(38)-N(4)-N(3)	119.77(16)	C(9)-C(10)-C(11)	109.62(17)
C(38)-N(4)-C(39)	122.93(16)	C(9)-C(10)-H(10A)	109.7
N(3)-N(4)-C(39)	114.57(14)	C(11)-C(10)-H(10A)	109.7
O(1)-C(1)-O(2)	122.3(3)	C(9)-C(10)-H(10B)	109.7
O(1)-C(1)-C(2)	122.9(3)	C(11)-C(10)-H(10B)	109.7
O(2)-C(1)-C(2)	114.77(18)	H(10A)-C(10)-H(10B)	108.2
C(3)-C(2)-C(7)	118.9(2)	C(12)-C(11)-C(10)	108.16(17)
C(3)-C(2)-C(1)	115.0(2)	C(12)-C(11)-H(11A)	110.1
C(7)-C(2)-C(1)	126.1(2)	C(10)-C(11)-H(11A)	110.1
C(4)-C(3)-C(2)	121.6(2)	C(12)-C(11)-H(11B)	110.1
C(4)-C(3)-H(3)	119.2	C(10)-C(11)-H(11B)	110.1
C(2)-C(3)-H(3)	119.2	H(11A)-C(11)-H(11B)	108.4
C(5)-C(4)-C(3)	119.4(2)	O(4)-C(12)-N(2)	120.01(19)
C(5)-C(4)-H(4)	120.3	O(4)-C(12)-C(11)	125.51(18)
C(3)-C(4)-H(4)	120.3	N(2)-C(12)-C(11)	114.37(18)
C(4)-C(5)-C(6)	120.2(3)	N(2)-C(13)-C(14)	112.07(16)
C(4)-C(5)-H(5)	119.9	N(2)-C(13)-P(1)	104.64(12)

C(14)-C(13)-P(1)	113.67(13)	O(8)-C(27)-C(28)	112.91(17)
N(2)-C(13)-H(13)	108.8	C(29)-C(28)-C(33)	119.88(18)
C(14)-C(13)-H(13)	108.8	C(29)-C(28)-C(27)	118.32(18)
P(1)-C(13)-H(13)	108.8	C(33)-C(28)-C(27)	121.73(17)
C(15)-C(14)-C(19)	117.42(19)	C(27)-O(8)-H(8O)	109.5
C(15)-C(14)-C(13)	120.34(18)	C(30)-C(29)-C(28)	121.4(2)
C(19)-C(14)-C(13)	122.23(18)	C(30)-C(29)-H(29)	119.3
C(14)-C(15)-C(16)	122.1(2)	C(28)-C(29)-H(29)	119.3
C(14)-C(15)-H(15)	118.9	C(29)-C(30)-C(31)	119.10(19)
C(16)-C(15)-H(15)	118.9	C(29)-C(30)-H(30)	120.5
C(17)-C(16)-C(15)	119.9(2)	C(31)-C(30)-H(30)	120.5
C(17)-C(16)-H(16)	120.1	C(32)-C(31)-C(30)	120.13(19)
C(15)-C(16)-H(16)	120.1	C(32)-C(31)-H(31)	119.9
C(18)-C(17)-C(16)	119.3(2)	C(30)-C(31)-H(31)	119.9
C(18)-C(17)-H(17)	120.3	C(31)-C(32)-C(33)	121.73(19)
C(16)-C(17)-H(17)	120.3	C(31)-C(32)-H(32)	119.1
C(17)-C(18)-C(19)	121.6(2)	C(33)-C(32)-H(32)	119.1
C(17)-C(18)-H(18)	119.2	C(32)-C(33)-C(28)	117.74(17)
C(19)-C(18)-H(18)	119.2	C(32)-C(33)-C(34)	120.27(17)
C(14)-C(19)-C(18)	119.6(2)	C(28)-C(33)-C(34)	121.99(16)
C(14)-C(19)-C(20)	124.5(2)	N(3)-C(34)-C(33)	112.38(15)
C(18)-C(19)-C(20)	115.9(2)	N(3)-C(34)-P(2)	105.99(12)
O(5)-C(20)-O(6)	123.1(2)	C(33)-C(34)-P(2)	111.23(12)
O(5)-C(20)-C(19)	121.7(2)	N(3)-C(34)-H(34)	109.0
O(6)-C(20)-C(19)	115.1(2)	C(33)-C(34)-H(34)	109.0
C(20)-O(6)-H(6O)	109.5	P(2)-C(34)-H(34)	109.0
C(22)-C(21)-C(26)	118.97(18)	O(9)-C(35)-N(3)	119.74(18)
C(22)-C(21)-P(1)	123.55(15)	O(9)-C(35)-C(36)	125.85(18)
C(26)-C(21)-P(1)	117.20(14)	N(3)-C(35)-C(36)	114.39(17)
C(23)-C(22)-C(21)	121.3(2)	C(35)-C(36)-C(37)	109.90(17)
C(23)-C(22)-H(22)	119.4	C(35)-C(36)-H(36A)	109.7
C(21)-C(22)-H(22)	119.4	C(37)-C(36)-H(36A)	109.7
C(24)-C(23)-C(22)	119.96(19)	C(35)-C(36)-H(36B)	109.7
C(24)-C(23)-H(23)	120.0	C(37)-C(36)-H(36B)	109.7
C(22)-C(23)-H(23)	120.0	H(36A)-C(36)-H(36B)	108.2
C(23)-C(24)-C(25)	119.91(19)	C(38)-C(37)-C(36)	110.60(18)
C(23)-C(24)-H(24)	120.0	C(38)-C(37)-H(37A)	109.5
C(25)-C(24)-H(24)	120.0	C(36)-C(37)-H(37A)	109.5
C(24)-C(25)-C(26)	121.21(19)	C(38)-C(37)-H(37B)	109.5
C(24)-C(25)-H(25)	119.4	C(36)-C(37)-H(37B)	109.5
C(26)-C(25)-H(25)	119.4	H(37A)-C(37)-H(37B)	108.1
C(25)-C(26)-C(21)	118.66(17)	O(10)-C(38)-N(4)	119.4(2)
C(25)-C(26)-P(2)	123.42(15)	O(10)-C(38)-C(37)	125.86(19)
C(21)-C(26)-P(2)	117.87(14)	N(4)-C(38)-C(37)	114.68(18)
O(7)-C(27)-O(8)	122.39(18)	N(4)-C(39)-C(40)	110.80(16)
O(7)-C(27)-C(28)	124.70(18)	N(4)-C(39)-P(2)	107.11(12)

C(40)-C(39)-P(2)	114.81(13)	C(43)-C(44)-H(44)	119.2
N(4)-C(39)-H(39)	108.0	C(45)-C(44)-H(44)	119.2
C(40)-C(39)-H(39)	108.0	C(44)-C(45)-C(40)	118.9(2)
P(2)-C(39)-H(39)	108.0	C(44)-C(45)-C(46)	118.7(2)
C(41)-C(40)-C(45)	118.9(2)	C(40)-C(45)-C(46)	122.4(2)
C(41)-C(40)-C(39)	118.36(19)	O(11)-C(46)-O(11A)	27.9(2)
C(45)-C(40)-C(39)	122.70(19)	O(11)-C(46)-O(12A)	109.7(3)
C(42)-C(41)-C(40)	121.0(3)	O(11A)-C(46)-O(12A)	114.1(4)
C(42)-C(41)-H(41)	119.5	O(11)-C(46)-O(12)	130.2(3)
C(40)-C(41)-H(41)	119.5	O(11A)-C(46)-O(12)	125.9(4)
C(43)-C(42)-C(41)	119.9(3)	O(12A)-C(46)-O(12)	22.88(18)
C(43)-C(42)-H(42)	120.1	O(11)-C(46)-C(45)	124.4(3)
C(41)-C(42)-H(42)	120.1	O(11A)-C(46)-C(45)	123.9(3)
C(44)-C(43)-C(42)	119.7(2)	O(12A)-C(46)-C(45)	121.6(3)
C(44)-C(43)-H(43)	120.1	O(12)-C(46)-C(45)	104.7(3)
C(42)-C(43)-H(43)	120.1	C(46)-O(12)-H(12O)	109.5
C(43)-C(44)-C(45)	121.6(3)	C(46)-O(12A)-H(12)	109.5

Symmetry transformations used to generate equivalent atoms:

Table 6.4 Anisotropic displacement parameters ($Å^2 x\ 10^3$) for tetraacid bisdiazaphos **1**. The anisotropic displacement factor exponent takes the form: $-2\pi^2[\ h^2\ a^{*2}U^{11} + ... + 2\ h\ k\ a^*\ b^*\ U^{12}\ ]$.

	U^{11}	U^{22}	U^{33}	U^{23}	U^{13}	U^{12}
P(1)	20(1)	22(1)	14(1)	0(1)	3(1)	0(1)
P(2)	18(1)	19(1)	16(1)	1(1)	3(1)	1(1)
O(1)	78(2)	92(2)	37(1)	-20(1)	37(1)	-32(1)
O(2)	51(1)	55(1)	16(1)	0(1)	9(1)	12(1)
O(3)	37(1)	26(1)	29(1)	2(1)	9(1)	-1(1)
O(4)	53(1)	47(1)	17(1)	-2(1)	11(1)	-19(1)
O(9)	21(1)	29(1)	40(1)	5(1)	6(1)	6(1)
O(10)	29(1)	34(1)	44(1)	-4(1)	-3(1)	-9(1)
N(1)	25(1)	24(1)	14(1)	0(1)	7(1)	-1(1)
N(2)	25(1)	25(1)	16(1)	0(1)	6(1)	-4(1)
N(3)	16(1)	21(1)	25(1)	3(1)	4(1)	-1(1)
N(4)	17(1)	21(1)	31(1)	1(1)	3(1)	-2(1)
C(1)	58(2)	25(1)	29(1)	-4(1)	23(1)	-10(1)
C(2)	37(1)	22(1)	39(1)	-9(1)	21(1)	-9(1)
C(3)	42(1)	37(1)	64(2)	-22(1)	34(1)	-13(1)
C(4)	27(1)	53(2)	87(2)	-37(2)	24(1)	-11(1)
C(5)	26(1)	53(2)	68(2)	-32(1)	1(1)	-1(1)
C(6)	24(1)	40(1)	39(1)	-15(1)	5(1)	0(1)
C(7)	25(1)	20(1)	30(1)	-6(1)	9(1)	-3(1)
C(8)	23(1)	23(1)	15(1)	-1(1)	5(1)	-2(1)
C(9)	20(1)	25(1)	24(1)	-2(1)	2(1)	1(1)
C(10)	27(1)	30(1)	28(1)	-8(1)	7(1)	0(1)
C(11)	33(1)	36(1)	18(1)	-5(1)	6(1)	-6(1)
C(12)	28(1)	35(1)	19(1)	-3(1)	6(1)	-3(1)
C(13)	23(1)	23(1)	19(1)	0(1)	5(1)	-2(1)
C(14)	21(1)	24(1)	29(1)	-1(1)	6(1)	-2(1)
C(15)	26(1)	30(1)	34(1)	6(1)	4(1)	0(1)
C(16)	29(1)	40(1)	41(1)	10(1)	-4(1)	0(1)
C(17)	23(1)	45(1)	50(2)	9(1)	-2(1)	0(1)
C(18)	22(1)	43(1)	50(1)	5(1)	11(1)	-2(1)
C(19)	27(1)	33(1)	32(1)	1(1)	6(1)	-3(1)
C(20)	22(1)	37(1)	35(1)	6(1)	7(1)	-3(1)
O(5)	32(1)	57(1)	36(1)	10(1)	14(1)	9(1)
O(6)	36(1)	37(1)	25(1)	7(1)	4(1)	-5(1)
C(21)	20(1)	24(1)	19(1)	2(1)	1(1)	0(1)
C(22)	28(1)	36(1)	19(1)	-1(1)	3(1)	3(1)
C(23)	30(1)	44(1)	17(1)	4(1)	0(1)	0(1)
C(24)	25(1)	36(1)	25(1)	8(1)	-3(1)	1(1)
C(25)	23(1)	28(1)	24(1)	2(1)	2(1)	1(1)

C(26)	20(1)	23(1)	17(1)	2(1)	2(1)	-3(1)
C(27)	22(1)	25(1)	24(1)	0(1)	5(1)	-4(1)
C(28)	20(1)	25(1)	21(1)	0(1)	4(1)	0(1)
O(7)	39(1)	36(1)	24(1)	-4(1)	6(1)	-17(1)
O(8)	38(1)	54(1)	30(1)	-5(1)	10(1)	-27(1)
C(29)	29(1)	35(1)	25(1)	3(1)	8(1)	-5(1)
C(30)	38(1)	41(1)	19(1)	-3(1)	5(1)	-1(1)
C(31)	32(1)	32(1)	24(1)	-6(1)	0(1)	-2(1)
C(32)	24(1)	24(1)	26(1)	-2(1)	3(1)	-4(1)
C(33)	17(1)	19(1)	21(1)	0(1)	2(1)	3(1)
C(34)	17(1)	18(1)	20(1)	1(1)	4(1)	-1(1)
C(35)	23(1)	24(1)	24(1)	2(1)	7(1)	4(1)
C(36)	31(1)	22(1)	34(1)	6(1)	8(1)	2(1)
C(37)	38(1)	22(1)	36(1)	0(1)	9(1)	-5(1)
C(38)	29(1)	26(1)	27(1)	0(1)	6(1)	-5(1)
C(39)	16(1)	22(1)	22(1)	-1(1)	2(1)	-1(1)
C(40)	20(1)	27(1)	28(1)	-6(1)	5(1)	-8(1)
C(41)	30(1)	55(2)	26(1)	0(1)	6(1)	-13(1)
C(42)	46(2)	86(2)	31(1)	-4(1)	15(1)	-33(2)
C(43)	42(2)	86(2)	52(2)	-33(2)	34(1)	-35(2)
C(44)	25(1)	47(2)	66(2)	-29(1)	19(1)	-14(1)
C(45)	18(1)	28(1)	47(1)	-13(1)	8(1)	-7(1)
C(46)	20(1)	25(1)	69(2)	-2(1)	3(1)	2(1)
O(11)	24(1)	37(2)	69(1)	26(1)	8(1)	3(1)
O(12)	24(1)	37(2)	69(1)	26(1)	8(1)	3(1)
O(11A)	24(1)	37(2)	69(1)	26(1)	8(1)	3(1)
O(12A)	24(1)	37(2)	69(1)	26(1)	8(1)	3(1)

Table 6.5 Hydrogen coordinates (x 10^4) and isotropic displacement parameters ($Å^2$x 10^3) for tetraacid bisdiazaphos **1**.

	x	y	z	U(eq)
H(2O)	2238	2834	1504	61
H(3)	4207	2996	2134	55
H(4)	4882	3079	3184	65
H(5)	4482	3071	4309	59
H(6A)	3409	2989	4384	41
H(8)	2232	3231	2968	24
H(10A)	1605	4820	4872	34
H(10B)	2236	5511	5022	34
H(11A)	2775	3898	5462	35
H(11B)	2202	4151	5934	35
H(13)	1713	1068	4497	26
H(15)	1144	2487	2911	36
H(16)	105	2832	2508	45
H(17)	-677	2522	3272	48
H(18)	-418	1846	4425	46
H(6O)	1074	265	5608	49
H(22)	2718	1123	4912	33
H(23)	3466	-18	5492	37
H(24)	4030	-1207	4818	35
H(25)	3839	-1261	3559	30
H(8O)	5174	1448	1637	61
H(29)	4473	445	240	35
H(30)	3880	-622	-604	39
H(31)	3188	-1912	-200	35
H(32)	3073	-2086	1027	30
H(34)	4010	-881	2480	22
H(36A)	3262	-3984	3216	35
H(36B)	3743	-4606	2747	35
H(37A)	3106	-4261	1668	38
H(37B)	2686	-4838	2230	38
H(39)	2189	-1119	1791	24
H(41)	2411	-2144	3572	44
H(42)	1679	-2184	4424	65
H(43)	724	-1294	4186	70
H(44)	496	-409	3094	54
H(12O)	428	536	1649	65
H(12)	726	1039	1641	65

Table 6.6 Torsion angles [°] for tetraacid bisdiazaphos **1**.

C(9)-N(1)-N(2)-C(12)	-40.8(3)	N(1)-N(2)-C(12)-C(11)	8.4(3)
C(8)-N(1)-N(2)-C(12)	152.50(18)	C(13)-N(2)-C(12)-C(11)	-174.62(18)
C(9)-N(1)-N(2)-C(13)	141.87(18)	C(10)-C(11)-C(12)-O(4)	-136.3(2)
C(8)-N(1)-N(2)-C(13)	-24.9(2)	C(10)-C(11)-C(12)-N(2)	40.0(2)
C(35)-N(3)-N(4)-C(38)	-41.5(3)	C(12)-N(2)-C(13)-C(14)	91.3(2)
C(34)-N(3)-N(4)-C(38)	145.51(18)	N(1)-N(2)-C(13)-C(14)	-91.54(19)
C(35)-N(3)-N(4)-C(39)	156.68(17)	C(12)-N(2)-C(13)-P(1)	-145.08(17)
C(34)-N(3)-N(4)-C(39)	-16.3(2)	N(1)-N(2)-C(13)-P(1)	32.08(18)
O(1)-C(1)-C(2)-C(3)	4.4(3)	C(21)-P(1)-C(13)-N(2)	81.37(13)
O(2)-C(1)-C(2)-C(3)	-175.2(2)	C(8)-P(1)-C(13)-N(2)	-23.91(13)
O(1)-C(1)-C(2)-C(7)	-175.3(2)	C(21)-P(1)-C(13)-C(14)	-156.05(14)
O(2)-C(1)-C(2)-C(7)	5.1(3)	C(8)-P(1)-C(13)-C(14)	98.67(15)
C(7)-C(2)-C(3)-C(4)	0.6(4)	N(2)-C(13)-C(14)-C(15)	90.2(2)
C(1)-C(2)-C(3)-C(4)	-179.1(2)	P(1)-C(13)-C(14)-C(15)	-28.2(2)
C(2)-C(3)-C(4)-C(5)	-0.1(4)	N(2)-C(13)-C(14)-C(19)	-88.2(2)
C(3)-C(4)-C(5)-C(6)	-0.2(4)	P(1)-C(13)-C(14)-C(19)	153.39(17)
C(4)-C(5)-C(6)-C(7)	0.0(4)	C(19)-C(14)-C(15)-C(16)	-0.9(3)
C(5)-C(6)-C(7)-C(2)	0.5(3)	C(13)-C(14)-C(15)-C(16)	-179.4(2)
C(5)-C(6)-C(7)-C(8)	177.9(2)	C(14)-C(15)-C(16)-C(17)	1.4(4)
C(3)-C(2)-C(7)-C(6)	-0.8(3)	C(15)-C(16)-C(17)-C(18)	-0.5(4)
C(1)-C(2)-C(7)-C(6)	178.9(2)	C(16)-C(17)-C(18)-C(19)	-0.8(4)
C(3)-C(2)-C(7)-C(8)	-178.1(2)	C(15)-C(14)-C(19)-C(18)	-0.3(3)
C(1)-C(2)-C(7)-C(8)	1.6(3)	C(13)-C(14)-C(19)-C(18)	178.1(2)
C(9)-N(1)-C(8)-C(7)	72.3(2)	C(15)-C(14)-C(19)-C(20)	179.5(2)
N(2)-N(1)-C(8)-C(7)	-121.41(17)	C(13)-C(14)-C(19)-C(20)	-2.1(3)
C(9)-N(1)-C(8)-P(1)	-161.93(15)	C(17)-C(18)-C(19)-C(14)	1.2(4)
N(2)-N(1)-C(8)-P(1)	4.34(18)	C(17)-C(18)-C(19)-C(20)	-178.6(2)
C(6)-C(7)-C(8)-N(1)	29.8(3)	C(14)-C(19)-C(20)-O(5)	134.7(2)
C(2)-C(7)-C(8)-N(1)	-152.86(18)	C(18)-C(19)-C(20)-O(5)	-45.5(3)
C(6)-C(7)-C(8)-P(1)	-92.6(2)	C(14)-C(19)-C(20)-O(6)	-48.6(3)
C(2)-C(7)-C(8)-P(1)	84.7(2)	C(18)-C(19)-C(20)-O(6)	131.2(2)
C(21)-P(1)-C(8)-N(1)	-88.84(14)	C(13)-P(1)-C(21)-C(22)	-17.55(19)
C(13)-P(1)-C(8)-N(1)	11.90(13)	C(8)-P(1)-C(21)-C(22)	76.10(19)
C(21)-P(1)-C(8)-C(7)	37.07(16)	C(13)-P(1)-C(21)-C(26)	156.36(15)
C(13)-P(1)-C(8)-C(7)	137.81(14)	C(8)-P(1)-C(21)-C(26)	-109.98(15)
N(2)-N(1)-C(9)-O(3)	-169.30(17)	C(26)-C(21)-C(22)-C(23)	-0.2(3)
C(8)-N(1)-C(9)-O(3)	-3.8(3)	P(1)-C(21)-C(22)-C(23)	173.64(17)
N(2)-N(1)-C(9)-C(10)	15.9(2)	C(21)-C(22)-C(23)-C(24)	0.6(3)
C(8)-N(1)-C(9)-C(10)	-178.59(17)	C(22)-C(23)-C(24)-C(25)	-0.3(3)
O(3)-C(9)-C(10)-C(11)	-141.2(2)	C(23)-C(24)-C(25)-C(26)	-0.5(3)
N(1)-C(9)-C(10)-C(11)	33.3(2)	C(24)-C(25)-C(26)-C(21)	0.8(3)
C(9)-C(10)-C(11)-C(12)	-61.0(2)	C(24)-C(25)-C(26)-P(2)	178.07(16)
N(1)-N(2)-C(12)-O(4)	-175.13(19)	C(22)-C(21)-C(26)-C(25)	-0.5(3)
C(13)-N(2)-C(12)-O(4)	1.9(3)	P(1)-C(21)-C(26)-C(25)	-174.73(15)

C(22)-C(21)-C(26)-P(2)	-177.91(15)
P(1)-C(21)-C(26)-P(2)	7.9(2)
C(34)-P(2)-C(26)-C(25)	-3.65(18)
C(39)-P(2)-C(26)-C(25)	87.41(18)
C(34)-P(2)-C(26)-C(21)	173.60(15)
C(39)-P(2)-C(26)-C(21)	-95.34(16)
O(7)-C(27)-C(28)-C(29)	176.1(2)
O(8)-C(27)-C(28)-C(29)	-4.2(3)
O(7)-C(27)-C(28)-C(33)	-6.8(3)
O(8)-C(27)-C(28)-C(33)	172.88(19)
C(33)-C(28)-C(29)-C(30)	0.5(3)
C(27)-C(28)-C(29)-C(30)	177.6(2)
C(28)-C(29)-C(30)-C(31)	-1.2(3)
C(29)-C(30)-C(31)-C(32)	1.0(3)
C(30)-C(31)-C(32)-C(33)	0.0(3)
C(31)-C(32)-C(33)-C(28)	-0.7(3)
C(31)-C(32)-C(33)-C(34)	179.43(18)
C(29)-C(28)-C(33)-C(32)	0.5(3)
C(27)-C(28)-C(33)-C(32)	-176.55(18)
C(29)-C(28)-C(33)-C(34)	-179.67(18)
C(27)-C(28)-C(33)-C(34)	3.3(3)
C(35)-N(3)-C(34)-C(33)	97.0(2)
N(4)-N(3)-C(34)-C(33)	-90.33(18)
C(35)-N(3)-C(34)-P(2)	-141.29(16)
N(4)-N(3)-C(34)-P(2)	31.36(18)
C(32)-C(33)-C(34)-N(3)	26.9(2)
C(28)-C(33)-C(34)-N(3)	-152.91(17)
C(32)-C(33)-C(34)-P(2)	-91.72(19)
C(28)-C(33)-C(34)-P(2)	88.43(19)
C(26)-P(2)-C(34)-N(3)	74.00(13)
C(39)-P(2)-C(34)-N(3)	-28.74(13)
C(26)-P(2)-C(34)-C(33)	-163.57(13)
C(39)-P(2)-C(34)-C(33)	93.69(13)
N(4)-N(3)-C(35)-O(9)	-172.08(17)
C(34)-N(3)-C(35)-O(9)	0.1(3)
N(4)-N(3)-C(35)-C(36)	9.6(3)
C(34)-N(3)-C(35)-C(36)	-178.24(17)
O(9)-C(35)-C(36)-C(37)	-141.5(2)
N(3)-C(35)-C(36)-C(37)	36.7(2)
C(35)-C(36)-C(37)-C(38)	-55.2(2)
N(3)-N(4)-C(38)-O(10)	-163.68(19)
C(39)-N(4)-C(38)-O(10)	-3.4(3)
N(3)-N(4)-C(38)-C(37)	18.8(3)
C(39)-N(4)-C(38)-C(37)	179.02(18)
C(36)-C(37)-C(38)-O(10)	-149.5(2)
C(36)-C(37)-C(38)-N(4)	27.8(3)
C(38)-N(4)-C(39)-C(40)	65.9(2)
N(3)-N(4)-C(39)-C(40)	-132.86(16)
C(38)-N(4)-C(39)-P(2)	-168.15(15)
N(3)-N(4)-C(39)-P(2)	-6.95(19)
C(26)-P(2)-C(39)-N(4)	-80.58(14)
C(34)-P(2)-C(39)-N(4)	20.46(13)
C(26)-P(2)-C(39)-C(40)	42.91(16)
C(34)-P(2)-C(39)-C(40)	143.95(15)
N(4)-C(39)-C(40)-C(41)	37.2(2)
P(2)-C(39)-C(40)-C(41)	-84.3(2)
N(4)-C(39)-C(40)-C(45)	-144.91(18)
P(2)-C(39)-C(40)-C(45)	93.6(2)
C(45)-C(40)-C(41)-C(42)	-0.4(3)
C(39)-C(40)-C(41)-C(42)	177.6(2)
C(40)-C(41)-C(42)-C(43)	-0.4(4)
C(41)-C(42)-C(43)-C(44)	0.8(4)
C(42)-C(43)-C(44)-C(45)	-0.4(4)
C(43)-C(44)-C(45)-C(40)	-0.4(3)
C(43)-C(44)-C(45)-C(46)	178.6(2)
C(41)-C(40)-C(45)-C(44)	0.8(3)
C(39)-C(40)-C(45)-C(44)	-177.13(19)
C(41)-C(40)-C(45)-C(46)	-178.2(2)
C(39)-C(40)-C(45)-C(46)	4.0(3)
C(44)-C(45)-C(46)-O(11)	168.2(4)
C(40)-C(45)-C(46)-O(11)	-12.9(5)
C(44)-C(45)-C(46)-O(11A)	-158.0(4)
C(40)-C(45)-C(46)-O(11A)	20.9(4)
C(44)-C(45)-C(46)-O(12A)	13.8(4)
C(40)-C(45)-C(46)-O(12A)	-167.3(3)
C(44)-C(45)-C(46)-O(12)	-3.0(4)
C(40)-C(45)-C(46)-O(12)	175.9(3)

Symmetry transformations used to generate equivalent atoms:

Table 6.7 Hydrogen bonds for tetraacid bisdiazaphos **1** [Å and °].

D-H...A	d(D-H)	d(H...A)	d(D...A)	<(DHA)
O(2)-H(2O)...O(4)#1	0.84	1.75	2.586(2)	174.1
O(8)-H(8O)...O(9)#2	0.84	1.76	2.597(2)	176.9

Symmetry transformations used to generate equivalent atoms:
#1 x,-y+1/2,z-1/2 #2 -x+1,y+1/2,-z+1/2

6.5 Crystallography Data for Tetraester Bisdiazaphos 2 (Chapter 3)

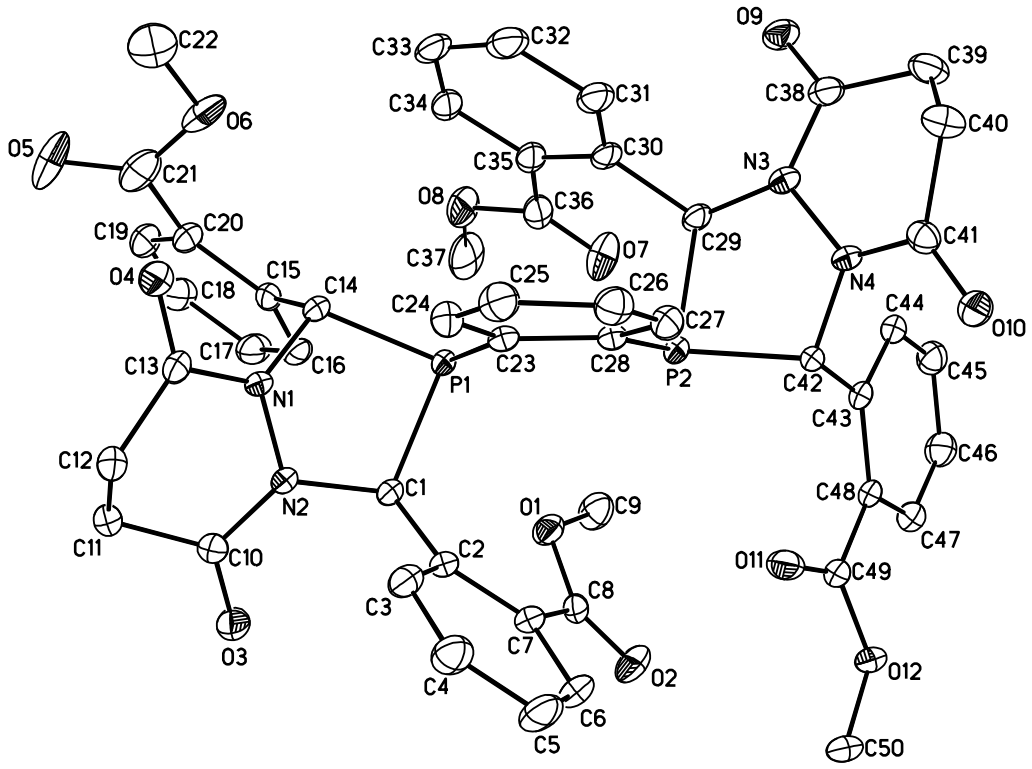

Figure 6.2 ORTEP drawing of tetraester bisdiazaphos **2**. Thermal ellipsoids are drawn at the 40% probability level. All hydrogens and THF solvent molecules are omitted for clarity. Only the (*S*,*S*) stereoisomer is shown; however, both exist in the structure.

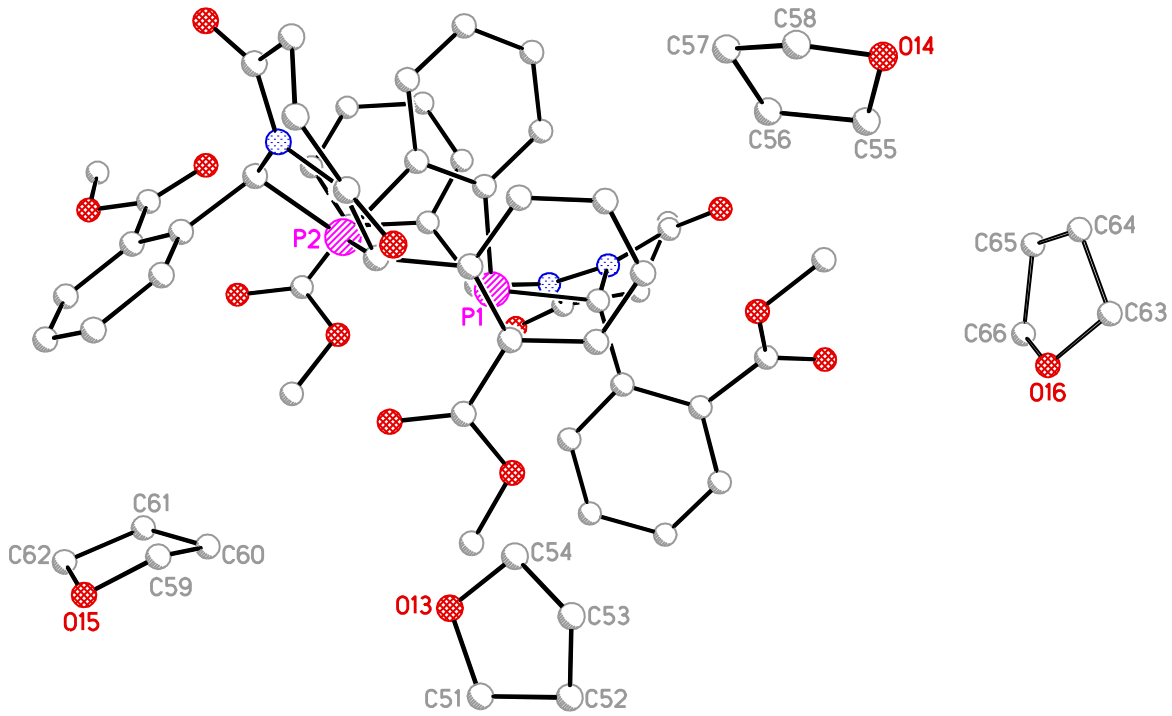

Figure 6.3 A molecular drawing of the unit cell content. All H atoms are omitted.

Data Collection

A colorless crystal with approximate dimensions 0.50 x 0.46 x 0.38 mm^3 was selected under oil under ambient conditions and attached to the tip of a MiTeGen MicroMount©. The crystal was mounted in a stream of cold nitrogen at 100(1) K and centered in the X-ray beam by using a video camera.

The crystal evaluation and data collection were performed on a Bruker CCD-1000 diffractometer with Mo K_α (λ = 0.71073 Å) radiation and the diffractometer to crystal distance of 4.9 cm.

The initial cell constants were obtained from three series of ω scans at different starting angles. Each series consisted of 20 frames collected at intervals of 0.3º in a 6º range about ω with the exposure time of 10 seconds per frame. A total of 67 reflections was obtained. The reflections were successfully indexed by an automated indexing routine built in the SMART program. The final cell constants were calculated from a set of 9947 strong reflections from the actual data collection.

The data were collected by using the full sphere data collection routine to survey the reciprocal space to the extent of a full sphere to a resolution of 0.73 Å. A total of 32825 data were harvested by collecting four sets of frames with 0.36º scans in ω and one set with 0.45º scans in φ with an exposure time 20 sec per frame. These highly redundant datasets were corrected for Lorentz and polarization effects. The absorption correction was based on fitting a function to the empirical transmission surface as sampled by multiple equivalent measurements. [1]

Structure Solution and Refinement

The systematic absences in the diffraction data were consistent for the space groups $P\bar{1}$ and $P1$. The *E*-statistics strongly suggested the centrosymmetric space group $P\bar{1}$ that yielded chemically reasonable and computationally stable results of refinement [2].

A successful solution by the direct methods provided most non-hydrogen atoms from the *E*-map. The remaining non-hydrogen atoms were located in an alternating series of least-squares cycles and difference Fourier maps. All non-hydrogen atoms were refined with anisotropic displacement coefficients unless otherwise specified. All hydrogen atoms were included in the structure factor calculation at idealized positions and were allowed to ride on the neighboring atoms with relative isotropic displacement coefficients.

There are also 3.5 THF molecules in the asymmetric unit. One THF molecule is disordered over an inversion center; it was refined with a DFT-optimized idealized envelope geometry and refined isotropically.

The final least-squares refinement of 753 parameters against 19179 data resulted in residuals *R* (based on F^2 for $I \geq 2\sigma$) and *wR* (based on F^2 for all data) of 0.0802 and 0.2206, respectively. The final difference Fourier map was featureless.

The molecular diagram is drawn with 40% probability ellipsoids.

References

[1] Bruker-AXS. (2000-2007) SADABS, SAINT, and SMART 5.622 Software Reference Manuals. Bruker-AXS, Madison, Wisconsin, USA.

[2] Sheldrick, G. M. (2008) SHELXL. *Acta Cryst.* **A64**, 112-122.

[3] Dolomanov, O.V.; Bourhis, L.J.; Gildea, R.J.; Howard, J.A.K.; Puschmann, H. "OLEX2: a complete structure solution, refinement and analysis program". *J. Appl. Cryst.* (2009) **42**, *339-341*.

Table 6.8 Crystal data and structure refinement for tetraester bisdiazaphos **2**.

Empirical formula	$C_{50}\ H_{44}\ N_4\ O_{12}\ P_2$. 3.5 THF	
Formula weight	1207.20	
Temperature	100(2) K	
Wavelength	0.71073 Å	
Crystal system	Triclinic	
Space group	$P\bar{1}$	
Unit cell dimensions	a = 12.420(3) Å	α= 71.998(3)°.
	b = 14.079(3) Å	β= 77.459(3)°.
	c = 19.532(4) Å	γ = 64.254(3)°.
Volume	2912.1(10) $Å^3$	
Z	2	
Density (calculated)	1.377 Mg/m^3	
Absorption coefficient	0.150 mm^{-1}	
F(000)	1276	
Crystal size	0.50 x 0.46 x 0.38 mm^3	
Theta range for data collection	1.10 to 25.00°.	
Index ranges	-14<=h<=14, -16<=k<=16, -23<=l<=23	
Reflections collected	32825	
Independent reflections	10179 [R(int) = 0.0343]	
Completeness to theta = 25.00°	99.2 %	
Absorption correction	Empirical with SADABS	
Max. and min. transmission	0.9452 and 0.9288	
Refinement method	Full-matrix least-squares on F^2	
Data / restraints / parameters	10179 / 10 / 753	
Goodness-of-fit on F^2	1.044	
Final R indices [I>2sigma(I)]	R1 = 0.0802, wR2 = 0.2144	
R indices (all data)	R1 = 0.0901, wR2 = 0.2206	
Largest diff. peak and hole	1.566 and -1.202 e.$Å^{-3}$	

Table 6.9 Atomic coordinates (x 10^4) and equivalent isotropic displacement parameters ($Å^2$x 10^3) for tetraester bisdiazaphos **2**. U(eq) is defined as one third of the trace of the orthogonalized U^{ij} tensor.

	x	y	z	U(eq)
P(1)	8751(1)	3329(1)	1818(1)	19(1)
P(2)	8617(1)	3781(1)	3338(1)	20(1)
O(1)	10055(2)	4740(2)	1808(2)	29(1)
O(2)	11668(3)	4766(2)	2117(2)	36(1)
O(3)	11570(3)	3159(3)	-154(2)	37(1)
O(4)	9002(2)	712(2)	871(2)	31(1)
O(5)	6735(4)	2099(3)	-136(2)	56(1)
O(6)	6387(3)	2132(2)	1026(2)	40(1)
O(7)	6298(3)	5811(3)	2536(2)	46(1)
O(8)	5591(3)	5683(3)	1632(2)	45(1)
O(9)	4969(2)	4098(2)	4666(2)	33(1)
O(10)	9284(2)	2282(2)	5665(1)	28(1)
O(11)	11228(2)	3518(2)	3685(2)	32(1)
O(12)	11815(2)	4757(2)	3794(1)	29(1)
N(1)	9460(3)	2090(2)	882(2)	22(1)
N(2)	10288(3)	2591(2)	698(2)	23(1)
N(3)	6982(3)	3525(3)	4484(2)	24(1)
N(4)	8058(2)	3276(2)	4780(2)	22(1)
C(1)	10240(3)	3156(3)	1228(2)	22(1)
C(2)	11355(3)	2580(3)	1634(2)	22(1)
C(3)	12004(3)	1483(3)	1687(2)	29(1)
C(4)	13055(4)	900(3)	2031(2)	34(1)
C(5)	13484(4)	1446(4)	2323(2)	37(1)
C(6)	12846(3)	2532(3)	2284(2)	32(1)
C(7)	11784(3)	3123(3)	1946(2)	25(1)
C(8)	11194(3)	4281(3)	1963(2)	25(1)
C(9)	9367(4)	5827(3)	1903(2)	36(1)
C(10)	10949(3)	2632(3)	44(2)	27(1)
C(11)	10904(4)	1887(3)	-359(2)	31(1)
C(12)	10817(3)	863(3)	173(2)	30(1)
C(13)	9698(3)	1171(3)	678(2)	24(1)
C(14)	8311(3)	2780(3)	1206(2)	21(1)
C(15)	7604(3)	3678(3)	596(2)	24(1)
C(16)	7727(3)	4670(3)	369(2)	26(1)
C(17)	7198(4)	5470(4)	-229(2)	33(1)
C(18)	6538(4)	5282(4)	-622(2)	36(1)
C(19)	6418(4)	4305(4)	-418(2)	35(1)
C(20)	6923(3)	3500(3)	189(2)	29(1)
C(21)	6706(4)	2505(4)	332(3)	41(1)
C(22)	6234(5)	1141(5)	1142(3)	55(1)
C(23)	9193(3)	2152(3)	2607(2)	21(1)

C(24)	9525(3)	1078(3)	2579(2)	26(1)
C(25)	9882(3)	218(3)	3179(2)	30(1)
C(26)	9923(3)	423(3)	3822(2)	29(1)
C(27)	9566(3)	1473(3)	3869(2)	26(1)
C(28)	9177(3)	2359(3)	3277(2)	20(1)
C(29)	6996(3)	4030(3)	3706(2)	22(1)
C(30)	6443(3)	3599(3)	3312(2)	26(1)
C(31)	6432(3)	2568(3)	3601(2)	32(1)
C(32)	6018(4)	2113(4)	3238(3)	40(1)
C(33)	5599(4)	2682(4)	2577(3)	44(1)
C(34)	5581(3)	3712(4)	2277(2)	37(1)
C(35)	6000(3)	4189(3)	2636(2)	31(1)
C(36)	5982(3)	5292(4)	2286(2)	34(1)
C(37)	5580(5)	6739(4)	1254(3)	54(1)
C(38)	5940(3)	3682(3)	4924(2)	27(1)
C(39)	6095(3)	3249(3)	5716(2)	33(1)
C(40)	7292(3)	2275(3)	5849(2)	32(1)
C(41)	8310(3)	2584(3)	5439(2)	24(1)
C(42)	8924(3)	3650(3)	4268(2)	19(1)
C(43)	8809(3)	4753(3)	4301(2)	21(1)
C(44)	7701(3)	5473(3)	4542(2)	24(1)
C(45)	7541(3)	6497(3)	4568(2)	30(1)
C(46)	8491(4)	6823(3)	4363(2)	31(1)
C(47)	9601(3)	6124(3)	4123(2)	28(1)
C(48)	9778(3)	5089(3)	4084(2)	22(1)
C(49)	10989(3)	4357(3)	3834(2)	24(1)
C(50)	13040(3)	4109(4)	3566(2)	35(1)
O(13)	2886(4)	7761(4)	2342(2)	73(1)
C(51)	2123(5)	8584(5)	1800(3)	61(1)
C(52)	1262(6)	8129(5)	1730(4)	72(2)
C(53)	1310(6)	7250(5)	2419(4)	66(2)
C(54)	2584(6)	6850(5)	2557(4)	65(2)
O(14)	2166(4)	-59(3)	4711(2)	61(1)
C(55)	2629(6)	469(5)	4050(3)	65(2)
C(56)	3558(6)	767(6)	4231(4)	77(2)
C(57)	3426(5)	517(6)	5033(4)	76(2)
C(58)	2262(5)	369(5)	5242(4)	62(2)
O(15)	6269(3)	9610(3)	2987(2)	56(1)
C(59)	6001(5)	8744(4)	2984(3)	62(2)
C(60)	6789(7)	8323(7)	2353(5)	98(3)
C(61)	7929(5)	8458(5)	2371(4)	66(2)
C(62)	7525(4)	9337(4)	2781(3)	51(1)
O(16)	4005(4)	1157(4)	-175(3)	112(2)
C(63)	3628(4)	281(4)	131(3)	112(2)
C(64)	4688(4)	-636(4)	526(3)	112(2)
C(65)	5787(4)	-456(4)	52(3)	112(2)
C(66)	5233(4)	695(4)	-447(3)	112(2)

Table 6.10 Bond lengths [Å] and angles [°] for tetraester bisdiazaphos **2**.

P(1)-C(23)	1.849(4)	C(9)-H(9B)	0.9800
P(1)-C(14)	1.884(3)	C(9)-H(9A)	0.9800
P(1)-C(1)	1.915(3)	C(9)-H(9C)	0.9800
P(2)-C(28)	1.847(3)	C(10)-C(11)	1.518(5)
P(2)-C(42)	1.875(3)	C(11)-C(12)	1.526(6)
P(2)-C(29)	1.899(3)	C(11)-H(11B)	0.9900
O(1)-C(8)	1.335(5)	C(11)-H(11A)	0.9900
O(1)-C(9)	1.441(5)	C(12)-C(13)	1.496(5)
O(2)-C(8)	1.206(4)	C(12)-H(12A)	0.9900
O(3)-C(10)	1.218(5)	C(12)-H(12B)	0.9900
O(4)-C(13)	1.225(4)	C(14)-C(15)	1.532(5)
O(5)-C(21)	1.207(6)	C(14)-H(14)	1.0000
O(6)-C(21)	1.334(6)	C(15)-C(16)	1.395(5)
O(6)-C(22)	1.431(6)	C(15)-C(20)	1.418(5)
O(7)-C(36)	1.216(5)	C(16)-C(17)	1.394(5)
O(8)-C(36)	1.333(5)	C(16)-H(16)	0.9500
O(8)-C(37)	1.437(6)	C(17)-C(18)	1.386(6)
O(9)-C(38)	1.234(5)	C(17)-H(17)	0.9500
O(10)-C(41)	1.229(4)	C(18)-C(19)	1.374(6)
O(11)-C(49)	1.199(5)	C(18)-H(18)	0.9500
O(12)-C(49)	1.348(4)	C(19)-C(20)	1.399(6)
O(12)-C(50)	1.448(5)	C(19)-H(19)	0.9500
N(1)-C(13)	1.362(5)	C(20)-C(21)	1.472(6)
N(1)-N(2)	1.413(4)	C(22)-H(22A)	0.9800
N(1)-C(14)	1.471(4)	C(22)-H(22B)	0.9800
N(2)-C(10)	1.360(5)	C(22)-H(22C)	0.9800
N(2)-C(1)	1.466(4)	C(23)-C(24)	1.401(5)
N(3)-C(38)	1.359(5)	C(23)-C(28)	1.419(5)
N(3)-N(4)	1.430(4)	C(24)-C(25)	1.385(6)
N(3)-C(29)	1.466(5)	C(24)-H(24)	0.9500
N(4)-C(41)	1.356(5)	C(25)-C(26)	1.388(6)
N(4)-C(42)	1.461(4)	C(25)-H(25)	0.9500
C(1)-C(2)	1.518(5)	C(26)-C(27)	1.373(5)
C(1)-H(1)	1.0000	C(26)-H(26)	0.9500
C(2)-C(3)	1.380(5)	C(27)-C(28)	1.398(5)
C(2)-C(7)	1.422(5)	C(27)-H(27)	0.9500
C(3)-C(4)	1.392(6)	C(29)-C(30)	1.520(5)
C(3)-H(3)	0.9500	C(29)-H(29)	1.0000
C(4)-C(5)	1.401(6)	C(30)-C(31)	1.390(6)
C(4)-H(4)	0.9500	C(30)-C(35)	1.406(6)
C(5)-C(6)	1.368(6)	C(31)-C(32)	1.381(6)
C(5)-H(5)	0.9500	C(31)-H(31)	0.9500
C(6)-C(7)	1.397(5)	C(32)-C(33)	1.367(7)
C(6)-H(6)	0.9500	C(32)-H(32)	0.9500
C(7)-C(8)	1.477(5)	C(33)-C(34)	1.379(7)

C(33)-H(33)	0.9500	C(54)-H(54B)	0.9900
C(34)-C(35)	1.403(5)	C(54)-H(54A)	0.9900
C(34)-H(34)	0.9500	O(14)-C(58)	1.398(7)
C(35)-C(36)	1.483(6)	O(14)-C(55)	1.416(7)
C(37)-H(37B)	0.9800	C(55)-C(56)	1.524(9)
C(37)-H(37A)	0.9800	C(55)-H(55B)	0.9900
C(37)-H(37C)	0.9800	C(55)-H(55A)	0.9900
C(38)-C(39)	1.499(6)	C(56)-C(57)	1.484(10)
C(39)-C(40)	1.529(6)	C(56)-H(56A)	0.9900
C(39)-H(39A)	0.9900	C(56)-H(56B)	0.9900
C(39)-H(39B)	0.9900	C(57)-C(58)	1.501(8)
C(40)-C(41)	1.501(5)	C(57)-H(57B)	0.9900
C(40)-H(40B)	0.9900	C(57)-H(57A)	0.9900
C(40)-H(40A)	0.9900	C(58)-H(58B)	0.9900
C(42)-C(43)	1.517(5)	C(58)-H(58A)	0.9900
C(42)-H(42)	1.0000	O(15)-C(59)	1.398(7)
C(43)-C(44)	1.395(5)	O(15)-C(62)	1.430(6)
C(43)-C(48)	1.414(5)	C(59)-C(60)	1.502(10)
C(44)-C(45)	1.383(5)	C(59)-H(59A)	0.9900
C(44)-H(44)	0.9500	C(59)-H(59B)	0.9900
C(45)-C(46)	1.384(6)	C(60)-C(61)	1.517(9)
C(45)-H(45)	0.9500	C(60)-H(60B)	0.9900
C(46)-C(47)	1.383(6)	C(60)-H(60A)	0.9900
C(46)-H(46)	0.9500	C(61)-C(62)	1.525(7)
C(47)-C(48)	1.400(5)	C(61)-H(61B)	0.9900
C(47)-H(47)	0.9500	C(61)-H(61A)	0.9900
C(48)-C(49)	1.487(5)	C(62)-H(62A)	0.9900
C(50)-H(50A)	0.9800	C(62)-H(62B)	0.9900
C(50)-H(50C)	0.9800	O(16)-C(63)	1.4215
C(50)-H(50B)	0.9800	O(16)-C(66)	1.4253
O(13)-C(54)	1.406(7)	C(63)-C(64)	1.5302
O(13)-C(51)	1.444(7)	C(63)-H(63A)	0.9900
C(51)-C(52)	1.512(8)	C(63)-H(63B)	0.9900
C(51)-H(51A)	0.9900	C(64)-C(65)	1.5470
C(51)-H(51B)	0.9900	C(64)-H(64B)	0.9900
C(52)-C(53)	1.512(9)	C(64)-H(64A)	0.9900
C(52)-H(52B)	0.9900	C(65)-C(66)	1.5472
C(52)-H(52A)	0.9900	C(65)-H(65B)	0.9900
C(53)-C(54)	1.486(8)	C(65)-H(65A)	0.9900
C(53)-H(53B)	0.9900	C(66)-H(66A)	0.9900
C(53)-H(53A)	0.9900	C(66)-H(66B)	0.9900

C(23)-P(1)-C(14)	102.19(16)	C(8)-O(1)-C(9)	116.4(3)
C(23)-P(1)-C(1)	102.94(15)	C(21)-O(6)-C(22)	111.6(4)
C(14)-P(1)-C(1)	89.77(14)	C(36)-O(8)-C(37)	115.4(3)
C(28)-P(2)-C(42)	103.71(15)	C(49)-O(12)-C(50)	116.4(3)
C(28)-P(2)-C(29)	100.31(15)	C(13)-N(1)-N(2)	121.6(3)
C(42)-P(2)-C(29)	88.14(15)	C(13)-N(1)-C(14)	127.2(3)

N(2)-N(1)-C(14)	110.6(3)	C(12)-C(11)-H(11B)	109.6
C(10)-N(2)-N(1)	121.0(3)	C(10)-C(11)-H(11A)	109.6
C(10)-N(2)-C(1)	124.7(3)	C(12)-C(11)-H(11A)	109.6
N(1)-N(2)-C(1)	113.9(3)	H(11B)-C(11)-H(11A)	108.1
C(38)-N(3)-N(4)	119.2(3)	C(13)-C(12)-C(11)	109.5(3)
C(38)-N(3)-C(29)	122.0(3)	C(13)-C(12)-H(12A)	109.8
N(4)-N(3)-C(29)	113.7(3)	C(11)-C(12)-H(12A)	109.8
C(41)-N(4)-N(3)	120.7(3)	C(13)-C(12)-H(12B)	109.8
C(41)-N(4)-C(42)	123.9(3)	C(11)-C(12)-H(12B)	109.8
N(3)-N(4)-C(42)	114.4(3)	H(12A)-C(12)-H(12B)	108.2
N(2)-C(1)-C(2)	111.9(3)	O(4)-C(13)-N(1)	121.1(3)
N(2)-C(1)-P(1)	106.2(2)	O(4)-C(13)-C(12)	125.9(3)
C(2)-C(1)-P(1)	115.4(2)	N(1)-C(13)-C(12)	112.9(3)
N(2)-C(1)-H(1)	107.7	N(1)-C(14)-C(15)	108.4(3)
C(2)-C(1)-H(1)	107.7	N(1)-C(14)-P(1)	104.5(2)
P(1)-C(1)-H(1)	107.7	C(15)-C(14)-P(1)	112.6(2)
C(3)-C(2)-C(7)	118.2(3)	N(1)-C(14)-H(14)	110.4
C(3)-C(2)-C(1)	118.6(3)	C(15)-C(14)-H(14)	110.4
C(7)-C(2)-C(1)	123.2(3)	P(1)-C(14)-H(14)	110.4
C(2)-C(3)-C(4)	122.3(3)	C(16)-C(15)-C(20)	117.4(3)
C(2)-C(3)-H(3)	118.8	C(16)-C(15)-C(14)	120.0(3)
C(4)-C(3)-H(3)	118.8	C(20)-C(15)-C(14)	122.2(3)
C(3)-C(4)-C(5)	119.1(4)	C(17)-C(16)-C(15)	122.1(3)
C(3)-C(4)-H(4)	120.5	C(17)-C(16)-H(16)	118.9
C(5)-C(4)-H(4)	120.5	C(15)-C(16)-H(16)	118.9
C(6)-C(5)-C(4)	119.5(4)	C(18)-C(17)-C(16)	119.7(4)
C(6)-C(5)-H(5)	120.3	C(18)-C(17)-H(17)	120.1
C(4)-C(5)-H(5)	120.3	C(16)-C(17)-H(17)	120.1
C(5)-C(6)-C(7)	121.9(3)	C(19)-C(18)-C(17)	119.4(4)
C(5)-C(6)-H(6)	119.0	C(19)-C(18)-H(18)	120.3
C(7)-C(6)-H(6)	119.0	C(17)-C(18)-H(18)	120.3
C(6)-C(7)-C(2)	119.0(3)	C(18)-C(19)-C(20)	121.6(4)
C(6)-C(7)-C(8)	115.1(3)	C(18)-C(19)-H(19)	119.2
C(2)-C(7)-C(8)	125.9(3)	C(20)-C(19)-H(19)	119.2
O(2)-C(8)-O(1)	122.8(4)	C(19)-C(20)-C(15)	119.7(4)
O(2)-C(8)-C(7)	124.4(3)	C(19)-C(20)-C(21)	114.6(3)
O(1)-C(8)-C(7)	112.8(3)	C(15)-C(20)-C(21)	125.7(4)
O(1)-C(9)-H(9B)	109.5	O(5)-C(21)-O(6)	122.5(4)
O(1)-C(9)-H(9A)	109.5	O(5)-C(21)-C(20)	123.6(4)
H(9B)-C(9)-H(9A)	109.5	O(6)-C(21)-C(20)	113.7(4)
O(1)-C(9)-H(9C)	109.5	O(6)-C(22)-H(22A)	109.5
H(9B)-C(9)-H(9C)	109.5	O(6)-C(22)-H(22B)	109.5
H(9A)-C(9)-H(9C)	109.5	H(22A)-C(22)-H(22B)	109.5
O(3)-C(10)-N(2)	121.7(3)	O(6)-C(22)-H(22C)	109.5
O(3)-C(10)-C(11)	125.3(3)	H(22A)-C(22)-H(22C)	109.5
N(2)-C(10)-C(11)	112.7(3)	H(22B)-C(22)-H(22C)	109.5
C(10)-C(11)-C(12)	110.3(3)	C(24)-C(23)-C(28)	118.7(3)
C(10)-C(11)-H(11B)	109.6	C(24)-C(23)-P(1)	123.5(3)

C(28)-C(23)-P(1)	117.8(3)	H(37A)-C(37)-H(37C)	109.5
C(25)-C(24)-C(23)	121.5(3)	O(9)-C(38)-N(3)	120.4(3)
C(25)-C(24)-H(24)	119.3	O(9)-C(38)-C(39)	124.7(3)
C(23)-C(24)-H(24)	119.3	N(3)-C(38)-C(39)	114.8(3)
C(24)-C(25)-C(26)	119.4(3)	C(38)-C(39)-C(40)	110.9(3)
C(24)-C(25)-H(25)	120.3	C(38)-C(39)-H(39A)	109.5
C(26)-C(25)-H(25)	120.3	C(40)-C(39)-H(39A)	109.5
C(27)-C(26)-C(25)	120.2(4)	C(38)-C(39)-H(39B)	109.5
C(27)-C(26)-H(26)	119.9	C(40)-C(39)-H(39B)	109.5
C(25)-C(26)-H(26)	119.9	H(39A)-C(39)-H(39B)	108.0
C(26)-C(27)-C(28)	121.7(3)	C(41)-C(40)-C(39)	110.2(3)
C(26)-C(27)-H(27)	119.1	C(41)-C(40)-H(40B)	109.6
C(28)-C(27)-H(27)	119.1	C(39)-C(40)-H(40B)	109.6
C(27)-C(28)-C(23)	118.4(3)	C(41)-C(40)-H(40A)	109.6
C(27)-C(28)-P(2)	122.6(3)	C(39)-C(40)-H(40A)	109.6
C(23)-C(28)-P(2)	118.9(3)	H(40B)-C(40)-H(40A)	108.1
N(3)-C(29)-C(30)	112.3(3)	O(10)-C(41)-N(4)	121.0(3)
N(3)-C(29)-P(2)	107.5(2)	O(10)-C(41)-C(40)	125.1(3)
C(30)-C(29)-P(2)	111.4(2)	N(4)-C(41)-C(40)	113.8(3)
N(3)-C(29)-H(29)	108.5	N(4)-C(42)-C(43)	113.1(3)
C(30)-C(29)-H(29)	108.5	N(4)-C(42)-P(2)	107.2(2)
P(2)-C(29)-H(29)	108.5	C(43)-C(42)-P(2)	107.6(2)
C(31)-C(30)-C(35)	118.3(3)	N(4)-C(42)-H(42)	109.6
C(31)-C(30)-C(29)	119.8(3)	C(43)-C(42)-H(42)	109.6
C(35)-C(30)-C(29)	121.8(3)	P(2)-C(42)-H(42)	109.6
C(32)-C(31)-C(30)	121.8(4)	C(44)-C(43)-C(48)	118.5(3)
C(32)-C(31)-H(31)	119.1	C(44)-C(43)-C(42)	118.9(3)
C(30)-C(31)-H(31)	119.1	C(48)-C(43)-C(42)	122.5(3)
C(33)-C(32)-C(31)	119.9(4)	C(45)-C(44)-C(43)	121.2(3)
C(33)-C(32)-H(32)	120.0	C(45)-C(44)-H(44)	119.4
C(31)-C(32)-H(32)	120.0	C(43)-C(44)-H(44)	119.4
C(32)-C(33)-C(34)	120.0(4)	C(44)-C(45)-C(46)	120.3(4)
C(32)-C(33)-H(33)	120.0	C(44)-C(45)-H(45)	119.9
C(34)-C(33)-H(33)	120.0	C(46)-C(45)-H(45)	119.9
C(33)-C(34)-C(35)	121.0(4)	C(47)-C(46)-C(45)	119.7(4)
C(33)-C(34)-H(34)	119.5	C(47)-C(46)-H(46)	120.2
C(35)-C(34)-H(34)	119.5	C(45)-C(46)-H(46)	120.2
C(34)-C(35)-C(30)	119.0(4)	C(46)-C(47)-C(48)	120.9(3)
C(34)-C(35)-C(36)	119.1(4)	C(46)-C(47)-H(47)	119.5
C(30)-C(35)-C(36)	121.9(3)	C(48)-C(47)-H(47)	119.5
O(7)-C(36)-O(8)	121.2(4)	C(47)-C(48)-C(43)	119.3(3)
O(7)-C(36)-C(35)	126.4(4)	C(47)-C(48)-C(49)	119.2(3)
O(8)-C(36)-C(35)	112.4(4)	C(43)-C(48)-C(49)	121.4(3)
O(8)-C(37)-H(37B)	109.5	O(11)-C(49)-O(12)	123.1(3)
O(8)-C(37)-H(37A)	109.5	O(11)-C(49)-C(48)	126.0(3)
H(37B)-C(37)-H(37A)	109.5	O(12)-C(49)-C(48)	110.9(3)
O(8)-C(37)-H(37C)	109.5	O(12)-C(50)-H(50A)	109.5
H(37B)-C(37)-H(37C)	109.5	O(12)-C(50)-H(50C)	109.5

H(50A)-C(50)-H(50C)	109.5	O(14)-C(58)-C(57)	105.7(5)
O(12)-C(50)-H(50B)	109.5	O(14)-C(58)-H(58B)	110.6
H(50A)-C(50)-H(50B)	109.5	C(57)-C(58)-H(58B)	110.6
H(50C)-C(50)-H(50B)	109.5	O(14)-C(58)-H(58A)	110.6
C(54)-O(13)-C(51)	109.2(4)	C(57)-C(58)-H(58A)	110.6
O(13)-C(51)-C(52)	105.2(5)	H(58B)-C(58)-H(58A)	108.7
O(13)-C(51)-H(51A)	110.7	C(59)-O(15)-C(62)	108.7(4)
C(52)-C(51)-H(51A)	110.7	O(15)-C(59)-C(60)	104.4(5)
O(13)-C(51)-H(51B)	110.7	O(15)-C(59)-H(59A)	110.9
C(52)-C(51)-H(51B)	110.7	C(60)-C(59)-H(59A)	110.9
H(51A)-C(51)-H(51B)	108.8	O(15)-C(59)-H(59B)	110.9
C(53)-C(52)-C(51)	104.5(5)	C(60)-C(59)-H(59B)	110.9
C(53)-C(52)-H(52B)	110.8	H(59A)-C(59)-H(59B)	108.9
C(51)-C(52)-H(52B)	110.8	C(59)-C(60)-C(61)	102.6(5)
C(53)-C(52)-H(52A)	110.8	C(59)-C(60)-H(60B)	111.2
C(51)-C(52)-H(52A)	110.8	C(61)-C(60)-H(60B)	111.2
H(52B)-C(52)-H(52A)	108.9	C(59)-C(60)-H(60A)	111.2
C(54)-C(53)-C(52)	100.7(5)	C(61)-C(60)-H(60A)	111.2
C(54)-C(53)-H(53B)	111.6	H(60B)-C(60)-H(60A)	109.2
C(52)-C(53)-H(53B)	111.6	C(60)-C(61)-C(62)	104.4(4)
C(54)-C(53)-H(53A)	111.6	C(60)-C(61)-H(61B)	110.9
C(52)-C(53)-H(53A)	111.6	C(62)-C(61)-H(61B)	110.9
H(53B)-C(53)-H(53A)	109.4	C(60)-C(61)-H(61A)	110.9
O(13)-C(54)-C(53)	106.8(5)	C(62)-C(61)-H(61A)	110.9
O(13)-C(54)-H(54B)	110.4	H(61B)-C(61)-H(61A)	108.9
C(53)-C(54)-H(54B)	110.4	O(15)-C(62)-C(61)	105.7(4)
O(13)-C(54)-H(54A)	110.4	O(15)-C(62)-H(62A)	110.6
C(53)-C(54)-H(54A)	110.4	C(61)-C(62)-H(62A)	110.6
H(54B)-C(54)-H(54A)	108.6	O(15)-C(62)-H(62B)	110.6
C(58)-O(14)-C(55)	105.8(4)	C(61)-C(62)-H(62B)	110.6
O(14)-C(55)-C(56)	107.0(5)	H(62A)-C(62)-H(62B)	108.7
O(14)-C(55)-H(55B)	110.3	C(63)-O(16)-C(66)	106.7
C(56)-C(55)-H(55B)	110.3	O(16)-C(63)-C(64)	104.8
O(14)-C(55)-H(55A)	110.3	O(16)-C(63)-H(63A)	110.8
C(56)-C(55)-H(55A)	110.3	C(64)-C(63)-H(63A)	110.8
H(55B)-C(55)-H(55A)	108.6	O(16)-C(63)-H(63B)	110.8
C(57)-C(56)-C(55)	104.2(5)	C(64)-C(63)-H(63B)	110.8
C(57)-C(56)-H(56A)	110.9	H(63A)-C(63)-H(63B)	108.9
C(55)-C(56)-H(56A)	110.9	C(63)-C(64)-C(65)	102.9
C(57)-C(56)-H(56B)	110.9	C(63)-C(64)-H(64B)	111.2
C(55)-C(56)-H(56B)	110.9	C(65)-C(64)-H(64B)	111.2
H(56A)-C(56)-H(56B)	108.9	C(63)-C(64)-H(64A)	111.2
C(56)-C(57)-C(58)	103.9(5)	C(65)-C(64)-H(64A)	111.2
C(56)-C(57)-H(57B)	111.0	H(64B)-C(64)-H(64A)	109.1
C(58)-C(57)-H(57B)	111.0	C(64)-C(65)-C(66)	103.8
C(56)-C(57)-H(57A)	111.0	C(64)-C(65)-H(65B)	111.0
C(58)-C(57)-H(57A)	111.0	C(66)-C(65)-H(65B)	111.0
H(57B)-C(57)-H(57A)	109.0	C(64)-C(65)-H(65A)	111.0

C(66)-C(65)-H(65A)	111.0	C(65)-C(66)-H(66A)	110.4
H(65B)-C(65)-H(65A)	109.0	O(16)-C(66)-H(66B)	110.4
O(16)-C(66)-C(65)	106.6	C(65)-C(66)-H(66B)	110.4
O(16)-C(66)-H(66A)	110.4	H(66A)-C(66)-H(66B)	108.6

Symmetry transformations used to generate equivalent atoms:

Table 6.11 Anisotropic displacement parameters ($Å^2 x\ 10^3$) for tetraester bisdiazaphos **2**. The anisotropic displacement factor exponent takes the form: $-2\pi^2[\ h^2\ a^{*2}U^{11} + ...\ + 2\ h\ k\ a^*\ b^*\ U^{12}\ ]$.

	U^{11}	U^{22}	U^{33}	U^{23}	U^{13}	U^{12}
P(1)	16(1)	26(1)	18(1)	-9(1)	-2(1)	-9(1)
P(2)	17(1)	26(1)	19(1)	-8(1)	-3(1)	-9(1)
O(1)	25(1)	33(1)	38(2)	-18(1)	-3(1)	-13(1)
O(2)	41(2)	40(2)	42(2)	-11(1)	-12(1)	-24(1)
O(3)	42(2)	57(2)	31(2)	-17(1)	7(1)	-36(2)
O(4)	32(1)	35(2)	35(2)	-17(1)	4(1)	-19(1)
O(5)	75(2)	53(2)	63(2)	-22(2)	-35(2)	-26(2)
O(6)	30(2)	38(2)	66(2)	-18(2)	-15(1)	-16(1)
O(7)	61(2)	43(2)	40(2)	-8(1)	-25(2)	-18(2)
O(8)	40(2)	66(2)	33(2)	-13(2)	-16(1)	-18(2)
O(9)	18(1)	46(2)	42(2)	-21(1)	1(1)	-12(1)
O(10)	25(1)	31(1)	26(1)	-4(1)	-6(1)	-10(1)
O(11)	24(1)	40(2)	39(2)	-20(1)	7(1)	-16(1)
O(12)	20(1)	45(2)	31(1)	-16(1)	1(1)	-17(1)
N(1)	16(1)	33(2)	26(2)	-15(1)	2(1)	-13(1)
N(2)	20(2)	34(2)	25(2)	-15(1)	1(1)	-16(1)
N(3)	16(1)	34(2)	25(2)	-8(1)	-3(1)	-12(1)
N(4)	15(1)	30(2)	24(2)	-8(1)	-2(1)	-11(1)
C(1)	17(2)	30(2)	24(2)	-12(2)	-1(1)	-10(1)
C(2)	18(2)	33(2)	22(2)	-11(1)	0(1)	-13(2)
C(3)	24(2)	36(2)	35(2)	-14(2)	-4(2)	-14(2)
C(4)	26(2)	35(2)	43(2)	-13(2)	-8(2)	-7(2)
C(5)	24(2)	43(2)	46(2)	-10(2)	-15(2)	-10(2)
C(6)	27(2)	44(2)	36(2)	-13(2)	-7(2)	-20(2)
C(7)	20(2)	37(2)	24(2)	-10(2)	-1(1)	-15(2)
C(8)	28(2)	37(2)	17(2)	-9(2)	1(1)	-20(2)
C(9)	35(2)	31(2)	45(2)	-16(2)	-8(2)	-11(2)
C(10)	25(2)	39(2)	23(2)	-10(2)	1(1)	-17(2)
C(11)	32(2)	49(2)	26(2)	-20(2)	7(2)	-24(2)
C(12)	26(2)	40(2)	33(2)	-22(2)	2(2)	-14(2)
C(13)	23(2)	31(2)	24(2)	-11(2)	-5(1)	-11(2)
C(14)	16(2)	31(2)	23(2)	-12(1)	-1(1)	-11(1)
C(15)	18(2)	36(2)	19(2)	-12(2)	-1(1)	-10(2)
C(16)	23(2)	41(2)	22(2)	-6(2)	-5(1)	-18(2)
C(17)	33(2)	42(2)	28(2)	-1(2)	-5(2)	-21(2)
C(18)	33(2)	52(3)	25(2)	0(2)	-10(2)	-21(2)
C(19)	27(2)	55(3)	30(2)	-14(2)	-9(2)	-16(2)
C(20)	21(2)	44(2)	31(2)	-16(2)	-4(2)	-14(2)
C(21)	35(2)	42(2)	52(3)	-9(2)	-22(2)	-13(2)
C(22)	60(3)	61(3)	55(3)	-16(3)	3(2)	-36(3)
C(23)	15(2)	28(2)	23(2)	-7(1)	-2(1)	-9(1)

C(24)	27(2)	28(2)	24(2)	-9(2)	-2(1)	-11(2)
C(25)	28(2)	26(2)	38(2)	-13(2)	-2(2)	-9(2)
C(26)	26(2)	29(2)	29(2)	-4(2)	-6(2)	-9(2)
C(27)	23(2)	30(2)	24(2)	-8(2)	-4(1)	-10(2)
C(28)	14(2)	26(2)	21(2)	-7(1)	-1(1)	-8(1)
C(29)	14(2)	29(2)	27(2)	-12(2)	-4(1)	-6(1)
C(30)	11(2)	39(2)	34(2)	-21(2)	0(1)	-8(2)
C(31)	20(2)	41(2)	43(2)	-23(2)	3(2)	-14(2)
C(32)	25(2)	52(3)	59(3)	-35(2)	11(2)	-21(2)
C(33)	21(2)	74(3)	61(3)	-48(3)	11(2)	-27(2)
C(34)	16(2)	68(3)	37(2)	-30(2)	1(2)	-16(2)
C(35)	15(2)	49(2)	33(2)	-22(2)	-1(2)	-9(2)
C(36)	16(2)	52(3)	30(2)	-19(2)	-6(2)	-3(2)
C(37)	53(3)	66(3)	39(3)	-7(2)	-27(2)	-13(2)
C(38)	20(2)	30(2)	36(2)	-14(2)	1(2)	-12(2)
C(39)	24(2)	40(2)	33(2)	-11(2)	7(2)	-15(2)
C(40)	28(2)	32(2)	35(2)	-4(2)	3(2)	-15(2)
C(41)	24(2)	23(2)	24(2)	-8(1)	2(1)	-9(1)
C(42)	16(2)	28(2)	15(2)	-7(1)	-1(1)	-11(1)
C(43)	20(2)	30(2)	17(2)	-6(1)	-5(1)	-11(1)
C(44)	22(2)	35(2)	20(2)	-10(2)	-2(1)	-13(2)
C(45)	27(2)	34(2)	31(2)	-15(2)	-3(2)	-8(2)
C(46)	35(2)	31(2)	34(2)	-14(2)	-3(2)	-15(2)
C(47)	30(2)	39(2)	25(2)	-11(2)	-1(2)	-20(2)
C(48)	20(2)	32(2)	17(2)	-7(1)	-4(1)	-13(2)
C(49)	21(2)	36(2)	18(2)	-7(2)	-2(1)	-14(2)
C(50)	19(2)	55(3)	39(2)	-20(2)	1(2)	-18(2)
O(13)	72(3)	94(3)	65(3)	-21(2)	-9(2)	-41(2)
C(51)	65(4)	56(3)	68(4)	-17(3)	0(3)	-29(3)
C(52)	64(4)	71(4)	80(4)	-7(3)	-28(3)	-23(3)
C(53)	63(4)	54(3)	85(4)	-17(3)	-15(3)	-24(3)
C(54)	63(4)	68(4)	68(4)	-11(3)	-17(3)	-29(3)
O(14)	73(3)	70(2)	60(2)	-22(2)	-1(2)	-43(2)
C(55)	68(4)	75(4)	60(3)	-10(3)	0(3)	-43(3)
C(56)	68(4)	86(5)	77(4)	9(3)	-15(3)	-47(4)
C(57)	49(3)	107(5)	93(5)	-62(4)	5(3)	-32(3)
C(58)	50(3)	64(3)	83(4)	-42(3)	4(3)	-21(3)
O(15)	39(2)	64(2)	64(2)	-30(2)	0(2)	-11(2)
C(59)	36(3)	49(3)	79(4)	9(3)	-13(3)	-10(2)
C(60)	69(4)	106(6)	158(8)	-90(6)	4(5)	-38(4)
C(61)	45(3)	82(4)	78(4)	-50(3)	6(3)	-15(3)
C(62)	47(3)	58(3)	50(3)	-23(2)	-2(2)	-17(2)

Table 6.12 Hydrogen coordinates (x 10^4) and isotropic displacement parameters (Å^{2}x 10^3) for tetraester bisdiazaphos **2**.

	x	y	z	U(eq)
H(1)	10204	3898	958	26
H(3)	11724	1112	1482	35
H(4)	13475	141	2067	41
H(5)	14213	1066	2547	45
H(6)	13132	2894	2492	38
H(9B)	9226	5808	2420	54
H(9A)	8594	6126	1703	54
H(9C)	9811	6286	1652	54
H(11B)	11636	1683	-699	38
H(11A)	10199	2274	-643	38
H(12A)	10802	377	-95	36
H(12B)	11528	468	452	36
H(14)	7842	2337	1493	26
H(16)	8187	4805	630	32
H(17)	7289	6142	-367	40
H(18)	6171	5824	-1030	43
H(19)	5981	4172	-696	42
H(22A)	5605	1269	856	83
H(22B)	6002	890	1656	83
H(22C)	6991	588	993	83
H(24)	9505	935	2138	31
H(25)	10098	-505	3151	36
H(26)	10198	-164	4230	34
H(27)	9583	1600	4316	31
H(29)	6525	4832	3634	27
H(31)	6718	2166	4061	38
H(32)	6023	1406	3447	48
H(33)	5320	2367	2325	53
H(34)	5281	4105	1820	44
H(37B)	5055	7268	1536	81
H(37A)	5281	6957	781	81
H(37C)	6397	6712	1186	81
H(39A)	5428	3028	5971	39
H(39B)	6063	3829	5915	39
H(40B)	7394	2024	6372	39
H(40A)	7297	1669	5690	39
H(42)	9758	3102	4359	22
H(44)	7044	5256	4691	29
H(45)	6776	6979	4728	37
H(46)	8382	7524	4387	38
H(47)	10252	6350	3982	34

H(50A)	13205	3336	3774	53
H(50C)	13593	4300	3733	53
H(50B)	13151	4253	3037	53
H(51A)	2603	8722	1333	73
H(51B)	1681	9274	1954	73
H(52B)	438	8700	1687	87
H(52A)	1519	7821	1301	87
H(53B)	750	7550	2817	79
H(53A)	1131	6670	2346	79
H(54B)	2680	6503	3077	77
H(54A)	3110	6309	2276	77
H(55B)	1976	1131	3813	78
H(55A)	3006	-21	3718	78
H(56A)	4378	328	4047	92
H(56B)	3392	1548	4020	92
H(57B)	3390	1124	5204	91
H(57A)	4102	-155	5236	91
H(58B)	2269	-138	5724	74
H(58A)	1579	1074	5256	74
H(59A)	5142	8995	2921	75
H(59B)	6186	8173	3441	75
H(60B)	6424	8757	1893	117
H(60A)	6947	7550	2415	117
H(61B)	8281	8689	1875	79
H(61A)	8532	7769	2625	79
H(62A)	7967	9060	3214	62
H(62B)	7669	9981	2469	62
H(63A)	3454	56	-251	135
H(63B)	2900	491	473	135
H(64B)	4713	-1358	549	135
H(64A)	4645	-574	1023	135
H(65B)	6215	-1008	-235	135
H(65A)	6354	-487	352	135
H(66A)	5658	1145	-439	135
H(66B)	5296	651	-951	135

Table 6.13 Torsion angles [°] for tetraester bisdiazaphos **2**.

C(13)-N(1)-N(2)-C(10)	37.6(5)	C(14)-N(1)-C(13)-O(4)	-13.6(6)
C(14)-N(1)-N(2)-C(10)	-133.9(3)	N(2)-N(1)-C(13)-C(12)	-7.5(5)
C(13)-N(1)-N(2)-C(1)	-149.6(3)	C(14)-N(1)-C(13)-C(12)	162.5(3)
C(14)-N(1)-N(2)-C(1)	38.9(4)	C(11)-C(12)-C(13)-O(4)	136.9(4)
C(38)-N(3)-N(4)-C(41)	40.7(5)	C(11)-C(12)-C(13)-N(1)	-39.0(4)
C(29)-N(3)-N(4)-C(41)	-164.1(3)	C(13)-N(1)-C(14)-C(15)	-91.6(4)
C(38)-N(3)-N(4)-C(42)	-150.5(3)	N(2)-N(1)-C(14)-C(15)	79.3(3)
C(29)-N(3)-N(4)-C(42)	4.7(4)	C(13)-N(1)-C(14)-P(1)	148.1(3)
C(10)-N(2)-C(1)-C(2)	-77.1(4)	N(2)-N(1)-C(14)-P(1)	-41.0(3)
N(1)-N(2)-C(1)-C(2)	110.5(3)	C(23)-P(1)-C(14)-N(1)	-77.3(2)
C(10)-N(2)-C(1)-P(1)	156.3(3)	C(1)-P(1)-C(14)-N(1)	25.9(2)
N(1)-N(2)-C(1)-P(1)	-16.2(3)	C(23)-P(1)-C(14)-C(15)	165.3(2)
C(23)-P(1)-C(1)-N(2)	95.9(2)	C(1)-P(1)-C(14)-C(15)	-91.5(3)
C(14)-P(1)-C(1)-N(2)	-6.6(2)	N(1)-C(14)-C(15)-C(16)	-91.0(4)
C(23)-P(1)-C(1)-C(2)	-28.7(3)	P(1)-C(14)-C(15)-C(16)	24.0(4)
C(14)-P(1)-C(1)-C(2)	-131.1(3)	N(1)-C(14)-C(15)-C(20)	81.4(4)
N(2)-C(1)-C(2)-C(3)	-24.3(4)	P(1)-C(14)-C(15)-C(20)	-163.5(3)
P(1)-C(1)-C(2)-C(3)	97.2(3)	C(20)-C(15)-C(16)-C(17)	0.7(5)
N(2)-C(1)-C(2)-C(7)	153.8(3)	C(14)-C(15)-C(16)-C(17)	173.5(3)
P(1)-C(1)-C(2)-C(7)	-84.7(4)	C(15)-C(16)-C(17)-C(18)	-0.9(6)
C(7)-C(2)-C(3)-C(4)	-0.2(6)	C(16)-C(17)-C(18)-C(19)	-0.3(6)
C(1)-C(2)-C(3)-C(4)	178.1(4)	C(17)-C(18)-C(19)-C(20)	1.5(6)
C(2)-C(3)-C(4)-C(5)	-1.2(6)	C(18)-C(19)-C(20)-C(15)	-1.7(6)
C(3)-C(4)-C(5)-C(6)	1.9(6)	C(18)-C(19)-C(20)-C(21)	179.8(4)
C(4)-C(5)-C(6)-C(7)	-1.4(6)	C(16)-C(15)-C(20)-C(19)	0.6(5)
C(5)-C(6)-C(7)-C(2)	0.0(6)	C(14)-C(15)-C(20)-C(19)	-172.1(3)
C(5)-C(6)-C(7)-C(8)	178.9(4)	C(16)-C(15)-C(20)-C(21)	178.9(4)
C(3)-C(2)-C(7)-C(6)	0.7(5)	C(14)-C(15)-C(20)-C(21)	6.2(6)
C(1)-C(2)-C(7)-C(6)	-177.4(3)	C(22)-O(6)-C(21)-O(5)	7.0(6)
C(3)-C(2)-C(7)-C(8)	-177.9(3)	C(22)-O(6)-C(21)-C(20)	-177.6(4)
C(1)-C(2)-C(7)-C(8)	3.9(5)	C(19)-C(20)-C(21)-O(5)	39.9(6)
C(9)-O(1)-C(8)-O(2)	-6.2(5)	C(15)-C(20)-C(21)-O(5)	-138.6(4)
C(9)-O(1)-C(8)-C(7)	172.3(3)	C(19)-C(20)-C(21)-O(6)	-135.5(4)
C(6)-C(7)-C(8)-O(2)	14.6(5)	C(15)-C(20)-C(21)-O(6)	46.1(6)
C(2)-C(7)-C(8)-O(2)	-166.6(4)	C(14)-P(1)-C(23)-C(24)	20.9(3)
C(6)-C(7)-C(8)-O(1)	-163.8(3)	C(1)-P(1)-C(23)-C(24)	-71.7(3)
C(2)-C(7)-C(8)-O(1)	14.9(5)	C(14)-P(1)-C(23)-C(28)	-158.3(3)
N(1)-N(2)-C(10)-O(3)	172.0(4)	C(1)-P(1)-C(23)-C(28)	109.1(3)
C(1)-N(2)-C(10)-O(3)	0.0(6)	C(28)-C(23)-C(24)-C(25)	-2.7(5)
N(1)-N(2)-C(10)-C(11)	-13.1(5)	P(1)-C(23)-C(24)-C(25)	178.1(3)
C(1)-N(2)-C(10)-C(11)	175.0(3)	C(23)-C(24)-C(25)-C(26)	-0.5(6)
O(3)-C(10)-C(11)-C(12)	140.9(4)	C(24)-C(25)-C(26)-C(27)	2.6(6)
N(2)-C(10)-C(11)-C(12)	-33.8(5)	C(25)-C(26)-C(27)-C(28)	-1.3(6)
C(10)-C(11)-C(12)-C(13)	60.3(4)	C(26)-C(27)-C(28)-C(23)	-2.0(5)
N(2)-N(1)-C(13)-O(4)	176.3(3)	C(26)-C(27)-C(28)-P(2)	176.7(3)

C(24)-C(23)-C(28)-C(27)	3.9(5)	C(39)-C(40)-C(41)-O(10)	140.8(4)
P(1)-C(23)-C(28)-C(27)	-176.9(2)	C(39)-C(40)-C(41)-N(4)	-37.2(4)
C(24)-C(23)-C(28)-P(2)	-174.8(3)	C(41)-N(4)-C(42)-C(43)	-97.0(4)
P(1)-C(23)-C(28)-P(2)	4.4(4)	N(3)-N(4)-C(42)-C(43)	94.6(3)
C(42)-P(2)-C(28)-C(27)	7.4(3)	C(41)-N(4)-C(42)-P(2)	144.5(3)
C(29)-P(2)-C(28)-C(27)	-83.2(3)	N(3)-N(4)-C(42)-P(2)	-23.8(3)
C(42)-P(2)-C(28)-C(23)	-173.9(3)	C(28)-P(2)-C(42)-N(4)	-73.0(2)
C(29)-P(2)-C(28)-C(23)	95.5(3)	C(29)-P(2)-C(42)-N(4)	27.2(2)
C(38)-N(3)-C(29)-C(30)	-66.0(4)	C(28)-P(2)-C(42)-C(43)	165.1(2)
N(4)-N(3)-C(29)-C(30)	139.5(3)	C(29)-P(2)-C(42)-C(43)	-94.8(2)
C(38)-N(3)-C(29)-P(2)	171.0(3)	N(4)-C(42)-C(43)-C(44)	-26.2(4)
N(4)-N(3)-C(29)-P(2)	16.6(3)	P(2)-C(42)-C(43)-C(44)	92.1(3)
C(28)-P(2)-C(29)-N(3)	78.8(2)	N(4)-C(42)-C(43)-C(48)	155.0(3)
C(42)-P(2)-C(29)-N(3)	-24.8(2)	P(2)-C(42)-C(43)-C(48)	-86.8(3)
C(28)-P(2)-C(29)-C(30)	-44.7(3)	C(48)-C(43)-C(44)-C(45)	0.3(5)
C(42)-P(2)-C(29)-C(30)	-148.3(3)	C(42)-C(43)-C(44)-C(45)	-178.6(3)
N(3)-C(29)-C(30)-C(31)	-25.3(4)	C(43)-C(44)-C(45)-C(46)	-0.9(6)
P(2)-C(29)-C(30)-C(31)	95.4(3)	C(44)-C(45)-C(46)-C(47)	0.7(6)
N(3)-C(29)-C(30)-C(35)	158.6(3)	C(45)-C(46)-C(47)-C(48)	0.0(6)
P(2)-C(29)-C(30)-C(35)	-80.7(4)	C(46)-C(47)-C(48)-C(43)	-0.6(5)
C(35)-C(30)-C(31)-C(32)	0.9(5)	C(46)-C(47)-C(48)-C(49)	-179.1(3)
C(29)-C(30)-C(31)-C(32)	-175.3(3)	C(44)-C(43)-C(48)-C(47)	0.5(5)
C(30)-C(31)-C(32)-C(33)	-0.2(6)	C(42)-C(43)-C(48)-C(47)	179.3(3)
C(31)-C(32)-C(33)-C(34)	-0.6(6)	C(44)-C(43)-C(48)-C(49)	178.9(3)
C(32)-C(33)-C(34)-C(35)	0.7(6)	C(42)-C(43)-C(48)-C(49)	-2.2(5)
C(33)-C(34)-C(35)-C(30)	0.0(5)	C(50)-O(12)-C(49)-O(11)	-0.8(5)
C(33)-C(34)-C(35)-C(36)	179.0(3)	C(50)-O(12)-C(49)-C(48)	179.1(3)
C(31)-C(30)-C(35)-C(34)	-0.8(5)	C(47)-C(48)-C(49)-O(11)	-169.5(4)
C(29)-C(30)-C(35)-C(34)	175.4(3)	C(43)-C(48)-C(49)-O(11)	12.0(5)
C(31)-C(30)-C(35)-C(36)	-179.8(3)	C(47)-C(48)-C(49)-O(12)	10.6(4)
C(29)-C(30)-C(35)-C(36)	-3.6(5)	C(43)-C(48)-C(49)-O(12)	-167.8(3)
C(37)-O(8)-C(36)-O(7)	0.3(6)	C(54)-O(13)-C(51)-C(52)	3.4(7)
C(37)-O(8)-C(36)-C(35)	-178.4(4)	O(13)-C(51)-C(52)-C(53)	19.3(7)
C(34)-C(35)-C(36)-O(7)	178.8(4)	C(51)-C(52)-C(53)-C(54)	-33.1(7)
C(30)-C(35)-C(36)-O(7)	-2.2(6)	C(51)-O(13)-C(54)-C(53)	-25.5(7)
C(34)-C(35)-C(36)-O(8)	-2.5(5)	C(52)-C(53)-C(54)-O(13)	36.2(6)
C(30)-C(35)-C(36)-O(8)	176.5(3)	C(58)-O(14)-C(55)-C(56)	28.7(7)
N(4)-N(3)-C(38)-O(9)	166.0(3)	O(14)-C(55)-C(56)-C(57)	-8.3(7)
C(29)-N(3)-C(38)-O(9)	12.9(5)	C(55)-C(56)-C(57)-C(58)	-13.6(7)
N(4)-N(3)-C(38)-C(39)	-17.9(5)	C(55)-O(14)-C(58)-C(57)	-37.8(7)
C(29)-N(3)-C(38)-C(39)	-171.0(3)	C(56)-C(57)-C(58)-O(14)	31.7(7)
O(9)-C(38)-C(39)-C(40)	147.2(4)	C(62)-O(15)-C(59)-C(60)	-37.0(6)
N(3)-C(38)-C(39)-C(40)	-28.8(5)	O(15)-C(59)-C(60)-C(61)	36.4(7)
C(38)-C(39)-C(40)-C(41)	56.6(4)	C(59)-C(60)-C(61)-C(62)	-22.8(8)
N(3)-N(4)-C(41)-O(10)	172.7(3)	C(59)-O(15)-C(62)-C(61)	21.8(6)
C(42)-N(4)-C(41)-O(10)	5.0(5)	C(60)-C(61)-C(62)-O(15)	2.0(7)
N(3)-N(4)-C(41)-C(40)	-9.2(5)	C(66)-O(16)-C(63)-C(64)	40.7
C(42)-N(4)-C(41)-C(40)	-176.9(3)	O(16)-C(63)-C(64)-C(65)	-32.7

C(63)-C(64)-C(65)-C(66)	13.5	C(64)-C(65)-C(66)-O(16)	9.8
C(63)-O(16)-C(66)-C(65)	-31.6		

Symmetry transformations used to generate equivalent atoms:

6.6 Crystallography Data for (2*S*)-2-(1,3-dioxolan-2-yl)-propanal 2,4-dinitrophenylhydrazone 6 (Chapter 4)

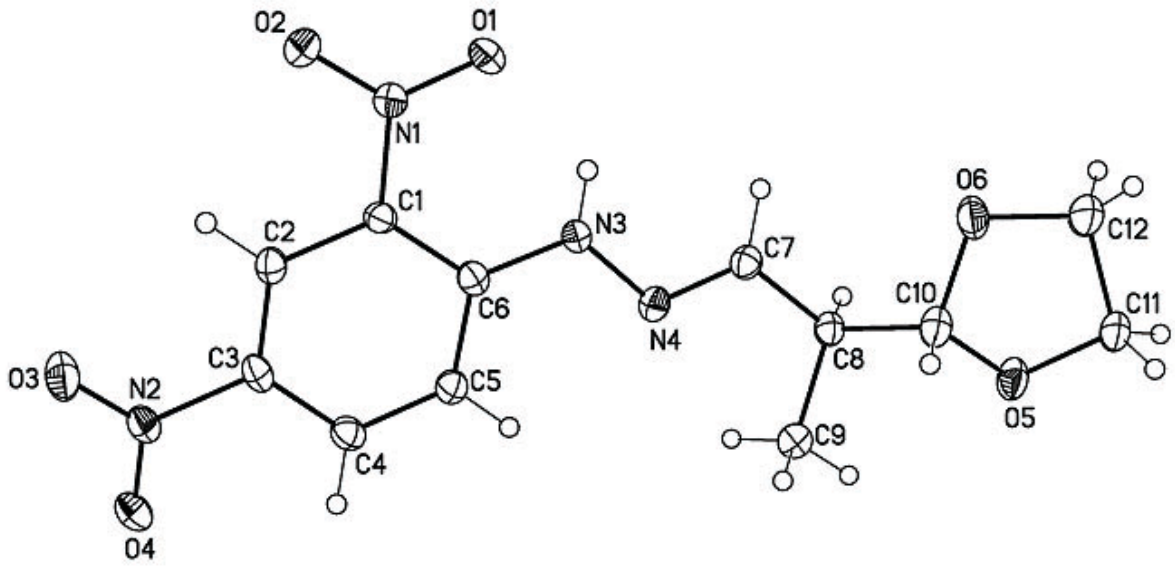

Figure 6.4 ORTEP drawing of (2*S*)-2-(1,3-dioxolan-2-yl)-propanal 2,4-dinitrophenylhydrazone **6**. Thermal ellipsoids are drawn at the 50% probability level.

Data Collection

A colorless crystal with approximate dimensions 0.44 x 0.13 x 0.12 mm^3 was selected under oil under ambient conditions and attached to the tip of a MiTeGen MicroMount©. The crystal was mounted in a stream of cold nitrogen at 100(1) K and centered in the X-ray beam by using a video camera.

The crystal evaluation and data collection were performed on a Bruker SMART APEXII diffractometer with Cu K_α (λ = 1.54178 Å) radiation and the diffractometer to crystal distance of 4.03 cm.

The initial cell constants were obtained from three series of ω scans at different starting angles. Each series consisted of 41 frames collected at intervals of 0.6º in a 25º range about ω with the exposure time of 10 seconds per frame. The reflections were successfully indexed by an automated indexing routine built in the APEXII program. The final cell constants were calculated from a set of 9901 strong reflections from the actual data collection.

The data were collected by using the full sphere data collection routine to survey the reciprocal space to the extent of a full sphere to a resolution of 0.82 Å. A total of 10691 data were harvested by collecting 15 sets of frames with 0.7º scans in ω with an exposure time 8-20 sec per frame. These highly redundant datasets were corrected for Lorentz and polarization effects. The absorption correction was based on fitting a function to the empirical transmission surface as sampled by multiple equivalent measurements. [1]

Structure Solution and Refinement

The systematic absences in the diffraction data were consistent for the space group $P2_1$ that yielded chemically reasonable and computationally stable results of refinement [2,3].

A successful solution by the direct methods provided most non-hydrogen atoms from the *E*-map. The remaining non-hydrogen atoms were located in an alternating series of least-squares cycles and difference Fourier maps. All non-hydrogen atoms were refined with anisotropic displacement coefficients. All hydrogen atoms were included in the structure factor calculation at idealized positions and were allowed to ride on the neighboring atoms with relative isotropic displacement coefficients.

The absolute configuration of the chiral C(8) center is *S*.

The final least-squares refinement of 205 parameters against 2436 data resulted in residuals *R* (based on F^2 for $I \geq 2\sigma$) and *wR* (based on F^2 for all data) of 0.0251 and 0.0695, respectively. The final difference Fourier map was featureless.

The molecular diagram is drawn with 50% probability ellipsoids.

References

[1] Bruker-AXS. (2007) APEX2, SADABS, and SAINT Software Reference Manuals. Bruker-AXS, Madison, Wisconsin, USA.

[2] Sheldrick, G. M. (2008) SHELXL. *Acta Cryst.* **A64**, 112-122.

[3] Dolomanov, O.V.; Bourhis, L.J.; Gildea, R.J.; Howard, J.A.K.; Puschmann, H. "OLEX2: a complete structure solution, refinement and analysis program". *J. Appl. Cryst.* (2009) **42**, *339-341*.

Table 6.14 Crystal data and structure refinement for (2*S*)-2-(1,3-dioxolan-2-yl)-propanal 2,4-dinitrophenylhydrazone **6**.

Empirical formula	$C_{12}\ H_{14}\ N_4\ O_6$	
Formula weight	310.27	
Temperature	100(2) K	
Wavelength	1.54178 Å	
Crystal system	Monoclinic	
Space group	$P2_1$	
Unit cell dimensions	a = 4.491(2) Å	α= 90°.
	b = 16.233(6) Å	β= 96.47(4)°.
	c = 9.274(5) Å	γ = 90°.
Volume	671.8(6) $Å^3$	
Z	2	
Density (calculated)	1.534 Mg/m^3	
Absorption coefficient	1.073 mm^{-1}	
F(000)	324	
Crystal size	0.44 x 0.13 x 0.12 mm^3	
Theta range for data collection	4.80 to 71.77°.	
Index ranges	-5<=h<=5, -19<=k<=19, -11<=l<=11	
Reflections collected	10691	
Independent reflections	2436 [R(int) = 0.0145]	
Completeness to theta = 67.00°	99.6 %	
Absorption correction	Empirical with SADABS	
Max. and min. transmission	0.8811 and 0.6484	
Refinement method	Full-matrix least-squares on F^2	
Data / restraints / parameters	2436 / 1 / 205	
Goodness-of-fit on F^2	0.964	
Final R indices [I>2sigma(I)]	R1 = 0.0251, wR2 = 0.0694	
R indices (all data)	R1 = 0.0251, wR2 = 0.0695	
Absolute structure parameter Flack x	0.10(13)	
Absolute structure parameter Hooft y	0.07(7)	
Largest diff. peak and hole	0.195 and -0.170 $e.Å^{-3}$	

Table 6.15 Atomic coordinates (x 10^4) and equivalent isotropic displacement parameters ($Å^2$x 10^3) for (2*S*)-2-(1,3-dioxolan-2-yl)-propanal 2,4-dinitrophenylhydrazone **6**. U(eq) is defined as one third of the trace of the orthogonalized U^{ij} tensor.

	x	y	z	U(eq)
O(1)	-1625(2)	2808(1)	7916(1)	24(1)
O(2)	-4062(2)	2178(1)	9461(1)	28(1)
O(3)	-3420(2)	2953(1)	14385(1)	26(1)
O(4)	162(2)	3753(1)	15303(1)	25(1)
O(5)	8479(2)	6508(1)	5676(1)	24(1)
O(6)	5623(3)	5462(1)	4648(1)	33(1)
N(1)	-2230(2)	2690(1)	9166(1)	18(1)
N(2)	-1264(2)	3400(1)	14270(1)	19(1)
N(3)	2365(2)	3953(1)	8746(1)	17(1)
N(4)	4398(2)	4584(1)	8642(1)	18(1)
C(1)	-745(3)	3200(1)	10320(1)	16(1)
C(2)	-1613(3)	3066(1)	11699(1)	18(1)
C(3)	-337(3)	3533(1)	12835(1)	18(1)
C(4)	1766(3)	4142(1)	12640(1)	19(1)
C(5)	2597(3)	4278(1)	11279(1)	19(1)
C(6)	1395(3)	3808(1)	10060(1)	16(1)
C(7)	5294(3)	4696(1)	7399(1)	18(1)
C(8)	7482(3)	5377(1)	7200(1)	18(1)
C(9)	8342(3)	5883(1)	8570(1)	22(1)
C(10)	6254(3)	5933(1)	5946(1)	22(1)
C(11)	7908(3)	6706(1)	4170(2)	24(1)
C(12)	6613(4)	5917(1)	3495(2)	34(1)

Table 6.16 Bond lengths [Å] and angles [°] for (2*S*)-2-(1,3-dioxolan-2-yl)-propanal 2,4-dinitrophenylhydrazone **6**.

O(1)-N(1)	1.2355(15)	C(4)-C(5)	1.3738(19)
O(2)-N(1)	1.2216(16)	C(4)-H(4)	0.9500
O(3)-N(2)	1.2236(16)	C(5)-C(6)	1.4192(18)
O(4)-N(2)	1.2325(16)	C(5)-H(5)	0.9500
O(5)-C(10)	1.4109(16)	C(7)-C(8)	1.5042(17)
O(5)-C(11)	1.4285(18)	C(7)-H(7)	0.9500
O(6)-C(12)	1.4115(19)	C(8)-C(10)	1.5244(18)
O(6)-C(10)	1.4264(18)	C(8)-C(9)	1.5251(19)
N(1)-C(1)	1.4533(17)	C(8)-H(8)	1.0000
N(2)-C(3)	1.4546(17)	C(9)-H(9A)	0.9800
N(3)-C(6)	1.3599(17)	C(9)-H(9B)	0.9800
N(3)-N(4)	1.3831(15)	C(9)-H(9C)	0.9800
N(3)-H(3)	0.858(19)	C(10)-H(10)	1.0000
N(4)-C(7)	1.2761(17)	C(11)-C(12)	1.513(2)
C(1)-C(2)	1.3955(18)	C(11)-H(11A)	0.9900
C(1)-C(6)	1.4176(18)	C(11)-H(11B)	0.9900
C(2)-C(3)	1.3705(19)	C(12)-H(12B)	0.9900
C(2)-H(2)	0.9500	C(12)-H(12A)	0.9900
C(3)-C(4)	1.3934(18)		

C(10)-O(5)-C(11)	105.65(10)	C(3)-C(4)-H(4)	120.3
C(12)-O(6)-C(10)	108.06(12)	C(4)-C(5)-C(6)	121.85(12)
O(2)-N(1)-O(1)	122.70(11)	C(4)-C(5)-H(5)	119.1
O(2)-N(1)-C(1)	119.17(11)	C(6)-C(5)-H(5)	119.1
O(1)-N(1)-C(1)	118.10(11)	N(3)-C(6)-C(1)	124.38(11)
O(3)-N(2)-O(4)	123.70(11)	N(3)-C(6)-C(5)	119.31(12)
O(3)-N(2)-C(3)	118.61(11)	C(1)-C(6)-C(5)	116.31(11)
O(4)-N(2)-C(3)	117.68(11)	N(4)-C(7)-C(8)	119.50(11)
C(6)-N(3)-N(4)	118.10(10)	N(4)-C(7)-H(7)	120.2
C(6)-N(3)-H(3)	115.9(12)	C(8)-C(7)-H(7)	120.2
N(4)-N(3)-H(3)	126.0(12)	C(7)-C(8)-C(10)	110.05(11)
C(7)-N(4)-N(3)	116.52(11)	C(7)-C(8)-C(9)	113.65(11)
C(2)-C(1)-C(6)	121.96(11)	C(10)-C(8)-C(9)	110.67(11)
C(2)-C(1)-N(1)	115.68(11)	C(7)-C(8)-H(8)	107.4
C(6)-C(1)-N(1)	122.34(11)	C(10)-C(8)-H(8)	107.4
C(3)-C(2)-C(1)	118.86(12)	C(9)-C(8)-H(8)	107.4
C(3)-C(2)-H(2)	120.6	C(8)-C(9)-H(9A)	109.5
C(1)-C(2)-H(2)	120.6	C(8)-C(9)-H(9B)	109.5
C(2)-C(3)-C(4)	121.60(11)	H(9A)-C(9)-H(9B)	109.5
C(2)-C(3)-N(2)	118.87(12)	C(8)-C(9)-H(9C)	109.5
C(4)-C(3)-N(2)	119.52(11)	H(9A)-C(9)-H(9C)	109.5
C(5)-C(4)-C(3)	119.42(11)	H(9B)-C(9)-H(9C)	109.5
C(5)-C(4)-H(4)	120.3	O(5)-C(10)-O(6)	106.38(11)

O(5)-C(10)-C(8)	108.92(11)	C(12)-C(11)-H(11B)	111.1
O(6)-C(10)-C(8)	110.35(12)	H(11A)-C(11)-H(11B)	109.0
O(5)-C(10)-H(10)	110.4	O(6)-C(12)-C(11)	105.59(12)
O(6)-C(10)-H(10)	110.4	O(6)-C(12)-H(12B)	110.6
C(8)-C(10)-H(10)	110.4	C(11)-C(12)-H(12B)	110.6
O(5)-C(11)-C(12)	103.43(11)	O(6)-C(12)-H(12A)	110.6
O(5)-C(11)-H(11A)	111.1	C(11)-C(12)-H(12A)	110.6
C(12)-C(11)-H(11A)	111.1	H(12B)-C(12)-H(12A)	108.8
O(5)-C(11)-H(11B)	111.1		

Symmetry transformations used to generate equivalent atoms:

Table 6.17 Anisotropic displacement parameters ($Å^2 x\ 10^3$) for (2*S*)-2-(1,3-dioxolan-2-yl)-propanal 2,4-dinitrophenylhydrazone **6**. The anisotropic displacement factor exponent takes the form: $-2\pi^2[\ h^2\ a^{*2}U^{11} + ... + 2\ h\ k\ a^*\ b^*\ U^{12}\ ]$.

	U^{11}	U^{22}	U^{33}	U^{23}	U^{13}	U^{12}
O(1)	32(1)	28(1)	14(1)	-3(1)	7(1)	-7(1)
O(2)	37(1)	26(1)	20(1)	-1(1)	5(1)	-15(1)
O(3)	24(1)	35(1)	19(1)	4(1)	5(1)	-6(1)
O(4)	32(1)	29(1)	13(1)	-2(1)	2(1)	-3(1)
O(5)	22(1)	26(1)	23(1)	7(1)	3(1)	-6(1)
O(6)	46(1)	35(1)	17(1)	7(1)	-4(1)	-20(1)
N(1)	22(1)	17(1)	16(1)	0(1)	4(1)	-1(1)
N(2)	21(1)	21(1)	14(1)	1(1)	3(1)	4(1)
N(3)	20(1)	18(1)	14(1)	0(1)	3(1)	-3(1)
N(4)	16(1)	19(1)	18(1)	1(1)	2(1)	0(1)
C(1)	19(1)	16(1)	14(1)	-1(1)	2(1)	2(1)
C(2)	18(1)	18(1)	16(1)	4(1)	3(1)	2(1)
C(3)	18(1)	22(1)	14(1)	3(1)	4(1)	5(1)
C(4)	19(1)	22(1)	16(1)	-1(1)	-1(1)	2(1)
C(5)	18(1)	20(1)	19(1)	2(1)	2(1)	-2(1)
C(6)	16(1)	18(1)	15(1)	2(1)	2(1)	5(1)
C(7)	18(1)	19(1)	17(1)	2(1)	0(1)	1(1)
C(8)	18(1)	21(1)	17(1)	1(1)	3(1)	0(1)
C(9)	24(1)	22(1)	19(1)	0(1)	3(1)	-2(1)
C(10)	19(1)	24(1)	22(1)	4(1)	1(1)	-4(1)
C(11)	32(1)	20(1)	22(1)	5(1)	8(1)	-2(1)
C(12)	55(1)	26(1)	25(1)	0(1)	17(1)	-7(1)

Table 6.18 Hydrogen coordinates (x 10^4) and isotropic displacement parameters ($Å^2$x 10^3) for (2*S*)-2-(1,3-dioxolan-2-yl)-propanal 2,4-dinitrophenylhydrazone **6**.

	x	y	z	U(eq)
H(3)	1590(40)	3649(12)	8044(19)	25(4)
H(2)	-3062	2657	11848	21
H(4)	2618	4461	13441	23
H(5)	4016	4698	11150	23
H(7)	4584	4352	6605	22
H(8)	9354	5116	6926	22
H(9A)	9144	5517	9360	32
H(9B)	6566	6168	8844	32
H(9C)	9868	6289	8385	32
H(10)	4408	6223	6185	26
H(11A)	9782	6859	3766	29
H(11B)	6459	7165	4008	29
H(12B)	4920	6037	2746	41
H(12A)	8159	5606	3041	41

Table 6.19 Torsion angles [°] for (2*S*)-2-(1,3-dioxolan-2-yl)-propanal 2,4-dinitrophenylhydrazone **6.**

C(6)-N(3)-N(4)-C(7)	179.07(11)
O(2)-N(1)-C(1)-C(2)	-1.22(17)
O(1)-N(1)-C(1)-C(2)	177.19(11)
O(2)-N(1)-C(1)-C(6)	-179.76(11)
O(1)-N(1)-C(1)-C(6)	-1.35(17)
C(6)-C(1)-C(2)-C(3)	-0.46(17)
N(1)-C(1)-C(2)-C(3)	-179.00(11)
C(1)-C(2)-C(3)-C(4)	0.79(18)
C(1)-C(2)-C(3)-N(2)	179.36(11)
O(3)-N(2)-C(3)-C(2)	-9.40(17)
O(4)-N(2)-C(3)-C(2)	171.36(11)
O(3)-N(2)-C(3)-C(4)	169.20(11)
O(4)-N(2)-C(3)-C(4)	-10.04(16)
C(2)-C(3)-C(4)-C(5)	-0.24(18)
N(2)-C(3)-C(4)-C(5)	-178.80(11)
C(3)-C(4)-C(5)-C(6)	-0.66(19)
N(4)-N(3)-C(6)-C(1)	178.07(10)
N(4)-N(3)-C(6)-C(5)	-2.97(16)
C(2)-C(1)-C(6)-N(3)	178.60(11)
N(1)-C(1)-C(6)-N(3)	-2.95(18)
C(2)-C(1)-C(6)-C(5)	-0.39(16)
N(1)-C(1)-C(6)-C(5)	178.06(11)
C(4)-C(5)-C(6)-N(3)	-178.09(11)
C(4)-C(5)-C(6)-C(1)	0.95(17)
N(3)-N(4)-C(7)-C(8)	179.38(10)
N(4)-C(7)-C(8)-C(10)	-126.02(13)
N(4)-C(7)-C(8)-C(9)	-1.27(17)
C(11)-O(5)-C(10)-O(6)	32.63(13)
C(11)-O(5)-C(10)-C(8)	151.58(11)
C(12)-O(6)-C(10)-O(5)	-19.87(15)
C(12)-O(6)-C(10)-C(8)	-137.88(12)
C(7)-C(8)-C(10)-O(5)	-173.45(10)
C(9)-C(8)-C(10)-O(5)	60.10(14)
C(7)-C(8)-C(10)-O(6)	-57.02(14)
C(9)-C(8)-C(10)-O(6)	176.54(10)
C(10)-O(5)-C(11)-C(12)	-31.66(14)
C(10)-O(6)-C(12)-C(11)	-0.03(17)
O(5)-C(11)-C(12)-O(6)	19.39(16)

Symmetry transformations used to generate equivalent atoms:

Table 6.20 Hydrogen bonds for (2*S*)-2-(1,3-dioxolan-2-yl)-propanal 2,4-dinitrophenylhydrazone **6** [Å and °].

D-H...A	d(D-H)	d(H...A)	d(D...A)	<(DHA)
N(3)-H(3)...O(1)	0.858(19)	1.981(19)	2.6350(16)	132.2(15)

Symmetry transformations used to generate equivalent atoms:

6.7 Synthesis of 3,4-Diazaphospholanes and 3,6-Diazaphosphacycles Using Chiral Auxillaries

The development of chiral phosphines was explored with enantioenriched aldehydes and from a racemic chiral diamine. Diastereoselective cyclization of (*S*)-2-(acetyloxy)-propanal azine was accomplished with phenylphosphine and succinyl chloride to the *rac*-diazaphospholane (Scheme 6.1). Although the synthesis of the monodentate diazaphospholane was diastereoselective, cyclization of 1,2-bis(phosphino)benzene resulted in many phosphine isomers indicating no selectivity in the bidentate analogue (12 peaks in the ^{31}P NMR).

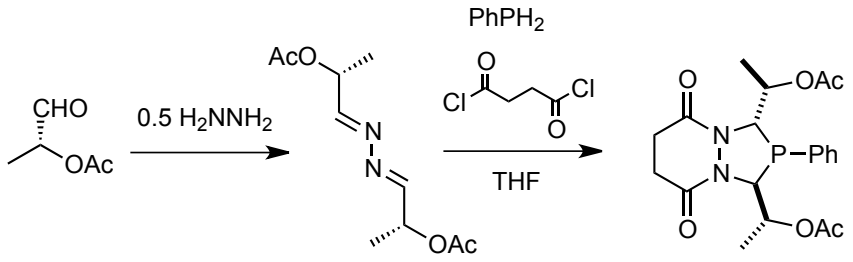

Scheme 6.1 Reaction scheme using enantiomerically enriched (*S*)-2-(acetyloxy)-propanal to diastereoselectively prepare an enantioenriched *rac*-3,4-diazaphospholane.

The cyclization of other types of diamines was explored. Condensation of 2-formylbenzoic acid with racemic trans-1,2-diaminocyclohexane was carried out in the presence of potassium carbonate (Scheme 6.2). Cyclization of this diimine salt to the 7-member phosphacycle was slow and resulted in a poor yield of the intramolecular amidation product **1**. 3,6-Diazaphosphacycle **1** was confirmed from ^{1}H NMR spectroscopy, mass spectrometry, and X-ray crystallography (Figure 6.5).

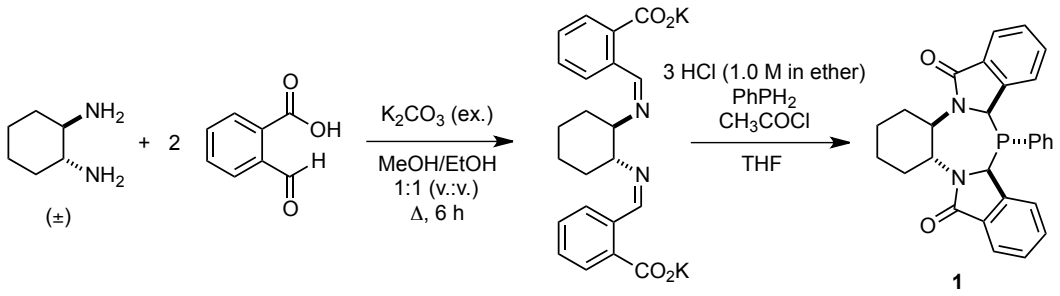

Scheme 6.2 Condensation of *trans*-1,2-diaminocyclohexane with 2-formylbenzoic acid results in the diimine potassium carboxylate salt. Cyclization of a diimine to the 7-member monophosphine (**1**) with phenylphosphine and acetyl chloride in low yield.

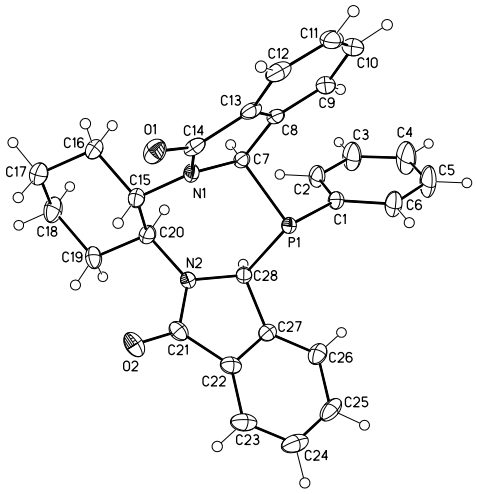

Figure 6.5 Crystal structure of 3,6-diazaphosphacycle **1**. The molecular diagram is drawn with 40% probability ellipsoids and both enantiomers exist in the structure.

6.8 Crystallography Data for 3,6-diazaphosphacycle 1 (Chapter 6)

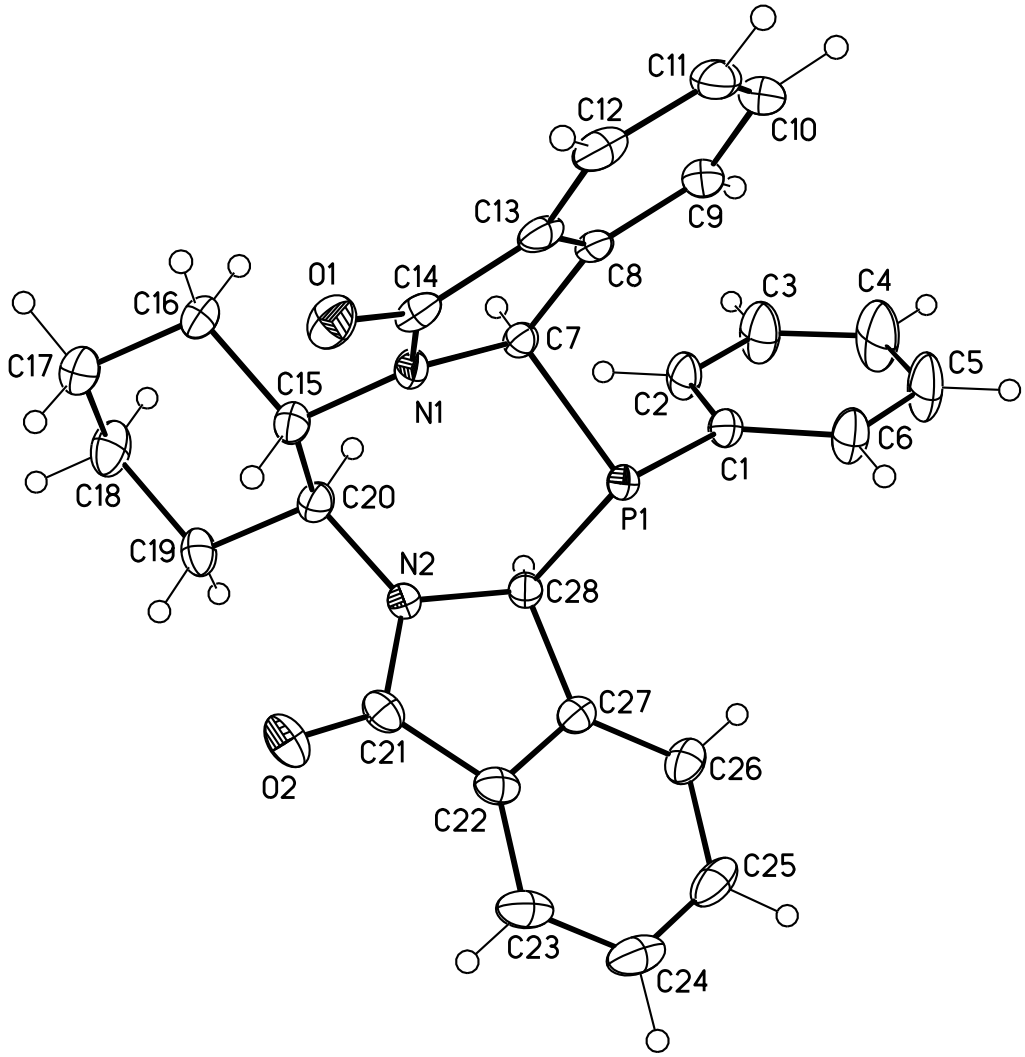

Figure 6.6 ORTEP drawing of 3,6-diazaphosphocycle **1**. Thermal ellipsoids are drawn at the 40% probability level.

Data Collection

A colorless crystal with approximate dimensions 0.46 x 0.27 x 0.18 mm^3 was selected under oil under ambient conditions and attached to the tip of a MiTeGen MicroMount©. The crystal was mounted in a stream of cold nitrogen at 100(2) K and centered in the X-ray beam by using a video camera.

The crystal evaluation and data collection were performed on a Bruker CCD-1000 diffractometer with Mo K_α (λ = 0.71073 Å) radiation and the diffractometer to crystal distance of 4.9 cm.

The initial cell constants were obtained from three series of ω scans at different starting angles. Each series consisted of 20 frames collected at intervals of 0.3º in a 6º range about ω with the exposure time of 10 seconds per frame. A total of 59 reflections was obtained. The reflections were successfully indexed by an automated indexing routine built in the SMART program. The final cell constants were calculated from a set of 10033 strong reflections from the actual data collection.

The data were collected by using the full sphere data collection routine to survey the reciprocal space to the extent of a full sphere to a resolution of 0.8 Å. A total of 30108 data were harvested by collecting four sets of frames with 0.36º scans in ω and one set with 0.45º scans in φ with an exposure time 31 sec per frame. These highly redundant datasets were corrected for Lorentz and polarization effects. The absorption correction was based on fitting a function to the empirical transmission surface as sampled by multiple equivalent measurements. [1]

Structure Solution and Refinement

The systematic absences in the diffraction data were uniquely consistent for the space group $P2_1/c$ that yielded chemically reasonable and computationally stable results of refinement [2].

A successful solution by the direct methods provided most non-hydrogen atoms from the *E*-map. The remaining non-hydrogen atoms were located in an alternating series of least-squares cycles and difference Fourier maps. All non-hydrogen atoms were refined with anisotropic displacement coefficients. All hydrogen atoms were included in the structure factor calculation at idealized positions and were allowed to ride on the neighboring atoms with relative isotropic displacement coefficients.

There was also a disordered solvate molecules of THF present in the asymmetric unit. A significant amount of time was invested in identifying and refining the disordered molecules. Bond length restraints were applied to model the molecules but the resulting isotropic displacement coefficients suggested the molecules were mobile. In addition, the refinement was computationally unstable. Option SQUEEZE of program PLATON [3] was used to correct the diffraction data for diffuse scattering effects and to identify the solvate molecule. PLATON calculated the upper limit of volume that can be occupied by the solvent to be 22% of the unit cell volume. The program calculated 218 electrons in the unit cell for the diffuse species. This very approximately corresponds to one molecule of THF molecule in the asymmetric unit (40 electrons). Please note that all derived results in the following tables are based on the known contents. No data are given for the diffusely scattering species.

The final least-squares refinement of 298 parameters against 5640 data resulted in residuals R (based on F^2 for $I \geq 2\sigma$) and wR (based on F^2 for all data) of 0.0548 and 0.1626, respectively. The final difference Fourier map was featureless.

The molecular diagram is drawn with 40% probability ellipsoids.

References

[1] Bruker-AXS. (2000-2007) SADABS, SAINT, and SMART 5.622 Software Reference Manuals. Bruker-AXS, Madison, Wisconsin, USA.

[2] Sheldrick, G. M. (2008) SHELXL. *Acta Cryst.* **A64**, 112-122.

[3] A.L. Spek (1990) Acta Cryst. A46, C34.

Table 6.21 Crystal data and structure refinement for 3,6-diazaphosphacycle **1**.

Empirical formula	$C_{28}H_{25}N_2O_2P$. THF	
Formula weight	524.57	
Temperature	100(2) K	
Wavelength	0.71073 Å	
Crystal system	Monoclinic	
Space group	$P2_1/c$	
Unit cell dimensions	a = 16.1072(16) Å	α= 90°.
	b = 15.3749(15) Å	β= 105.5300(10)°.
	c = 11.5092(11) Å	γ = 90°.
Volume	2746.2(5) $Å^3$	
Z	4	
Density (calculated)	1.269 Mg/m^3	
Absorption coefficient	0.136 mm^{-1}	
F(000)	1112	
Crystal size	0.46 x 0.27 x 0.18 mm^3	
Theta range for data collection	2.26 to 26.45°.	
Index ranges	-20<=h<=20, -19<=k<=19, -14<=l<=14	
Reflections collected	30108	
Independent reflections	5640 [R(int) = 0.0373]	
Completeness to theta = 26.45°	99.5 %	
Absorption correction	Empirical with SADABS	
Max. and min. transmission	0.9759 and 0.9400	
Refinement method	Full-matrix least-squares on F^2	
Data / restraints / parameters	5640 / 0 / 298	
Goodness-of-fit on F^2	1.045	
Final R indices [I>2sigma(I)]	R1 = 0.0548, wR2 = 0.1548	
R indices (all data)	R1 = 0.0645, wR2 = 0.1626	
Largest diff. peak and hole	0.736 and -0.248 $e.Å^{-3}$	

Table 6.22 Atomic coordinates (x 10^4) and equivalent isotropic displacement parameters ($Å^2$x 10^3) for 3,6-diazaphosphacycle **1**. U(eq) is defined as one third of the trace of the orthogonalized U^{ij} tensor.

	x	y	z	U(eq)
P(1)	2767(1)	5430(1)	7090(1)	18(1)
O(1)	3512(1)	7764(1)	9698(1)	32(1)
O(2)	533(1)	7148(1)	7473(1)	34(1)
N(1)	3149(1)	7116(1)	7823(1)	22(1)
N(2)	1450(1)	6612(1)	6404(1)	22(1)
C(1)	3207(1)	4747(1)	6095(2)	24(1)
C(2)	3342(1)	5047(1)	5016(2)	30(1)
C(3)	3741(2)	4526(2)	4347(2)	47(1)
C(4)	4023(2)	3702(2)	4752(3)	60(1)
C(5)	3884(2)	3391(2)	5812(3)	54(1)
C(6)	3467(2)	3904(1)	6472(2)	37(1)
C(7)	3474(1)	6424(1)	7182(2)	19(1)
C(8)	4307(1)	6188(1)	8071(2)	22(1)
C(9)	4944(1)	5604(1)	7949(2)	30(1)
C(10)	5638(1)	5476(1)	8941(2)	37(1)
C(11)	5699(1)	5892(1)	10013(2)	36(1)
C(12)	5074(1)	6479(1)	10150(2)	32(1)
C(13)	4374(1)	6622(1)	9145(2)	25(1)
C(14)	3648(1)	7228(1)	8974(2)	24(1)
C(15)	2496(1)	7767(1)	7277(2)	25(1)
C(16)	2934(1)	8590(1)	6969(2)	30(1)
C(17)	2270(2)	9282(1)	6418(2)	36(1)
C(18)	1650(2)	8928(1)	5272(2)	38(1)
C(19)	1195(1)	8094(1)	5539(2)	28(1)
C(20)	1867(1)	7415(1)	6149(2)	25(1)
C(21)	807(1)	6550(1)	6979(2)	25(1)
C(22)	534(1)	5624(1)	6860(2)	25(1)
C(23)	-114(1)	5213(2)	7243(2)	34(1)
C(24)	-244(2)	4342(2)	6997(2)	39(1)
C(25)	255(1)	3885(1)	6402(2)	37(1)
C(26)	912(1)	4296(1)	6016(2)	29(1)
C(27)	1036(1)	5178(1)	6252(2)	22(1)
C(28)	1708(1)	5782(1)	6031(2)	20(1)

Table 6.23 Bond lengths [Å] and angles [°] for 3,6-diazaphosphacycle **1**.

P(1)-C(1)	1.8319(19)	C(12)-C(13)	1.400(3)
P(1)-C(28)	1.8901(18)	C(12)-H(12)	0.9500
P(1)-C(7)	1.8915(18)	C(13)-C(14)	1.466(3)
O(1)-C(14)	1.233(2)	C(15)-C(20)	1.517(3)
O(2)-C(21)	1.224(2)	C(15)-C(16)	1.535(3)
N(1)-C(14)	1.364(2)	C(15)-H(15)	1.0000
N(1)-C(15)	1.467(2)	C(16)-C(17)	1.521(3)
N(1)-C(7)	1.468(2)	C(16)-H(16A)	0.9900
N(2)-C(21)	1.374(3)	C(16)-H(16B)	0.9900
N(2)-C(28)	1.444(2)	C(17)-C(18)	1.526(3)
N(2)-C(20)	1.471(2)	C(17)-H(17A)	0.9900
C(1)-C(6)	1.395(3)	C(17)-H(17B)	0.9900
C(1)-C(2)	1.396(3)	C(18)-C(19)	1.548(3)
C(2)-C(3)	1.382(3)	C(18)-H(18A)	0.9900
C(2)-H(2)	0.9500	C(18)-H(18B)	0.9900
C(3)-C(4)	1.384(3)	C(19)-C(20)	1.533(3)
C(3)-H(3)	0.9500	C(19)-H(19A)	0.9900
C(4)-C(5)	1.383(4)	C(19)-H(19B)	0.9900
C(4)-H(4)	0.9500	C(20)-H(20)	1.0000
C(5)-C(6)	1.387(3)	C(21)-C(22)	1.485(3)
C(5)-H(5)	0.9500	C(22)-C(27)	1.385(3)
C(6)-H(6)	0.9500	C(22)-C(23)	1.388(3)
C(7)-C(8)	1.498(2)	C(23)-C(24)	1.373(3)
C(7)-H(7)	1.0000	C(23)-H(23)	0.9500
C(8)-C(13)	1.383(3)	C(24)-C(25)	1.380(4)
C(8)-C(9)	1.398(3)	C(24)-H(24)	0.9500
C(9)-C(10)	1.382(3)	C(25)-C(26)	1.403(3)
C(9)-H(9)	0.9500	C(25)-H(25)	0.9500
C(10)-C(11)	1.370(3)	C(26)-C(27)	1.386(3)
C(10)-H(10)	0.9500	C(26)-H(26)	0.9500
C(11)-C(12)	1.392(3)	C(27)-C(28)	1.499(3)
C(11)-H(11)	0.9500	C(28)-H(28)	1.0000
C(1)-P(1)-C(28)	101.20(8)	C(2)-C(1)-P(1)	123.03(14)
C(1)-P(1)-C(7)	99.84(8)	C(3)-C(2)-C(1)	120.63(19)
C(28)-P(1)-C(7)	103.37(8)	C(3)-C(2)-H(2)	119.7
C(14)-N(1)-C(15)	119.91(15)	C(1)-C(2)-H(2)	119.7
C(14)-N(1)-C(7)	112.52(15)	C(2)-C(3)-C(4)	120.2(2)
C(15)-N(1)-C(7)	126.20(15)	C(2)-C(3)-H(3)	119.9
C(21)-N(2)-C(28)	113.27(15)	C(4)-C(3)-H(3)	119.9
C(21)-N(2)-C(20)	126.79(16)	C(5)-C(4)-C(3)	119.8(2)
C(28)-N(2)-C(20)	119.94(15)	C(5)-C(4)-H(4)	120.1
C(6)-C(1)-C(2)	118.65(18)	C(3)-C(4)-H(4)	120.1
C(6)-C(1)-P(1)	118.20(15)	C(4)-C(5)-C(6)	120.2(2)

C(4)-C(5)-H(5)	119.9	C(18)-C(17)-H(17A)	109.8
C(6)-C(5)-H(5)	119.9	C(16)-C(17)-H(17B)	109.8
C(5)-C(6)-C(1)	120.4(2)	C(18)-C(17)-H(17B)	109.8
C(5)-C(6)-H(6)	119.8	H(17A)-C(17)-H(17B)	108.2
C(1)-C(6)-H(6)	119.8	C(17)-C(18)-C(19)	111.03(17)
N(1)-C(7)-C(8)	101.97(14)	C(17)-C(18)-H(18A)	109.4
N(1)-C(7)-P(1)	108.88(12)	C(19)-C(18)-H(18A)	109.4
C(8)-C(7)-P(1)	104.96(12)	C(17)-C(18)-H(18B)	109.4
N(1)-C(7)-H(7)	113.4	C(19)-C(18)-H(18B)	109.4
C(8)-C(7)-H(7)	113.4	H(18A)-C(18)-H(18B)	108.0
P(1)-C(7)-H(7)	113.4	C(20)-C(19)-C(18)	109.95(17)
C(13)-C(8)-C(9)	121.11(18)	C(20)-C(19)-H(19A)	109.7
C(13)-C(8)-C(7)	109.50(16)	C(18)-C(19)-H(19A)	109.7
C(9)-C(8)-C(7)	129.35(18)	C(20)-C(19)-H(19B)	109.7
C(10)-C(9)-C(8)	117.5(2)	C(18)-C(19)-H(19B)	109.7
C(10)-C(9)-H(9)	121.3	H(19A)-C(19)-H(19B)	108.2
C(8)-C(9)-H(9)	121.3	N(2)-C(20)-C(15)	111.39(15)
C(11)-C(10)-C(9)	121.7(2)	N(2)-C(20)-C(19)	111.03(16)
C(11)-C(10)-H(10)	119.2	C(15)-C(20)-C(19)	112.10(16)
C(9)-C(10)-H(10)	119.2	N(2)-C(20)-H(20)	107.4
C(10)-C(11)-C(12)	121.7(2)	C(15)-C(20)-H(20)	107.4
C(10)-C(11)-H(11)	119.2	C(19)-C(20)-H(20)	107.4
C(12)-C(11)-H(11)	119.2	O(2)-C(21)-N(2)	125.61(19)
C(11)-C(12)-C(13)	117.1(2)	O(2)-C(21)-C(22)	128.99(18)
C(11)-C(12)-H(12)	121.4	N(2)-C(21)-C(22)	105.40(16)
C(13)-C(12)-H(12)	121.4	C(27)-C(22)-C(23)	121.7(2)
C(8)-C(13)-C(12)	120.95(19)	C(27)-C(22)-C(21)	108.87(16)
C(8)-C(13)-C(14)	108.59(16)	C(23)-C(22)-C(21)	129.5(2)
C(12)-C(13)-C(14)	130.39(19)	C(24)-C(23)-C(22)	117.7(2)
O(1)-C(14)-N(1)	125.15(19)	C(24)-C(23)-H(23)	121.2
O(1)-C(14)-C(13)	127.90(18)	C(22)-C(23)-H(23)	121.2
N(1)-C(14)-C(13)	106.92(16)	C(23)-C(24)-C(25)	121.5(2)
N(1)-C(15)-C(20)	111.16(15)	C(23)-C(24)-H(24)	119.3
N(1)-C(15)-C(16)	109.90(16)	C(25)-C(24)-H(24)	119.3
C(20)-C(15)-C(16)	109.87(16)	C(24)-C(25)-C(26)	121.1(2)
N(1)-C(15)-H(15)	108.6	C(24)-C(25)-H(25)	119.4
C(20)-C(15)-H(15)	108.6	C(26)-C(25)-H(25)	119.4
C(16)-C(15)-H(15)	108.6	C(27)-C(26)-C(25)	117.4(2)
C(17)-C(16)-C(15)	110.96(17)	C(27)-C(26)-H(26)	121.3
C(17)-C(16)-H(16A)	109.4	C(25)-C(26)-H(26)	121.3
C(15)-C(16)-H(16A)	109.4	C(22)-C(27)-C(26)	120.71(19)
C(17)-C(16)-H(16B)	109.4	C(22)-C(27)-C(28)	108.95(16)
C(15)-C(16)-H(16B)	109.4	C(26)-C(27)-C(28)	130.18(18)
H(16A)-C(16)-H(16B)	108.0	N(2)-C(28)-C(27)	102.66(14)
C(16)-C(17)-C(18)	109.58(18)	N(2)-C(28)-P(1)	110.05(12)
C(16)-C(17)-H(17A)	109.8	C(27)-C(28)-P(1)	106.36(12)

N(2)-C(28)-H(28)	112.4	P(1)-C(28)-H(28)	112.4
C(27)-C(28)-H(28)	112.4		

Symmetry transformations used to generate equivalent atoms:

Table 6.24 Anisotropic displacement parameters ($Å^2 x\ 10^3$) for 3,6-diazaphosphacycle **1**. The anisotropic displacement factor exponent takes the form: $-2\pi^2[\ h^2\ a^{*2}U^{11} + ... + 2\ h\ k\ a^*\ b^*\ U^{12}\ ]$.

	U^{11}	U^{22}	U^{33}	U^{23}	U^{13}	U^{12}
P(1)	19(1)	16(1)	20(1)	-1(1)	6(1)	0(1)
O(1)	42(1)	27(1)	29(1)	-8(1)	14(1)	-5(1)
O(2)	34(1)	39(1)	30(1)	-2(1)	11(1)	13(1)
N(1)	23(1)	16(1)	26(1)	-2(1)	4(1)	0(1)
N(2)	19(1)	18(1)	30(1)	0(1)	6(1)	1(1)
C(1)	25(1)	18(1)	29(1)	-3(1)	9(1)	0(1)
C(2)	41(1)	21(1)	34(1)	-2(1)	19(1)	6(1)
C(3)	73(2)	32(1)	48(1)	2(1)	39(1)	15(1)
C(4)	94(2)	36(1)	68(2)	-2(1)	54(2)	23(1)
C(5)	82(2)	24(1)	63(2)	3(1)	35(2)	20(1)
C(6)	52(1)	23(1)	39(1)	2(1)	20(1)	7(1)
C(7)	21(1)	18(1)	20(1)	0(1)	7(1)	-2(1)
C(8)	17(1)	19(1)	30(1)	5(1)	6(1)	-4(1)
C(9)	23(1)	26(1)	43(1)	5(1)	12(1)	0(1)
C(10)	21(1)	32(1)	57(1)	6(1)	10(1)	-1(1)
C(11)	20(1)	36(1)	47(1)	16(1)	-1(1)	-4(1)
C(12)	32(1)	32(1)	30(1)	3(1)	4(1)	-14(1)
C(13)	23(1)	24(1)	26(1)	6(1)	6(1)	-9(1)
C(14)	28(1)	22(1)	24(1)	-4(1)	10(1)	-10(1)
C(15)	27(1)	19(1)	29(1)	2(1)	9(1)	2(1)
C(16)	32(1)	19(1)	40(1)	2(1)	12(1)	-3(1)
C(17)	37(1)	24(1)	45(1)	5(1)	10(1)	1(1)
C(18)	50(1)	26(1)	35(1)	10(1)	4(1)	5(1)
C(19)	31(1)	24(1)	27(1)	2(1)	2(1)	8(1)
C(20)	27(1)	20(1)	28(1)	3(1)	7(1)	0(1)
C(21)	21(1)	30(1)	21(1)	-1(1)	1(1)	5(1)
C(22)	18(1)	34(1)	20(1)	4(1)	1(1)	0(1)
C(23)	23(1)	52(1)	29(1)	11(1)	7(1)	-3(1)
C(24)	28(1)	51(1)	34(1)	17(1)	1(1)	-13(1)
C(25)	36(1)	29(1)	36(1)	8(1)	-9(1)	-14(1)
C(26)	32(1)	24(1)	26(1)	-1(1)	-2(1)	-5(1)
C(27)	20(1)	23(1)	18(1)	2(1)	0(1)	-2(1)
C(28)	20(1)	19(1)	20(1)	0(1)	6(1)	1(1)

Table 6.25 Hydrogen coordinates (x 10^4) and isotropic displacement parameters ($Å^2$x 10^3) for 3,6-diazaphosphacycle **1**.

	x	y	z	U(eq)
H(2)	3158	5615	4738	37
H(3)	3821	4734	3607	56
H(4)	4312	3352	4303	72
H(5)	4075	2824	6088	64
H(6)	3358	3679	7187	44
H(7)	3544	6612	6383	23
H(9)	4901	5308	7211	36
H(10)	6083	5089	8877	44
H(11)	6180	5777	10680	43
H(12)	5121	6770	10893	39
H(15)	2169	7924	7873	30
H(16A)	3337	8822	7711	36
H(16B)	3271	8442	6393	36
H(17A)	2565	9806	6225	43
H(17B)	1946	9449	7003	43
H(18A)	1973	8795	4672	46
H(18B)	1213	9376	4923	46
H(19A)	824	8237	6073	34
H(19B)	825	7855	4777	34
H(20)	2206	7262	5566	30
H(23)	-455	5524	7660	41
H(24)	-687	4047	7242	47
H(25)	152	3282	6251	45
H(26)	1258	3983	5608	35
H(28)	1725	5782	5169	24

Table 6.26 Torsion angles [°] for 3,6-diazaphosphacycle **1**.

C(28)-P(1)-C(1)-C(6)	-126.83(18)	C(7)-N(1)-C(15)-C(20)	29.4(2)
C(7)-P(1)-C(1)-C(6)	127.29(18)	C(14)-N(1)-C(15)-C(16)	73.1(2)
C(28)-P(1)-C(1)-C(2)	57.19(19)	C(7)-N(1)-C(15)-C(16)	-92.5(2)
C(7)-P(1)-C(1)-C(2)	-48.68(19)	N(1)-C(15)-C(16)-C(17)	-179.12(17)
C(6)-C(1)-C(2)-C(3)	-1.2(3)	C(20)-C(15)-C(16)-C(17)	58.3(2)
P(1)-C(1)-C(2)-C(3)	174.7(2)	C(15)-C(16)-C(17)-C(18)	-59.3(2)
C(1)-C(2)-C(3)-C(4)	-1.0(4)	C(16)-C(17)-C(18)-C(19)	58.1(2)
C(2)-C(3)-C(4)-C(5)	1.9(5)	C(17)-C(18)-C(19)-C(20)	-55.8(2)
C(3)-C(4)-C(5)-C(6)	-0.4(5)	C(21)-N(2)-C(20)-C(15)	75.3(2)
C(4)-C(5)-C(6)-C(1)	-1.9(4)	C(28)-N(2)-C(20)-C(15)	-105.03(19)
C(2)-C(1)-C(6)-C(5)	2.7(4)	C(21)-N(2)-C(20)-C(19)	-50.3(2)
P(1)-C(1)-C(6)-C(5)	-173.5(2)	C(28)-N(2)-C(20)-C(19)	129.29(17)
C(14)-N(1)-C(7)-C(8)	-5.86(19)	N(1)-C(15)-C(20)-N(2)	56.7(2)
C(15)-N(1)-C(7)-C(8)	160.60(16)	C(16)-C(15)-C(20)-N(2)	178.61(15)
C(14)-N(1)-C(7)-P(1)	104.72(15)	N(1)-C(15)-C(20)-C(19)	-178.16(16)
C(15)-N(1)-C(7)-P(1)	-88.83(18)	C(16)-C(15)-C(20)-C(19)	-56.3(2)
C(1)-P(1)-C(7)-N(1)	172.49(12)	C(18)-C(19)-C(20)-N(2)	-179.57(16)
C(28)-P(1)-C(7)-N(1)	68.37(13)	C(18)-C(19)-C(20)-C(15)	55.1(2)
C(1)-P(1)-C(7)-C(8)	-78.95(13)	C(28)-N(2)-C(21)-O(2)	173.04(17)
C(28)-P(1)-C(7)-C(8)	176.94(12)	C(20)-N(2)-C(21)-O(2)	-7.3(3)
N(1)-C(7)-C(8)-C(13)	7.20(18)	C(28)-N(2)-C(21)-C(22)	-7.1(2)
P(1)-C(7)-C(8)-C(13)	-106.32(14)	C(20)-N(2)-C(21)-C(22)	172.52(16)
N(1)-C(7)-C(8)-C(9)	-175.31(18)	O(2)-C(21)-C(22)-C(27)	-178.73(18)
P(1)-C(7)-C(8)-C(9)	71.2(2)	N(2)-C(21)-C(22)-C(27)	1.4(2)
C(13)-C(8)-C(9)-C(10)	0.3(3)	O(2)-C(21)-C(22)-C(23)	2.2(3)
C(7)-C(8)-C(9)-C(10)	-176.90(18)	N(2)-C(21)-C(22)-C(23)	-177.58(19)
C(8)-C(9)-C(10)-C(11)	0.9(3)	C(27)-C(22)-C(23)-C(24)	-0.1(3)
C(9)-C(10)-C(11)-C(12)	-1.3(3)	C(21)-C(22)-C(23)-C(24)	178.86(19)
C(10)-C(11)-C(12)-C(13)	0.5(3)	C(22)-C(23)-C(24)-C(25)	0.6(3)
C(9)-C(8)-C(13)-C(12)	-1.2(3)	C(23)-C(24)-C(25)-C(26)	-0.5(3)
C(7)-C(8)-C(13)-C(12)	176.57(16)	C(24)-C(25)-C(26)-C(27)	-0.3(3)
C(9)-C(8)-C(13)-C(14)	176.11(17)	C(23)-C(22)-C(27)-C(26)	-0.7(3)
C(7)-C(8)-C(13)-C(14)	-6.2(2)	C(21)-C(22)-C(27)-C(26)	-179.82(16)
C(11)-C(12)-C(13)-C(8)	0.7(3)	C(23)-C(22)-C(27)-C(28)	-176.50(17)
C(11)-C(12)-C(13)-C(14)	-175.86(18)	C(21)-C(22)-C(27)-C(28)	4.4(2)
C(15)-N(1)-C(14)-O(1)	12.9(3)	C(25)-C(26)-C(27)-C(22)	0.8(3)
C(7)-N(1)-C(14)-O(1)	-179.72(17)	C(25)-C(26)-C(27)-C(28)	175.63(18)
C(15)-N(1)-C(14)-C(13)	-164.94(15)	C(21)-N(2)-C(28)-C(27)	9.50(19)
C(7)-N(1)-C(14)-C(13)	2.5(2)	C(20)-N(2)-C(28)-C(27)	-170.17(15)
C(8)-C(13)-C(14)-O(1)	-175.34(19)	C(21)-N(2)-C(28)-P(1)	-103.41(15)
C(12)-C(13)-C(14)-O(1)	1.6(3)	C(20)-N(2)-C(28)-P(1)	76.92(17)
C(8)-C(13)-C(14)-N(1)	2.4(2)	C(22)-C(27)-C(28)-N(2)	-8.15(18)
C(12)-C(13)-C(14)-N(1)	179.31(18)	C(26)-C(27)-C(28)-N(2)	176.57(18)
C(14)-N(1)-C(15)-C(20)	-165.08(16)	C(22)-C(27)-C(28)-P(1)	107.45(14)

C(26)-C(27)-C(28)-P(1)	-67.8(2)	C(1)-P(1)-C(28)-C(27)	96.95(13)
C(1)-P(1)-C(28)-N(2)	-152.54(12)	C(7)-P(1)-C(28)-C(27)	-159.98(12)
C(7)-P(1)-C(28)-N(2)	-49.47(13)		

Symmetry transformations used to generate equivalent atom